ISSN 1097-8135

Life Science Journal

Acta Zhengzhou University Overseas Edition

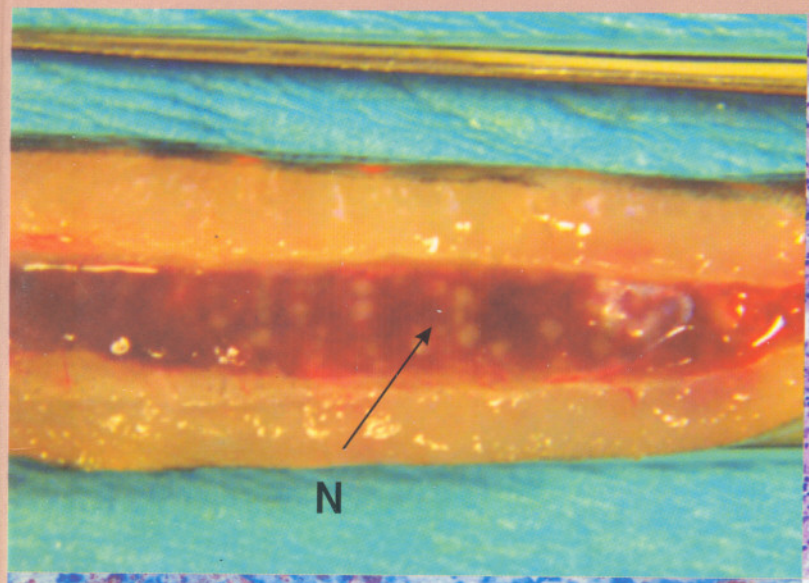

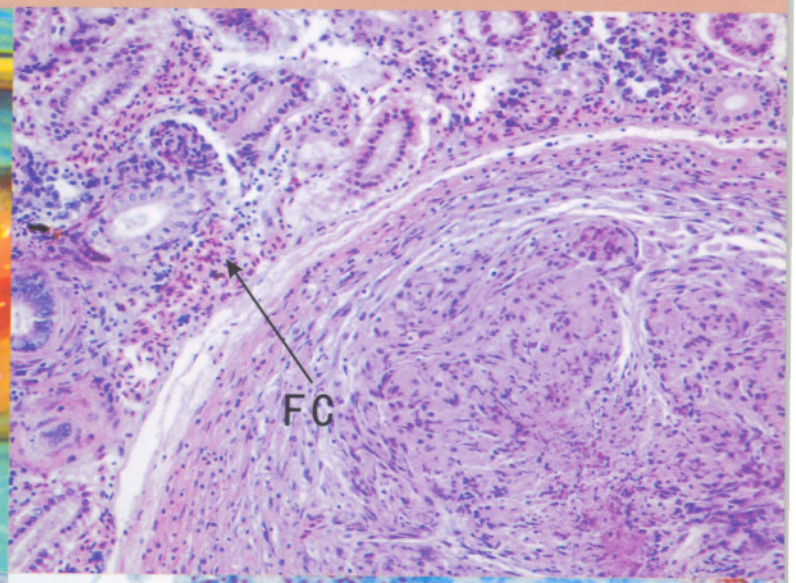

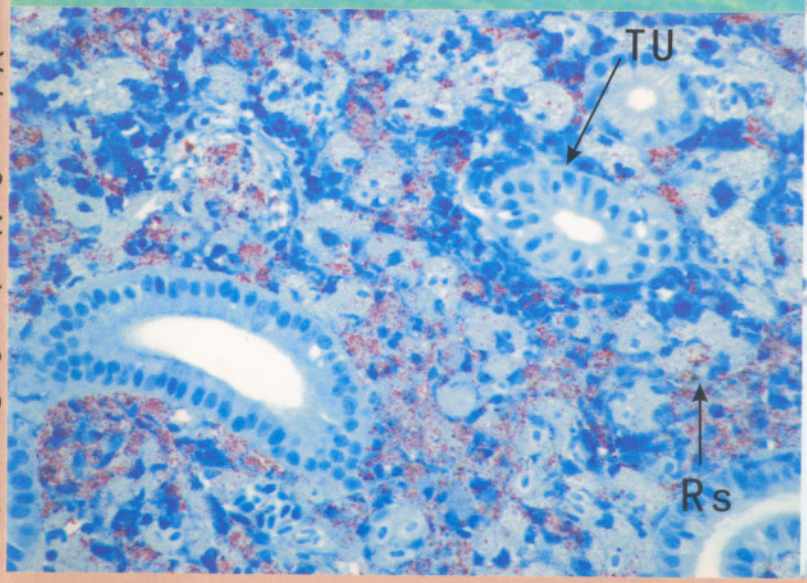

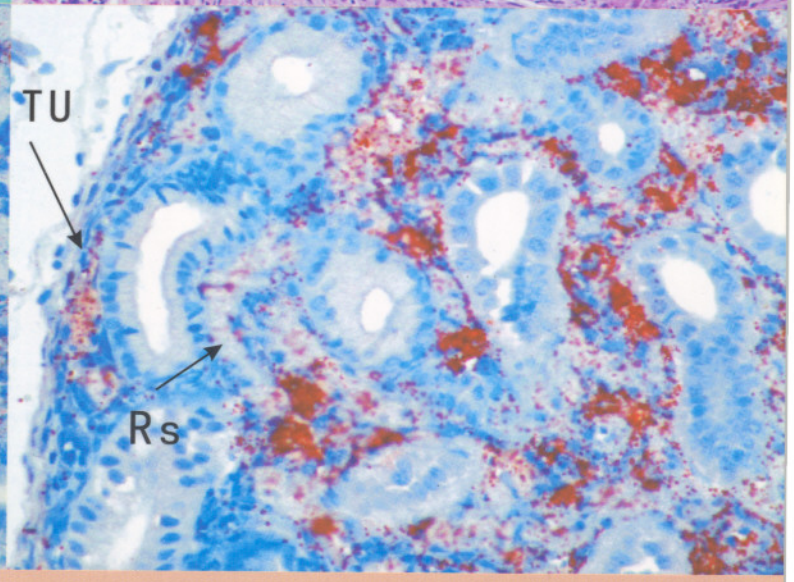

Volume 3 Number 3, September 2006

Life Science Journal

Volume 3 Number 3 September 2006

Life Science Journal

Acta Zhengzhou University Overseas Edition

Life Science Journal, the Acta Zhengzhou University Overseas Edition, is an international journal with the purpose to enhance our natural and scientific knowledge dissemination in the world under the free publication principle. The journal is calling for papers from all who are associated with Zhengzhou University – home and abroad. Any valuable papers or reports that are related to life science are welcome. Other academic articles that are less relevant but are of high quality will also be considered and published. Papers submitted could be reviews, objective descriptions, research reports, opinions/debates, news, letters, and other types of writings. All publications of *Life Science Journal* are under vigorous peer-review. Let's work together to disseminate our research results and our opinions.

CONTENTS

On the cover : Iron River Brook trout with Bacterial Kidney Disease.

The top left one showed the swollen kidney with multiple creamy- whitish nodules (N). The top right one showed HE stained slide of kidney with a severe granulomatous reaction that is replacing kidney tissues of a 3 years old Assinica brook trout. The bottom left one showed kidney tissue of Iron River brook trout fingerling with heavy *Renibacterium salmoninarum* infection stained by an anti-*Renibacterium salmoninarum* antibody based streptavidin-immunoperoxidase immmunolbeling. The bottom right one showed kidney tissue of Iron River brook trout fingerling with heavy *Renibacterium salmoninarum* infection after enhanced antigen retrieval procedures using Alkaline Phosphatase Red and goat anti-*Renibacterium salmoninarum* antibody and counterstained with Mayer's Hematoxylin (Blue background). See *An Overview on Bacterial Kidney Disease* by Eissa AE & Elsayed EE, page 58 – 76 in this issue.

Review and Progress of the Pathologic Research on Esophageal Carcinoma in Henan, China

Yunhan Zhang, Fengyu Cao

Henan Key Laboratory of Tumor Pathology; Department of Pathology, The First Affiliated Hospital of Zhengzhou University, Zhengzhou, Henan 450052, China

Abstract: In the first part of this paper, we briefly reviewed the history of pathologic research on esophageal carcinoma in Henan Province of China. In the research, the excellent work of Professor Qiong Shen, a famous pathologist, is prominently introduced, that includes cytologic diagnosis of esophageal carcinoma, classification of early esophageal carcinoma and the prevention of the esophageal carcinoma, etc. And then, the advance of pathologic research on esophageal carcinoma in Henan province is described as follows: 1. Morphometry research of esophageal carcinoma. 2. The relationship between Langerhans cells and esophageal carcinoma. 3. The relationship between apoptosis and esophageal carcinoma. 4. The related immunohistochemical markers of esophageal carcinoma. 5. The molecular biology and therapy research on esophageal carcinoma. [Life Science Journal. 2006;3(3):1-5] (ISSN: 1097-8135).

Keywords: Henan Province; esophageal tumor; carcinoma; pathology

Abbreviations: AME: alternariol monomethyl ether; AOH: alternariol; ASODN: antisense oligodeoxyribonucleotide; BM: basement membrane; DC: dendritic cells; EC9706: esophageal carcinoma cell-9706; Eca109: esophageal carcinoma cell-109; ECM: extracellular matrix; GST: glutathione s transferring enzyme; HPV: human papilloma virus; ICE: interleukin1-β converting enzyme; LC: Langerhans cells; NDRG: N-myc downstream regulated gene; nm23-H1: Non-metastatic gene; PCR-SSCP: PCR single strand conformation polymorphism; SSH: suppression subtractive hybridization; TRAP-ELISA: telomeric repeat amplification protocol-ELISA; TUNEL: T-mediated d UTP nick end labeling

1 Introduction

Esophageal carcinoma is a kind of common malignant tumors which is seriously harmful to human being. In the world, it appears striking and puzzling differences in geographic incidence. Statistics from WHO (World Health Organization) show that the morbidity and mortality of esophageal carcinoma was the highest in China. The morbidity and mortality of esophageal carcinoma of Chinese male was 6.4/100,000, 31.66/100,000 and that of Chinese female was 20.0/100,000, 15.93/100,000. In 1997, 46.6% of the dead who died of esophageal carcinoma were Chinese. Meanwhile, in China, the highest morbidity and mortality of esophageal carcinoma was in Henan Province. In 1980, the mean mortality of esophageal carcinoma was 33.22/100.000, which was higher than that of any other areas in China.

In 1958, a preliminary survey on epidemiology of esophageal carcinoma was finished. It was found that the prevalence of esophageal carcinoma was much more severe in north of Henan Province than in other regions, especially in Linxian County (Linzhou City now). In 1959, under the guidance of China national leading pathologists, a doctor team from Henan Medical College worked in Linxian County and studied on etiology, pathogenesis, and cytologic diagnosis of esophageal carcinoma. Professors, such as Qiong Shen, Guiting Liu, and Songliang Qiu *et al*, were prominent members in the research group.

2 Cytologic Diagnosis and Pathologic Research on Early Esophageal Carcinoma

At the beginning of the research, autopsy was resisted by local people because of some of the obsolete traditional concepts. At that time, diagnosis of esophageal carcinoma mainly depended on X-ray barium meal visualization or esophagoscope, which was rough and made patients suffer a lot. Above all, most of the patients lost ideal chance for operation when they were found ill by the above two diagnostic methods. Placed in such a predicament, Professor Qiong Shen and his staff members decided to try cellular examination on esophageal carcinoma diagnosis. They invented the "Abrasive Cytological Balloon" and tried many times on themselves. After clinical test, the Balloon was proved to be effective and convenient for diagnosis of

esophageal carcinoma. From 1962, using the general survey with the Balloon in high-incidence areas, the diagnostic accuracy of advanced esophageal carcinoma had been 98.1%[1], and a lot of precancerous lesions of severe atypical hyperplasia and early esophageal carcinoma of asymptomatic patients were found. From the above data it was known that the Abrasive Cytological Balloon applied to the diagnosis of esophageal carcinoma[2,3]. At that time, the applications and disseminations of the Balloon gained high appraisal throughout the world.

Using the Balloon, a lot of asymptomatic or mild-symptomatic patients who suffered from esophageal carcinoma were found. The team with the leader of Professor Shen and Professor Qiu *et al* collected all the available materials of 362 cases of early esophageal carcinoma specimens and made the following conclusions: (1) Most minimal lesions were too small to be found. Only 10%-formalin-fixed lesions and iodine-smeared lesions could be found by naked eyes. (2) Peak morbidity of early esophageal carcinoma arose among people of 41-50 years old (51.1%), which was 6.3 years earlier than that of advanced esophageal carcinoma. (3) Based on the gross features, they, for the first time, distinguished esophageal carcinoma into 4 types: insidious type, erosion type, plaque type and papillary type, which was widely accepted and cited. (4) As for histological features, 35 insidious lesions were squamous cell carcinoma *in situ*, most erosion lesions were carcinoma *in situ* or were confined in mucosa, and more than half of plaque lesions invaded sub-mucosa. (5) Esophageal carcinoma always arose in more than one site, and it often progressed in the following way: normal mucosa → simple hyperplasia → atypical hyperplasia → carcinoma *in situ* →invasive carcinoma[4].

3 Etiology of Esophageal Carcinoma

3.1 Fungi

Much on-site inspection showed that people of Linxian County usually took mildewed and rotten food (such as pickle). Liu *et al*, for the first time, succeeded in inducing esophageal carcinoma on albino rats with natural rotten food, and made such conclusion that rotten food enhanced the carcinogenesis of nitrosamine[5]. He isolated the fungi from local grain and found that five kinds of fungi, including *Alternaria alternata*, had much higher contaminating possibility than that in low-incidence areas. It was known by animal studies that alternariol monomethyl ether (AME) and alternariol (AOH) were active components of *Alternaria alternata*, and both of them enhanced hyperplasia of fetal esophageal epithelia *in vitro* and even cancerization[6].

3.2 Virus

With electron microscope, for the first time, Hu found virus-like particles in the cytoplasm of esophageal carcinoma cells[7]. Then, with *in situ* hybridization, Chang *et al* detected DNA of HPV6, 11, 16, 18 within precancerous lesions and cancer tissues, which indicated that infection of HPV might be concerned with development of esophageal carcinoma[8].

4 Prevention of the Cancerization among High-risk Group

As we know that epithelia hyperplasia was the only way to cancerization. Based on this theory, using rough riboflavin and rabdosia rubesens, Professor Shen *et al* began the research of preventing cancerization. From 1988 to 1992, the results proved that long-term taking rough riboflavin could prevent 57.1% of severe atypical hyperplasia from cancerization, which indicated that rough riboflavin had obvious function of preventing cancerization[9].

5 Morphometry Research of Esophageal Carcinoma

At the first time of esophageal cellular research, microscope micrometer was used to measure the nuclear dimension of hyperplasia cells and made quantification to different hyperplasia grades. In 1990, Professor Zhang *et al* started a new method. Using computer image texture analysis and correlation grid methods, different texture features of normal mucosa, atypical hyperplasia epithelia and carcinoma *in situ* of human esophagus were observed. The texture measures and the data of correlation grid test showed significant difference between severe atypical hyperplasia epithelia and carcinoma *in situ*. The computer image texture analysis might correctly distinguish atypical hyperplasia in esophageal precancerous change from carcinoma *in situ*. With double-blind detection, the accuracy of this technique reached above 90%. This method might have affirmative practical value in the early diagnosis of esophageal carcinoma[10].

6 Relationship between Langerhans Cells and Esophageal Carcinoma

Langerhans cells (LC) were members of dendritic cells (DC). They were successively found in epidermis and other squamous cells covered mucosa, such as oral cavity, pharynx, larynx, rectum, cervix and vagina. They inlayed among ker-

atinocytes and were not able to be found with HE stain. While, with ATPase cellular chemistry or immunohistochemistry of S-100 and OKT6, their morphous could be clearly observed. The main function of them was to present antigens to T lymphocytes. There were Fc-receptors, C3b and immune associated antigen (Ia antigen) on the surface of LC. LC could be classified into 6 types according to their different dendrites.

From 1990, Zhang took the lead in observing the morphous, distribution, and quantity of LC with ATPase (+), S-100 (+), OKT6 (+) in esophageal lesions. Conclusions were made as follows: the expression of S-100 and OKT6 decreased as the lesion progressed, least ATPase positive LC were found in severe atypical hyperplasia epithelia, and most were found in carcinoma *in situ*. Most LC in normal mucosa had less but long and obvious dendrites. While the dendrites became more but shorter in severe atypical hyperplasia epithelia and in carcinoma. LC mainly distributed in the lower layers of normal epithelia, but appeared anywhere in carcinoma *in situ*. At the same time, LC were found to be close to T-lymphocytes and cancer cells. All of the above indicated that different subtypes of LC took part in the progress of esophageal carcinoma[11].

Combining the observation of HPV infection and LC' change, it was found that HPV infection decreased the quantity of LC, which might cooperate with other carcinogens and worked in the progress of esophageal carcinoma[12].

7 Relationship between Apoptosis and Esophageal Carcinoma

With TUNEL technique and immunohistochemistry, apoptosis was found to be related to differentiation of esophageal carcinoma. Change of ICE protein could be an indicator of early cancerization. Cisplatin could induce apoptosis of Eca-109 cells, and DNA degradation was the important change during apoptosis[13].

8 Immunohistochemical Markers of Esophageal Carcinoma

More than 20 targets had been involved in this research and 4 of them would be briefly mentioned.

8.1 P53 protein

The research indicated that 60.0% of carcinoma presented P53 protein stain positive, while 42.9% – 66.7% of atypical hyperplasia epithelia and carcinoma *in situ* presented P53 protein stain positive. The positive rate of P53 protein staining was related to the differentiation, infiltration and metastasis of esophageal carcinoma[14].

8.2 P16 protein

The positive rate of P16 protein staining decreased in the order of normal mucosa, atypical hyperplasia epithelia and cancer tissue, and it decreased as differentiation became poorer[15].

8.3 nm23-H1

In the adjacent non-cancerous mucosa, the positive rate of nm23-H1 staining decreased as the lesion became poorer; in the cancerous tissue, the poorer the lesion was, the lower the positive rate of nm23-H1 staining was; and it was the lowest in lymph node metastasis cases[16].

8.4 GST-π

The positive rate of GST-π staining was relatively high in normal and simple hyperplasial epithelia, while it decreased in atypical hyperplasia epithelia and cancer tissues. The result indicated that GST-π was early enzymologic change of esophageal carcinoma[17].

9 Molecular Biology and Therapy on Esophageal Carcinoma

9.1 p53 gene

With PCR-SSCP silver staining, mutation of exon 5, 6, 7, 8 of p53 gene could be observed. It was found that 32.5% cases presented p53 gene mutation, and the mutation rate of lymph node metastasis group was obviously higher than that of non-metastasis group, suggesting that mutation of p53 gene might contribute to the development of esophageal carcinoma.

9.2 p16 gene

Through observing the mutation of p16 gene in adjacent non-cancerous mucosa and in cancer tissue, it was found that the mutation rate was 27.5% in cancerous mucosa and no mutation occurred in adjacent non-cancerous mucosa. Meanwhile, the mutation rate decreased as differentiation became poorer and it increased as adventitia infiltration and lymph node metastasis happened[18].

9.3 GSTs isoenzyme gene

Through RNA dot blot hybridization, it was found that transcriptional level of GST gene was higher in cancer tissue. GST-π was active form of GSTs isoenzyme in esophageal carcinoma. Altofrequency of positive GST-π might indicate its important role in the process of esophageal carcinoma.

9.4 Telomerase activity and targeted therapy of esophageal carcinoma by antisense oligodeoxynucleotide

Applying TRAP-ELASA quantitative analysis and TRAP silver staining, telomerase activity was respectively detected in cancer tissues, atypical

hyperplasia tissues and normal esophageal mucosa. With *in situ* hybridization, expression of catalytic subunit hTR mRNA of telomerase was detected. With Southern blot and chemiluminescence methods, the length of the telomere was measured. 5 synthetic ASODN with different blocked gene locus were respectively transfected into esophageal cancer cells, and then the cells were subcutaneously planted to nude mice. By this way, the apoptosis induced by ASODN and its inhibitory effect on cell proliferation could be directly observed. All results indicated that activation of telomerase was an early event of tumorigenesis in esophagus and ASODN-t3 could induce apoptosis of tumor cells through inhibiting telomerase activity[19].

9.5 DNA polymerase β gene (polβ)

Professor Dong was the first to do systemic study on mutation of polβ in esophageal carcinoma[20]. With RT-PCR, SSCP and sequence analysis, polβ was studied in cancer tissues and adjacent non-cancerous mucosa. It could be seen that mutation rate of polβ was as high as 44% in cancer tissues, while it was only 4% in adjacent non-cancerous mucosa. So such conclusion could be made that mutation of polβ was related to progression of esophageal carcinoma.

9.6 Screening and identification of esophageal cancer associated gene

With mRNA differential display and suppression subtractive hybridization (SSH), three esophageal cancer associated genes 3y59, c57 and ECAG1 were found in specimens from high-incidence areas. Through homology search in GenBank, no identical genes were found. They all had been registered in GenBank. The work is going on[21].

9.7 Relationship between heparanase and infiltration, metastasis of esophageal carcinoma

It was proved that heparanase was able to destroy extracellular matrix (ECM) and basement membrane (BM) and played some roles in cancerous angiogenesis, infiltration and metastasis. But the definite relationship and mechanism was unclear. To find the answer, with the guidance of Professor Zhang, the following studies had recently been finished:

A. 54 cases of specimens were obtained from high-incidence areas. With *in situ* hybridization and RT-PCR, expression of heparanase was detected respectively in cancer tissues, atypical hyperplasia of adjacent non-cancerous mucosa and normal mucosa of the above 54 specimens. It was found that the protein and mRNA expression of heparanse was related not only to metastasis but also to infiltration depth of esophageal carcinoma[22,23].

B. With RT-PCR, the expression of heparanse in peripheral blood lymphocytes of patients with esophageal cancer was detected. The study suggested that the level of hepatanase expression was higher in group with metastasis than that in group without metastasis. The result indicated that expression of heparanse in peripheral blood lymphocytes, to some extent, could reflect the metastatic state of esophageal carcinoma[24].

C. Using antiesense oligodeoxynucleotide technique, ASODN of different concentration were transfected into EC9706, and then the expression of protein and mRNA of heparanase was detected. It was found that heparanase ASODN could weaken the infiltrative and metastatic ability of cancer cells by inhibiting the expression of heparanase[25].

D. Expression of heparanase in nude mice transplanted tumor indicated that hepatanase ASOND could inhibit the expression of heparanase *in vivo*, which confirmed the above conclusion.

9.8 Expression of differentiation-related gene NDRG Ⅰ and differentiation-induced therapy

Discovered in 1997, NDRG Ⅰ (N-myc downstream regulated gene Ⅰ) was a kind of gene which was related to differentiation. It always presented low expression in many tumors. Until now, no article reported about NDRG Ⅰ expression in esophageal carcinoma. Recently, using molecular biological tech and IHC, we studied on expression of NDRG Ⅰ mRNA and protein in normal esophageal mucosa, atypical hyperplasia and cancer tissues. Differentiation-induced therapy was involved, too. The study indicated that phorbol ester, ratinoic acid, Vit D_3 and sodium butyrate could induce the expression of NDRG Ⅰ in esophageal cancer cells, which showed us a new clue for gene therapy of esophageal carcinoma[26,27].

Based on hard work of more than 40 years, we have made some progresses in the field of esophageal carcinoma. At present, we have built Henan Key Laboratory of Tumor Pathology, and a lot of young doctors have been trained to be eligible researchers. Although there still are a lot of problems to deal with in this field, we are deeply convinced that we will have a bright future.

Acknowledgment

During 40 years of the research, a lot of staff members showed their devotions. The authors would like to express sincere thanks to predecessors for their preliminary studies and to the young generation for their hard works. We are grateful to leaders at different levels for their moral encourage-

ment and financial support. We also would like to express heartfelt thanks to the patients and medical workers in high-incidence areas for their warm assistance.

Correspondence to:
Yunhan Zhang
Henan Key Laboratory of Tumor Pathology
Pathological Department of the First Affiliated Hospital of Zhengzhou University
Zhengzhou, Henan 450052, China
Telephone: 86-371-6665-8175
Email: yhzhang@zzu.edu.cn

References

1. Shen Q, Qiu SL, Zhang YH, *et al*. The study of exfoliative cytology on esophagus. Henan Medical College Journal 1966;23:4-9.
2. Shen Q, Qiu SL, Zhang YH, *et al*. Early cytological diagnosis of esophageal carcinoma. Henan Medical College Journal 1966;23:10-2.
3. Shen Q, Qiu SL, Zhang YH, *et al*. The use of exfoliative cytology in clinical diagnosis and mass surveys for cancer of the esophagus. China's Medicine 1967; 6:479-84.
4. Qiu SL, Shen Q, Zhang YH, *et al*. Pathology of early esophageal squamous cell carcinoma. Chinese Medical Journal 1977;3(3):180-92.
5. Liu GT, Miao J, Zhen YZ, *et al*. The progress of research on the carcinogenicity of fungi in the esophagus in Henan Province, China. Journal of Henan Medical University 1988;2:4-11.
6. Liu GT, Qian YZ, Zhang P, *et al*. Etiological role of Alternaria alternata in human esophageal cancer. Chinese Medical Journal 1992; 105(5):394-400.
7. Hu ZL, Chang KL, Yen CX, *et al*. Virus-like particles in cytoplasm and vermicellar bodies in nuclei of epithelial cell from patients with esophageal carcinoma. Ultrastructural Pathology 1986; 10(5):459-61.
8. Chang F, Shen Q, Zhou J, *et al*. Detection of Human papilloma virus DNA in cytologic specimens derived from esophageal precancerous lesions and cancer. Scand Journal Gastroenterology 1990; 25(4):383-8.
9. Shen Q, Wang DY, Xiang YY, *et al*. The research report of preventive treatment on precancerous hyperplasia of esophagus using rough riboflavin. Chinese Journal of Clinical Oncology 1994; 21(4):250-1.
10. Zhang YH, Huang CZ, Zhang SM, *et al*. The study of computer texture analysis of atypical hyperplasia epithelia and carcinoma *in situ* of human esophagus. Journal of Henan Medical University 1993; 28(3):199-203.
11. Zhang YH, Zhang SM, Gao DL, *et al*. The quantitative observation of the relation between Langerhans cells and pathogenesis of esophageal carcinoma. Henan Medical Research 1993; 2(3):193-7.
12. Li J, Zhang YH, Gao DL, *et al*. Study on the interrelationship between human papilloma virus infection and Langerhans cell in carcinogenesis of esophagus. Chinese Journal of Pathology 1996; 25(2):83-5.
13. Deng LY, Zhang YH, Xu P, *et al*. Expression of interleukin Ⅰβ converting enzyme in 5-Fu induced apoptosis in esophageal carcinoma. World Journal of Gastroenterology. 1999; 5(1):50-2.
14. Wang YH, Zhang YH, Gao DL, *et al*. Expression of P53 protein in carcinogenesis of human esophageal squamous cell carcinoma. Journal of Henan Medical University 1995; 30(3):215-8.
15. Wang J, Zhang YH, Li YN, *et al*. Alteration of P16 protein expression in the carcinogenesis of esophageal squamous cell carcinoma. Journal of Henan Medical University 1997; 32(3):28-30.
16. Zhao GF, Zhang YH, Gao DL, *et al*. Expression of nm23-H1 during the carcinogenesis and development of human esophageal squamous cell carcinoma. Journal of Henan Medical University 1997; 32(3):65-7.
17. Fu BJ, Zhang YH, Wang YH, *et al*. Expression of GST-π gene in human esophageal carcinoma. Chinese Journal of Cancer Research 1999; 11(4):264-6.
18. Wang J, Zhang YH, Fu BJ, *et al*. Detection of mutation of p16 tumor-suppressing gene in esophageal squamous cell carcinoma. Journal of Henan Medical University. 1997; 32(2):30-3.
19. Zhang L, Geng L, Zhang YH, *et al*. Effect on cell proliferation and telomerase activity of esophageal carcinoma EC9706 cells transfected by ASODN blocking different human telomerase RNA sites. Journal of Zhengzhou University(Medical Science) 2006; 41(3):406-9.
20. Dong ZM, Zheng NG, Wu JL, *et al*. Difference in expression level and localization of DNA polymerase beta among human esophageal cancer focus, adjacent and coresponding normal tissues. Dis Esophagus 2006;19(3):172-6.
21. Zhang YH, Yin ZR, Wen HT, *et al*. Screening and identification of esophageal cancer associated gene. Journal of Henan Medical University 2001; 36(5):519-21.
22. Chen KS, Zhang L, Zhang YH, *et al*. Expression of heparanase gene in esophageal carcinoma tissue with different depth of infiltration. Journal of Zhengzhou University (Medical Science) 2004; 39(2):176-8.
23. Chen KS, Tang L, Zhang YH, *et al*. Relation between heparanase mRNA expression and metastasis of esophageal carcinoma. Journal of Zhengzhou University (Medical Science) 2004; 39(2):179-81.
24. Chen KS, Zhang YH, Gao DL, *et al*. Expression of heparanase gene in peripheral blood lymphocytes of patients with esophageal cancer. Journal of Zhengzhou University (Medical Science) 2003; 38(6):908-10.
25. Chen KS, Zhang L, Tang L, *et al*. Expression of heparanase mRNA in human esophageal cancer EC9706 cells transfected by antisense oligodeoxynucleotide. World Journal Gastroenterology 2005; 11(31):4916-7.
26. He FC, Zhang L, Gao DL, *et al*. Expression of NDRG Ⅰ mRNA and protein in esophageal squamous cell carcinoma tissue. Journal of Zhengzhou University 2006; 41(3):395-8.
27. He FC, Zhang YH, Gao DL, *et al*. The protein expression of NDRG Ⅰ in esophageal squamous cell carcinoma and its relationship with clinical pathologic factors. Life Science Journal 2006; 3(1):18-22.

Received July 2, 2006

Expressions of C-erbB2 and C-myc in Esophageal and Gastric Cardia Multistage Carcinogenesis from the Subjects at High-risk Area in Linxian, Northern China

Lidong Wang[1], Xiaoshan Feng[1,2], Bin Liu[3], Yanrui Zhang[4], Yongjie Lu[1], Yongmin Bai[1], Zongmin Fan[1], Xin He[1], Changwei Feng[5], Shanshan Gao[1], Jilin Li[6], Xinying Jiao[6], Fubao Chang[7]

1. Henan Key Laboratory for Esophageal Cancer; Laboratory for Cancer Research, Basic Medical College; The First Affiliated Hospital of Zhengzhou University, Zhengzhou, Henan 450052, China

2. Department of Oncology, The First Affiliated Hospital of Henan Science and Technology University, Luoyang, Henan 471001, China

3. Department of Gastroenterology, Tongren Hospital, Capital Medical University, Beijing 100013, China

4. Department of Gastroenterology, Henan Provincial People's Hospital, Zhengzhou, Henan 450003, China

5. Department of Gastroenterology, The Second Affiliated Hospital, Zhengzhou University, Zhengzhou, Henan 450014, China

6. Department of Pathology, Linzhou Esophageal Cancer Hospital, Linzhou, Henan 456500, China

7. Department of Surgery, Linzhou Center Hospital, Linzhou, Henan 456500, China

Abstract: Linxian and nearby counties in Henan Province, northern China have been well-recognized as the highest incidence area for both esophageal squamous cell carcinoma (SCC) and gastric cardia adenocarcinoma (GCA). The molecular mechanism for SCC and GCA is largely unknown. Recent studies indicate that aberrations of DNA copy numbers at 8q and 17p in which the genes of C-myc and C-erbB2 reside, are very common events in SCC and GCA from the patients in Linxian. The present study was undertaken to characterize the changes of C-erbB2 and C-myc in protein level on the subjects with different esophageal and gastric cardia precancerous and cancerous lesions from Linxian. In the study, 144 samples were collected, including 30 SCC and 30 GCA from Linxian Esophageal Cancer Hospital and 84 biopsies from symptom-free subjects (16 cases with normal esophageal epithelia (ENOR), 34 with esophageal basal cell hyperplasia (BCH), 8 with esophageal dysplasia (EDYS), 7 with normal gastric cardia epithelia (GNOR), 6 with chronic superficial gastritis (CSG), 10 with chronic atrophic gastritis (CAG), and 3 with gastric cardia dysplasia (GDYS)). The avidin-biotin-peroxidase complex (ABC) method was performed for the expression of C-erbB2 and C-myc. No immunoreactivity was observed for C-erbB2 in normal esophagus, BCH and EDYS. However, 50% of SCC was positive for C-erbB2 immunostaining. In contrast, positive immunostaining for C-myc was observed in normal esophageal epithelia and different lesions. With lesions progressed from ENOR-EDYS-SCC, the positive immunostaining rates for C-myc increased apparently. In gastric cardia, positive immunoreactivity for both C-erbB2 and C-myc was observed in normal gastric cardia epithelia and different lesions. With the lesions progressed from GNOR-CSG-CAG-GDYS-GCA, an apparent increasing tendency was observed for both C-erbB2 and C-myc. In gastric cardia multistage carcinogenesis, the positive immunostaining rate for C-erbB2 and C-myc was much higher than in esophagus. The present results demonstrate that the immunostaining patterns for C-erbB2 and C-myc are different between esophageal and gastric cardia carcinogenesis from the population at same high-risk area in Linxian. Overexpression of both C-erbB2 and C-myc is a common event in gastric cardia multistage carcinogenesis, which may be a promising early biomarker for gastric cardia carcinogenesis. C-erbB2 may be a late event for esophageal carcinogenesis. [Life Science Journal. 2006;3(3):6-12] (ISSN: 1097-8135).

Keywords: squamous cell carcinoma; gastric cardia adenocarcinoma; precancerous lesion; C-erbB2; C-myc

Abbreviations: BCH: basal cell hyperplasia; CAG: chronic atrophic gastritis; CGH: comparative genomic hybridization; CSG: chronic superficial gastritis; EC: esophageal carcinoma; EDYS: esophageal dysphasia; ENOR:

normal esophageal epithelium; GDYS: gastric cardia dysphasia; GCA: gastric cardia adenocarcinoma; GNOR: normal gastric cardia epithelium; SCC: esophageal squamous cell carcinoma

1 Introduction

Linxian and nearby counties in Henan, northern China have been well-recognized as the highest incidence areas for esophageal squamous cell carcinoma (SCC)[1], and gastric cardia adenocarcinoma (GCA) seems to occur together with SCC in these areas[2] and in other countries[3]. SCC and GCA have a very poor prognosis and remain the leading cause of cancer-related death in Linxian. In clinic, more than 80% of the patients with SCC and GCA are diagnosed at late stage in these areas, whose five-year survival rates are less than 10%. In contrast, the five-year survival rates for the early SCC and GCA are more than 90%[4]. Apparently, early detection and high-risk subject screening is of great importance in decreasing the mortality rate for SCC and GCA. The early indicator for the subjects predisposed to SCC and GCA is the epithelial cell hyperproliferation, morphologically, manifested as basal cell hyperplasia (BCH), dysplasia (DYS) and carcinoma *in situ* (CIS) in esophagus[5] and chronic atrophic gastritis (CAG) with intestinal metaplasia (IM), DYS and CIS in gastric cardia[6]. All or part of these lesions could be considered as precancerous lesions for SCC and GCA[2]. These lesions are unstable, i.e., they may progress to more severe type, or stay in the same stage for long time, or return to less severe type, even to normal, which is difficult to explain based on morphological changes only[7]. Thus it becomes crucial to characterize the molecular changes in the early stage of SCC and GCA carcinogenesis to identify the biomarker for high-risk subject screening and early diagnosis. However, the underlying key molecular changes for multistage carcinogenesis of SCC and GCA are largely unknown.

Recent studies with comparative genomic hybridization (CGH) demonstrate that aberrations in DNA copy number at chromosome 8q and 17q, in which the genes of C-myc and C-erbB2 reside, are frequently observed in SCC and GCA tissues from the patients in Linxian[8]. C-myc, an oncogene, belongs to a family of nuclear phosphoproteins. Myc family of proteins influences the expression of around 10% of all human genes[9]. The expression of C-myc protein is an important factor in cell proliferation via activating the cell division cycle gene cdc25A, the product of which catalyses the dephosphorylation of the cyclin-E / cyclin dependent / kinase 2c (CDK2) complex[10]. The expression of C-myc also induces apoptosis via interaction with a number of apoptotic pathways[11]. Amplification of C-myc both in mRNA and protein level has been found frequently in SCC[11-13], especially in advanced stages of SCC. Antisense myc gene introduced into esophageal cancer cell line (EC8712) is capable of inhibiting cell proliferation and malignancy[14]. Evidence for the expression of C-myc in GCA is very limited. Luo *et al* reported a 62% of positive immunostaining for C-myc in sporadic GCA from Chinese people[15]. But, the expression pattern of C-myc is largely unknown both in esophageal and gastric cardia precancerous lesion.

The C-erbB2 (HER-2/neu) oncoprotein is a 185-kDa transmembrane receptor[16]. Over expression of C-erbB2 has been found not only in breast and ovarian, but also in gastric and many other human cancers[17]. The C-erbB2 amplification has been known as independent predictor for neoplastic recurrence and overall survival rate[18,19]. The accumulated evidences indicate that C-erbB2 aberrant expression occurs more frequently in primary esophageal adenocarcinoma, but not in SCC[20-22]. The expression pattern for C-erbB2 in gastric cardia carcinogenesis is not clear. To define whether C-myc and C-erbB2 is the target gene in multistsge carcinogenesis of SCC and GCA at 8q and 17q aberrations as indicated by CGH from the SCC and GCA patients at Linxian, the highest incidence area for both SCC and GCA in northern China, the present study was undertaken to characterize C-myc and C-erbB2 expression in both esophageal and gastric cardia multistage carcinogensis from the patients at same high incidence areas for both SCC and GCA in Linxian, northern China.

2 Materials and Methods

2.1 Endoscopic examination and biopsy

Esophageal endoscopic examination and biopsy were performed on 84 symptom-free subjects who volunteered to participate in a routine endoscopic screening for esophageal cancer (EC) in Linxian, the highest incidence area for EC in Henan Province, northern China. No selection process was involved. Of these subjects, there were 45 males (35 – 71 years of age with a mean ± SD of 51 ± 10 years) and 39 females (32 – 71 years of age with a mean ± SD of 49 ± 11 years). Esophageal endoscopic examination was performed with Olympus GIF-V70 (Olympus Com., Japan).

Esophageal biopsies were taken from each subject at the middle third of the esophagus (30 – 32 cm from incisor teeth). Gastric cardia biopsies were taken within 2 cm lower from the esophageal and gastric cardia junction. Additional biopsies were taken when there were macroscopic lesions. The biopsy specimens were fixed in 85% alcohol, embedded in paraffin, and sectioned at 5 μm.

2.2 SCC and GCA specimen collection and processing

A total of 30 surgically resected primary SCC specimens (52 – 72 years of age with a mean ± SD of 56 ± 11 years) and 30 surgically resected primary GCA specimens (50 – 71 years of age with a mean ± SD of 53 ± 10 years) were collected from Linxian Esophageal Cancer Hospital from October to December, 2005. All the patients had received neither chemotherapy nor radiotherapy before surgery. All the tissues were fixed with 85% alcohol, embedded with paraffin, and sectioned at 5 μm. Five adjacent ribbons were collected for histopathologic and immunohistochemical analysis.

2.3 Histopathological analysis

Histopathological diagnosis for esophageal epithelia was made based on the changes in cell morphology and tissue architecture using previously established criteria[2]. In brief, the normal esophageal epithelium contained one to three proliferating basal cell layers; the papillae were confined to the lower half of the whole epithelium thickness. In BCH, the proliferating basal cells surpassed 15% of the total epithelial thickness. Dysplasia was characterized by nuclear atypia (enlargement, pleomorphism, and hyperchromasia), loss of normal cell polarity, and abnormal tissue maturation. SCC was characterized by confluent and invasive sheets of cohesive, polymorphous cells with hyperchromatic nuclei. The following histopathological classification was used for the gastric cardia epithelia: chronic superficial gastritis (CSG), inflammation manifested by mild lymphocyte and plasma cell infiltration; chronic atrophic gastritis (CAG), glandular morphology disappeared partially or completely absent in the mucosa and replaced by connective tissue, interglandular space infiltrated mainly by plasma cells and lymphocytes; gastric cardia dysplasia (GDYS), neoplastic features including nuclear atypia and /or architectural abnormalities confined to the gastric cardia epithelium, without invasion; gastric cardia adenocarcinoma (GCA), invasion of neoplastic gastric cells through the basement membrane[6].

2.4 Immunohistochemical staining

Anti-C-erbB2 antibody is a monoclonal mouse antiserum against the human C-erbB2 (DAKO, Carpinteria, CA, USA). Anti-C-myc antibody is a polyclonal rabbit antiserum against human C-myc (Oncogene Science, Manhasset, NY, USA). The avidin-biotin-peroxidase complex (ABC) method was used for the immunostaining of C-erbB2 and C-myc. In brief, after dewaxing, inactivating endogenous peroxidase activity and blocking cross-reactivity with normal serum (Vectastain Elite Kit; Vector, Burlingame, CA, USA), the sections were incubated overnight at 4 ℃ with a diluted solution of the primary antibodies (1:200 for C-erbB2 and 1:150 for C-myc). Location of the primary antibodies was achieved by subsequent application of a biotinylated anti-primary antibody, an avidin-biotin complex conjugated to horseradish peroxidase, and diaminobenzidine (Vectastain Elite Kit, Burlingame, CA, USA). Normal serum blocking and omission of the primary antibodies were used as negative controls. Clear nuclear staining was the criterion for a positive reaction of C-myc. C-erbB2 positive immunoreactivity was localized at cytoplasm.

2.5 Statistical analysis

The χ^2 test was used for the percentage of lesions with positive immunostaining. Spearman correlation test and linear tendency test were used for the correlation between positive rates and different severities of the lesions ($P < 0.05$ was considered significant).

3 Results

3.1 Histopathological findings

Of the 84 biopsies, 58 esophageal mucosa and 26 gastric cardia mucosa were identified, respectively. Histopathological examination showed that, of the 58 esophageal biopsies, 16 biopsies were identified with normal epithelia (ENOR) (28%), 34 with esophageal basal cell hyperplasia (BCH) (59%), 8 with esophageal dysphasia (EDYS) (13%). In 26 gastric cardia biopsies, there were 7 biopsies identified with normal gastric cardia epithelia (GNOR) (27%), 6 with chronic superficial gastritis (CSG) (23%), 10 with chronic atrophic gastritis (CAG) (36%), 3 with gastric cardia dysplasia (GDYS) (11%). Histopathologically, all the surgically resected esophageal specimens were confirmed as SCC, and all the gastric cardia cancer specimens were confirmed as GCA.

3.2 Immunohistochemical staining for C-myc and C-erbB2

In esophagus (Table 1): positive immunoreactivity for C-myc was observed both in esophageal precancerous and cancerous lesions (Figure 1). With the lesions progressed from BCH-EDYS-

SCC, the positive immunostaining rate for C-myc increased. A good correlation between the C-myc positive staining rate and lesion progression was observed ($P < 0.05$). However, the positive immunoreactivity for C-erbB2 was identified only in SCC (Figure 2). All the normal esophagi and the precancerous lesions were negative for C-erbB2 expression.

Table 1. Immunoreactivity of C-erbB2 and C-myc in esophageal multistage carcinogenesis*

Histological types	C-erbB2		C-myc**	
	Cases of samples examined	Samples with positive staining (n (%))	Cases of samples examined	Samples with positive staining (n (%))
ENOR	12	0 (0)	16	1 (6)
BCH	34	0 (0)	14	3 (21)
EDYS	8	0 (0)	4	1 (25)
SCC	30	15 (50)	27	16 (59)

* Part of the slide tissue lost during the immunohistochemistry processing. ** BCH *vs*. EDYS, $P<0.05$ (χ^2 test).

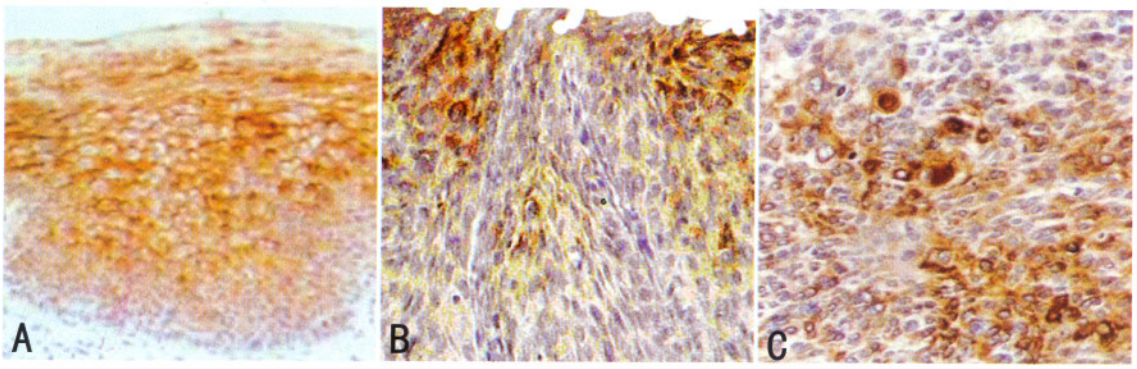

Figure 1. Microphotograph for C-myc immunostaining in esophageal basal cell hyperplasia (A: ×200), dysphasia (B: ×200) and squamous cell carcinoma (C: ×200). Immunoreactivity is mostly located in the nuclia. The positive cells were invariably associated with cell proliferative activity.

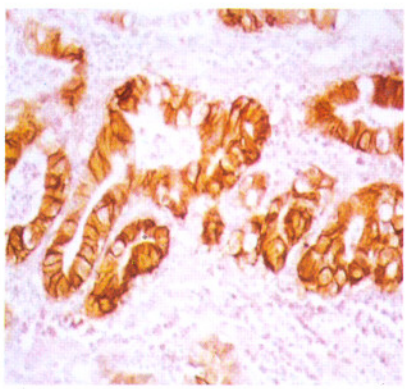

Figure 2. Microphotograph for C-erbB2 immunostaining in esophageal squamous cell carcinoma. Immunoreactivity is mostly located in the cytoplasm and cell membrane. The positive cells are in variably associated with cell proliferative activity (×400).

In gastric cardia (Table 2): positive immunoreactivity for both C-myc and C-erbB2 was observed in gastric cardia precancerous and cancerous lesions (Figure 3 and Figure 4). The positive immunostaining rate apparently increased with the lesions progressed from CSG-CAG-GDYS-GCA. The positive immunostaining rate for C-erbB2 and C-myc was very low in normal gastric cardia epithelia, and increased significantly in EDYS and GCA ($P<0.05$).

It was noteworthy that the positive immunostaining rate for C-erbB2 and C-myc in gastric cardia multistage carcinogenesis was higher than in esophageal carcinogenesis. Furthermore, the "diffuse" immunostaining pattern in C-erbB2 was predominant in gastric cardia carcinogenesis, in contrast, the "focal" immunostaining pattern was frequently observed in esophageal carcinogenesis.

Table 2. Immunoreactivity of C-erbB2 and C-myc in gastric cardia carcinogenesis*

Histological types	C-erbB2		C-myc**	
	Cases of samples examined	Samples with positive staining (n (%))	Cases of samples examined	Samples with positive staining (n (%))
GNOR	7	2 (9)	5	2 (40)
CSG	6	5 (83)	5	4 (80)
CAG	10	9 (90)	6	5 (83)
GDYS	3	3 (100)	2	2 (100)

* Part of the slide tissue lost during the immunohistochemistry processing. ** Normal *vs*. CAG, Normal *vs*. GCA, $P<0.05$.

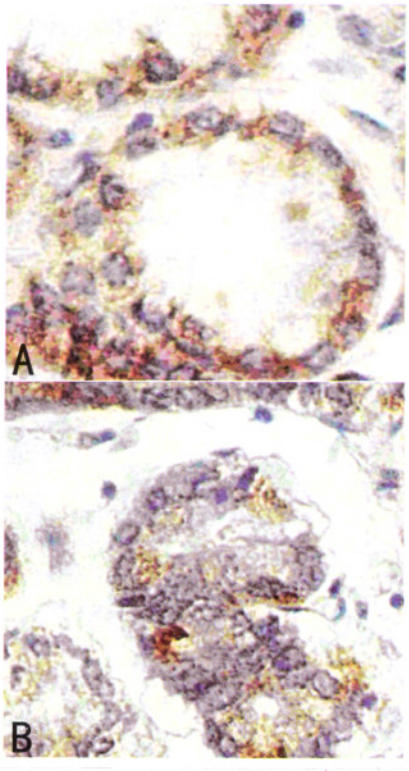

Figure 3. Microphotograph for C-myc immunostaining in gastric cardia dysphasia (A: ×400) and chronic atrophic gastritis (B: ×400). Immunoreactivity is mostly located in the nuclia. The positive cells are in variably associated with cell proliferative activity.

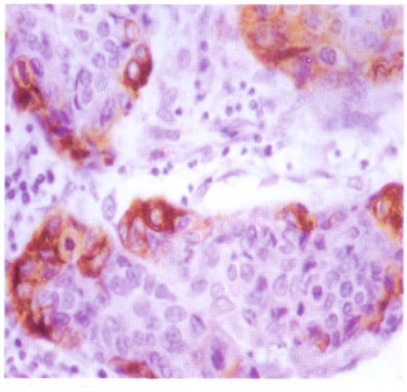

Figure 4. Microphotograph for C-erbB2 immunostaining in gastric cardia adenocarcinoma. Immunoreactivity is mostly located in the cytoplasm and cell membrane. The positive cells are in variably associated with cell proliferative activity (×200).

4 Discussion

The present study demonstrates that over-expression of C-erB2 and C-myc is a very early frequent event in gastric cardia multistage carcinogenesis. These aberrant protein expressions are well correlated with gastric cardia epithelial lesion progressions, suggesting that C-erbB2 and C-myc may play an important role in gastric cardia multistage carcinogenesis. These results are consistent with our CGH work[4], indicating that CGH is a good technique in narrowing down the scope for identifying the key related genes with cancers. The present results also indicate that C-erbB2 and C-myc aberrant expression may be a promising early biomarker to predict the gastric cardia carcinogenesis. The recent studies by our group and other laboratories have showed that autoantibodies to C-myc could be detected through cancer patient's blood serum, including esophageal and gastric cardia cancers, and could increase the early detection of these cancers[23-27].

An interesting result in this study is that aberrant C-erbB2 expression occurs only in SCC, none in normal esophagus and esophageal precancerous lesions, suggesting that C-erbB2 may be a late event for esophageal carcinogenesis. Accumulated evidences have demonstrated that aberrant C-erbB2 expression occurs more frequently in adenocarcinoma, e.g. in GCA and Barrett's esophagus-related esophageal adenocarcinoma, not in SCC[20]. These different expression patterns may be related with the different tissue types occurring of tumor cells, which could explain the different immunostaining patterns observed in GCA and SCC for C-erbB2 and C-myc in this study.

Many studies suggest that tumor occurring and progression are the result of a multistage and progressive process which may be related with the deactivity of tumor suppressor gene and the activity of the tumor oncogene in different stages. The present studies demonstrate that, in the multistage progression of the esophageal carcinogenesis, there is few expression of C-erbB2 in the early stage but some in SCC; however, the overexpression of C-myc is positive during the esophageal multiple carcinogenesis, suggesting the possibility of multiple genetic changes involved in esophageal carcinogenesis.

Historically, EC and GCA have been considered as a single clinical entity for incidence and mortality-rate calculations in Linxian because of the common syndrome of dysphagia[28]. The similar geographic distributions of SCC and GCA in China suggest that there may be similar risk factors and genetic changes involved in these two cancers. GCA is an under-studied subject. The molecular changes in the early stage of GCA carcinogenesis have not been characterized. There is evidence, however, that GCA differs from cancer of the rest of stomach in terms of time trend, risk factors and histopathogenesis[29]. Because of the common occurrence both of SCC and GCA in Henan, it is of great interest to know whether the molecular changes observed in SCC also occur in GCA. The

present results demonstrate that the aberrant expressions of C-erbB2 and C-myc occur similarly in SCC and GCA, however, the immunostaining pattern for C-erbB2 and C-myc in precancerous lesions of the esophagus and gastric cardia is different, especially in C-erbB2. The significance of these observations needs to be further analyzed.

Acknowledgment

We are grateful to the helps of Drs. Tao Guo, Shaohua Li, Weina Liu, Xianjuan Du and Hui Fan in preparation of the manuscript.

This work was supported in part by: National Outstanding Young Scientist Award of China 30025016 and Foundations of Henan Education and Health Committees of China.

Correspondence to:
Lidong Wang, M.D., Ph.D.
Henan Key Laboratory for Esophageal Cancer; Laboratory for Cancer Research; Basic Medical College
Zhengzhou University
Zhengzhou, Henan 450052, China
Telephone and Fax: 86-371-6665-8335
Email: ldwang@zzu.edu.cn

References

1. Yang CS. Research on esophageal cancer in China: a review. Cancer Res 1980; 40: 2633－44.
2. Wang LD, Shi ST, Zhou Q, *et al*. Changes in p53 and cyclin D1 protein levels and cell proliferation in different stages of human esophageal and gastric-cardia carcinogenesis. Int J Cancer 1994; 59: 514－9.
3. Victor T, Du Toit R, Jordan AM, *et al*. No evidence for point mutations in codons 12, 13, and 61 of the ras gene in a high-incidence area for esophageal and gastric cancers. Cancer Res 1990; 50: 4911－4.
4. Wang LD, Zheng S, Zheng ZY, *et al*. Primary adenocarcinomas of lower esophagus, esophagogastric junction and gastric cardia: in special references. World J Gastroenterol 2003; 9:1156－64.
5. Wang LD, Qiu SL, Yang GR, *et al*. A randomized double-blind intervention study on the effect of calcium supplementation on esophageal precancerous lesions in a high-risk population in China. Cancer Epidemiol Biomarkers Prev 1993; 2: 71－8.
6. Wang LD, Zhou Q, Yang CS. Esophageal and gastric cardia epithelial cell proliferation in northern Chinese subjects living in a high-incidence area. J Cell Biochem Suppl 1997; 28－29: 159－65.
7. Wang LD, Zhou Q, Feng CW, *et al*. Intervention and follow-up on human esophageal precancerous lesions in Henan, northern China, a high-incidence area for esophageal cancer. Gan To Kagaku Ryoho 2002; 29:159－72.
8. Wang LD, Qin YR, Fan ZM, *et al*. Comparative genomic hybridization: comparison between esophageal squamous cell carcinoma and gastric cardia adenocarcinoma from the patients at high-incidence area for both esophageal and gastric cardia cancers in Henan, northern China. Dis Esophagus 2006 (in press).
9. Shervington A, Cruickshanks N, Wright H, *et al*. Glioma: What is the role of C-myc, hsp90 and telomerase? Mol Cell Biochem 2006; 283: 1－9.
10. Zornig M, Evan G. Cell cycle: on target with Myc. Curr Biol 1996; 6: 1553－6.
11. Packham G, Cleveland J. C-myc and apoptosis. Biochim Biophys Acta 1995; 1242: 11－28.
12. Bitzer M, Stahl M, Arjumand J, *et al*. C-myc gene amplification in different stages of esophageal squamous cell carcinoma: prognostic value in relation to treatment modality. Anticancer Res 2003; 23: 1489－93.
13. Sarbia M, Arjumand J, Wolter M, *et al*. Frequent C-myc amplification in high-grade dysplasia and adenocarcinoma in Barrett esophagus. Am J Clin Pathol 2001; 115: 835－40.
14. Ye X, Wu M. Retrovirus mediated transfer of antisense human C-myc gene into human esophageal cancer cells suppressed cell proliferation and malignancy. Sci China B 1992; 35: 76－83.
15. Luo B, Wang Y, Wang XF, *et al*. Correlation of Epstein-Barr virus and its encoded proteins with Helicobacter pylori and expression of c-met and C-myc in gastric carcinoma. World J Gastroenterol 2006; 12: 1842－8.
16. Akiyama T, Sudo C, Ogawara H, *et al*. The product of the human c-erbB-2 gene: a 185-kilodalton glycoprotein with tyrosine kinase activity. Science 1986; 232: 1644－6.
17. James T. C-erbB2 oncoprotein and its soluble ectodomain: a new potential tumor marker for prognosis early detection and monitoring patients undergoing Herceptin treatment. Clin Chim Acta 2002; 322: 11－9.
18. Slamon DJ, Clark GM, Wong SG, *et al*. Human breast cancer correlation of relapse and survival with amplification of the HER-2/c-erbB-2 oncogene. Science 1987; 235: 177－81.
19. Kyrgidis A, Kountouras J, Zavos C, *et al*. New molecular concepts of Barrett's esophagus: clinical implications and biomarkers. J Surg Res 2005; 125: 189－212.
20. Bahnassy AA, Zekri AR, Abdallah S, *et al*. Human papillomavirus infection in Egyptian esophageal carcinoma: correlation with p53, p21, mdm2, C-erbB2 and impact on survival. Pathol Int 2005; 55: 53－62.
21. Trudgill NJ, Suvarna SK, Royds J A, *et al*. Cell cycle regulation in patients with intestinal metaplasia at the gastro-oesophageal junction. Mol Pathol 2003; 56: 313－7.
22. Suo Z, Holm R, Nesland JM. Squamous cell carcinomas, an immunohistochemical and ultrastructural study. Anticancer Res 1992; 12: 2025－31.
23. Du F, Wang LD, Qi YJ, *et al*. Detection of multiple serum autoantibody in the subjects with esophageal and gastric cardia precancerous and cancerous lesion using tumor-associated antigens mini-array. Chin J Cancer Prev Treat 2006 (in press in Chinese).
24. Zhang JY, Chan EK, Peng XX, *et al*. A novel cytoplasmic protein with RNA-binding motifs is an autoantigen in human hepatocellular carcinoma. J Exp Med 1999; 189: 1101－10.

25. Zhang JY, Wang X, Peng XX, *et al*. Autoantibody responses in Chinese hepatocellular carcinoma. J Clin Immunol 2002; 22: 98－105.
26. Megliorino R, Shi FD, Peng XX, *et al*. Autoimmune response to anti-apoptotic protein surviving and its association with antibodies to p53 and C-myc in cancer detection. Cancer Detect Prev 2005; 29: 241－8.
27. Wang ZQ, Wang LD. DNA methylation and esophageal squamous cell carcinoma: special reference to research in China. Life Science Journal 2006;3(2):1－11.
28. Li JY. Epidemiology of esophageal cancer in China. Monogr Natl Cancer Inst 1982; 62: 113－20.
29. Wang HH, Antonioli DA, Gao HK, *et al*. Comparative features of esophageal and gastric adenocarcinomas. Hum Pathol 1986; 17: 482－7.

Received June 25, 2006

Expression of MMP-2 and MMP-9 and Its Correlation with Invasion and Metastasis in Human Esophageal Squamous Cell Carcinoma

Hongtao Wen[1], Lei Zhang[2], Qiumin Zhao[3], Jichang Li[1]

1. *Department of Gastroenterology, The First Affiliated Hospital of Zhengzhou University, Zhengzhou, Henan 450052, China*
2. *Department of Oncology, The First Affiliated Hospital of Zhengzhou University, Zhengzhou, Henan 450052, China*
3. *Editorial Board of Journal of Zhengzhou University (Medical Sciences), Zhengzhou, Henan 450052, China*

Abstract: Objective. To investigate the significance of MMP-2 mRNA and MMP-9 mRNA expression in human esophageal squamous cell carcinoma (ESCC). **Methods.** MMP-2 mRNA, MMP-9 mRNA and proteins were examined by immunohistochemistry, *in situ* hybridization, RT-PCR, zymographic analysis and Western blot for 41 cases of ESCC. **Results.** The expression rate and value of MMP-9 was significantly higher than that of MMP-2 in tumor tissues. **Conclusions.** MMP-9 has higher sensitivity and specificity in predicting the biologic behavior of invasion and metastasis in ESCC. [Life Science Journal. 2006;3(3):13-18] (ISSN: 1097-8135).

Keywords: MMP-2; MMP-9; esophageal carcinoma; invasion; metastasis

Abbreviations: BM: basement membrane; ECM: extracellular matrix; ESCC: esophageal squamous cell carcinoma; MMP: matrix metalloproteinase; PAGE: polyacrylamide gel electrophoresis; SDS: sodium dodecyl sulfate; TBS: Tris-HCl buffered saline

1 Introduction

Esophageal carcinoma is one of the most common cancers and acts as the fourth leading cause of cancer death in China. It is characterized by poor prognosis and rapid clinical progression with a high frequency of lymph node metastasis and recurrence. The transition from *in situ* to invasive tumors is a very complicated process. Proteolysis of extracellular matrix (ECM) is essential step in tumor invasion and metastasis. Numerous proteolytic enzymes including the matrix metalloproteinase (MMP) have been implicated in this process. Reports showed that both MMP-2 and MMP-9 were highly expressed in esophageal tumor tissues[1,2]. In the current study, MMP-2 mRNA and MMP-9 mRNA and their proteins were examined by immunohistochemistry, *in situ* hybridization, RT-PCR, zymographic analysis and Western blot in 41 cases of ESCC as well as the matched normal mucosa tissues, to compare the potential value of MMP-2 and MMP-9 in estimation of the biologic behavior of ESCC.

2 Materials and Methods

2.1 Tissue samples

41 specimens of patients with esophageal squamous cell caricinoma were collected from the First Affiliated Hospital of Zhengzhou University and the Henan Tumor Hospital. All of them were identified by pathology. The resected specimens including the ESCC samples and the normal adjacent tissues were snap-frozen in liquid nitrogen.

2.2 Immunohistochemistry

Specimens were fixed with 10% neutral buffered formaldehyde solution and embedded in low-melting paraffin. Sections of esophageal tumors were immunostained with monoclonal antibodies to MMP-2 and MMP-9. Immunohistochemistry for the individual MMP was performed by an alkaline phosphatase anti-alkaline phosphatase technique. After the immunohistochemistry, the sections were examined under microscope. The MMP status of the tumors was assessed as positive if any of the tumor cells showed significant immunostaining. Negative controls were done by replacing the primary antibody with TBS and by liquid phase pre-absorp-

tion of primary antibody with the corresponding immunogen at 10 nmol/ml antibody. The positive controls for both MMP-2 and MMP-9 were lung containing intra-alveolar macrophages.

2.3 *In situ* hybridization

In situ hybridization was performed on sections (4 μm). After deparaffinization and rehydration all samples were treated with proteinase K and washed in 0.1 M triethanolamine buffer containing 0.25% acetic anhydride. Sections were hybridized overnight at 50 ℃ to 55 ℃ with ^{35}S-labelled RNA probe. After hybridization, slides were washed under stringent conditions and treated with RNase to remove unhybirdized probe. Previously positive samples for each anti-sense probe were used as positive controls. The slides were independently assessed by two experienced investigators.

2.4 RT-PCR

Total RNA was extracted from shock-frozen tissue samples with RNA extract kit. First strand complementary DNA was synthesized from 2 μg of DNA-free total RNA in a 20 μl system of: 1 mmol/L dNTP; 10 U RNAsin; 20 mmol/L DTT; 1 μmol Random Hexamer Primer and 100 U MM-LV. Follow the procedure of 37 ℃ 10 min, 42 ℃ 1 hour and 95 ℃ for 5 min. PCR was done in a 50 μl system including both MMP and β-actin primers. The annealing temperatures of MMP-9 and MMP-2 were 66 ℃ and 65 ℃, respectively. Raw data from each samples, were quantified using the eagle eye system (Stratagene, American). Data from MMP cDNA were normalized to the respective content of β-actin cDNA. T/N>2.0 was recognized as positive.

2.5 Zymographic analysis

Equal amounts of total lysates of esophageal tissue samples were used for determining protein amounts with the Bio-Rad DC protein assay kit and stored at −20 ℃ until assayed. MMP activity in the lysates was assessed by gelatin zymography: lanes were loaded with 2 μg of total protein each. The concentrated media were run on nonreducing sodium dodecyl sulfate (SDS)-polyacrylamide gel (10%) containing 1 mg/ml gelatin. After electrophoresis in 25 mM Tris base, 250 mM glycine, and 1% SDS, the gel was washed at room temperature in solution (2.5% Triton X-100, 5 mM $CaCl_2$, 50 mM Tris-HCl, pH 7.5), and was incubated again in the same buffer twice for 1 hour each. After rinsing the gel extensively with six changes of distilled water, it was incubated overnight at 37 ℃ in 5 mM $CaCl_2$ and 50 mM Tris-HCl, pH7.5, followed by Coomassie blue staining and destaining in solution of methanol, acetic acid and water(50:10:40). Gelatin zymography depicts MMP as negatively staining bands of gelatinolytic activity.

2.6 Western blot

Tissue lysates were separated by SDS-PAGE using separating gels and stacking gels of 3% polyacrylamide. Lane was loaded with 2 μg of total protein each. After electrophoresis, the proteins were transferred to PVDF membrane. Protein bands were localized by staining with Ponceau S. Blots were blocked with Tris-buffered saline-NaCl, pH 7.6, containing 10% bovine serum albumin, 20 mM Tris, 137 mM NaCl, and 0.1% Nonidet P40; washed; blocked with 10% milk and incubated with antibodies against MMP-2 or MMP-9. Experiments were done in triplicate. The bands were scanned by computer analysis. Data from all tissue samples analyzed were normalized by setting the protein amount in the healthy tissue to 1.0 in each sample[3].

2.7 Statistical analysis

The SPSS statistical package program was used for all analysis. Associations between the variables were tested by χ^2 test, Student's t test. $\alpha = 0.05$ were set significant.

3 Results

3.1 Immunohistochemistry

The results revealed that there were 26 cases of positive reaction for MMP-9 in 41 ESCC and 5 cases of positive reaction in matched normal mucosa tissues. The percentage of positive cases in ESCC was significantly higher than that in matched normal mucosa tissues ($P<0.01$). Faint staining was also found in monocyts, fibroblasts, endothelial and smooth muscle cells. Positive reaction for MMP-9 showed a tendency to be stronger in deeply invading nests, especially in peripheral fronts. On the contrary, MMP-2 levels were lower and positive reaction in carcinoma cells was generally weaker than that in stromal cells. There were distinct difference between the MMP-9 and MMP-2 expression in ESCC ($P<0.01$) (Table 1, Figure 1 and Figure 2).

Table 1. Expressions of MMP-2 and MMP-9 by immunohistochemistry

MMP type	Cases (n)	Expression	
		Positive cases (n)	Positive rate (%)
MMP-9	41	26	63.41
MMP-2	41	7	17.07

$P<0.01$

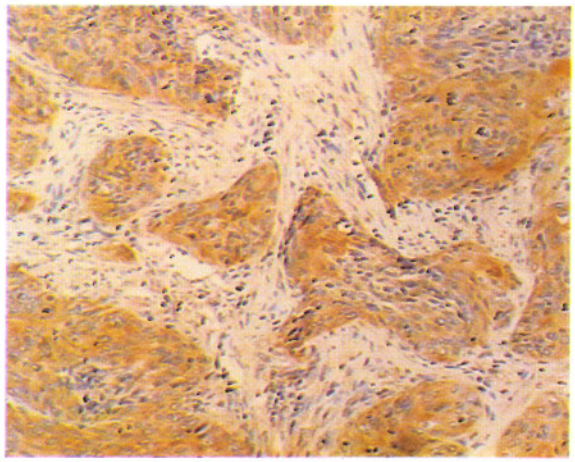

Figure 1. Detection of MMP-9 protein in ESCC by immunohistochemical staining SP×200

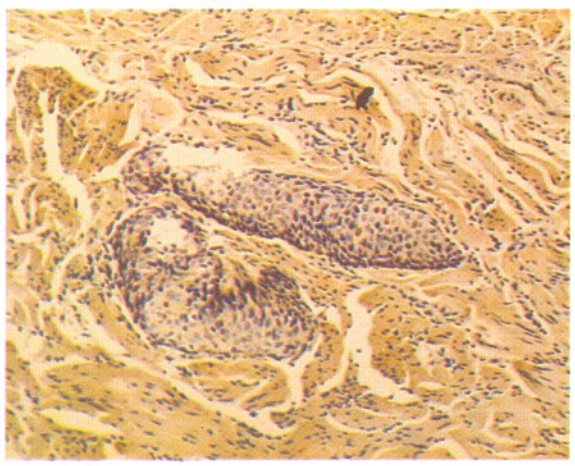

Figure 2. Detection of MMP-2 protein in ESCC by immunohistochemical staining SP×200

3.2 *In situ* hybridization

The results revealed that there were 22 cases of positive reaction for MMP-9 mRNA in 41 ESCC and 5 cases of positive reaction in matched normal mucosa tissues. The percentage of positive cases in ESCC was significant higher than that in matched normal mucosa tissues ($P<0.01$). Faint staining was also detected in macrophages, fibroblasts, endothelial and smooth muscle cells but stronger staining was observed in plasmacytes. Positive reaction for MMP-9 mRNA showed a tendency to be stronger in deeply invading nests, especially in peripheral fronts. On the contrary, MMP-2 levels were lower and positive reaction in carcinoma cells was generally weaker than that in stromal cells. There was distinct difference between the MMP-9 mRNA and MMP-2 mRNA expression in ESCC ($P<0.01$) (Table 2, Figure 3 and Figure 4).

Table 2. Expressions of MMP-2 mRNA and MMP-9 mRNA by *in situ* hybridization

MMP type	Cases (n)	mRNA expression	
		Positive case (n)	Positive rate (%)
MMP-9	41	22	53.66
MMP-2	41	4	9.76

$P<0.01$

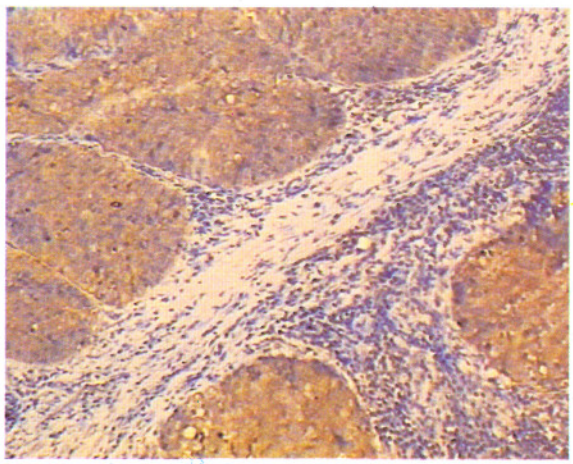

Figure 3. Detection of MMP-9 mRNA in ESCC by *in situ* hybridization×200

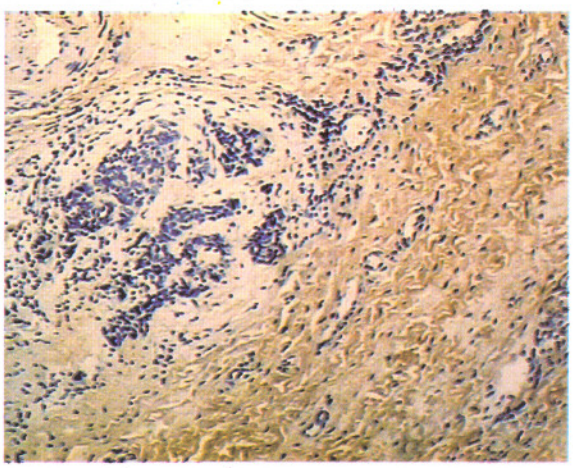

Figure 4. Detection of MMP-2 mRNA in ESCC by *in situ* hybridization×200

3.3 RT-PCR

RT-PCR inspect showed that the positive rate and semi-quantitative value of MMP-9 mRNA were 80.49% (33/41) and 0.57 ± 0.43 in ESCCs, respectively. The positive rate and the semi-quantitative value of MMP-2 mRNA were 58.54% (24/41) and 0.21 ± 0.21 in ESCC, respectively. The positive rate and the semi-quantitative value of MMP-2 mRNA were distinctly lower than those of MMP-9 mRNA ($P<0.05$, $P<0.01$) (Table 3, Figure 5 and Figure 6).

Table 3. Expressions of MMP-2 and MMP-9 mRNA by RT-PCR

MMP type	Cases (n)	mRNA expression		
		Positive case (n)	Positive rate(%)	Absorbance value
MMP-9	41	33	80.49#	0.57±0.44*
MMP-2	41	24	58.54#	0.21±0.21*

#: *vs*. MMP-9, $P<0.05$; *: *vs*. MMP-9, $P<0.01$

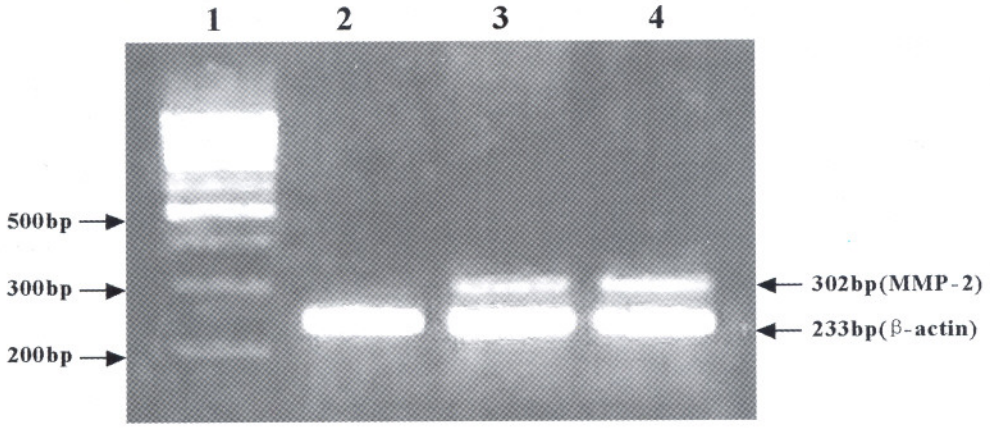

Figure 5. Detection of MMP-2 mRNA in ESCC, tissue adjacent to tumor and matched mormal mucosa tissue by RT-PCR
Lane 1: Marker; Lane 2: normal tissue; Lane 3: tissue adjacent to tumor; Lane 4: ESCC

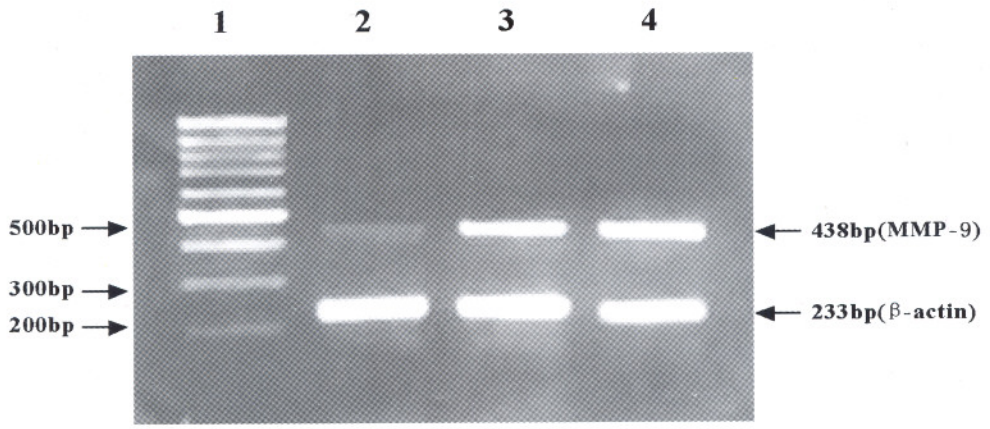

Figure 6. Detection of MMP-9 mRNA in ESCC, tissue adjacent to tumor and matched mormal mucosa tissue by RT-PCR
Lane 1: Marker; Lane 2: normal tissue; Lane 3: tissue adjacent to tumor; Lane 4: ESCC

3.4 Zymographic analysis

By zymographic analysis, there were small amount secretions of proMMP-9 (92 kD) and proMMP-2(72 kD) in matched normal mucosa tissues. The activated MMP-2(62 kD) was detected in 31 biopsy specimens, but no activated MMP-9 (82 kD) could be found. The semi-quantitative values of proMMP-9, activated MMP-2 and proMMP-2 in ESCC were 2.52±0.75, 1.92±0.42 and 1.51±0.42, respectively. There were distinct differences between proMMP-9 and activated MMP-2 ($P<0.01$), proMMP-9 and proMMP-2 ($P<0.01$). The activated MMP-9 could be detected in 24 biopsy specimens (Figure 7).

3.5 Western blot

By Western blot analysis, the semi-quantitative values of MMP-9 and MMP-2 in ESCC were 3.02±0.56 and 2.26±0.51, respectively. There were distinct differences between MMP-9 and MMP-2($P<0.05$) (Figure 8).

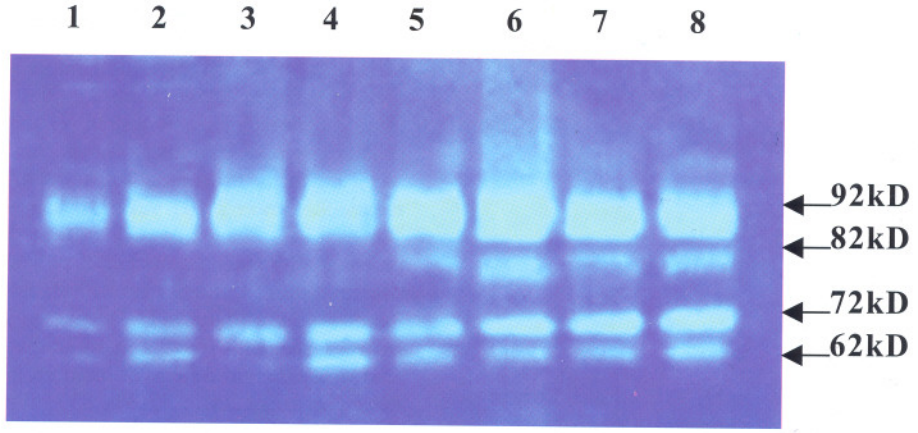

Figure 7. Detections of MMP-2, MMP-9 in ESCC and matched normal mucosa tissues by zymographic analysis
Lane 1: standard of collagenase IV; Lane 2 – 4: normal tissues; Lane 5 – 8: ESSC

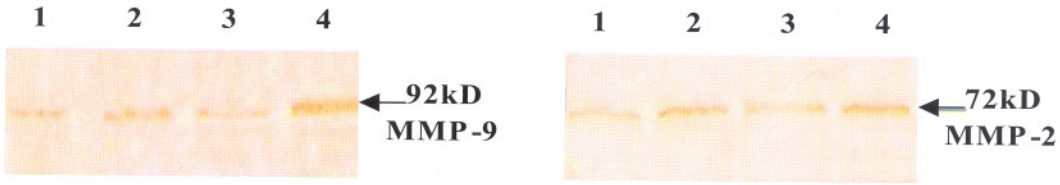

Figure 8. Detections of TIMP in ESCC by Western blot
Lane 1, 3: matched normal mucosa tissues; Lane 2, 4: ESSC

4 Discussion

Matrix metalloproteinase (MMP) is a family of Zn^{2+} metalloproteinase, involved in degradation of the extra cellular matrix macromolecules. They have been classified into four classes based on substrate specificities such as collagenases, gelatinases, stromelysins and membrane-type MMP. Collagenases, gelatinases and stromelysins are solubale while membrane-type metalloproteinsaes attach to the surface of the cell[4]. MMP-2 and MMP-9 are capable of cleaving basement membrane type Ⅳ collagen, but their enzymatic activity is far greater against gelatins, hence they are often referred to as gelatinases. MMP-2 and MMP-9 are also responsible for further degradation of the large 3/4 and 1/4 collagen fragments and other proteins including fibronectin, laminin, and elastin[5]. Reports showed that both MMP-2 and MMP-9 played an important role in tumor invasion and metastasis[6-9].

In the current study, MMP-2 mRNA, MMP-9 mRNA and their proteins were examined by immunohistochemistry, *in situ* hybridization, RT-PCR, zymographic analysis and Western blot for 41 cases of ESCC as well as matched normal mucosa tissues, in order to compare the potential value of MMP-2 and MMP-9 in estimation of the biologic behavior of ESCC. Our results showed that the expression rate and semi-quantitative value of MMP-9 was significantly higher than those of MMP-2 in tumor tissues, which suggested that MMP-9 had higher sensitivity in predicting the biologic behavior of invasion and metastasis in ESCC.

Most of MMP are secreted as inactive zymogens (proMMPs), and extracelluar activation mechanisms are required for their function. Through separating the Zn^{2+} and cysteine, the Zn^{2+} active center are exposed. Activation of MMP shows waterfall effect[10]. Zymographic analysis is a special technique to detect the activity of MMP by polyacrylamidedel electrophoresis (PAGE), which can differentiates proenzyme and activated enzyme and detects a group of MMP with identical substrate at the same time. It has the behavior of convenient and susceptible[11].

In our study, there was small amount of secretion of proMMP-9 (92 kD) and proMMP-2 (72 kD) in all 41 cases of normal mucosa tissues. The activated MMP-2 (62 kD) was detected in 31 biopsy specimens, but no activated MMP-9 (82 kD) was found. Also, the expression of proMMP-9 was significantly higher than both proMMP-2 and activated MMP-2 in ESCC tissues. The activated MMP-9 could be detected in 24 biopsy specimens of all 41 cases of ESCC tissues. All these strongly suggested that MMP-9 has higher sensitivity and specificity in predicting the biologic behavior of in-

vasion and metastasis in ESCC.

Correspondence to:
Hongtao Wen
Department of Gastroenterology
The First Affiliated Hospital
Zhengzhou University
Zhengzhou, Henan 450052, China
Telephone: 86-371-6516-9173
Email: wenhongtao68@163.com

References

1. Suzuki T, Kuwabara Y, Iwata H, *et al*. Role of matrix metalloproteinase-9 in *in vitro* invasion of esophageal carcinoma cells. J Surg Oncol 2002; 81:80 – 6.
2. Yu Y, Zhou Y, Miao X, *et al*. Functional haplotypes in the promoter of matrix metalloproteinase-2 predict risk of the occurrence and metastasis of esophageal cancer. Cancer Res 2004;64:7622 – 8.
3. Roeb E, Dietrich CG, Winograd R, *et al*. Activity and cellular origin of gelatinases in patients with colon and rectal carcinoma differential activity of matrix metalloproteinase-9. Cancer 2001; 92:2680 – 91.
4. Kahari VM, Saarialho-Kere U. Matrix metalloproteinases and their inhibitor in tumor growth and invasion. Ann Med 1999; 31: 34 – 5.
5. Zucker S, Cao J, Chen WT. Critical appraisal of the use of matrix metalloproteinase inhibitors in cancer treatment. Oncogene 2000; 19,6642 – 50.
6. Roeb E, Dietrich CG, Winograd R, *et al*. Activity and cellular origin of gelatinases in patients with colon and rectal carcinoma differential activity of matrix metalloproteinase-9. Cancer 2001; 92(10):2680 – 91.
7. Wu X, Li H, Kang L, *et al*. Activated matrix metalloproteinase-2-a potential marker of prognosis for epithelial ovarian cancer. Gynecol Oncol 2002; 84(1): 126 – 34.
8. Nordqvist AC, Smurawa H, Mathiesen T. Expression of matrix metalloproteinases 2 and 9 in meningiomas associated with different degrees of brain invasiveness and edema. J Neurosurg 2001; 95(5): 839 – 44.
9. Scorilas A, Karameris A, Arnogiannaki N, *et al*. Overexpression of matrix-metalloproteinase-9 in human breast cancer: a potential favourable indicator in node-negative patients. Br J Cancer 2001; 84(11): 1488 – 96.
10. Murphy G, Stanton H, Cowell S, *et al*. Mechanisms for pro matrix metalloproteinase activation. APMIS 1999; 107: 38 – 44.
11. Kleiner DE, Stetler-Stevenson WG. Quantitative zymography: detection of picogram quantities of gelatinases. Anal Biochem 1994; 218: 325 – 9.

Received June 26, 2006

Expression of Cathepsin B and Its Relationship with Esophageal Squamous Carcinoma

Kuisheng Chen[1,2], Zhihua Zhao[1], Miaomiao Sun[1,2], Xin Lou[1,2], Dongling Gao[1,2]

1. Department of Pathology, The First Affiliated Hospital of Zhengzhou University, Zhengzhou Henan 450052, China

2. The Key Laboratory of Tumor Pathology of Henan, Zhengzhou, Henan 450052, China

Abstract: Objective. To explore the relations between expression of Cathepsin B (CB) and development, invasion and metastasis of esophageal squamous cell carcinoma. **Methods.** The expression of CB protein and of CB mRNA were determined by immunihistochemitry and *in situ* hybridization. **Results.** CB protein expression and CB mRNA expression couldn't be detected in normal esophageal mucosa, while positive in matastatic group and non-metastatic group. CB protein expression and CB mRNA expression was significantly decreased. The out layer invasion group, rate of CB protein expression and CB mRNA expression in the tumor tissues and atypical hyperplasia in tumor-adjacent tissues was significantly elevated compared with low-muscle invasion group and deep-muscle invasion group. The positive rates was slightly higher in deep-muscle invasion than in low-muscle invasion without statistical significance. The positive rates of CB protein expression and of CB mRNA expression in the carcinoma tissues were significantly higher than atypical hyperplasia tissues in both the metastatic and non-metastatic group. **Conclusion.** CB protein expression and CB mRNA expression in human esophageal squamous cell carcinoma were increased, which indicated that CB is related to the development, invasion and metastasis of esophageal carcinoma [Life Science Journal. 2006;3(3):19-24] (ISSN: 1097-8135).

Keywords: esophageal squamous cell carcinoma; Cathepsin B; invasion; metastasis

Abbreviations: CB: Cathepsin B

1 Introduction

Invasion and metastasis of tumor is a complicated process, in which the relationship of extracellular matrix and metastasis of tumor is extremly close. A series of dynamic change develop between tumor cells and extracellular matrix. There are a lot of enzymes released that degrade the extracellular matrix and facilitate the invasion and metastasis of tumor cells[1]. It is known that Cathepsin B (CB) is a lysosomal cysteine proteinase that can degrade laminin, fibronectin, Ⅳ type collagen and so on the extracellular matrix, and participating in the invasion and metastasis of tumor cells. In recent years, the research discovered that CB showed an obivious increase in varieties of malignant tumors such as prostate carcinoma, melanocytoma, cancinoma of colon and so on. It also participates in the invasion and metastasis of tumor. While both domestic and foreign scholors haven't carried out the research for CB and its relationship with invasion and metastasis of esophageal carcinoma. This research adopted the technique of immunohistochemistry and *in situ* hybridization, to investigate CB expression and its relationship with the development, invasion and metastasis of esophageal carcinoma.

2 Materials and Methods

2.1 Materials

2.1.1 Reagents

CB immunohistochemiscal SP kit was provided by Wuhan Boster Biological Technology Company; SA-AP and BCIP/NBT were from American Promera corporation; CBcDNA probe with 5 teminal biotin marked (5′-GTTGACCAGCTCATCCGACAGG-3′) was synthesized by Beijing Oker Biological Technology Limited Corporation.

2.1.2 Specimens

Forty-nine fresh samples of human esophageal carcinoma were obtained from oncological hospital of Anyang and the First Affiliated Hospital of Zhengzhou University. These samples were all confirmed by pathology as squamous cell carcinoma. There were 49 cases, 25 males and 24 females, with median age 58.3±17.8 years old (from 40.5 years old to 76.1 years old).

According to lymphotic metastasis: metastatic group (20 cases) and non-metastatic group (29 cases); according to the depth of invasion: low-muscle group (10 cases), deep-muscle group (15 cases) and out layer group (24 cases); according to development: esopheal carcinoma group (49 cases), atypical hyperplasia of tumor-adjacent group (30 cases) and normal group (49 cases).

2.2 Methods

2.2.1 Specimen preparation

The tissues of carcinoma, atypical hyperplasia of tumor-adjacent and normal tissues obtained were formalined-fixed and paraffin-embeded respectively for immunohistochemistry and *in situ* hybridization.

2.2.2 Immunohistochemistry

Paraffin sections were de-paraffined routinely, rinsed in PBS 3 times for 5 min each. Under the high pressure, samples were treated with 0.01 mol/L Citrate Tris-sodium for 15 min. Samples were rinsed 3 times with PBS for 5 min each, and blocked by serum for 30 min, to remove non-specific staining. Then drop wise 1:100 rabbit antihuman CB antibody was added and incubated at 4 ℃ overnight. The next day sections were taken for 30 min at room temperature, rinsed with PBS 3 times for 5 min each. So did the secondary antibody and the tertiary antibody. After the following DAB staining, hematoxylin staining, samples was dehydrated and mounted. PBS replaced the primary antibody in the negative control slices.

2.2.3 *In situ* hybridization

Paraffin sections were deparaffined to water routinely, and performed in 3% hydrogen peroxide for 30 min at room temperature for blocking endogenous peroxidase activity. Sections were rinsed with H_2O 3 times for 5 min each time and digested for 20 min with pepsin to expose mRNA nuclear section, rinsed once with H_2O for 5 min, fixed with 1% formalin / 0.1 M PBS (pH 7.2 – 7.6, contain 0.1% DEPC) for 10 min at room temperature. Rinsed by H_2O 3 times for 5 min each time, and dropwised 20 μl /slice hybridization solution. The sections were set in 20% glyerine to prehybridize for 3 – 4 h at 42 ℃ dropwise 20 μl labeled probe added to specimen, then coved paraffin membrane to hybridize for 12 – 16 h at 42 – 43 ℃. The next day, sections were dropwised with 0.1 × SSC for 4 times for 15 min each time to elute non-specific hybridization. Sections were processed with 1% acetylatel BSA for 10 min at 20 ℃. Sections were in Streptavdin Alkaline Phoshates (SA-AP) for 20 min at 37 ℃, Tris-HCl buffer I 3 times for 10 min each, and Tris-HCl buffer Ⅱ 2 times for 1 min. Sections were dropwised BCIP/NBT (33 μl NBT and 16.5 μl BCIP added to 5 ml buffer Ⅱ) substrate solution freshly, stained in the darkness for 10 – 120 min, nuclear fast red after stained for a few min, neutral gum mounted, prehybridization solution without probe hybridized and before hybridization specimens were processed as negative control by RNase.

The results were judged according to Naoki method[3]. Positive cells accout for 0% for (–), 0 – 20% for (±), 20 – 80% for (+), 80% for (+ +), (–) and (±) were set as negative, (+) and (+ +) were positive.

2.2.4 Statistical analysis

All the data were analyzed by spass 10.0 system. Comparison between positive rates adopted chi-square test (χ^2-test).

3 Results

3.1 CB protein expression and CB mRNA expression in esophageal carcinoma tissues, atypical hyperplasia tissues and normal tissues

The positive signals of CB protein were localized in cytoplasm or membrane of esophageal carcinoma or atypical hyperplasia cell and showed brown granules. Periphery matrix of carcinoma nest showed positive as well (Figure 1) but not in negative control. Positive signals of CB mRNA was localized in cytoplasm of esophageal carcinoma or atypical hyperplasia cells and showed blue granules (Figure 2). Normal esophageal mucosa cells couldn't be stained. No positive signals appeared in the negative control.

3.2 Relationships of CB and esophageal carcinoma metastasis

3.2.1 Relationship of CB protein and esophageal carcinoma metastasis

In the 20 cases with lymphatic metastasis, the positive rates of expression of CB protein in the tissues of esophageal carcinoma, atypical hyperplasia tissues and normal tissues were 100% (20/20), 60% (6/10) and 0% (0/20), respectively; while in the 29 cases without lymphatic metastasis, the the positive rates CB protein expression in the esophageal carcinoma tissues, atypical hyperplasia tissues and normal tissues were 62.07% (18/29), 10% (2/20) and 0% (0/29), respectively. The difference of CB had statistical significance (carcinoma tissues group *vs*. normal tissues group, $P < 0.01$; atypical hyperplasia group *vs*. normal tissues group, $P < 0.01$). Table 1 showed the details.

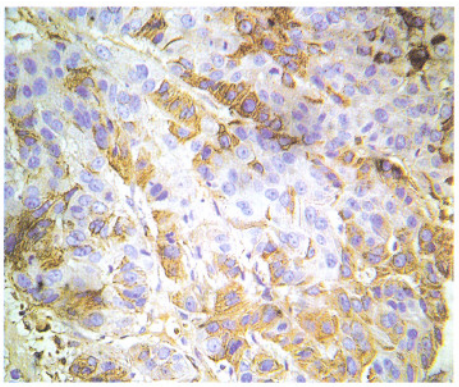

Figure 1. Immunohistochemical staining of esophageal squamous carcinoma (×400)

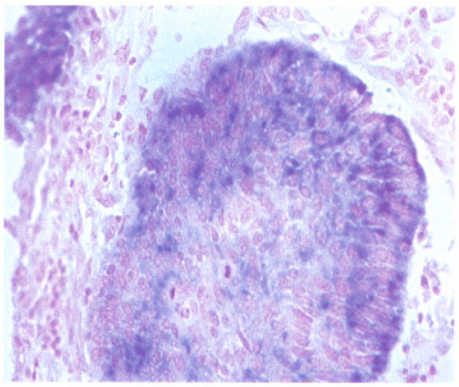

Figure 2. *In situ* hybridization staining of esophageal squamous carcinoma (×400)

Table 1. Relationship of CB expression and lymphatic metastasis

Group	Tissues	Cases(n)	Positive cases(n)	Positive rate (%)
Metastatic group	Tissues of carcinoma	20	20	100
	Tissues of tumor-adjacent	10	6	60
Non-metastatic group	Tissues of carcinoma	29	18	62.07
	Tissues of tumor-adjacent	20	2	10

Note: comparison of CB mRNA expression in carcinoma tissues between two groups: $\chi^2=9.782$, $P=0.000$; comparison of CB mRNA expression in atypical hyperplasia tissues between two groups: $\chi^2=8.523$, $P=0.004$

3.2.2 Relationship of CB mRNA expression and esophageal carcinoma metastasis

In the 20 cases with lymphatic metastasis, the positive rates of CB mRNA expression in esophageal carcinoma tissues, atypical hyperplasia tissues and normal tissues were 95% (19/20), 50% (5/10) and 0% (0/20), respectively; in the 29 cases without lymphatic metastasis, the positive rates of CB mRNA expression in the tissues of esophageal carcinoma, atypical hyperplasia and normal tissues were 55.2% (16/29), 10% (2/20) and 0% (0/29), respectively. The positive rates of CB mRNA in the esophageal carcinoma tissues and atypical hyperplasia between two groups were statistically significant. Table 2 showed the details.

Table 2. Relationship of CB mRNA and esophageal carcinoma metastasis

Group	Tissues	Cases(n)	Positive cases(n)	Positive rate (%)
Metastatic group	Tissues of carcinoma	20	19	95
	Tissues of tumor-adjacent	10	5	50
Non-metastatic group	Tissues of carcinoma	29	16	55.2
	Tissues of tumor-adjacent	20	2	10

Note: comparison of CB mRNA expression in carcinoma tissues between two groups: $\chi^2=9.2$, $P=0.002$; comparison of CB mRNA expression in atypical hyperplasia tissues between two groups: $\chi^2=5.963$, $P=0.015$

3.3 CB protein, CB mRNA and esophageal carcinoma invasion

3.3.1 Relationship of CB protein expression and esophageal carcinoma invasion

In tissues of esophageal aquamous cell carcinoma with low-muscle invasion, deep-muscle invasion and out layer invasion, the positive rates of CB protein were 50% (5/10), 60% (9/15) and 100% (24/24), respectively; in atypical hyperplasia tissues in different invasion depths, the positive rates of CB protein were 0% (0/8), 10% (1/10) and 58.33% (7/12). In the tissues of esophageal carcinoma and atypical hyperplasia of tumor-adjacent with out layer invasion, the positive rates of CB protein was obviously higher than the other two with statistical significance. While in the tissues of esophageal carcinoma and atypical hyperplasia with deep-muscle invasion, the difference of the positive rates of expression of CB protein in comparison with low-muscle invaded wasn't statistically significant ($P>0.05$). Table 3 showed the details.

Table 3. CB protein Expression and esophageal carcinoma invasion

Depth of invasion	Tissues of carcinoma			Tissues of atypical hyperplasia		
	Positive cases(n)	Negative cases(n)	Positive rates(%)	Positive cases(n)	Negative cases(n)	Positive rates(%)
Low-muscle layer[a]	5	5	50	0	8	0
Deep-muscle layer[b]	9	6	60	1	9	10
Out layer[c]	24	0	100	7	5	58.33

Note: tissues of carcinoma: a *vs*. b: $\chi^2=0.244$, $P=0.612$; a *vs*. c: $\chi^2=14.069$, $P=0$; b *vs*. c: $\chi^2=11.345$, $P=0.001$; tissues of tumor-adjacent: a *vs*. b: $\chi^2=0.847$, $P=0.357$; a *vs*. c: $\chi^2=7.179$, $P=0.007$; b *vs*. c: $\chi^2=5.507$, $P=0.019$

3.3.2 Relationship of CB mRNA and esophageal carcinoma invasion

In tissues of esophageal aquamous cell carcinoma with low-muscle invasion, deep-muscle invasion and out layer invasion, the positive rates of CB mRNA were 30% (3/10), 53.33% (8/15) and 95.83% (23/24), respectively; in atypical hyperplasia tissues in different invasion depths, the positive rates of CB mRNA were 0% (0/8), 10% (1/10) and 50% (6/12), respectively. In tissues of esophageal carcinoma and atypical hyperplasia with deep-muscle invasion, the CB mRNA expression was higher compared with low-muscle invasion, but the difference wasn't of statistical significance ($P>0.05$). While CB mRNA expression in the tissues of esophageal carcinoma and atypical hyperplasia with out layer invasion in comparison with the former both, the difference of the positive rates was statisticalLy significant. Table 4 showed the details.

Table 4. CB mRNA and esophageal carcinoma invasion

Depth of invasion	Tissues of carcinoma			Tissues of tumor-adjacent		
	Positive cases(n)	Negative cases(n)	Positive rates(%)	Positive cases(n)	Negative cases(n)	Positive rates(%)
Low-muscle layer[a]	4	6	40	0	8	0
Deep-muscle layer[b]	8	7	53.33	1	9	10
Outer layer[c]	23	1	95.83	6	6	50

Note: tissues of carcinoma: a *vs*. b: $\chi^2=0.427$, $P=0.513$; a *vs*. c: $\chi^2=13.459$, $P=0$; b *vs*. c: $\chi^2=10.226$, $P=0.001$; tissues of tumor-adjacent: a *vs*. b: $\chi^2=0.847$, $P=0.357$; a *vs*. c $\chi^2=5.714$, $P=0.017$; b *vs*. c $\chi^2=4.023$, $P=0.045$

3.4 Relationship of CB protein, CB mRNA and esophageal carcinoma development

Above-mentioned results showed, in the tissues of normal esophageal mucosa, CB protein expression and CB mRNA expression were seldom detected. In the carcinoma tissues of metastatic group, the positive rates of CB protein expression and CB mRNA expression were 100% (20/20), 95% (19/20), respectively. In the matched tissues of tumor-adjacent atypical hyperplasia, the positive rates of CB protein expression and CB mRNA expression were 60% (6/10), 50% (5/10), respectively; in the carcinoma tissues of non-metastatic group, the positive rates of CB protein expression and CB mRNA expression were 62.07% (18/29), 55.2% (16/29) respectively. In the matched tissues of tumor-adjacent atypical hyperplasia, both of the positive rates of CB protein expression and CB mRNA expression were 10% (2/20). The positive rates of CB protein expression and CB mRNA expression were compared to those in the matched tumor-adjacent atypical hyperplasia, with the statistically significant difference ($P<0.01$). Table 5 showed the details.

Table 5. Correlations of CB protein expression, CB mRNA expression and esophageal carcinoma development

Group	Tissues of carcinoma#		Tissues of tumor-adjacent*	
	Expression of protein(%)	Expression of mRNA (%)	Expression of protein (%)	Expression of mRNA (%)
Metastatic group[a]	100.00	95.00	60.00	50.00
Non-metastatic group[b]	62.07	55.20	10	10

Note: #: correlation of a and CB mRNA expression, $r=20.328$, $P=0.000$; *: correlation of b and CB mRNA expression, $r=3.649$, $P=0.01$

3.5 Correlations of CB protein and CB mRNA

In the metastatic group and non-metastatic group, the expression of CB protein and mRNA in the tissues of carcinoma and atypical hyperplasia of tumor-adjacent had positively relative tendency, the difference had statistical significance (carcinoma tissues: $P<0.01$; atypical hyperplasia tissues: $P<0.01$). Table 6 showed the details.

Table 6. Correlations between CB protein expression and of CB mRNA expression

Group	Tissues	Cases (n)	Expression of protein		Expression of mRNA	
			Positive cases(n)	Positive rates	Positive cases(n)	Positive rates
Metastatic group	Tissues of carcinoma	20	20	100.00	19	95.00
	Tissues of tumor-adjacent	10	6	60.00	5	50.00
Non-metastaticgroup	Tissues of carcinoma	29	18	62.07	16	55.2
	Tissues of tumor-adjacent	20	2	10	2	10

Note: correlation of carcinoma tissues and CB mRNA expression: $r=20.328, P<0.01$; correlation of atypical hyperplasia tissues and CB mRNA expression: $r=3.649, P<0.01$

4 Disscusion

The mechanism of tumor is unclear, but it's known that metastasis would lead to worse prognosis. Therefore index, which is relevant to metastasis of tumor has been reseach hot-spot domestically and abroad. Recent years, CB was found to participated in extracelluar matrix and facilitated the metastasis of tumor. Miyake *et al*[5] discovered that in the serum of prostate carcinoma with lymphatic metastasis, the level of CB protein was obviously increased compared to those without lymphatic metastasis; Yu *et al*[6] discovered that the positive rates of expression of CB protein in the tissues of colorectal carcinoma with lymphatic metastasis was also elevated. Xu *et al*[7] determined expression of CB protein and mRNA of hepatoma tissues and found that CB participated in the metastasis of hepatoma.

Experiments may suggest that the highly expressed CB have relationship with the metastasis of prostate cancer, colorectal cancer, and liver cancer, but its relationship with the metastasis of esophageal carcinoma hasn't been reported. This experiment measured the CB protein expression and CB mRNA in the esophageal carcinoma tissues, tumor-adjacent atypical hyperplasia tissues and normal esophageal tissues and explored relationship of CB expression with esophageal carcinoma. Immunohistochemical results demonstrated in 20 cases with the lymphatic metastasis, the positive rates of CB protein expression in the tissues of esophageal carcinoma, tumor-adjacent atypical hyperplasia and normal tissues were 100%, 60% and 0%, respectively; in the 29 cases without lymphatic metastasis, the positive rates of expression of CB protein in the tissues of esophageal carcinoma, tumor-adjacent atypical hyperplasia and normal tissues were 62.07%, 10% and 0%, respectively. CB protein expression in metastasis group was significantly increased in tissues of carcinoma and tumor-adjacent atypical hyperplasia tissues compared with the non-matastasis group. *In situ* hybridization results demonstrated in 20 cases with lymphatic metastasis, the positive rates of CB mRNA expression were 95%, 50% and 0%, respectively; while in non-lyphatic metastasis group, the positive rates of expression of CB mRNA were 55.2%, 6% and 0%, respectively. The difference of the positive rates of CB mRNA expression in the carcinoma tissues and tumor-adjacent atypical hyperplasia tissues between the lymphatic group and non-lymphatic group was statistically significant. Above-mentioned results demonstrated that both CB protein and mRNA have close relationship with the metastasis of esophageal carcinoma.

CB is a lysosomal cysteine proteinase that can degrade the extracellular matrix and facilitate to go through barrier of basement membrane and extracellular matrix, which results in the invasion and metastasis of tumor cells. Accordingly, attentions were paid to the relationship between CB and the invasion of tumor, as well. Ejian *et al*[8] analyzed the tissues of transitional bladder carcinoma by Western blot, and the results demonstrated that the expression of CB protein was higher in invasive type than that in superficial type, which suggested that CB protein expression was related to the invasion of bladder carcinoma; Dohchin *et al*[9] discovered that in the gastric carcinoma tissues with muscle layer invasion, CB protein expression was higher than tissues with the mucosa layer invasion, and relevant to the invasion of gastric carcinoma. This research results demonstrated: in the carcinoma tissues and tumor-adjacent atypical hyperplasia tissues with low-muscle invasion, deep-muscle invasion

and out layer invasion, the positive rates of CB protein expression and CB mRNA expression were both elevated. In the tissues of carcinoma and tumor-adjacent atypical hyperplasia of the out layer invasion, the positive rates of CB protein and CB mRNA were significantly highly expressed significantly comprared with the low-muscle invasion and deep-muscle invasion both. So CB protein expression and CB mRNA expression was related not only to the metastasis but also to the invasion of esophageal carcinoma. Therefore CB may be a marker of invasion and metastasis of tumor cells and at the same time, provided important guidance for clinical therapy to prevent the invasion and metastasis.

Many abroad and domestic studies carried out were on CB and its relationship with the cancer invasion and metastasis of tumor, but seldom on relationship of CB and cancer development. This research observed also explored CB and its relationship with esophageal carcinoma development. Results demonstrated: CB protein and CB mRNA couldn't be detected in normal tissues, while in the lymphatic and non-lymphatic group, the positive rates of expression of CB protein and CB mRNA in the esophageal carcinoma tissues were higher than those in the tumor-adjacent atypical hyperplasia with statistical significance, which demonstrated that CB participated in the development of esophageal carcinoma.

Furthermore, this experiment results suggested, and non-metastatic group, the positive rates of CB protein expression and CB mRNA expression in carcinoma tissues and tumor-adjacent atypical hyperplasia tissues in metastasis group was significantly higher than that in non-metastasis group. This results further showed that except non-metastasis group, the positive rates of CB protein expression was consistent with CB mRNA expression, in carcinoma tissues and in the atypical hyperplasia tissues, but the positive rates of CB mRNA was lower than CB protein. To some extent, investigation of CB by immunohistochemistry was more sensitive than that by *in situ* hybridization.

It was noteworthy of the different location of CB protein positive staining. Positive staining in the tumor-adjacent mucosa and normal mucosa was only in the cytoplasm, while positive staining in the esophageal carcinoma was scattered in the cytoplasm, cellular membrane and peripheral cells. Weiss *et al* injected invasion tumor cell and non-invasion tumor cell to athmic mice respectively, and got the similar results, suggesting that tumor cells secreted CB protein to peripheral matrix, which could degrade the matrix component and facilitated the invasion and metastasis of tumor.

Acknowledgments

This work was supported by the Building Foundation for 211 Key Fields during the 15th Five-year-Plan Period of Miniatry of Education, No. 2002.

Corresponence to
Kuisheng Chen
Department of Pathology
The First Affiliated Hospital of Zhengzhou University; The Key Laboratory of Henan Tumor Pathology
Zhengzhou University
Zhengzhou, Henan 450052, China
Telephone: 86-371-6691-2412
Email: chenksh2002@yahoo.com.cn

References

1. Li MN. Cathepsin B and tumor. Foreign Med Sci Oncol Sect 2005; 32(6): 429-32.
2. Anna M, Szpaderska AM, Frankfater A. An intracellular form of Cathepsin B contributes to invasiveness in Cancer. Cancer Res 2001; 61(8): 3493-500.
3. Naoki F, Atsushi N, Yashitaka T, *et al*. Prognostic impact of Cathepsin B and matrix metalloproteinase-9 in pulmonary adenocarcinomas by immunohistochemical study. Lung Can 2000; 27(1):19-26.
4. Gong Q, Chan Sj, Bajkowski AS, *et al*. Characterization of the Cathepsin B gene and multiple mRNAs in human tissues: evidence for alternative splicing of Cathepsin B pre-mRNA. DNA cell Biol 1993; 12(4):299-309.
5. Miyake H, Hara I, Eto H. Serum level of Cathepsin B and its density in men with prostate cancer as novel markers of disease progression. Anticancer Res 2004; 24(4):2573-7.
6. Yu B, Li SY, An P, *et al*. Expression of Cathepsin B and its clinical importance in colorectal cancer. Chinese Journal of Gastrointestinal Surgery 2005; 8(6):507-9.
7. Xu CL, Huang ZM, Chen MX, *et al*. Expression and effects of Cathepsin B and its mRNA in hepatocelluar carcinoma. Journal of Wenzhou Medical College 2004; 34(6): 414-6.
8. Ejian AM, Sandes EO, Riveros MD, *et al*. High expression of Cathepsin B in transitional bladder carcinoma correlates with tumor invasion. Cancer 2003; 98(2):262-8.
9. Dohchin A, Suzuki JI, Seki H, *et al*. Immunostained Cathepsins B and L correlate with depth of invasion and different metastatic pathways in early stage gastric carcinoma. Cancer 2000;89(3):482-7.

Received March 1, 2006

Alteration of Telomere Length in Gastric Carcinoma

Shuman Liu[1], Jie Fang[2], Wei Zhang[1], Qinxian Zhang[1]

1. Department of Histology and Embryology, Basic Medical College, Zhengzhou University, Zhengzhou, Henan 450052, China

2. Department of Internal Medicine, Huaxian People's Hospital, Huaxian, Henan 456400, China

Abstract: Objective. To evaluate the alteration of telomere length in gastric carcinoma. **Methods.** Southern blot was used to detect the telomere length in gastric carcinoma, matched adjacent tumor tissue and normal gastric mucosa. **Results.** In 32 samples, the telomere length in gastric carcinoma, matched adjacent tumor tissue and corresponding normal gastric mucosa were 5.088 ± 1.712 kb, 5.969 ± 1.659 kb and 6.728 ± 1.707 kb respectively. There was no significant correlation between the telomere shortening in gastric carcinoma and the pathological grades, invasion depth, lymph node metastasis and tumor size. **Conclusion.** Telomere length in gastric carcinoma shortened obviously than that in corresponding normal gastric mucosa and adjacent tumor tissue. Telomere shortening may not be used as a sensitive biomarker to judge the malignance of gastric carcinoma. [Life Science Journal. 2006;3(3):25-28] (ISSN: 1097-8135).

Keywords: gastric carcinoma; telomere length; Southern blot

Abbreviations: BCIP: 5-bromo-4-chloro-3-inddylphosphate; DIG: digoxin; NBT: nitro-blue tetrazolium; TRF: terminal restriction fragments; SSC: sodium saline citrate

1 Introduction

Telomeres are unique structures at the physical ends of linear eukaryotic chromosomes. In most eukaryotes, telomeric DNA consists of simple repetitive sequences with G-rich 3′ terminal. In human somatic cells, telomeres have 500 - 3000 repeats of TTAGGG, which gradually shorten with age *in vivo* and *in vitro*[1]. It has been reported that telomere shortening occurs in a subset of tumors[2], but the alteration of telomere length in gastric carcinoma remained to be elucidated. About this there are different opinions[3,4]. In this study, we examined the telomere length in gastric carcinoma, matched adjacent tumor tissue and corresponding normal gastric mucosa by using analysis of terminal restriction fragments (TRF), with special reference to their clinical features and histological findings. From the accumulated data, we determined whether the telomere length is associated with gastric carcinogenesis and the development of gastric carcinoma.

2 Materials and Methods

2.1 Materials

Thirty-two samples from gastric carcinoma, with matched adjacent tumor tissue and corresponding normal gastric mucosa, were studied. In each case, tumor tissue, matched adjacent tumor tissue and corresponding normal mucosa, at least 5 cm apart, were obtained from surgically dissected stomach. The patients never received radiotherapy and chemotherapy, including twelve males and twenty females. The age of the patients varied in the range of 25 - 69 years old. All tissues were frozen in liquid nitrogen. Considering the morphological characteristics, all of the samples from the gastric carcinoma were identified as ulcerating, papillary and infiltrating carcinoma. Histological examination revealed 14 cases of well differentiated adenocarcinoma, 16 cases of poorly differentiated adenocarcinoma and 2 cases of mucous signet-ring cell adenocarcinoma.

2.2 Genomic DNA isolation and Southern blot

Took out the fresh frozen samples from liquid nitrogen and rapidly ground into powder. High-molecula-weight DNA was prepared from each sample by digestion with proteinase K and extraction with phenol/chloroform. Deposited and condensed genomic DNA with ethanol. Identified DNA purity and concentration with ultraviolet spectrophotometer(HITACHI). 1% agarose gel electrophoresis revealed the genomic DNA integrity. Equivalent amounts of tumor and constitutional DNA (3 μg) were digested overnight at 37 ℃ with 5 μl *Hinf* Ⅰ (TaKaRa, Kyoto, Japan). Thus, the terminal restriction fragments (TRFs), containing both the subtelomeric repetitive DNA and telomeric 5′-TTAGGG-3′ repeats, were liberated. The TRF de-

termining telomeric length were separated by 0.6% agarose gel electrophoresis, denatured and neutralized, and then transferred by capillary transfer onto positive nylon membranes (Osmonics) for Southern blotting. The filters were prehybridized in a hybridization buffer (Sangon) for 6 h at 42 ℃, then hybridized with telomere probe 5′-$(CCCTAA)_3$-3′ labeled with digoxin (DIG) random labeling and detection kit (Boshide, Wuhan, China) in hybridization buffer overnight at 42 ℃. The filters were washed twice in 2 × sodium saline citrate (SSC)/0.1% sodium dodecyl sulfate (SDS) for 5 min at room temperature and then washed twice in 0.2 × SSC/0.1% SDS for 10 min at 58 ℃. The filters were blocked for 1 h at room temperature with blocking buffer (Pierce) and incubated for 1 h at 37 ℃ in a Anti-Dig-Ap mixture that had been diluted 1∶2500 in the blocking buffer. The filters were washed twice in washing buffer for 30 min. Then incubated for 2 min at room temperature in coloring buffer. After mixing with NBT and BCIP (2∶1, Promega), the filters were kept still in shaded corner for color development until the ribbon appeared.

2.3 Densitometry and mean telomere length measurements

The telomeric lengths were quantified by densitometric analysis of the ribbon using Gel imaging analysis system(Gene Genius). The mean telomere length in each sample was calculated as reported[5].

2.4 Statistical analysis

The analysis were conducted with SPSS 10.0 statistical software. Results were expressed as $\bar{x} \pm s$. χ^2 tests, t and K-W tests were used, and a P value < 0.05 was set statistically significant.

3 Results

3.1 Mean telomere length in gastric carcinoma, matched adjacent tumor tissue and normal gastric mucosa

In 32 samples, the telomere length in normal gastric mucosa varied in the range of 4.0 kb − 11.0 kb, the mean telomere length was 6.728 ± 1.707 kb. The telomere length in matched adjacent tumor tissue varied in the range of 3.0 kb − 10.0 kb, the mean telomere length was 5.969 ± 1.659 kb. The telomere length in gastric carcinoma varied in the range of 2.0 kb − 9.0 kb, the mean telomere length was 5.088 ± 1.712 kb. There were significantly statistical differences between three groups ($F = 7.529$, $P = 0.01$). The mean telomere length in normal gastric mucosa, matched adjacent tumor tissue and gastric carcinoma shortened obviously in turn(Table 1, Figure 1). Otherwise, in 3 cases of gastric carcinoma, the mean telomere length slightly shortened, and was even a little longer than that of the normal mucosa(Figure 2).

Table 1. The mean telomere length in gastric carcinoma, adjacent tumor tissues and normal gastric mucosa

Lesions	TRF(kb, $\bar{x} \pm s$)	Significance
Carcinoma	5.088 ± 1.712	
Adjacent tumor tissues	5.969 ± 1.659	$P = 0.01$
Normal tissues	6.728 ± 1.707	

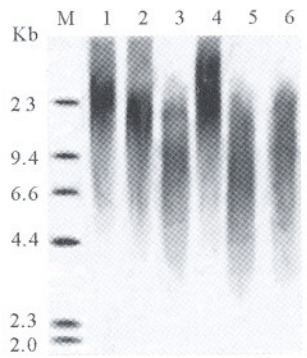

Figure 1. Southern blotting
M: Dig MW marker; Lane 1 and Lane 4: matched normal gastric mucosa; Lanes 2 and 5: adjacent tumor tissue; Lane 3 and Lane 6: gastric carcinoma

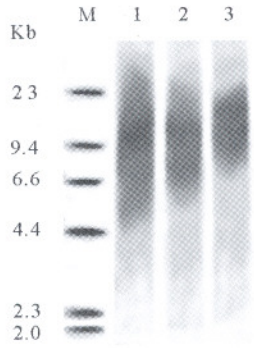

Figure 2. Southern blotting
M: Dig MW marker; Lane 1: matched normal gastric mucosa; Lane 2: adjacent tumor tissue; Lanes 3: gastric carcinoma

3.2 Correlation between telomere length shortening and clinical factors in gastric carcinoma

Several variables, such as age, sex, tumor size, histology, infiltrating depth and tumor stage with lymph node metastasis, were examined for potential links with telomere shortening in the gastric carcinoma group. Age was significantly associated with telomere shortening in normal gastric mucosa. While the mean telomere length showed shortening tendency with age in carcinoma group

and adjacent tumor group, obvious statistical significance was absent (Table 2). Similarly, tumor size, histology, infiltrating depth, tumor stage with lymph node metastasis and sex were not significantly correlated with telomere shortening in gastric carcinoma($P>0.05$).

Table 2. Mean telomere length in different age group

Age(year)	Cases(n)	TRF(kb, $\bar{x}\pm s$)		
		Normal tissue	Adjacent tumor tissue	Carcinoma
20－29	3	10.767±0.252	9.533±0.643	8.476±0.503
30－39	7	7.471±0.214	6.900±0.252	6.229±0.263
40－49	10	6.780±0.235	5.980±0.308	5.010±0.538
50－59	4	6.275±0.457	5.650±0.311	4.825±0.624
60－69	8	4.725±0.656	3.936±0.940	3.050±1.149
P		$P<0.05$	$P>0.05$	$P>0.05$

4 Discussion

A telomere is a group of tandem-repeat DNA sequences located at the ends of eukaryotic chromosomes. Telomere is thought to stabilize chromosomes and protect them from end-to-end fusion or exonucleolytic degradation[1].

Telomere has close relationship with tumorigenesis. Telomeres cannot be replicated completely by DNA polymerases because the enzymes cannot accomplish the coping processes to the very end of DNA strands. Therefore, the length of telomere decreases gradually with the increasing number of cell divisions and therefore with aging, resulting in chromosome instability and genetic changes that may lead to tumor development[6]. Alterations of telomere length have been reported in a subset of tumors including colorectal carcinoma[7], hepatic carcinoma[8], skin base cell carcinoma and renal cell carcinoma[9,10], but they were not consistent, and even can examine longer telomere in carcinoma. Some papers revealed that telomere shortening was related to tumor size, histological type, infiltrating depth, lymph node metastasis[11,12]. Kondo[13] believed that telomere shortened progressively in gastric carcinoma with development of tumor.

Our current finding that the mean telomere length shortened in the order of normal gastric mucosa, matched adjacent tumor tissue and gastric carcinoma may also suggest reduction of telomere occurs in early period of gastric carcinogenesis, causes chromosome instability and accelerates development of gastric carcinoma. This is consistent with theory set by Meeker[14]. Another finding of the current study is that in 3 cases of gastric carcinoma, the mean telomere length slightly shortened, and was even a little longer than that of the normal mucosa. There are several possible reasons about this: telomerase activation was expressed at the early stage of tumorigenesis and compensate shortened telomere; stroma cells are abundant in tumor tissues, and their DNA may affect analysis of TRFs; telomere prolonged mechanism beyond telomerase activation exists. Our current study also indicated that telomere shortening in gastric carcinoma was not related to clinical pathological parameters.

From all the above, though reduction of telomere is one early molecular event of gastric carcinogenesis, the mean telomere length in gastric carcinoma is also decided by other factors and lack of significant correlation with clinical pathological parameters. We deduce that telomere shortening may not be used as a sensitive biomarker to diagnose gastric carcinoma and judge the malignant degree.

Correspondence to:
Shuman Liu
Department of Histology and Embryology
Basic Medical College
Zhengzhou University
Zhengzhou, Henan 450052, China
Telephone: 86-137-8362-1327
Email: donna79320@126.com

References

1. Blackburn. Structure and function of telomeres. Nature 1991; 350(3):569－73.
2. Meeker AK, Argani P. Telomere shortening occurs early during breast tumorigenesis: a cause of chromosome destabilization underlying malignant transformation? J Mammary Gland Biol Neoplasia 2004; 9(3):285－96.
3. Furugori E, Hirayama R, Nakamura KI, *et al*. Telomere shortening in gastric carcinoma with aging despite telomerase activation. Cancer Res Clin Oncol 2000; 126(8):481－5.
4. Maruyama Y, Hanai H, Kaneko E. Telomere length and telomerase activity in intestinal metaplasia, adenoma and

well differentiated adenocarcinoma of the stomach. Nippon Rinsho 1998; 56(5): 1186 - 9.
5. Hastie ND, Dempster M, Dunlop MG, *et al*. Telomere reduction in human colorectal carcinoma and with aging. Nature 1990; 346(6287):866 - 8.
6. Shay JW. Molecular pathogenesis of aging and cancer: are telomeres and telomerase the connection? J Clin Pathol 1997; 50(10):799 - 800.
7. Kim HR, Kim YJ, Kim HJ, *et al*. Telomere length changes in colorectal cancers and polyps. Korean Med Sci 2002; 17(3):360 - 5.
8. Yokota T, Suda T, Igarashi M, *et al*. Telomere length variation and maintenance in hepatocarcinogenesis. Cancer 2003; 98(1): 110 - 8.
9. Wainwright J, Middleton PG, Rees JL. Changes in mean telomere length in basal cell carcinomas of the skin. Genes Chromosome Cancer 1995; 12(6):45 - 9.
10. Dahse R, Fiedler W, Ernst G, *et al*. Changes in telomere lengths in renal cell carcinomas. Cell Mol Biol 1996; 42(9): 477 - 85.
11. Gordon KE, Ireland H, Roberts M, *et al*. High levels of telomere dysfunction bestow a selective disadvantage during the progression of human oral squamous cell carcinoma. Cancer Res 2003; 63(2): 458 - 67.
12. Frazil PA, Glickman J, Jiang S, *et al*. Differential impact of telomere dysfunction on initiation and progression of hepatocellular carcinoma. Cancer Res 2003; 63(16): 5021 - 7.
13. Kondo T, Oue N, Yoshida K, *et al*. Expression of POT1 is associated with tumor stage and telomere length in gastric carcinoma. Cancer Res 2004; 64(2): 523 - 9.
14. Meeker AK, De Marzo AM. Recent advances in telomere biology: implications for human cancer. Curr Opin Oncol 2004; 16(1): 32 - 8.

Received June 10, 2006

Mage-α_x mRNA Level in Lung Cancer of Mice Derived by Coal Tar Pitch

Yue Ba, Huizhen Zhang, Qingtang Fan, Xiaoshan Zhou, Yiming Wu

Department of Labor and Environmental Health, College of Public Health, Zhengzhou University, Henan 450052, China

Abstract: Objective. To investigate the expression of *Mage-a_x* mRNA in lung cancer tissues of mice induced by coal tar pitch (CTP) fume and to discuss the possibility of the lung cancer animal model induced by CTP as a model for lung cancer immunotherapy with *MAGE-A*. **Methods.** Tumor tissue samples of lung cancer and paired non-tumor tissues of the lung were obtained from 8 lung cancer mice. Total RNA was extracted and cDNA was synthesized. Nested PCR amplification using *Mage-a_x* specific primers was then performed to detect the expression of *Mage-a*. The 2 clones of 1 sample of *Mage-a_x* mRNA positive PCR products were DNA sequenced by using DNAs sequencer (PE-377). **Results.** Of 29 mice in the experimental group, 8 were induced to lung cancer. Of 8 lung cancers, 5 (62.5%) expressed *Mage-a_x* mRNA. The expression of *Mage-a_x* gene was not recognized in adjacent lung tissues at all. The DNA sequence confirmed that the target gene fragments in all 2 samples of PCR products were *Mage-a_x* cDNA. **Conclusion.** The *Mage-a* gene was expressed highly in tumor tissues with lung cancer in mice induced by CTP fume. This suggests that this kind of lung cancer mouse model may be an ideal animal model for lung cancer therapeutic experiment by *MAGE-A*. [Life Science Journal. 2006;3(3):29-34] (ISSN: 1097-8135).

Keywords: *Mage-a_x* mRNA; mouse; CTP fume; lung cancer

Abbreviations: CTP: coal tar pitch; CTL: cytotoxic T lymphocyte; TAs: tumor antigens

1 Introduction

Although the enormous manpower and material resources have been spent, there are still no effective methods developed to prevent and treat malignant tumor. The incidence rate of malignant tumor is increasing and the onset age is tending to be younger along with the changes of environment and lifestyle of human being. In China, the increasing magnitude of lung cancer is in the first place in recent 20 years according to the information derived from a more recent national conference on oncology in 2000[1].

Using a gene transfection approach to identify antigens recognized by CTL (cytolytic T lymphocytes) on a human melanoma cell line, Boon *et al* isolated the gene *MAGE-A* family that is located in the Xq28 region and the gene family includes at least 12 related genes[2-4]. *MAGE-B*, including 4 genes, was identified in the Xp21.3 region[5-7]. *MAGE-C1* is on band Xq26[8]. Most of these *MAGE* genes are expressed in a significant proportion of tumors of various histological origins, whereas no expression has been observed in normal tissues except on placenta and male germ cells.

The *MAGE*-encoded antigens are recognized by cytolytic T cells in the form of antigenic peptides presented by HLA class I molecules. Because male germ cells do not express the HLA class I genes, they fail to present MAGE antigens even though they express *MAGE* genes. The *MAGE*-encoded antigens are therefore strictly tumor-specific. Several immunogenic peptide epitopes from tumor-associated antigens (such as MAGE-A3, MAGA-A1 etc.) have served as targets for cellular immune responses in numerous clinical trials for therapeutic vaccinations[9, 10].

In 1999, Boon *et al* found *Mage-a*, a new family of mouse genes homologous to the human *MAGE-A* genes[11]. *Mage-a* genes were mapped on X chromosome. Like human *MAGE-A*, *Mage-a* genes were transcribed in adult testis, but not in other tissues. Expression of some *Mage-a* genes was also detected in tumor cell lines. *Mage-a* genes are higher degree homologous to the human *MAGE-A* genes. Like *MAGE-A* genes, they encode acidic proteins. As the ideal tumor animal model, it is possible to research the immunotherapy by using *MAGE* tumor antigens(TAs). There is, however, little information on their expression in lung carcinoma of mice. This experiment studied the expression of *Mage-a* gene in mice lung cancer and compared its sequence with that in GenBank, then discussed the possibility of the lung cancer ani-

mal model induced by CTP as a model for lung cancer immunotherapy with the use of *MAGE-A*. *Mage-a*$_1$, a_2, a_3, a_5, a_6, a_8 of *Mage-a* are arranged in a cluster located in a region syntenic to Xp22 and they share more than 93% nucleotide identity. The above 6 genes which were amplified in this study were called as *Mage-a*$_x$.

2 Materials and Methods

2.1 Sample collection and RNA extraction

Animal : 64 Kunming mice, 32 males and 32 females, were provided by Henan Animal Center (Zhengzhou, Henan, China). The mice were divided into experiment group and control group randomly. The experiment group was exposed to CTP fume 2 h per day for 12 weeks. The mice were killed in the 12th week and the 24th week, respectively. The lung tissues were frozen in liquid nitrogen. All the samples were confirmed by pathology.

Total cellular RNA was isolated using the flash column total RNA preparation kit (QIAGEN, German) according to the manufacture's instructions.

2.2 Nested RT-PCR

For nested RT-PCR analysis of *Mage-a*$_x$ transcripts, 5 μg of total RNA were reverse-transcribed with the first round PCR specific primers: 5′-AATACCAAGTCCTCCCCAG-3′ (forward), 5′-CTTGGGCCCCACAGGAACC-3′ (reverse) in a 30 μl reaction mixture containing reverse transcriptase buffer, 5 mmol dNTP, 25 pmol primer and 10 U AMV reverse transcriptase (Promega, USA). The mixture was incubated at 42 ℃ for 60 min, heated at 95 ℃ for 5 min and then stored under −20 ℃. 3 μl of RT reaction were used in one round of PCR with 1 × Taq buffer, 5 mmol dNTPs, 25 pmol first round PCR specific primers and 2 U of Taq DNA polymerase (Promega, USA). PCR amplification was 35 cycles at 94 ℃ for 50 sec, 55 ℃ for 50 sec and 72 ℃ for 60 sec with an initial one-cycle predenaturation at 94 ℃ for 120 sec and a final elongation cycle at 72 ℃ for 300 sec. Under the same PCR condition, a second round of PCR was performed using nested primer 5′-AGCGGATCC-CTCTCTCCCCAGGCC-3′ (forward), 5′-ACG *AAGCTT*CCAATTTCCGACGACACTCC-3′ (reverse), and 1 μl of first-round PCR products as template. The nested primers were added appropriate *Bam*HI and *Hind* III restricted site respectively.

2.3 Cloning and sequencing of recombinant plasmids

For the construction of recombinant pUC18 plasmids, a PCR fragment of *Mage-a*$_x$ cDNA was obtained with the nested primer. pUC18 plasmids and the target fragments were digested by *Bam*HI and *Hind* III respectively. Bands were isolated from low melting point agarose and purified by UNIQ-5 column DNA gel reextraction kit (Sangon, Shanghai, China) respectively, and then PCR product was ligated directly into pUC18 plasmid with T_4 DNA ligase. The mixture was transfered into *E. coli* cell, strain DH5α according to the method of *Molecular Cloning*[12]. At least 3 positive clones were picked up and amplified. Then, the ligated PCR products were isolated and sequenced by dideoxy method using DNAs sequencer (PE377). The sequencing results were analyzed using DNAsis software.

3 Results

3.1 The results of CTP induced cancer

Of 29 mice in the experiment group, 8 were induced to lung cancer, 7 were carcinoid and 1 was adenocarcinoma within 24 weeks. There were 5 specimens with squamous metaplasia, 2 were hyperplasia and the rest were normal. All the 32 mice in control group were normal. The cancer incidence was significantly different between two groups ($P < 0.01$). Detail results were shown in Table 1.

Table 1. Comparison of tumor induced in control group and experiment group

Group	Cases(n)	Mice with tumor(n)	Mice without tumor(n)	Ratio
Control group	32	0	32	0
Experiment group	29	8	21	27.6

$P<0.01$

3.2 Expression of *Mage-a*$_x$ gene at mRNA level in mice lung cancer tissues

Of 8 mice with cancers, *Mage-a*$_x$ mRNA was expressed in 5 (62.5%). The expression of *Mage-a*$_x$ gene was not recognized in adjacent and normal lung tissues at all. *Mage-a*$_x$ gene was also expressed in one squamous metaplasia. The PCR products were then digested by restriction endonucleas *Sca* I. The two fragments, 300 bp and 200 bp, were shown respectively. Representative gels were shown in Figure 1 and Figure 2. Results were shown in Table 2.

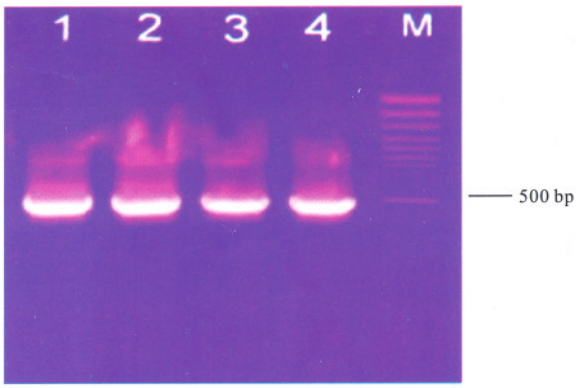

Figure 1. Amplification of target gene
Amplified product of *Mage-α_x* cDNA was 492 bp. Lane 1,2,3,4: lung cancer tissues which expressed *Mage-α_x* mRNA; Lane M: marker

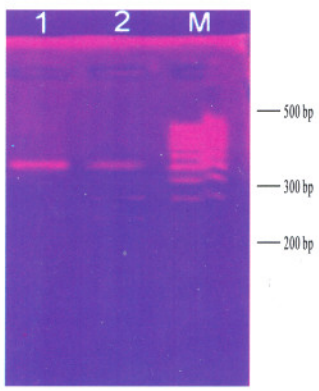

Figure 2. Identification of target gene
Lane 1: amplified target gene; Lane 2: fragments digested with *Sca* I; Lane M: marker

Table 2. Expression of *MAGE-α_x* gene in lung tumors in mice

Pathology	Proportion of positive samples
Carcinoid	4/7 (57.1%)
Adenocarcinoma	1/1 (100%)
Squamous metaplasia	1/5 (20%)
Hyperplasia	0/2
Adjacent lung tissues	0/8
Normal lung tissues	0/32

3.3 Construction, identification and sequencing of mouse *Mage-α_x* gene

The amplified DNA fragment was digested with *Bam* HI and *Hind* Ⅲ. The target fragment was ligated into a predigested (with *Bam* HI and *Hind* Ⅲ) clone vector pUC18. Initial transformation was carried out with *E. coli* DH5α host strain. Positive clone was identified via preparing the plasmid DNA from a number of clones and analyzed by using amplification with universal primer of pUC18 on agarose gel electrophoresis, and was sequenced by using primer M13 (or pUC18 universal primer). The target gene fragments in samples of PCR products were *Mage-α_x* cDNA. The results were shown in Figure 3 and Figure 4.

4 Discussion

The identification of TAs and their recognition by tumor-specific CTL has fuelled the development of immunotherapeutic strategies in cancer[13]. Although numerous TAs and their epitopes have been identified, the majority of these are quite restricted in expression and their clinical utility remains limited. Therefore, it is imperative to evaluate the possibility of tumor immunotherapy by using TAs/epitopes that are widely expressed in tumor. It has many benefit to research the *MAGE* genes' function in mice such as sample got easier, dynamic observation and so on. It may, therefore, be the ideal animal model for the lung cancer's therapeutic experiment by using *MAGE*.

4.1 Reliability, sensitivity and specificity of the experiment

The authors took the following measures to ensure the reliability of the experiment: (1) Remove the necrosis tissues to refrain from RNA degradation caused by necrosis. (2) RNA extracted was all verified by ethidium bromide fluorescence electrophoresis and by ultraviolet radiomete (A260/A280 > 1.9). (3) To ensure RNA was not degraded, a PCR assay with primers specific for β-actin was carried out in each case. (4) To avoid the false positive results, all the samples of extracted RNA were incubated with DNase. (5) Random sampling the positive clones sequenced and confirmed the amplified products being *Mage-α_x* (The sequence is the same as that of GenBank).

Method of nested PCR can improve the sensitivity and specificity of the experiment. The first round PCR will be carried out using the exo-primers firstly, and then the second round PCR will amplify the smaller regions of the first round PCR products by using the nested-primers. So the continuous twice enlargement may increase both the sensitivity and the specificity of PCR greatly. For the extreme-trace target fragments, it's very difficult to get the better results for once amplification, but satisfactory results can be obtained using nested PCR.

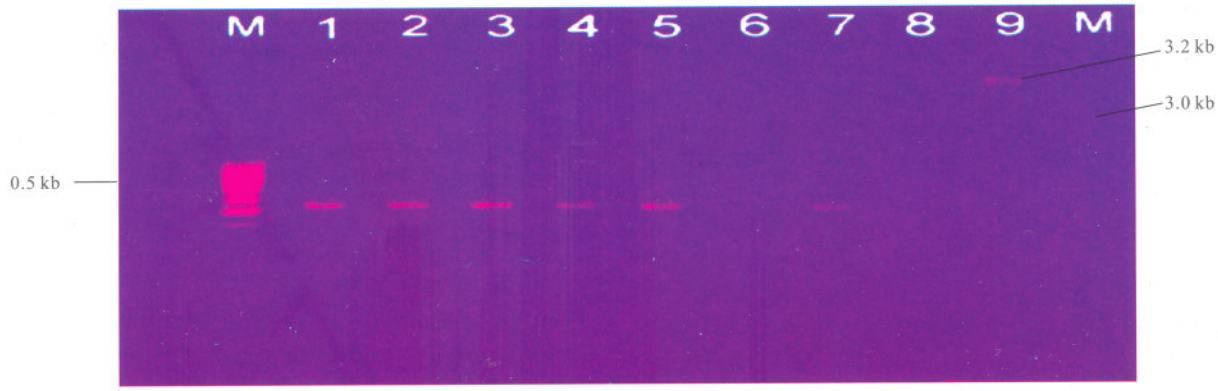

Figure 3. Identification of recombinant-plasmid amplified by pUC18 universal primer
Lane 1,2,3,4,5,7: the inserted target fragments amplified by universal primer; Lane 6: plasmid without inserted the target gene; Lane 8: the negative control; Lane 9: plasmid inserted the target gene

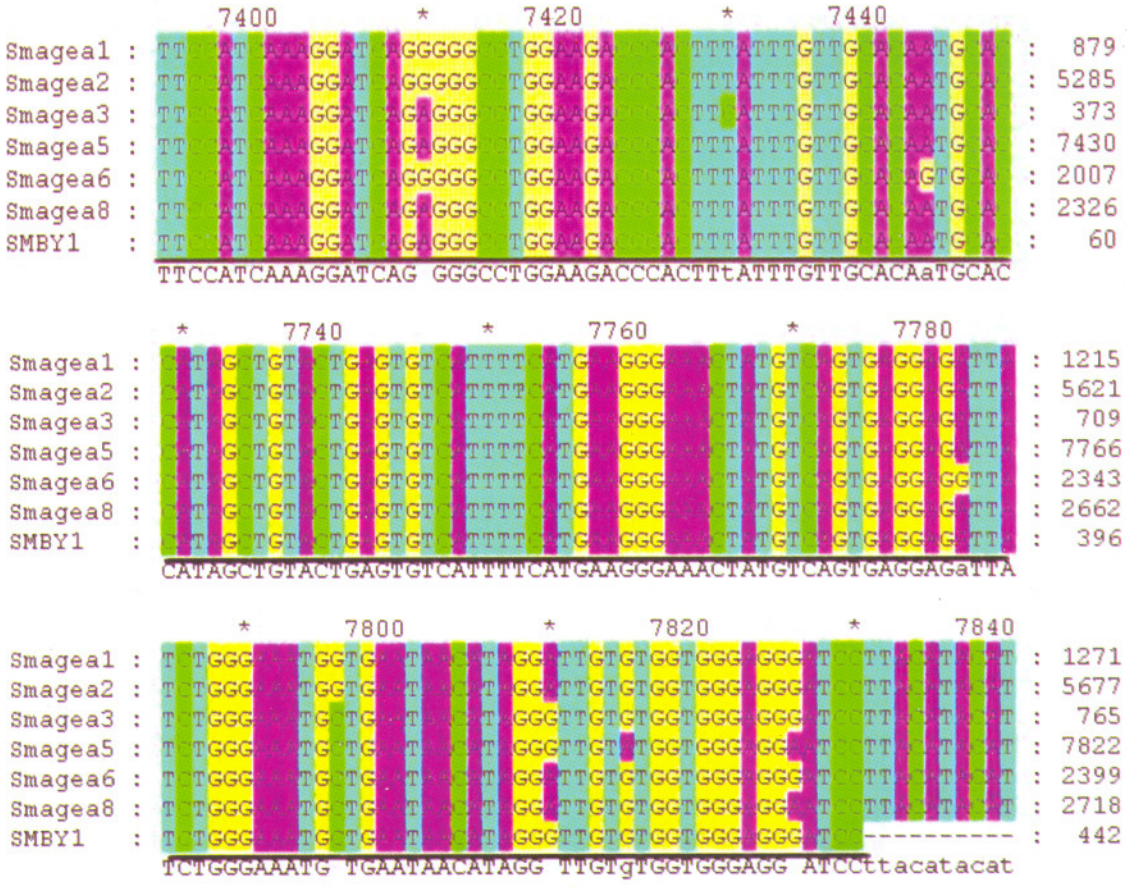

Figure 4. Comparing the sample sequence with *Mage-α_x* sequence in GenBank (The underlined parts were the sample sequences)

4.2 Expression of *Mage-α_x* mRNA of mouse lung cancer tissues

As the results of CTP fume inducing lung cancer among 29 mice in the experiment group within 24 weeks, 8 were induced to lung cancer, 7 were carcinoid and 1 was adenocarcinoma, respectively. PCR results showed that the majority of lung tumors in mice (5 of 8 tested) were positive for the *Mage-α_x* gene by gene-specific primers and the nested-PCR method. These results suggested that more than 60% of lung cancers were expressed *Mage-α_x* gene, which was also expressed in one

squamous metaplasia, but not recognized in adjacent and normal lung tissues at all. Although there are some mouse models used to evaluate human immune responses to *MAGE*-based tumor vaccine, there is no other information about the expression of *Mage-a* in lung carcinoma in mice. Gravekamp *et al*. found high expression levels of *Mage-b* (another *Mage* family of mouse genes homologous to human *MAGE-B* genes) in almost all metastases, regardless of age. The expression levels were 2- to 3-fold higher in the metastases than in the primary 4TO7cg breast tumors[14]. It suggests that *Mage*-encoded tumor antigen will be used as model to study various anti-tumor immunization modalities *in vivo*.

MAGE-A Ags were detected in primary and metastatic tumors of various histological types including melanoma, lung, bladder, ovarian, and breast carcinomas. Individual *MAGE-A* expression varies from one tumor type to another, but overall the majority of tumors express at least one of the *MAGE-A* family. Targeting epitopes shared by all *MAGE-A* Ags would be of interest against a broad spectrum of cancers. At present, *MAGE* peptide-based vaccines have been used in clinical trials with tumorous patients, but with limited success[15,16]. A suitable animal tumor model that would permit the optimization of *MAGE*-encoding cancer vaccines in mice is very necessary to immunotherapy of tumors using *MAGE* gene products. Researchers have used different tumor animal models to evaluate the possibility of tumor immunotherapy by using *MAGE* Ags. Eggert *et al* demonstrated the immunogenicity of two Kb-restricted peptide epitopes derived from mouse MAGE proteins which may serve as valuable tool for preclinical evaluation of vaccination strategies[17]. Ni found that rSFV vaccine could elicit human MAGE-3-specific antibody and CTL response in the Trimera mice[18]. The results of Gravekamp indicated that the metastatic and nonmetastatic breast tumor models could be useful model systems to analyze how breast cancer vaccines for humans[14].

However, a suitable mouse tumor model of lung cancer that would permit the optimization of *MAGE*-encoding cancer vaccines in mice is currently not available. In this study, it shows that *Mage-α_x* gene was expressed highly in tumor tissues with lung cancer induced by CTP fume. This suggests that this lung tumor mice expressing *Mage-α_x* may be an ideal animal model for lung cancer therapeutic experiment by using *MAGE-A*.

Correspondence to:
Yiming Wu
Department of Labor and Environmental Health
College of Public Health
Zhengzhou University
Zhengzhou, Henan 450051, China
Telephone: 86-371-6778-1797
Email: ymwu@zzu.edu.cn

Acknowledgments

This work was finished in Key Molecular Lab of Henan Province. We are particularly grateful to Professor Yi Zhang (Ludwig Institute for Cancer Research, Brussels Branch, Belgium) for his great help.

This work is supported by grants from the Key Project of Scientific Committee of Henan Province (No. 524410067) and the Natural Science Research Fundation of Henan Educational Bureau(No. 2006330003).

References

1. Xu GW. The review and perspective for prevention and treatment of tumor of China. Conference on Oncology, 2000 (Educational Book).
2. Van der Bruggern P, Traversari C, Chomez P, *et al*. A gene encoding an antigen-recognized by cytolytic T lymphocytes on a human melanoma. Science 1991;254: 1643 – 7.
3. De Plaen, Arden K, Van der Bruggen P, *et al*. Structure, chromosomal, localization, and the expression of 12 genes of the *MAGE* family. Immunogenetics 1994; 40(5): 360 – 9.
4. Rogner UC, Wilke K, Steck E, *et al*. The melanoma antigen gene (*MAGE*) family is clustered in the chromosomal band Xq28. Genomics 1995; 29(3):725 – 31.
5. Muscatelli F, Walker AP, De Plaen E, *et al*. Isolation and characterization of a *MAGE* gene family in the Xp21.3 region. Proc Natl Acad Sci USA 1995;92(11): 4987 – 91.
6. Dabovic B, Zanaria E, Bardoni B. A family of rapidly evolving genes from the sex reversal critical region in Xp21. Mamm Genome 1995;6(9):571 – 80.
7. Lurquin C, De Smet C, Brasseur F. Two members of the human *MAGE-B* gene family located in Xp21.3 are expressed in tumors of various histological origins. Genomic 1997; 46(3):397 – 408.
8. Lucas S, De Smet C, Arden KC, *et al*. Identification of a new *MAGE* gene with tumor-specific expression by representational difference analysis. Cancer Res 1998; 58 (4):743 – 52.
9. Ma JH, Sui YF, Ye J, *et al*. Heat shock protein 70/ *MAGE*-3 fusion protein vaccine can enhance cellular and humoral immune responses to *MAGE*-3 *in vivo*. Cancer Immunol Immunother 2005;54(9):907 – 14.
10. Ye J, Chen GS, Song HP, *et al*. Heat shock protein 70 / *MAGE*-1 tumor vaccine can enhance the potency of *MAGE*-1-specific cellular immune responses *in vivo*. Cancer Immunol Immunother 2004;53(9):825 – 34.

11. De Plaen E, De Backer D, Arnaud D, *et al*. A new family of mouse genes homologous to the *MAGE* genes. Genomics 1999; 55(2): 176 – 84.
12. Sambrook J, Fritsch EF, Maniatis T. Molecular cloning: a laboratory manual. 2nd. Cold Spring Harbor, NY: Cold Spring Harbor Laboratory, 1989.
13. Graff-Dubois S, Faure O, Gross DA, *et al*. Generation of CTL recognizing an HLA-A^{*}_{0201}-restricted epitope shared by *MAGE*-A_1, -A_2, -A_3, -A_4, -A_6, -A_{10}, and-A_{12} tumor antigens: Implication in a broad-spectrum tumor immunotherapy. J Immuno 2002; 169(1): 575 – 80.
14. Gravekamp C, Sypniewska R, Gauntt S, *et al*. Behavior of metastatic and nonmetastatic breast tumors in old mice. Exp Biol Med (Maywood) 2004; 229(7): 665 – 75.
15. Anichini A, Molla A, Mortarini R, *et al*. An expanded peripheral T cell population to a cytotoxic T lymphocyte (CTL)-defined, melanocyte-specific antigen in metastatic melanoma patients impacts on generation of peptide-specific CTLs but does not overcome tumor escape from immune surveillance in metastatic lesions. J Exp Med 1999; 190: 651 – 68.
16. Marchand M, van Baren N, Weynants P, *et al*. Tumor regressions observed in patients with metastatic melanoma treated with an antigenic peptide encoded by gene *MAGE*-3 and presented by HLA-A1. Int J Cancer 1999; 80:219 – 30.
17. Eggert AO, Andersen MH, Voigt H, *et al*. Characterization of mouse *MAGE*-derived H-2Kb-restricted CTL epitopes. Eur J Immunol 2004; 34(11): 3285 – 90.
18. Ni B, Gao W, Zhu B, *et al*. Induction of specific human primary immune responses to a Semliki Forest virus-based tumor vaccine in a Trimera mouse model. Cancer Immunol Immunother 2005; 54(5): 489 – 98.

Received April 2, 2006

Effect of Folate and Vitamin B12 on Tau Phosphorylation in Aged Rat Brain

Jiewen Zhang[1], Fen Lu[1], Xu Li[2], Aiqin Suo[1]

1. Department of Neurology, Henan People's Hospital, Zhengzhou, Henan 450003, China

2. Department of Pathology, Henan Tumor Hospital, Zhengzhou, Henan 450008, China

(All the authors contribute to the work equally)

Abstract: Alzheimer's disease (AD) is the cause of one of the most common types of dementia. In AD brain, abnormal hyperphosphorylated tau composed the major protein of neurofibrillary tangles (NFTs), one of the two neuropathological hallmarks of AD. To prevent and relieve the tau protein abnormal hyperphosphorylation in AD patients' brain is thought to be the key point of therapy. Recent study suggested that there is some relationship between folates, vitamin B12 and AD. In our study we aim to investigate the possible mechanism of AD especially the correlation between folates, vitamin B12 and tau phosphorylation. We examined tau protein phosphorylation state in rats' hippocampus of different age stages: two and forty months old by phosphorylation dependent and independent tau antibodies. We found that tau phosphorylation in aged rats' brain showed significant high level than these two months old. And we also found that folates plus vitamin B12 can decrease the level of tau phosphorylation in aged rats' brain. It suggests folates and vitamin B12 may play an important role in preventing the neurodegenerative change by influencing tau phosphorylation in brain. [Life Science Journal. 2006;3(3):35 - 40] (ISSN: 1097 - 8135).

Keywords: Alzheimer's disease; aged; folate; vitamin B12

Abbreviations: AD: Alzheimer's disease; BCA: bicinchoninic acid; CSF: cerebrospinal fluid; DAB: diaminobenizidine; NFTs: neurofibrillary tangles; PHF: paired helical filaments; SDS-PAGE: sodium dodecyl sulphate polyacrylamide gel electrophoresis

1 Introduction

Dementia is a syndrome characterized by an acquired global impairment of memory and other cognitive functions sufficient to interfere with normal life[1]. Alzheimer's disease (AD) is the cause of one of the most common types of dementia. The World Health Organization has estimated that 25 - 29 million people in the world suffer from dementia. Approximately 6% - 8% of all older people over the age of 65 years have AD[2], and the prevalence increases steeply with age[3]. AD is characterized by the presence of two histopathological hallmarks called senile plaques and neurofibrillary tangles, which are involved in the process leading to progressive neuronal degeneration and death. It is reported that neurofibrillary tangles (NFTs) are structures present in the neuronal body and consist of paired helical filaments (PHF), mainly composed of highly phosphorylated tau protein[4,5]. Tau is a microtubule-associated protein expressed mostly, but not exclusively, in the nervous system, and its normal physiological function is to bind and stabilize microtubules[6]. In AD brain, tau is found aberrantly hyperphosphorylated[7]. Abnormal phosphorylation of tau in brain seemed to be an important pathogenesis of AD.

The possible involvement of nutritional factors in the aetiology (causes) or pathogenesis (mechanisms of brain damage) of dementia has been widely considered. In particular, dietary deficiency of folates has been postulated as contributing to the aetiology AD. Folates are vitamins essential to the development of the central nervous system. And researcher also found that vitamin B12 deficiency not only produces anaemia but also causes irreversible damage to the central and peripheral nervous systems. In this study we aim to investigate the mechanism of the relationship between AD and folates and vitamin B12. We focus on the tau protein and to study whether folates plus vitamin B12 have effect on its phosphorylation status.

2 Materials and Methods

2.1 Animal

Male Wistar rats were from Experimental Animal Central of Henan Medical College. All animals were observed daily for clinical signs of disease. All

animal experiments were performed according to *Policies on the Use of Animals and Humans in Neuroscience Research*, revised and approved by the Society for Neuroscience in 1995. The subjects were allocated into two groups: two months old rats and forty months old rats. Group of forty months old rats were treated with folates (40 mg/kg diet) by the gut and vitamin B12 (20 μg/kg) by intraperitoneal injection every day for one month.

2.2 Antibodies and reagents

Antibodies to tau are listed in Table 1. Rabbit polyclonal antibody R134d against total tau, monoclonal antibodies PHF-1 against PHF-tau phosphorylated at Ser396/404, and Tau-1 against PHF-tau unphosphorylated at Ser199/202 were gifts from Dr. Chengxin Gong (New York State Institute for Basic Research, Staten Island, NY, USA). Bicinchoninic acid (BCA) protein detection kit, goat anti-rabbit peroxidase-conjugated secondary antibody, chemiluminescent substrate kit and phosphocellulose units were obtained from Pierce Chemical Company (Rockford, IL, USA). Detection kit (Histostain-SP) for immunohistochemistry. Goat anti-mouse and goat anti-rabbit alkaline phosphatase-conjugated secondary antibodies, diaminobenizidine (DAB) and other chemicals were purchased from Maixin Biotechnology Company (Fu Zhou, China). Folates were from Peking University Pharmaceutical Co. Ltd. and vitamin B12 was from Yangzhou Zhong Bao Pharmaceutical Co. Ltd.

Table 1. Tau antibodies employed and their properties

Antibody	Dilution	Type[a]	Specificity	Phosphorylation sites[b]
Tau-1	1:30000	Mono-	unP	Ser-198/Ser-199/Ser-202
PHF-1	1:500	Mono-	P	Ser-396/Ser-404
R134d	1:2000	Poly-	P + unP	

[a] Poly-, polyclonal; mono-, monoclonal; unP, unphosphorylated epitope; P, phosphorylated epitope

[b] Numbered according to the largest isoform of human brain tau

2.3 Preparation of rat brain extracts

The rat is deeply anesthetized with sodium pentobarbital (75 mg/kg, *i. p.*) and then decapitated. Immediately remove the brain and separate the brain sagittally into hemisphere and put into ice-chilled PBS. The left hemisphere was fixed for immunohistochemistry. And the right hippocampus was homogenated and supernatant was for Western blot.

2.4 Western blot

Western blots of hippocampus homogenate were to determine the phosphorylation state of tau of different aged rats. The homogenizer contained cold homogenizing buffer containing 50 mM Tris-HCl, pH 7.0, 10 mM β-mercaptoethanol, 1.0 mM EDTA, 0.1 mM phenylmethylsufonyl fluoride, and 2.0 μg/ml each of aprotinin, leupeptin, and pepstatin A. Then they were homogenized in the same buffer at a ratio of 9.0 ml of buffer/1.0 g tissue with phosphatase inhibitor mixture containing 20 mM β-glycerophosphate, 1.0 mM Na_3VO_4, and 50 mM NaF, pH 7.0. The homogenates were spin at 15,000 rpm for 3 min at 4 ℃ for biochemical analysis. The phosphorylation of tau in the above samples was analyzed by Western blots using 10% SDS-PAGE. The separated protein bands were transferred into nitrocellulose membrane and probed with specific anti-tau antibodies. Then all blots were probed with peroxidaseconjugated secondary antibody and developed with chemiluminescent substrate kit. The protein bands were quantitatively analyzed, and the amount of protein was expressed as relative level of total optical density.

2.5 Immunohistochemistry

The hippocampus of the left hemisphere were fixed by 10% neutrality formaldehyde, 90% 0.01 M PBS solution at room temperature for 6 h, paraffin embedded, and cut into 5 μm-thick sections. Dry the slides (processed by acetone and APES) with tissue sections in an 80 °C oven for 30 min. Sections were blocked with 0.3% H_2O_2 in absolute methanol for 20 min and non-specific sites were blocked with instant calf serum for 60 min at 37 ℃. Then incubate sections overnight at room temperature with primary antibodies as described. The slides were developed by biotinylated secondary antibodies (1:200) and Avidin-peroxidase conjugate (1:200)/diaminobenzidine tetrachloride (0.05%) system.

2.6 Statistical analysis

Data were expressed as $\bar{x} \pm SD$ and analyzed using SPSS 11.0 statistical software (SPSS Inc, Chicago, Illinois, USA). The One-Way ANOVA procedure followed by LSD's *post hoc* tests was used to determine the different means among groups ($P<0.05$).

3 Results

3.1 Tau phosphorylation at ser396/404 site

To study whether folates and vitamin B12 affect tau protein phosphorylation and their possible

relationship, the status of tau phosphorylation of different ages in rats' hippocampus were analyzed. The status of tau of different age rat were carried out by Western blot using three well characterized phosphorylation-dependent and site-specific tau antibodies as listed in Table 1. Compared with two months old rats group, a remarkable increase of phosphorylated tau for forty months old rats was detected by PHF-1 which recognize phosphorylated tau at ser396/404 site. And tau-1 recognizes unphosphorylated tau at ser199/ser202 sites. Tau phosphorylation in forty months old rats group have the high expression (Figure 1 A and B). The level of total tau was indicated by blot developed with R134d, a phosphorylation-independant antibody. Data showned that there was no remarkable difference between two months old group and forty months old group (Figure 1C). So the phosphorylation of tau protein in rat's hippocampus is notably increased with the aging process. And based this result we do the next step.

3.2 Folates plus vitamin B12 can decrease hyperphosphorylation of tau in aged rat brain

After rats were treated with folates and vitamin B12, the status of tau protein phosphorylation were detected on different age stage groups in rats' brain. Gained the extract of rats' hippocampus was for immunoblot analysis. We found that bands of the drug treated group were sharply decreased compared to the group which was not treated with drugs (Figure 2A). It indicates a large decrease in phosphorylation of tau at Ser396/404 sites. This result was corroborated by the greatly diminished staining of tau bands by phosphorylation-independent anti-tau antibody tau-1, which has an optimal immunoreactivity when tau is dephosphorylated at ser199/ser202 (Figure 2B). It demonstrated that folates and vitamin B12 have the effect on decreasing the tau phosphorylation in aged rat brain. We also found that the level of total tau still had no remarkable difference between groups(Figure 2C).

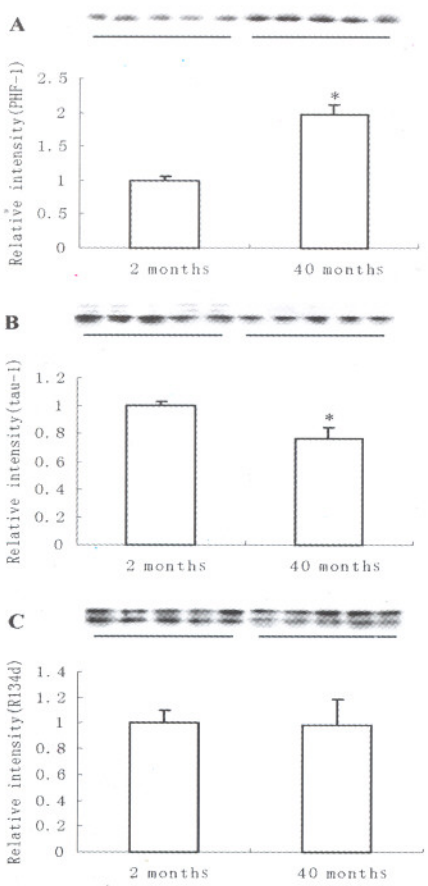

Figure 1. Level of tau phosphorylation in different age rat brain by Western blot.
15 μg of protein per lane was employed with antibody PHF-1, tau-1 and R134d. * $P < 0.05$, *vs*. 2 months old rat.

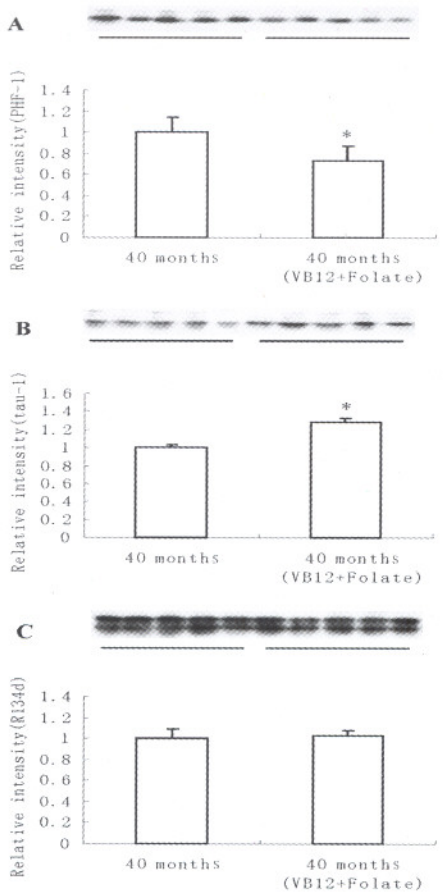

Figure 2. Effect of folate plus vitamin B12 on tau phosphorylation in 40 months aged rat brain by Western blots.
15 μg of protein per lane was employed with antibody PHF-1, tau-1 and R134d. * $P < 0.05$, *vs*. aged rat that was not treated with folate and vitamin B12.

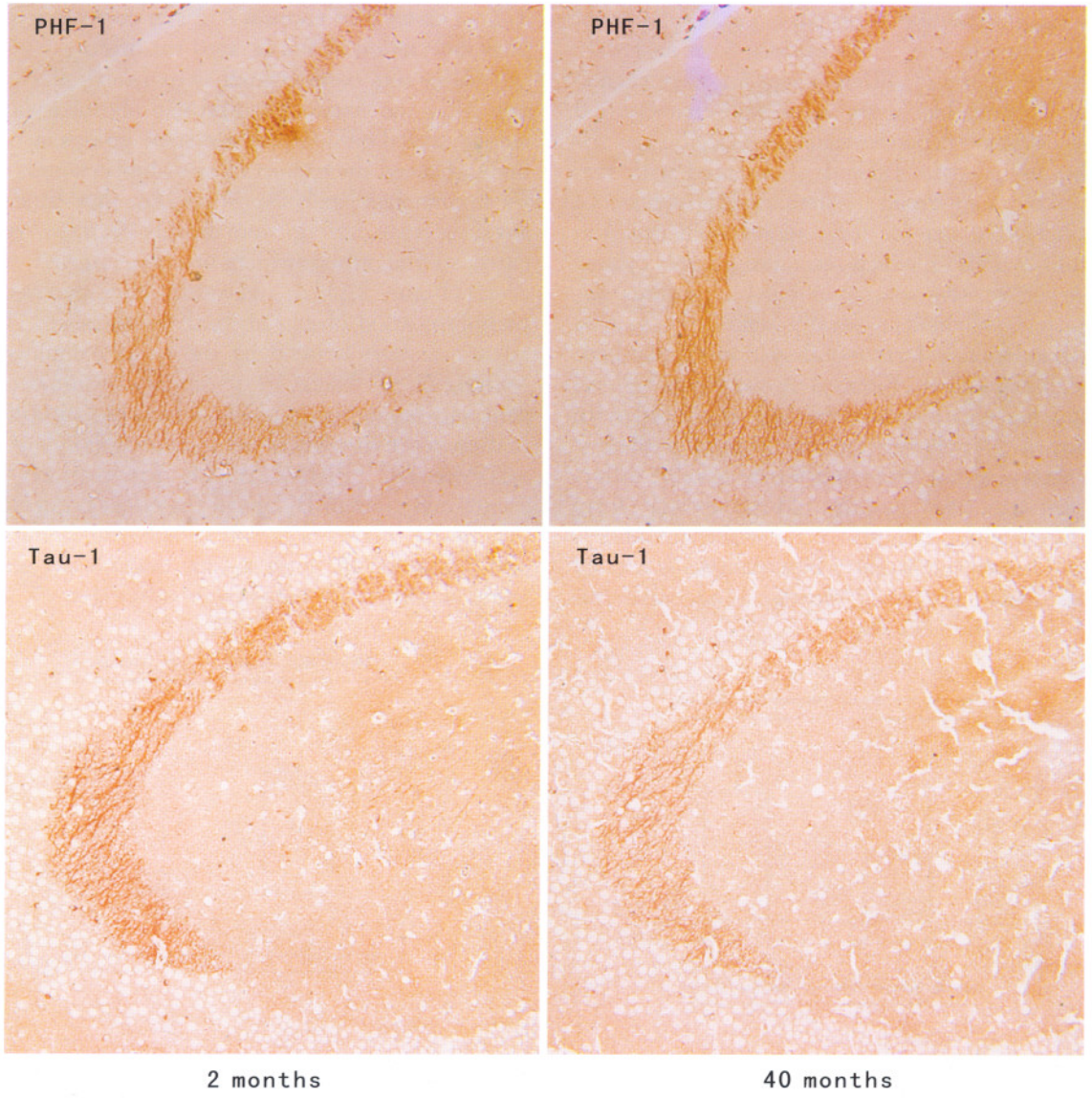

Figure 3. Level of tau phosphorylation in different age rat brain by immunohistochemistry
Paraffin embedded (5 μm-thick) sections were immunostained with PHF-1 and tau-1.

To learn the change of phosphorylation state of tau and its topographical distribution correlate with folates and vitamin B12 treatment in the brain tissue, we immunostained the sections cut from the left hemisphere with phosphorylation dependent and phosphorylation independent anti-tau antibodies. From these pictures we found that the immunohistochemistry results were consistent with Western blots results. The level of tau phosphorylation in 40 months aged rat brain is higher than that of 2 months old rat (Figure 3). After treated with folates and vitamin B12 for one month we can see that at ser396/404(PHF-1) the rat brain sections were stained gradually weak. Oppositely, they were stained gradually increased when detected by antibodies tau-1 (Figure 4). Immunohistochemistry results also demonstrated that folates and vitamin B12 could decrease the level of tau phosphorlation in rats' hippocampus.

4 Discussion

This experiment studied the possible associations between vitamin B12/folate and tau protein phosphorylation in aged rat brain. In the study we detected the phosphorylation state of the aged and young adult rats. We found that the level of tau phosphorylation in aged rat brain was higher than that of young adult rat. The result suggests that the phosphorylation of protein tau changes dynamically according to the physiological state associated

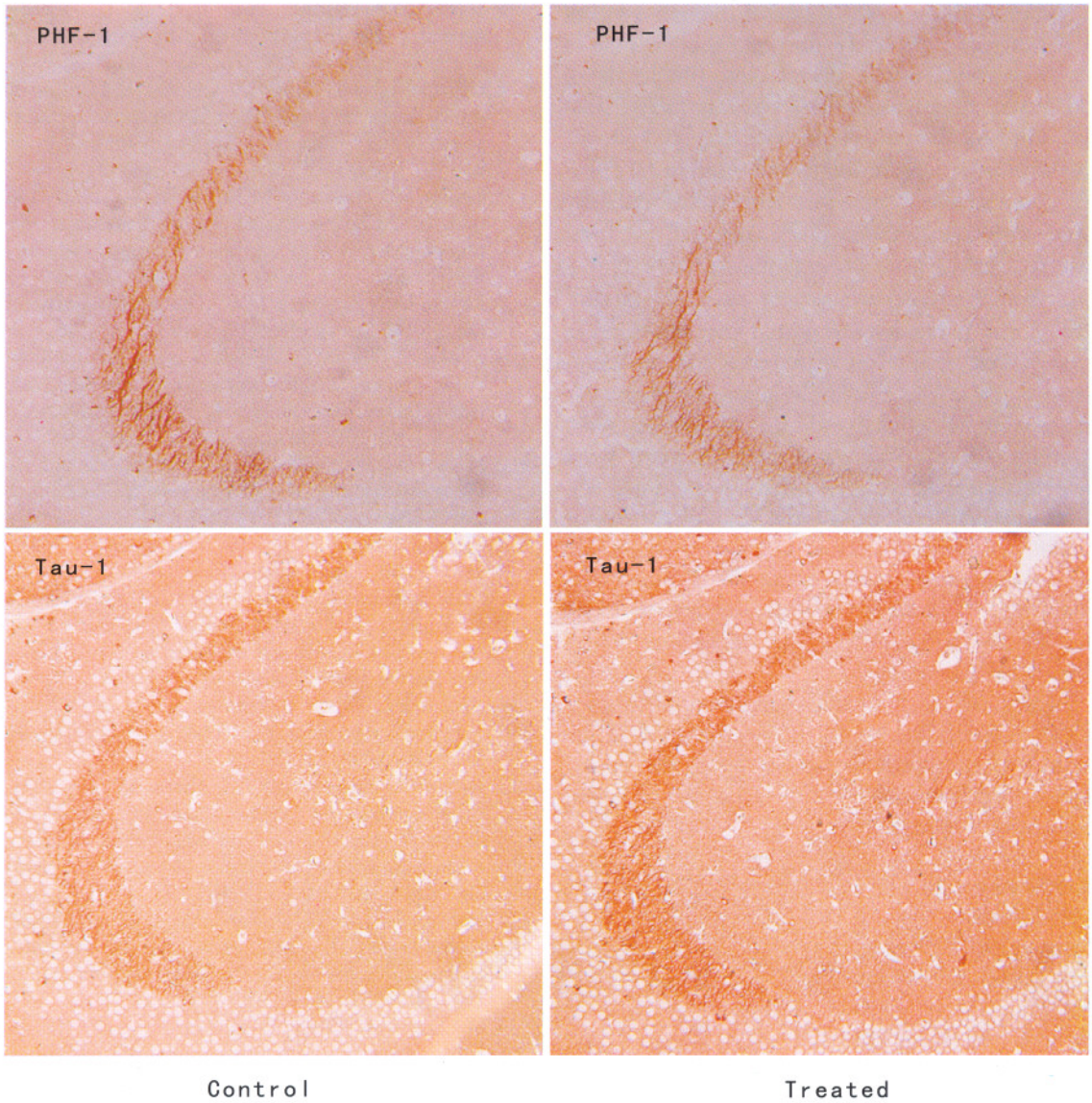

Figure 4. Effect of folate plus vitamin B12 on tau phosphorylation in 40 months aged rat brain by immunohistochemistry. Paraffin embedded (5 μm-thick) sections were immunostained with PHF-1 and tau-1.

with the aging process. In fact, recent studies had reported that high incidence rate of AD in aged population. And abnormal hyperphosphorylation of tau protein is closely related to AD. Biochemical and anatomy also had proven these foundings. But the mechanism of the tau phosphorylation in aged people which probably cause AD is still not clear. Recently, researcher found that older people with low levels of folate are twice as likely to develop AD as are those with normal levels[8]. In some observational studies, researchers found that low serum folate levels have been associated with AD and with all types of dementia[9, 10]. Red blood cell folate and CSF folate levels are lower in patients with AD than in controls[11]. It is known that low folate levels can be the result of inadequate dietary intake, diminished absorption from the gastrointestinal tract or increased utilization. In older people folate metabolism disturbance usually happened probably because body regular function becomes declined. So supplement folate could be reasonable for these older people.

In our study we treated the aged rat with folate and vitamin B12 for one month the level of hyperphosphorylation of tau in rat brain extract decreased. It suggested that folate and vitamin B12

could improve abnormal hyperphosphorylation of tau, which composed NFT, one of the hallmarks of AD. This result probably due to supplemental of folate and vitamin B12 decreaseing the levels of blood homocysteine. It has been reported that blood levels of homocysteine was elevated in patients who were lack of folate and vitamin B12[12]. High homocysteine levels are associated with decreased cognitive function and dementia[13]. Individuals with AD have been found to have higher plasma homocysteine levels than agematched controls[14], and it has been reported that elevation of plasma homocysteine levels precedes clinical manifestations of AD[15]. The underlying mechanisms of homocysteine as a risk factor for Alzheimer's dementia are still uncertain, but there are many ways in which homocysteine could damage neurons, including through endothelial dysfunction, cerebral microangiopathy and increased oxidative stress. In rats, homocysteine induces apoptosis in hippocampal neurons, and *in vivo* it increases excitotoxicity and oxidative damage[16]. The detail mechanism still need further study.

In summary, this study demonstrated that folate and vitamin B12 could relieve the level of tau protein hyperphosphorylation in aged rat brain. And this founding could be a reference for clinicians and medicine researchers.

Correspondence to:
Jiewen Zhang
Department of Neurology
Henan People's Hospital
Zhengzhou, Henan 450003, China
Telephone: 86-371-6558-0171
Email: gointo2001@hotmail.com

References

1. Gottfries CG, Lehmann W, Regland B. Early diagnosis of cognitive impairment in the elderly with the focus on Alzheimer's disease. J Neural Transm 1998;105:773-86.
2. Small GW, Rabins PV, Barry PP, *et al*. Diagnosis and treatment of Alzheimer disease and related disorders. Consensus Statement of the American Association for Geriatric Psychiatry, the Alzheimer's Association, and the American Geriatrics Society. JAMA 1997;278:1363-71.
3. Jorm AF, Korten AE, Henderson AS. The prevalence of dementia: a quantitative integration of the literature. Acta Psychiatr Scand 1987;76:465-79.
4. Grundke-Iqbal I, Iqbal K, Quinlan NM, *et al*. Microtubule-associated protein tau: a component of Alzheimer paired helical filaments. J Biol Chem 1986;261: 6084-9.
5. Godert M, Spillantini MG, Cairns NJ, *et al*. Tau proteins of Alzheimer paired helical filaments: abnormal phosphorylation of all six brain isoforms. Neuron 1992; 8:159-68.
6. Drubin DG, Kirschner MW. Tau protein function in living cells. J Cell Biochem 1986;103:2739-46.
7. Kopke E, Tung YC, Shaikh S, *et al*. Microtubule associated protein tau: abnormal phosphorylation of a nonpaired helical filament pool in Alzheimer disease. J Biol Chem 1993;268:24374-84.
8. Wang HX, Wahlin A, Basun H, *et al*. Vitamin B12 and folate in relation to the development of Alzheimer's disease. Neurology 2001;56, 1188-94.
9. Clarke R, Smith AD, Jobst KA, *et al*. Vitamin B12, and serum total homocysteine levels in confirmed Alzheimer disease. Arch Neurol 1998;55:1449-55.
10. Ebly EM, Schaefer JP, Campbell NR, *et al*. Folate status, vascular disease and cognition in elderly Canadians. Age Ageing 1998;27:485-91.
11. Abalan F, Zittoun J, Boutami C, *et al*. Plasma, red cell, and cerebrospinal fluid folate in Alzheimer's disease. Encephale 1996;22:430-4.
12. Kado DM, Karlamangla AS, Huang MH, *et al*. Homocysteine versus the vitamins folate, B6, and B12 as predictors of cognitive function and decline in older high-functioning adults: MacArthur Studies of Successful Aging. Am J Med 2005;118:161-7.
13. Hofman A, Ott A, Breteler MM, *et al*. Atherosclerosis, apolipoprotein E, and prevalence of dementia and Alzheimer's disease in the Rotterdam Study. Lancet 1997;349:151-4.
14. McCaddon A, Davies G, Hudson P, *et al*. Total serum homocysteine in senile dementia of Alzheimer type. Int J Geriatr. Psychiatry 1998; 13: 235-9.
15. Seshadri S, Beiser A, Selhub J, *et al*. Plasma homocysteine as a risk factor for dementia and Alzheimer's disease. New England Journal of Medicine 2002;346:476-83.
16. Kruman II, Kumaravel TS, Lohani A, *et al*. Folic acid deficiency and homocysteine impair DNA repair in hippocampal neurons and sensitize them to amyloid toxicity in experimental models of Alzheimer's disease. J Neurosci 2002;22(5):1752-62.

Received June 20, 2006

Peroxynitrite Mediated Oxidation Damage and Cytotoxicity in Biological Systems

Xu Zhang, Dejia Li

Department of Biochemistry, Basic Medical College, Zhengzhou Univercity, Zhengzhou, Henan 450052, China

Abstract: Peroxynitrite is the product of the diffusion-controlled termination reaction between two radicals, nitric oxide and superoxide and is a strong oxidant and nitrating regeant. Critical biomolecules like proteins, lipids and DNA react with peroxynitrite via direct or radical-mediated mechanisms, resulting in alterations in enzyme activities and signaling pathways. The biological consequences of peroxynitrite-mediated oxidative modifications depend on the levels of oxidant achieved *in vivo* and its cellular site of production. In this article we overview multiple biological toxicity of peroxynitrite including the biological reactivity of peroxynitrite, peroxynitrite mediated oxidation damage of biomacromolecules such as proteins, lipids and DNA and the cytotoxic effects (apoptosis and necrosis) of peroxynitrite. [Life Science Journal. 2006;3(3):41-44] (ISSN: 1097-8135).

Keywords: peroxynitrite; toxicity; cytotoxicity; oxidation damage

Abbreviations: NOS: nitric oxide synthase; PARP-1: poly(ADP-ribose) polymerase-1

1 Production of peroxynitrite in biological systems

$ONOO^-$, formed by the reaction of nitric oxide with superoxide (O_2^-) which is a byproduct of cellular respiration at near diffusion controlled rates[1], is very likely to occur even in the presence of physiological concentrations of SOD. Nitric oxide is enzymatically produced from L-arginine by nitric oxide synthase (NOS). Three isoforms of this enzyme have been described: nNOS (neuronal), eNOS (endothelial) and iNOS (induced, inflammatory). On the other hand, superoxide can be catalytically produced (for example, by xanthine oxidase or NADPH oxidase), and also formed by partial reduction of oxygen in the mitochondrial membrane or non-enzymatic monoelectron reduction of oxygen (for example, hemoglobin autoxidation). Peroxynitrite has a short biological half-life (10 - 20 ms) but can cross biological membranes and diffuse one to two cell diameters[2]. *In vivo* formation of peroxynitrite is supported by the growing experimental evidence[3].

2 Reactivity of Peroxynitrite

Peroxynitrite mediated oxidation damage by a decomposition intermediate with the biological activity of hydroxyl radical[4]. The decomposition of peroxynitrite to nitrate is intimately coupled with the oxidation chemistry of this species, and both reactions have been the subject of recent investigations. $ONOO^-$ is a relatively stable at alkaline pH, but at physiological pH it is capable of effecting one and two electron reactions akin to those of HO^+, NO_2, and nitrosonium cation. Oxidations of ascorbate[5], transition metal complexes, halide ions, thiols, sulfides[6], olefins, benzenes, phenols[7] and other aromatics by peroxynitrite have been described. Peroxynitrite is a particularly effective oxidant of aromatic molecules and organosulfur compounds that include free amino acids and peptide residues. Cysteine and glutathione, which are significant components of antioxidant reservoirs, are converted to disulfides. Methionine is converted to sulfoxide or is fragmented to ethylene and dimethyldisulfide. Tyrosine and tryptophan undergo one-electron oxidations to radical cations, which are competitively hydroxylated, nitrated and dimerized[8]. Purine nucleotides are vulnerable to oxidation and to adduct formation[9]. Other reports have more detailed reviews on the chemistry, decomposition and reactivity of peroxynitrite, peroxynitrous acid and its activated isomer[10]. The various reactions of peroxynitrite when occurring during the reaction of peroxynitrite with enzymes, macromolecules and lipids, have been shown to influence cellular functions.

3 Peroxynitrite Mediated Oxidation of Biomacro-Molecules

3.1 Protein oxidation

Peroxynitrite-induced protein modifications include protein oxidation (on methionine, cysteine, tryptophane or tyrosine residues) and nitration (of tyrosine or tryptophane residues). However, enzymes containing a redox active transition metal center are the prime targets of the oxidant[11]. Reactions of peroxynitrite are affected by the local pH and the microenvironment with hydrophobic membrane compartments favoring nitration and aqueous environments favoring oxidation. Moreover, carbon dioxide reacts with peroxynitrite resulting in the formation of nitroso-peroxocarbonates[1]. The ubiquitous presence of CO_2 at high concentration may favor this reaction route. As nitroso-peroxocarbonates divert peroxynitriteinduced protein modifications toward nitration, CO_2 is now considered as key determinant of peroxynitrite chemistry.

As just mentioned above, peroxynitrite can directly oxidize the prosthetic group of a protein, for example, hemoglobin, or directly react with the peptide chain leading to conformational and functional changes with potential severe biological consequences. Enzymes with critical cysteine residues can be inactivated by peroxynitrite[12]. In contrast, oxidation of a critical cysteine has been shown to activate an enzyme, that is the case of matrix metalloproteinases where the cysteine residue is in the autoinhibitory domain of the proenzyme[13].

In some cases, the oxidation of a cysteine residue to disulfide (via sulfenic acid) is part of the catalytic cycle, as is the case of peroxiredoxins, thiol-dependent peroxidases[14]. Critical methionine residues can be oxidized by peroxynitrite to yield methionine sulfoxide with loss of protein function as the case α1-antiproteinase[15] which lose its ability to inhibit proteases, in particular, elastase. The oxidation of methionine is readily reversed by methionine sulfoxide reductase at the expenses of thioredoxin. Peroxynitrite does not directly react with tyrosine residues[16] but can oxidize and nitrate them. Nitration (i. e. addition of a NO_2 group) of protein tyrosines to 3-nitrotyrosine has been interpreted as a footprint of peroxynitrite *in vivo* and which can inactivate the enzymes[17] or the proteins loss function after nitration[18].

3.2 DNA oxidation

Peroxynitrite can mediate DNA damage such as the oxidative modification of nitrogen bases and the sugar moiety as well as strand breaks[19]. The most reactive nitrogen base is guanine to yield 8-oxoguanine and 8-nitroguanine. The formation of strand breaks have been shown to activate poly-ADP ribose synthase (PARS) which catalyze the poly-ADP ribosylation of histones, topoisomerases, DNA ligase Ⅱ, triggering signaling towards cell cycle arrest[20]. Excessive PARS activation may lead to NAD consumption and energy depletion[21].

3.3 Lipid peroxidation

Peroxynitrite can initiate oxidation of lipids (membranes, liposomes and lipoproteins) yielding lipid hydroperoxides, conjugated dienes, aldehydes, and even nitrated lipids have been detected[22]. In contrast to the well-known oxygen radical dependent lipid peroxidation that requires transition metal ion catalysis, no iron is required to initiate lipid peroxidation by peroxynitrite[1]. Oxidation of polyunsaturated fatty acids and cholesterol in the process of lipoperoxidation causes membrane permeability and fluidity changes with biological consequences. In addition, the intermediate products of lipoperoxidation (lipid hydroperoxides, malondialdehyde, 4-hydroxynonenal, isoprostanes) are not inert and can initiate secondary oxidative events. A significant correlation has been found between these products plasma concentration and several disorders like Alzheimer[23] or diabetes. The reactivity and functions of novel nitrated derivatives found after peroxynitrite-mediated lipoperoxidation are under study and their participation in cell signaling has been suggested[24].

4 Cytotoxicity of Peroxynitrite

4.1 Peroxynitrite-induced apoptosis

When peroxynitrite-induced cellular damage reaches a level that cannot be handled by the repair mechanisms, cells will undergo one of the basic cell death pathways, apoptosis or necrosis. Apoptosis is the "default" death pathway characterized, among other parameters, by a compact morphology, maintenance of plasma membrane integrity, mitochondrial depolarization, secondary oxidant production, activation of caspases (cysteinyl aspartate specific proteases) and oligonucleosomal DNA fragmentation[25]. Pryor had the first report that peroxynitrite can trigger apoptotic death. They have detected DNA fragmentation in peroxynitrite treated thymocytes[26]. Later, activation of caspase-3, a key player in the caspase cascade has also been detected in thymocytes and HL-60 cells[27]. Prototypical apoptosis models utilize apoptosis inducers such as tumor necrosis factor acting upon cell surface death receptors. Channeling the death signal from these receptors to apoptotic effector machineries is well

described[25]. However, it is not quite clear, how peroxynitrite triggers the apoptotic machinery. Mitochondria are likely sites for peroxynitrite induced apoptosis initiation. Mitochondria are now recognized as central organizators of apoptosis[25]. A characteristic sequence of events including opening of mitochondrial permeability transition pore, mitochondrial depolarization, secondary superoxide production, release of apoptotic mediators from the intermembrane space to the cytoplasm, takes place in apoptosing cells[25]. Furthermore, adenosine nucleotide translocator, a member of the permeability pore is also targeted by peroxynitrite[28]. The role of mitochondria in peroxynitrite-induced apoptosis is also supported by findings that bcl-2, a mitochondrial antiapoptotic protein inhibits peroxynitrite-induced apoptosis[29]. The cellular energetics may become compromised by peroxynitrite also via alternative mechanisms (e. g. inactivation of creatine kinase in cardiomyocytes) which may also contribute to peroxynitrite cytotoxicity[30].

4.2 Peroxynitrite-induced necrosis

It has been found that low concentrations of peroxynitrite trigger apoptosis, higher concentrations of the oxidant compromise the apoptotic machinery forcing the cells to die by necrosis[30]. Recently, a new method has emerged identifying an active element in oxidative stress-induced necrosis. According to method, degree of the activation of poly(ADP-ribose) polymerase-1 (PARP-1) determines the fate of the oxidatively-injured cells[31]. PARP-1 is activated by DNA strand breakage. Activated PARP-1 cleaves NAD^+ into nicotinamide and ADP-ribose and polymerizes the latter on nuclear acceptor proteins. Peroxynitrite-induced over activation of PARP consumes NAD^+ and consequently ATP culminating in cell dysfunction, apoptosis or necrosis. These findings indicate that PARP-1 activation diverts the default apoptotic process toward necrosis[31].

Moreover, peroxynitrite-induced DNA breakage activates PARP leading to NAD^+ and ATP depletion and consequently to necrosis. The concerted action of PARP-1 and PARG maintains a highly accelerated ADP-ribose turnover in peroxynitrite treated cells. As a result, NAD^+ becomes depleted in the cells leading to malfunctioning glycolysis, Krebs cycle, mitochondrial electron transport and eventually to ATP depletion[32]. The deterioration of cellular energetic status may play a central role in the "cell death switch" of PARP-1[33].

5 Conclusions

Peroxynitrite formed *in vivo* from superoxide and nitric oxide can mediate selective oxidation and nitration of biomolecules via direct or radical-dependent pathways. Depending on the levels and cellular sites of peroxynitrite produced, these oxidative modifications can lead to conformational changes, impaired functions, enzyme inactivation, or signaling pathways alterations, apoptotic or necrotic cell death and result in various diseases. Pharmacological approaches to ameliorate peroxynitrite-mediated drug toxicity could be focused on diminishing the flux of precursor radicals (nitric oxide and superoxide) or on scavenging the peroxynitrite formed.

Correspondence to:
Xu Zhang
Department of Biochemistry
Basic Medical College
Zhengzhou Univercity
Zhengzhou, Henan 450052, China
Email: cleaner 0369@yahoo.com.cn

References

1. Radi R, Peluffo G, Alvarez MN, Naviliat M, Cayota A. Unraveling peroxynitrite formation in biological system. Free Radic Biol Med 2001; 30: 463-88.
2. Denicola A, Souza JM, Radi R. Diffusion of peroxynitrite across erythrocyte membranes. Proc Natl Acad Sci 1998; 95: 3566-71.
3. Fries DM, Paxinou E, Themistocleous M, Swanberg E. Expression of inducible nitricoxide synthase and intracellular protein tyrosine nitration in vascular smooth muscle cells: role of reactive oxygen species. J Biol Chem 2003; 278: 22901-7.
4. Pryor WA, Squadrito GL. The chemistry of peroxynitrite: a product from the reaction of nitric oxide with superoxide. Am J Physiol 1995; 268: L699-L722.
5. Barlett D, Church DF, Bounds, PL, Koppenol WH. The kinetics of the oxidation of L-ascorbic acid by peroxynitrite. Free Radic Biol Med 1995; 18: 85-90.
6. Padmaja S, Squadrito GL, Lemercier JN, Cueto R, Pryor WA. Rapid oxidation of DL-selenomethionine by peroxynitrite. Free Radic Biol Med 1996; 21: 317-24.
7. Ischiropoulos H, Zhu L, Chen J, Tsai M, Martin J C, Smith CD, Beckman JS. Peroxynitrite-mediated tyrosine nitration catalyzed by superoxide dismutase. Arch Biochem Biophys 1992; 298:431-7.
8. Ramezanian MS, Padmaja S, Koppenol WH. Nitration and hydroxylation of phenolic compounds by peroxynitrite. Chem Res Toxicol 1996; 9: 232-7.
9. Douki T, Cadet J. Peroxynitrite mediated oxidation of purine bases of nucleosides and isolated DNA. Free Radic Res 1996; 24: 369-80.
10. Groves JT. Peroxynitrite: reactive, invasive and enigmatic. Curr Opin Chem Biol 1999; 3: 226-35.
11. Beckman JS, Koppenol WH. Nitric oxide, superoxide,

and peroxynitrite: the good, the bad, and ugly. Am J Physiol 1996; 271: C1424 – 37.
12. Takakura K, Beckman JS, MacMillan-Crow LA, Crow JP. Rapid and irreversible inactivation of protein tyrosine phosphatases PTP1B, CD45, and LAR by peroxynitrite. Arch Biochem Biophys 1999; 369: 197 – 207.
13. Okamoto T, Akaike T, Nagano T, Miyajima S, Suga M, Ando M, Ichimori K, Maeda H. Activation of human neutrophil procollagenase by nitrogen dioxide and peroxynitrite: a novel mechanism for procollagenase activation involving nitric oxide. Arch Biochem Biophys 1997; 342: 261 – 74.
14. Bryk R, Griffin P, Nathan C. Peroxynitrite reductase activity of bacterial peroxiredoxins. Nature 2000; 407: 211 – 5.
15. Moreno JJ, Pryor WA. Inactivation of alpha 1-proteinase inhibitor by peroxynitrite. Chem Res Toxicol 1992; 5: 425 – 31.
16. Alvarez B, Radi R. Peroxynitrite reactivity with amino acids and proteins. Amino Acids 2003;25, 295 – 311.
17. Greenacre SA, Ischiropoulos H. Tyrosine nitration: localisation, quantification, consequences for protein function and signal transduction. Free Radic Res 2001; 34: 541 – 81.
18. Crow JP, Ye YZ, Strong M, Kirk M, Barnes S, Beckman JS. Superoxide dismutase catalyzes nitration of tyrosines by peroxynitrite in the rod and head domains of neurofilament-L. J Neurochem 1997; 69: 1945 – 53.
19. Burney S, Caulfield JL, Niles JC, Wishnok JS, Tannenbaum SR. The chemistry of DNA damage from nitric oxide and peroxynitrite. Mutat Res 1999; 424: 37 – 49.
20. Satoh MS, Lindahl T. Role of poly(ADP-ribose) formation in DNA repair. Nature 1992; 356: 356 – 8.
21. Szabo C, Zingarelli B, O'Connor M, Salzman AL. DNA strand breakage, activation of poly (ADP-ribose) synthetase, and cellular energy depletion are involved in the cytotoxicity of macrophages and smooth muscle cells exposed to peroxynitrite. Proc Natl Acad Sci 1996; 93: 1753 – 8.
22. O'Donnell VB, Eiserich JP, Chumley PH, Jablonsky MJ, Krishna NR, Kirk M, Barnes S, Darley-Usmar VM, Freeman BA. Nitration of unsaturated fatty acids by nitric oxide-derived reactive nitrogen species peroxynitrite, nitrous acid, nitrogen dioxide, and nitronium ion. Chem Res Toxicol 1999; 12: 83 – 92.
23. Cecchi C, Fiorillo C, Sorbi S, Latorraca S, Nacmias B, Bagnoli S, Nassi P, Liguri G. Oxidative stress and reduced antioxidant defenses in peripheral cells from familial Alzheimer's patients. Free Radic Biol Med 2002; 33: 1372 – 9.
24. Lim DG, Sweeney S, Bloodsworth A, White CR, Chumley PH, Krishna NR, Schopfer F, O'Donnell VB, Eiserich JP, Freeman BA. Nitrolinoleate, a nitric oxide-derived mediator of cell function: synthesis, characterization, and vasomotor activity. Proc Natl Acad Sci 2002; 99: 15941 – 6.
25. Green D, Kroemer G. The central executioners of apoptosis: caspases or mitochondria? Trends Cell Biol 1998; 8: 267 – 71.
26. Salgo MG, Squadrito GL, Pryor WA. Peroxynitrite causes apoptosis in rat thymocytes. Biochem Biophys Res Commun 1995; 215: 1111 – 8.
27. Lin KT, Xue JY, Lin MC, Spokas EG, Sun FF, Wong PY. Peroxynitrite induces apoptosis of HL-60 cells by activation of a caspase-3 family protease. Am J Physiol 1998; 274: C855 – 60.
28. Vieira HL, Belzacq AS, Haouzi D, Bernassola F, Cohen I, Jacotot E, Ferri KF, El Hamel C, Bartle L M, Melino G, Brenner C, Goldmacher V, Kroemer G. The adenine nucleotide translocator: a target of nitric oxide, peroxynitrite, and 4-hydroxynonenal. Oncogene 2001; 20: 4305 – 16.
29. Virag L, Szabo C. Bcl-2 protects peroxynitrite-treated thymocytes from poly(ADP-ribose) synthase (PARS) independent apoptotic but not from PARS-mediated necrotic cell death. Free Radical Biol Med 2000; 29: 704 – 13.
30. Mihm MJ, Coyle CM, Schanbacher BL, Weinstein, DM, Bauer, JA. Peroxynitrite induced nitration and inactivation of myofibrillar creatine kinase in experimental heart failure. Cardiovasc Res 2001a; 49: 798 – 807.
31. Virag L, Szabo C. The therapeutic potential of poly (ADP-ribose) polymerase inhibitors. Pharm Rev 2002; 54: 375 – 429.
30. Virag L, Salzman AL, Szabo C. Poly(ADP-ribose) synthetase activation mediates mitochondrial injury during oxidant-induced cell death. J Immunol 1998; 161: 3753 – 9.
32. Berger SJ, Sudar DC, Berger NA. Metabolic consequences of DNA damage: DNA damage induces alterations in glucose metabolism by activation of poly (ADP-Ribose) polymerase. Biochem Biophys Res Commun 1986; 134: 227 – 32.
33. Ying W, Chen Y, Alano CC, Swanson RA. Tricarboxylic acid cycle substrates prevent PARP-mediated death of neurons and astrocytes. J Cereb Blood Flow Metab 2002; 22: 774 – 9.

Received March 14, 2006

Arsenic Compounds in Carcinogenesis: Cytotoxic Testing by Liver Stem Cells in Culture

Shen Cherng[1], Hongbao Ma[2], Jinlian Tsai[3]

1. *Graduate Institute of Electrical Engineering, Chengshiu University, Niausong, Kaohsiung, Taiwan 830, ROC*
2. *School of Medicine, Michigan State University East Lansing, MI 48823, USA*
3. *Graduate Institute of Occupational Safety and Health, Kaohsiung Medical University, Kaohsiung City, Taiwan 801, ROC*

Abstract: Much of the work conducted on adult stem cells has focused on the application for carcinogenesis. By using stem cell model and gap junctional intracellular communication (GJIC) assay for studying the role of arsenic compounds in carcinogenesis including the cytotoxicity comparison of arsenic (Ⅲ) oxide, arsenic (V) oxide, dimethyl arsenic acid and disodium methyl arsenate are demonstrated in this article. From cell surviving curve of human liver stem cell (HL1), rat epithelial cell (WB) and liver cancer cell line (Malhava cells) in culture, the doses and time period of the arsenic exposure for 50% cell surviving were obtained. Conclusively arsenite and arsenate significantly affected GJIC within the cells in 50% cell surviving dose dependent inhibition. [Life Science Journal. 2006;3(3): 45-48] (ISSN: 1097-8135).

Keywords: arsenate; carcinogenesis; cytotoxicity; gap junctional intracellular communication; stem cell

Abbreviations: BPE: bovine pituitary extract; DMA: dimethylarsinic acid; EGF: epidermal growth factor; FBS: fetal bovine serum; GJIC: gap junctional intracellular communication; MMA: monomethylarsonic acid; PKC: protein kinase C; SL/DT: scrape-loading/dye-transfer; TMAO: trimethylarsine oxide; WB: WB-F344 rat liver epithelial cells

1 Introduction

Arsenic is a known human carcinogen and being initiated different tumours in many sites of the body organs, such as skin, lung, liver, urinary bladder, prostate, and many others[1]. The adverse effects of arsenic are dependent on its chemical form and metabolism. Inorganic arsenicals were basically more acutely toxic than organic species since the methylation of inorganic arsenic was involved in the detoxification process[2]. However, more evidences indicate that the trivalent organic arsenicals being as metabolic products of inorganic arsenic can be more toxic than the parent compound[3,4]. It is well known that As(V) can be first reduced to As(Ⅲ) and As(Ⅲ) being produced by this reduction or from direct ingestion can be methylated primarily to pentavalent organic arsenicals including monomethylarsonic acid [MMA(V)] and dimethylarsinic acid DMA(V). MMA and DMA are the predominant metabolites of inorganic arsenic. However, DMA may be further methylated to. The forms of arsenic being exposed either directly or via metabolism may complicate toxic and carcinogenic mechanisms of action. Drinking ground water was reported being arsenic contaminated by electroplating industry severely in regions of west-south seashore of Taiwan fifteen years ago. At that time, people exposed into drinking water in high concentration of arsenic (~300 ppb) being affected to lung cancer probability was four times, bladder cancer probability was eight times, skin cancer probability was twenty times, prostate cancer probability was three times more than in low concentration (~0.1 ppb)[5]. However, no publication expresses that any cell or animal model can successfully propose the mechanism of arsenic being initiated cancers.

In a cell, six connexin 43 subunits oligomerze in the Golgi apparatus into a connexon, called hemi channel and be transported to plasma membrane of the cell. Before pairing process, hemi channels are closed to avoid leakage of cellular contents and entry of extra-cellular materials. During the pairing of connexons and aggregation into plaques at the plasma membrane, connexin 43 is phosphorylated at least twice and connexons are attracted to those located on the adjacent cells. Two connexons join in an end-to-end manner to form a complete channel.

The channel aggregate into large gap junction plaques open to connect two cells for cell-to-cell communication and is called gap junctional intracellular communication (GJIC)[6], which can be modulated by environmental factors, such as effects of arsenic compounds. Since the function of the GJIC, cultured cells coupled together *in vitro*. The scrape loading dye transfer technique can identify the GJIC modulation by observing the diffusive range of the fluorescence[7]. The varied diffuse range of Lucifer yellow fluorescence expresses the cellular response under the exposure of arsenic toxic compounds. Since GJIC is affiliated with many pathological endpoints, GJIC modulation can be a good factor to evaluate the cellular response to the reaction of chemical toxicities. In this article, a liver stem cell model is proposed to investigate the order of cell toxicity of arsenic compounds by the Lucefer yellow dye mobility of the GJIC within the cells in a concentration and time dependent manner.

2 Materials and Methods

2.1 Reagents

Keratinocyte serum-free medium, Dulbecco's modified Eagle medium, modified Eagle's minimum essential medium, recombinant human epidermal growth factor (EGF), bovine pituitary extract (BPE), fetal bovine serum (FBS), penicillin, streptomycin, trypsin-EDTA and Trizol reagent were purchased from Invitrogen (GIBCO-Invitrogen Corporation, Carlsbad, CA, USA). Arsenic (Ⅲ) oxide, arsenic (V) oxide, dimethylarsenic acid, disodium methyl arsenate, N-acetyl-L-cysteine, DMSO, L-ascorbic acid 2-phosphate and nicotinamide were obtained from Sigma Chemical Co. (St Louis, MO, USA). Anti-THY1.1, AFP, albumin, and Oct4 monoclonal antibodies were purchased from Santa Cruz (Santa Cruz, CA, USA).

2.2 Cell culture

The medium used to develop the putative human liver stem/progenitor cell cultures (HL-1) is a modified MCDB 153 (Keratinocyte-SFM, GIBCO - Invitrogen Corporation, Carlsbad, CA, USA) supplemented with N-acetyl-L-cysteine (NAC) (2 mM) and L-ascorbic acid 2-phosphate (Asc 2P) (0.2 mM) (referred to as K-NAC medium). WB-F344 rat liver epithelial cells (WB), originally isolated in the laboratory of Joe W. Grisham, National Cancer Institute, Bethesda, MD, USA, were kindly provided by Chia-Cheng Chang (Michigan State University, East Lansing, MI, USA). Cells were grown in modified Eagle's minimum essential medium (Formula No. 03-5045EF, Gibco, Rockville, MD, USA), supplemented with 5% FBS. The hepatoma cells (Malhava) were grown in Dulbecco's modified Eagle medium supplemented with 10% FBS. All cell cultures were incubated at 37 ℃ in incubators supplied with humidified air and 5% CO_2.

2.3 Treatment of cells with arsenic compounds

HL-1, WB and Malhava cells were grown to approximately 80% confluence and then treated with arsenic (Ⅲ) oxide, arsenic (V) oxide, DMA and MMA for one day. The culture medium was changed before treatment with arsenic compounds. Arsenic compounds were dissolved in distilled water and then applied to the cells at carious concentrations in medium. The control cells were either not treated with any arsenic chemicals.

2.4 GJIC assay

GJIC was measured using scrape-loading/dye-transfer (SL/DT)[8]. The image pro plus software (Media Cybernetics, Georgia, USA) was used for scanning the size of the fluorescence area along the scrape line on monolayers to quantitate the levels of GJIC.

2.5 Statistical analysis

All data were presented as the mean group value ± standard error of the mean (SEM). The data were analyzed using one-way analysis of variance (ANOVA). Significant differences between control and arsenic compounds treatment were evaluated using Dunnett's method. The level of statistical significance was set at $P < 0.05$.

3 Results

3.1 Effects of arsenic exposure to cell toxicity

Tests of different concentrations of the 24 hours inorganic arsenic exposure to three different liver cells, HL-1 liver stem cell, WB cell line and Malhava cell line appear the results being depicted in Figure 1. Cell toxicity is to be in the order of As(Ⅲ) > As(V) > MMA > DMA for all cell lines and arsenic-dose dependent. In the arsenic (Ⅲ) concentration of 5 ppb, no WB cells can be found in surviving but 50% HL-1 cells was survived. In comparison, the cell toxicity of As(Ⅲ) is forty times more than As(V) and two hundred times more than DMA or MMA. The cell line came from different sources has different sensitivity to the arsenic toxicity. Normal liver cell (WB cell line) can only be survived less in 50% under concentration of As(Ⅲ) at 1.25 ppb. However, under the same dosage, 83% of the HL-1 liver stem cell can be survived and no effects to the cells of Malhava cell line.

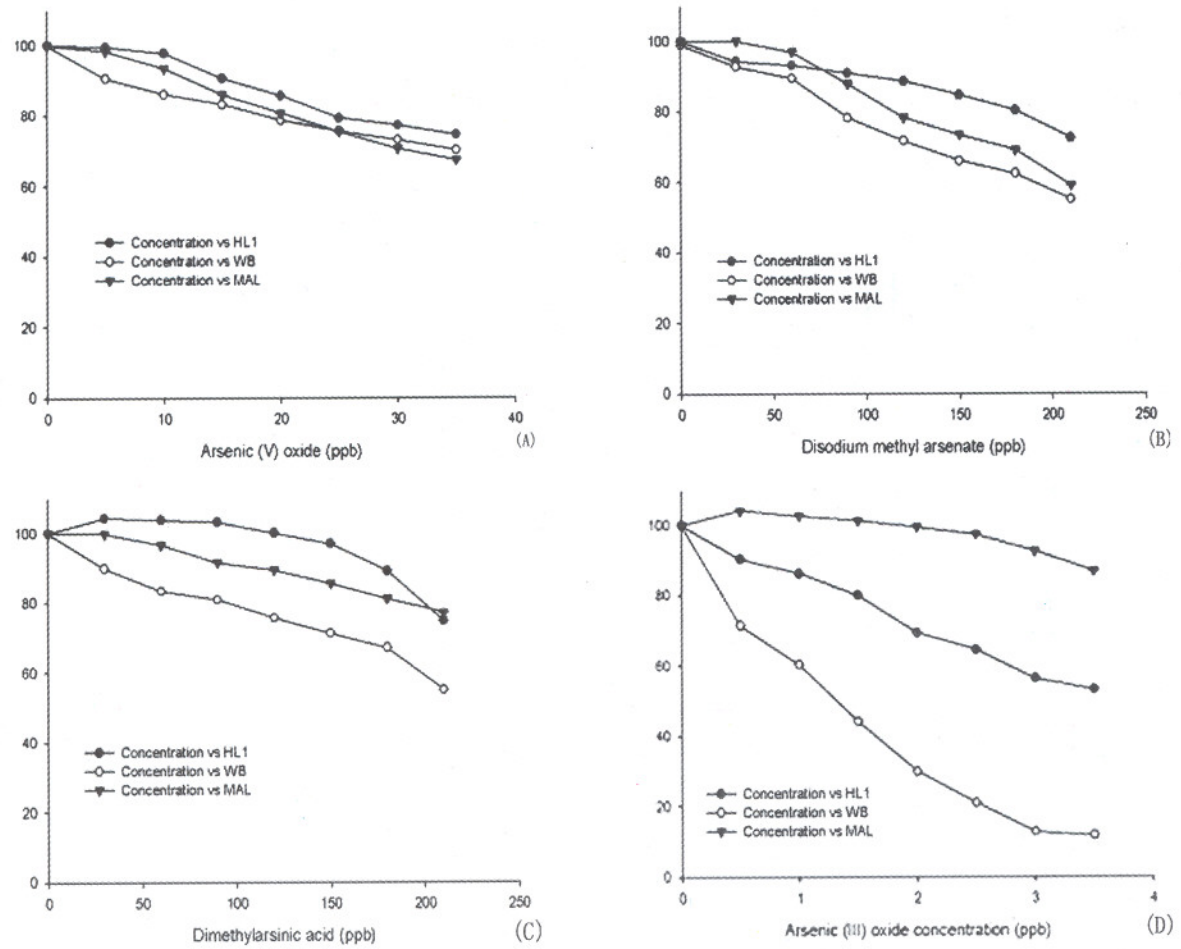

Figure 1. Inhibition of the proliferation of HL1, WB and Malhare cells by arsenic compounds. The cells were treated with various concentrations of arsenic compounds for 24 h. (A) arsenic (V) oxide, (B) disodium acid-treated oxide, (C) methyl arsenate dimethylarsenic, (D) arsenic (Ⅲ), and untreated HL1, WB and Malhava cells from quaternary determinations.

3.2 Effects of arsenic exposure to cell lines by expression of GJIC

Under the arsenic As(Ⅲ) exposure of 60 hours at 25 μg/ml, the GJIC within WB cells was completely inhibited. In Figure 2, it depicts the statistic difference($P<0.05$) of the GJIC inhabitation among As(Ⅲ) arsenic exposure at concentration of 50, 100 and 200 μg/L for cell toxic test of WB cells being exposed 24 hours. The arsenic As(Ⅲ)-dose dependent correlation is thus can be expressed *vs*. the inhabitation of GJIC being exposed to 12, 24 and 60 hours. The arsenic As(V)-dose dependent GJIC correlation also is depicted under the concentration of 5, 10, 30 and 50 μg/ml for WB cell being exposed to 10 hours. Under the treatments repeated for DMA and MMA in contrary, same GJIC inhabitation response required dosage is about 500 to 700 times more than As(Ⅲ).

4 Discussion

The homeostasis is mediated by cell to cell GJIC being associated with cell differentiation, proliferation and apoptosis[8]. Thus, the factors affected connexin gene, such as the mutant, reduced expression, degrading, changing of the transcription of connexin protein, can alter the GJIC from normal to block process and create the cancer promotion phase of carcinogenesis within the cells. In addition, gene mutant and epigenetic events must be happened in a multi-stage and multi-mechanism process in carcinogenesis. The metabolism of the arsenic compounds is in liver for the mammals. The catabolism of As(V) to As(Ⅲ) will continue being demethylated to MMA and then to DMAA. This pathway is not reversible and poisoned to the organs. The observation of the inhibition of the GJIC of the WB cells reflected the effect of consequence of cell toxicity of the arsenic exposure at dose and

time dependent manner. The mediated connexin protein has no doubt played an important role in carcinogenesis[9] under the arsenic exposure. The early research of the peroxisome proliferator activated receptor (PPAR) revealed the interaction of peroxisome proliferators being mediated by inhibition of PPAR under As(Ⅲ) exposure[10]. However, the connection of PPAR and GJIC is still unknown. No published papers or reports suggested the mechanism or model for the study. Deng demonstrated As(Ⅲ) and As(V) can inhibit the GJIC within skin fiberblast cells through the interaction of increasing of protein kinase C (PKC)[11]. Tsuchiya reported that both As(Ⅲ) and As(V) can inhibit the GJIC of the cells of V79 in dose dependent manner[12]. The toxicity concentration of As(Ⅲ) is about 10 times more than As(V) exposure. However, in our experiments, the DMA and MMA are not very dose sensitive to the inhibition of GJIC within WB cells.

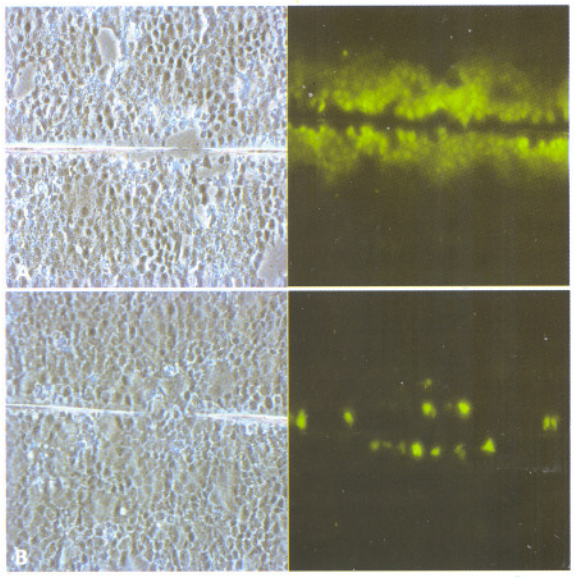

Figure 2. Gap junctional intercellular communication in WB cells as measured by the SL/DT technique. Cells were untreated (A) and 25 μg/L arsenic (Ⅲ) oxide (B) for 60 hours.

5 Conclusion

GJIC assay revealed WB cells being cancerized after enough time and dose arsenic exposure. This report depicted again that arsenic compound must be the carcinogen in carcinogenesis. Based upon the basic theory of the GJIC, the possible mechanism in arsenic carcinogenesis is that arsenic compound blocks the connexin gene expression and its phosphorylation to inhibit the GJIC of the normal cells. Further and advance study of this mechanism will be investigated later.

Correspondence to:
Shen Cherng, P.E., Ph.D., M.D.
Associate Professor
Graduate Institute of Electrical Engineering
Chengshiu University
Niausong, Kaohsuing, Taiwan, 833, ROC
Telephone: 86-7732-0489
Email: cherng@msu.edu

References

1. IARC. Arsenic in drinking water. International Agency for Research on Cancer Monographs on the Evaluation of Carcinogenic Risk to Humans, Vol. 84. IARC Press, Lyon, 2004; 269－477.
2. Aposhian HV. Enzymatic methylation of arsenic species and other new approaches to arsenic toxicity. Annu Rev Pharmacol Toxicol 1997; 37: 397－419.
3. Petrick JS, Jagadish B, Mash EA, Aposhian HV. Monomethylarsonous acid (MMA(Ⅲ)) and arsenite: LD (50) in hamsters and *in vitro* inhibition of pyruvate dehydrogenase. Chem Res Toxicol 2001; 14:651－6.
4. Styblo M, Del Razo LM, Vega L. Comparative toxicity of trivalent and pentavalent inorganic and methylated arsenicals in rat and human cells. Arch Toxicol 2000; 74: 289－99.
5. Chiang HS, Guo HR, Hong CL, Lin SM, Lee EF. The incidence of bladder cancer in the black foot disease endemic area in Taiwan. British Journal of Urology 1993; 71:274－8.
6. Trosko JE, Ruch RJ. Cell-cell communication in carcinogencic. Frontiers in Bioscience 1998; 3:208－36.
7. Upham BL, Weis LM, Trosko JE. Modulated gap junctional intercellular communication as a biomarker of PAH epigenetic toxicity: Structure-function relationship. Environ. Health Perspect 1998; 106(Suppl. 4): 975－81.
8. Loewenstein WR, Kanno Y. Intercellular communication and the control of tissue growth: lack of communication between cancer cells. Nature 1966; 209: 1248－9.
9. Yamasaki H, Mesnil M, Omori Y, Mironov N, Krutovskikh V. Intercellular communication and carcinogenesis. Mutat Res 1995; 333: 181－8.
10. Wauson EM, Langan AS, Vorce RL. Sodium arsenite inhibits and reverses expression of adipogenic and fat cell-specific genes during *in vitro* adipogenesis. Toxicological Sciences 2002; 65: 211－9.
11. Deng F, Guo X. Effect of inorganic arsenic on gap junctional intercellular communication between human skin fibroblasts. Chinese Journal of Preventive Medicine 2001; 35:51－4.
12. Tsuchiya T, Tanaka-Kagawa T, Jinno H, Tokunaga H, Sakimoto K, Ando M, Umeda M. Inorganic arsenic compounds and methylated metabolites induce morphological transformation in two-stage BALB/c 3T3 cell assay and inhibit metabolic cooperation in V79 cell assay. Toxicological Sciences 2005; 84:344－51.

Received April 8, 2006

Stable Expression of the *hBDNF* Gene in CHO Cells

Yaodong Zhao, Haifeng Zhang, Weihua Sheng, Yufeng Xie, Jicheng Yang,
Li Miao, S Sarode Bhushan, Jingcheng Miao

Department of Cell and Molecular Biology, Medical School of Suzhou University, Suzhou Industry Park, Jiangsu 215123, China

Abstract: objective. To transfect the *hBDNF* (human brain-derived neurotrophic factor) gene into CHO cells, establish a stable expression system, and to detect the biological activity of the expressed hBDNF protein. **Methods.** Liposomes were used to mediate the transfection, and RT-PCR, Western-blotting and MTT method were to detect. **Results.** *hBDNF* mRNA was detected in the transfected CHO cells, and hBDNF protein, promoting PC12 cells' growth, can be detected in the supernatant. **Conclusion.** The stable expression system of hBDNF-CHO was successfully established, which could produce hBDNF protein with biologic activity. [Life Science Journal. 2006;3(3):49-52] (ISSN: 1097-8135).

Keywords: hBDNF; eucaryon transfection; stable expression; function

Abbreviations: BDNF: brain derived neurotrophic factor; CGM: complete growth medium; CHO cell: Chinese hamster ovary cell; COS-7 cell: African green monkey SV40-transformed kidney fibroblast cell; CS: calf serum; SM: screening medium

1 Introduction

The brain derived neurotrophic factor (BDNF) belongs to the neurotrophin family[1], and plays important roles in the development and maturation process of nervous system. It is good for the regeneration, recovery and protection of neurocytes from degeneration after trauma. The most recent researches show that BDNF has high biologic activities upon the survival and development of many types of neurons, including the septal cholinergic neuron[2], mesencephalic dopaminergic neuron[3], and motor neuron in cornu anterius medullae spinalis[4]. They are potential in the treatment of nervous system disease. Our department successfully introduced the *hBDNF* gene into Chinese hamster ovary cell (CHO) cells by gene-engineering technology and cell-engineering technology; the hBDNF protein secreted by the hBDNF-CHO cells has a certain biologic activity, which establishes the experimental base of biologic hBDNF.

2 Materials and Methods

2.1 Materials

The plasmid of pTracer^{TM}-EV/V5-His-hBDNF was constructed by our department, CHO cells PC12 cells and *E. coli* DH5α all were from our department. Calf serum (CS) and cation liposome were purchased from GIBCO (USA); zeocin was from Invitrogen (America); thiazolyl blue was from Sigma (USA). Primers were synthesized by Shenggong Shanghai. Rabbit polyclonal antibodies against hBDNF were purchased from Santa Cruz Biotechnology, and the goat anti-rabbit antibodies together with its substrate were purchased from Shanjing, Shanghai.

2.2 Methods

2.2.1 *hBDNF* gene's introduction into CHO cells: The day before transfection, 2×10^5 CHO cells were seeded per well of a 6-well plate in 2 ml complete growth medium (CGM) with serum and incubated at 37 ℃ in a 5% CO_2 incubator until cells were 40% - 60% confluent overnight. Solution A: diluting 10 μg DNA (plasmids pTracer^{TM}-EV/V5-His or plasmids pTracer^{TM}-EV/V5-His) to 100 μl with medium DMEM without serum; solution B: diluting 15 μg cation liposomes to 100 μl with the same medium as above. Solution A and B were gently mixed and incubated at the room temperature for 30 min to form DNA-liposome complexes. For each transfection, 0.8 ml medium without serum was added to the tube containing the complexes, then mixed gently and overlaid onto the rinsed CHO cells. The cells with complexes subsequently were incubated at 37 ℃ with 5% CO_2. After 18 - 24 hours the medium was replaced with fresh CGM containing 10% CS.

2.2.2 Screening for positive clones: seventy-two hours after transfection we began to screening the positive clones by replacing the CGM with screening medium (SM), which was made up with 10% CS, DMEM and 800 μg/ml *zeocin*. After most cells were killed we changed the SM into main

medium, which was made up with CGM containing 10% CS and 200 μg/ml *zeocin*. Forty days later we got the two cloned lines i. e. CHO-pTracer™-EV/V5-His and CHO-pTracer™-EV/V5-His-hBDNF.

2.2.3 RT-PCR: The total RNA of the two cloned lines of CHO-pTracer™-EV/V5-His and CHO-pTracer™-EV/V5-His-hBDNF were respectively extracted, then the first-strand cDNA was synthesized from the mRNA template using reverse transcriptase and subsequently were amplified by PCR with above-mentioned primers as the following program: 95 ℃ for 5 min; degeneration 95 ℃ for 30 sec, primers annealing 52 ℃ for 40 sec, extension 72 ℃ for 45 sec for 35 cycles and a final extension 72 ℃ for 5 min. Finally 10 μl PCR products and DNA Marker were electrophoresed on 1.5% agarose gel.

2.2.4 Concentration dialysis and filtration the supernatants of these CHO cells: The above two cell lines were cultivated on large scale, and 72 hours later their supernates were collected, and concentrated 20 – 50 times by Polyethylene glycol 6000. Afterwards, the concentrated solution in bag filters were dialyzed with PBS and filtrated sterilization.

2.2.5 Western-blot analysis: 100 μl concentrated supernatants of the two kinds of CHO cells were respectively mixed with 100 μl 2 × loading buffer, and the two mixtures were boiled for 5 min, then followed with SDS-PAGE electrophoresis, incubation of the blot with primary antibody in the antibody binding buffer overnight at 4 ℃, washing the blot 5 times in TBST buffer, incubate the blot with second antibody, washing the blot 5 times in TBST buffer again in order, at last the blot was developed following DAB (p-dimethylaminoazobenzene) substrate instruction.

2.2.6 Biological activity detection

Promote PC12 cells' growth: The density of PC12 cells was adjusted to 4×10^5/ml by 2% DMEM, then 1 ml of such cells' suspension and 1.7 ml 2% DMEM were added to every small square bottle, subsequently we added 0.3 ml concentrated supernatant of pTracer™-EV/V5-His-hBDNF-CHO cells into the experimental group, 0.3 ml concentrated supernatant of pTracer™-EV/V5-His-CHO cells into the control group and 0.3 ml 2% DMEM into the blank group. All these small bottles of cells were cultivated at 37 ℃ with 5% CO_2. Seventy-two hours later the PC12 cells were observed and counted.

Activity detection by MTT assay: A 96-well-plate was divided into a blank group, a control group and an experiment group. Every well in the blank group contained 50 μl PC12 cells at the density of 1.2×10^5/ml and 50 μl 2% DMEM complete medium in each well; each well in the control group contained 50 μl PC12 cells at the density of 1.2×10^5/ml and 50 μl pTracer™-EV/V5-His-CHO cells' concentrated supernatant, which was diluted with 1:2, 1:4, 1:8, 1:16, 1:32, 1:64; and every well in the experiment group contained 50 μl PC12 cells also at the density of 1.2×10^5/ml and 50 μl pTracer™-EV/V5-His-hBDNF-CHO cells' concentrated supernatants, which was also diluted by 1:2, 1:4, 1:8, 1:16, 1:32, 1:64. Then the plate was put into a incubator at 37 ℃ with 5% CO_2. 72 hours later, 10 μl 5 mg/L thiazolyl blue was added into each well, and 3 – 4 hours later 100 μl 10% acidation SDS were added into all wells to terminate reaction, then the A_{570} value of each well was measured after 12 – 14 hours. Finally, all these date were analyzed by SPSS statistics software.

3 Results

3.1 *hBDNF* gene's introduction into CHO cells

72 hours after transfection CHO cells were observed under fluorescence microscope, and sporadic cells with green fluorescence could be seen (Figure 1). After 40 days' screening the CHO cells were again observed under fluorescence microscope, all cells were found to emit green fluorescence (Figure 2). This proved that the plasmids had been transfected into CHO cells and the GFP (green flurescence protein) gene in the plasmid of pTracer™-EV/V5-His could normally be expressed.

3.2 RT-PCR analysis

The products of RT-PCR were electrophoresed on 1.5% agarose gel, and a band can be seen near 750 bp. This demonstrated the gene *hBDNF* introduced into CHO cells could be effectively transcribed into mRNA (Figure 3).

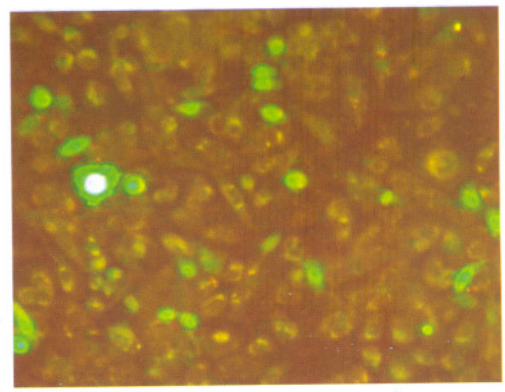

Figure 1. CHO cells 72 h after transfection

3.3 Westen-blot analysis

A brown band appeared on the lane of experiment group (EG), but no strap appeared on the control group's (CG), which illustrated that the target protein had been expressed in pTracer^{TM}-EV/V5-His-hBDNF-CHO cells, but not in the pTracer^{TM}-EV/V5-His-CHO cells (Figure 4).

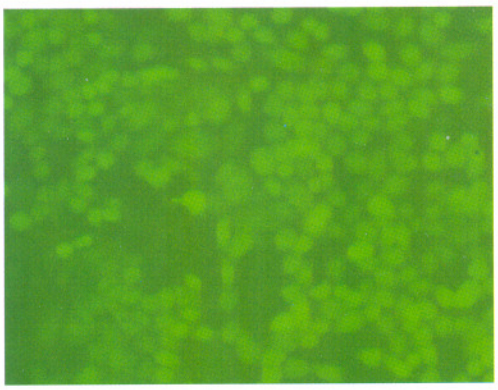

Figure 2. CHO cells after 40 days' screening

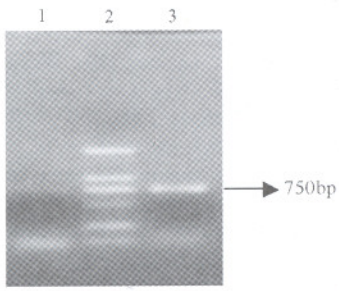

Figure 3. Lane 1 and 3 respectively showed the RT-PCR results of cells pTracer^{TM}-EV/V5-His-CHO and pTracer^{TM}-EV/V5-His-hBDNF-CHO; Lane 2 showed DNA Marker

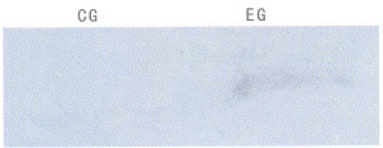

Figure 4. CG and EG respectively showed the Western-blot results of enriched supernatants of the two kinds of CHO cells: pTracer^{TM}-EV/V5-His-CHO and pTracer^{TM}-EV/V5-His-hBDNF-CHO

3.4 Activity detection for the eukaryotic expression product of *hBDNF* gene

3.4.1 Promoting PC12 cells' growth: After incubation for 72 hours, cells in the blank group (BG) adhered and stretched, but in small number. Cells in vacant plasmid group adhered, stretched were a little more than blank group. Cells in experiment group adhered, stretched were in high density (Figure 5A, B, C). The total number in each bottle was 1.8×10^5, 2.5×10^5 and 4.0×10^5, respectively.

3.4.2 Activity detection by MTT assay: The A_{570} value of the blank group was 0.137 ± 0.009, the A_{570} values of the vacant plasmid group (VG) and the experiment group (EG) in different dilute strength were shown in Table 1.

3.4.3 Statistics analysis results: The t test of the A_{570} value between two groups of EG and VG shows $P<0.01$, ($\bar{x}\pm s, n=3$).

4 Discussion

BDNF, a kind of protein, which was first found and isolated from a pig's brain in 1982 by German neurobiologist Barde and his colleagues, can promote neurons' growth; generally its active form exists as a dimeride combined by non-covalent bonding. The binding of BDNF to its receptor tyrosine kinase (TrkB) leads to the dimerization and autophosphorylation of tyrosine residues in the intracellular domain of the receptor and subsequent activation of cytoplasmic signal transmission[5-6]. At present, we get BDNF mainly from tissue's isolation and purification or recombined gene's expression. Large-scale preparation of these natural hBDNF proteins directly isolated from tissues is very difficult, in spite of their better activities.

The BDNF proteins, expressed by prokaryocytes through the technology of recombination *in vitro*, have relatively lower activities because these synthetic polypeptides cannot properly fold. However, proteins expressed in eukaryocytes are more approximate to the natural hBDNF protein and have higher activities. There are some merits for those proteins expressed in eukaryocytes than in prokaryocytes: first, acquiring more elaboration, e.g. α-helix and β-pleated sheet, glycosylation and phosphorylation; second, acquiring mature mRNA by recognizing and eliminating the introns of exogenous genes; third, eukaryocytes transfected with target genes can stably express target proteins even after frezeeing and revivals.

We have constructed the plasmid pTracer^{TM}-EV/V5-His-hBDNF. By comparing the difference of promoting PC12 cells' growth between the concentrated supernatants of the two kinds of CHO cells, pTracer^{TM}-EV/V5-His-hBDNF-CHO and pTracer^{TM}-EV/V5-His-CHO, we concluded that CS and hBDNF could promote PC12 cells' growth synergistically, for CS in both kinds of enriched supernatants were in some higher concentration. And PC12 cells grow better in VG than in BG, but worse

Table 1. Comparison between the EG and VG in different dilute strength

1/64(A)	1/32(B)	1/16(C)	1/8(D)	1/4(E)	1/2(F)	
EG	0.273±0.009	0.27±0.037	0.283±0.021	0.310±0	0.350±0.014	0.493±0.0286
VG	0.163±0.009	0.173±0.005	0.207±0.009	0.227±0.009	0.247±0.025	0.363±0.024

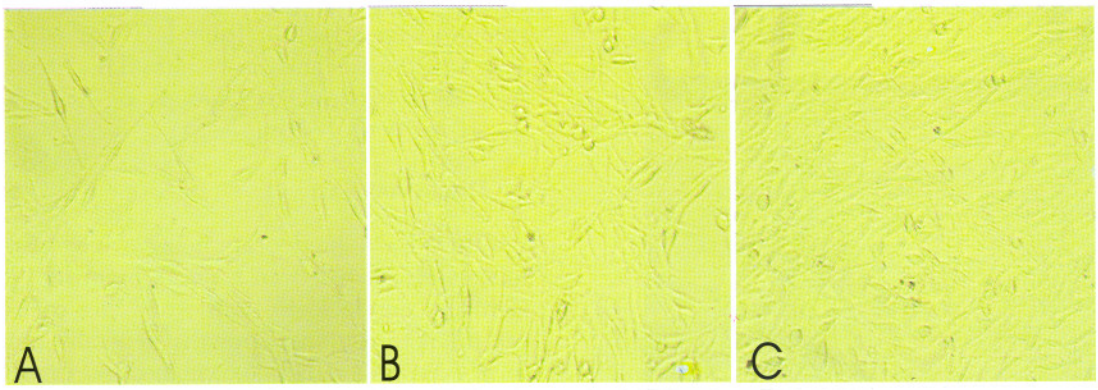

Figure 5. A: cells in the blank group B: cells in the vacant plasmid group C: cells in the experiment group

than in EG. In addition, we selected CHO cells as host cells but not African green monkey SV40-transformed kidney fibroblast cell (COS-7) cells, it was because that exogenous genes' expressions in CHO cells are stable and long-term after screening with G418, but not in COS-7 cells, which are only used to be the transient expression host cells. As a result, gene-engineering pharmacy prefers CHO cells than COS-7 cells.

Our subject establishes the experiment base for further research on developing these kind bioengineered medicines and treatments for some nervous system problems.

Correspondence to:
Jingcheng Miao
Department of Cell and Molecular Biology
Medical School
Suzhou University
Suzhou, Jiangsu 215123, China
Telephone: 86-512-6588-0107
Email: jcm@suda.edu.cn

References

1. Maness LM, Kastin AJ. The neurotrophins and their receptors: structure function and neuropathology. Neuroscience and Bio-behavioral Reviews 1994; 18(1):143-59.
2. Phillips HS, Hans JM, Laramee GR. Widespread expression of BDNF but not NT-3 by target areas of basal forebrain cholinergic neurons. Science 1990;250 (4978):290-4.
3. Ostergaard K, Jones SA, Hyman C, *et al*. Effects of donor age and brain-derived neurotrophic factor on the survival of dopaminergic neurons. Neuro Clin 1996;142(2):340-50.
4. Yan Q, Elliott J, Snider WD. Brain-derived neurotrophic factor rescues spinal motor neurons from axotomy induced cell death. Nature 1992; 360(6406):753-5.
5. Barde YA, Edger D, Thoenen H. Purification of a new neurotrophic factor from mammalian brain. EMBOJ 1982; 1(5): 549-53.
6. Leibrock J, Lottspeich H, Hohn A, *et al*. Molecular cloning and expression of brain derived neurotrophic factor. Nature 1989; 341:149-52.

Received May 13, 2006

OL-PCR for Site-directed Mutagenesis of Full-length cDNA of DEN-2

Wei Zhao[1], Beiguo Long[2], Zhuqiong Hu[2], Hao Zhou[2], Li Zhu[1], Hong Cao[2]

1. *Institute of Virology School of Public Health and Tropical Medicine, Southern Medical University, Guangzhou, Guangdong 510515, China*
2. *Department of Microbiology, School of Public Health and Tropical Medicine, Southern Medical University, Guangzhou, Guangdong 510515, China*

Abstract: Aim. To generate the oligonucleotide-directed mutants of the full length cDNA clone of dengue 2 virus. **Methods.** Two DNA fragments with single point mutation (E62 or E203) were amplified with four pairs of oligonucleotide primers by OL-PCR and then cloned into pGEM-T vectors respectively. The recombinant T vectors, TB62 and TB203, were digested with *Cla* I + *Sph* I and *Sph* I + *Nhe* I, then ligated to pDVWS501 with T4 DNA ligase respectively. The recombinant plasmids, TB62 and TB203, were sequenced. **Results.** The results of DNA sequencing indicated that TB62 and TB203 with point mutation were obtained. **Conclusion.** OL-PCR could be applied to site-directed mutagenesis of large plasmid (>16 Kb). [Life Science Journal. 2006;3(3):53-57] (ISSN: 1097-8135).

Keywords: dengue 2 virus; full-length cDNA clone; site-directed mutagenesis; OL-PCR

1 Introduction

The site-directed mutagenesis *in vitro* to target DNA sequence is a common-used way of molecular biology, but it is still a big problem to mutagenesize a large plasmid at present. What researchers always explore, under the operated conditions, is to maintain the sequences other than the sites of mutation intact. In this research, by using the technique of OL-PCR, the site-directed mutagenesis to a large plasmid of 16 kb has been established successfully. According to the sequenced results, there has been a consistence between the sequences of the mutagenesized plasmid and the designed ones.

By comparing the amino acids sequences of protein E of 3 dengue virus strains in our laboratory, 2 loci discovered, which locate in site 62 and 203 of protein E respectively, may be relevant to suckling mice neurovirulence. When the E62 is Glu and the E203 is Asp, the virulence is decreased; While the E62 is Lys and the E203 is Trp, the virulence is increased. pDVWS501 is a plasmid containing the full-length cDNA of D2-MON501, and RNA *in virto* transcripts from pDVWS501 could be recovered to infectious virus (MON501) upon electroporation into BHK cells. Then, the infected suckling mice with MON501 appeared to be the encephalitis symptom. By OL-PCR, we want to mutagenesize the amino acids of E62 and E203 in pDVWS501, and then mutated MON501 would not show neurovirulence on suckling mice. In a word, we hope this research would lay a base for further study on the influence of the 2 amino acids upon suckling mice neurovirulence.

2 Materials and Methods

2.1 Strains and plasmids

The pDVWS501 is a plasmid which contains the full-length cDNA clone of DEN-2, and this plasmid was kindly provided by Dr. Wright of Monash University in Australia. AF038403 is the Accession Number of complete genome sequence of D2-MON501. The *E. coli* DH5a was stored in our laboratory and the clone vector pGEM-T was purchased from Promega Company.

2.2 Enzymes and other reagents

The restriction enzymes were purchased from Biolab Company. The T4-DNA ligase was purchased from Promega Company. The IPTG and X-gal were purchased from Huamei Biology Engineering Company. The Pwo DNA polymerase, expand high fidelity PCR system and DNA recoverying kit were provided by Boeringer Mannheim Company. QIAGEN plasmid midi kit was purchased from QUIAGEN Company.

2.3 Primers

The primers were designed with the DNAstar's Quickpri software package and synthesized by Sangon Co. Ltd. The New3 and New4

hold the E62 site with point mutation (GAG→AAA). The New5 and New6 carry the E203 site with point mutation (AAT→GAC). In Table 1, the italics with underlines in the primers sequences are the ones after point mutagenesis.

Table 1. Oligonucleotide primers used for amplification

Primer name	Genome position*	Primer sequence(5′→3′)
New-1	1638-1656	CGGGCCTCTTCGCTATTAC
New-3	2968-2992	GGTCAGCTTTGC TTTTATACAGTAC
New-4	2968-2992	GTACTGTATA AAAGCAAAGCTGACC
New-7	3026-3042	GGAGAACCCAGCCTAAA
New-5	3391-3413	GCCAAGCTTT GTCTTCCATTTGC
New-6	3391-3413	GCAAATGGAA GACAAAGCTTGGC
R1566	3400-3423	CTGTGCACCAGCCAAGCTTTATTT
New-2	4388-4411	TGAAGCTAGCTTTGAAGGGGATTC

* Genome positions are given according to the sequence of pDVWS501

2.4 Plasmid PCR

With pDVWSK501 as templates and New1, New3, New4, R1566, New7, New5, New6, New2 as primers, we've amplified the segments which were named as pm1, pm2, pm4 and pm5 by PCR. These segments have been purified by DNA recovery kit.

PCR reaction system: 10 mmol/L dNTPs 0.6 μl, upstream primer 1.5 μl, downstream primer 1.5 μl, plasmid as template (about 10 ng/μl) 1 μl, 10× buffer 3 μl and water 22 μl. After denaturation of 2 min at 94 ℃, we added 0.5 μl Pwo DNA Polymerase into the PCR reaction system, then starting PCR cycling. Reaction parameters are as followed: ① pm1 and pm4:94 ℃ for 15 sec, 55 ℃ for 30 sec, 72 ℃ for 1.25 min, after 25 cycles, 72 ℃ continuously lasted for 7 min; ② pm2 and pm5:94 ℃ for 15 sec, 55 ℃ for 30 sec, 72 ℃ for 45 sec, after 25 cycles, 72 ℃ continuously lasted for 7 min.

2.5 OL-PCR

After making electrophoresis with 1% agarose gel and estimating the content of pm1, pm2 pm4 and pm5, we diluted the four segments to 0.5 ng/μl, respectively and then mixed pm1 and pm2 together, so did pm4 and pm5. PCR reaction system: 10 mmol/L dNTPs 0.6 μl, templates (pm1 and pm2 or pm4 and pm5) 2 μl, 10× buffer 3 μl and 21.9 μl water. After denaturation of 2 min at 94 ℃, 0.25 μl expand high fidelity DNA polymerase was put into the above mixture, then followed PCR cycling. Reaction parameters: 94 ℃ for 15 sec, 55 ℃ for 1 min, 72 ℃ for 2 min, after 3 cycles, 72 ℃ lasted for 5 min. After the primer New1 1 μl and R1566 1 μl or New7 1 μl and New2 1 μl were respectively added into the PCR mixture above and denatured of 2 min at 94 ℃, 0.25 μl expand high fidelity DNA polymerase was added into the before system then running the second PCR cycles. Reaction parameters: 94 ℃ for 15 sec, 55 ℃ for 1 min, 72 ℃ lasting for 3 min, after 25 cycles, 72 ℃ continuously kept for 7 min.

2.6 Constitution of plasmid T-TB62 and T-TB203

After purifying the pm3 and pm6 fragments obtained by OL-PCR, according to the specification of pGEM-T vector system kit, the two segments were ligated to pGEM-T vectors and transformed into DH5a with these recombiant plasmids, and the positive clones of T-TB62 and T-TB203 were selected. We identified the recombinant plasmids by digesting them with endorestriction enzymes and ran the PCR. The recombinant plasmids were sequenced with automatic-sequenator of ABI377 version.

2.7 Constitution and clone of plasmids TB62 and TB203

T-TB62 was digested with *Cla* I + *Sph* I for 2 h, therefore, we've got the segments tb62 about 1463 bp through purifying. Another plasmid T-TB203 was digested with *Sph* I + *Nhe* I for 2 h and then tb203 about 1167 bp was purified. Plasmid pDVWS501 was mono-digested by *Cla* I for 3 h and then being purified. The purified segments were mono-digested again with *Sph* I for 3 h and then the longer segments ZT-203 were purified. pDVWS501 plasmid was digested with *Sph* I + *Nhe* I at the same time for 1.5 h. In order to digest the pDVWS501 completely, we added *Sph* I + *Nhe* I into the previous mixture once again and lasted for another 1.5 h. Consequently the longer fragment ZT-203 was acquired and purified. The puri-

fied segment ZT62 was amplified by PCR with New7 and New5 as primers and another purified segment ZT203 was amplified with New4 and R1566 as primers. If the results were negative, the following proceure would be done.

Tb-62 and ZT-62, tb-203 and ZT-203 were respectively diluted to 3:1 in moles and ligated with T4 DNA ligase. With the recombinant plasmids before, DH5a was transformed again and the positive clones were selected. TB62 and TB203, the full-length cDNA clone of DEN-2 with point mutation should be tested for their correctness with digestion and plasmid PCR.

2.8 Sequencing

Plasmids TB62 and TB203 were extracted with QIAGEN plasmid midi kit and sequenced with automatic-sequenator of ABI377 version.

3 Results

The establishment of the method to dengue 2 virus full-length cDNA site-directed mutagenesis bases on the facts that, in the plasmid pDVWS501 with the cDNA, both ends of the E62 have mono-digestion sites of *Cla* I and *Sph* I; both ends of the E203 have mono-digestion sites of *Sph* I and *Nhe* I.

3.1 Constitution and clone of plasmid T-TB62 and T-TB203

Firstly with pDVWS501 as templates 2 groups of short segments were amplified: pm1 and pm2, pm4 and pm5, which were 1355 bp, 456 bp, 1021 bp, 388 bp in length, respectively and partly overlapped one another. Then pm1 and pm2, pm4 and pm5 were mixed in equal quantity separately. Long templates were acquired by the first PCR and the long segments pm3 and pm6 were obtained through the second PCR running, which were 1786 bp and 1386 bp in length, respectively (Figure 1). After pm3 and pm6 were cloned into pGEM-T vectors separately, the recombinant plasmids T-TB62 and T-TB203 were obtained. The two plasmids were transformed into DH5a. Running PCR to plasmid T-TB62 with primers New1 and R1566, a segment was about 1786 bp in length. After the two plasmids were digested with *Cla* I and *Sph* I, 2 segments of 1463 bp and 3323 bp in length separately were got. Running PCR to the plasmid with primers New7 and New2, the target segment about 1386 bp in length. After the same plasmid was digested with *Sph* I and *Nhe* I, other two target segments of 1167 bp and 3219 bp in length respectively were got (Figure 2). The sequencing results indicated that there were expected shifts only in mutated loci and the other loci were the same as before by comparing T-TB62 and T-TB203 with pDVWS501.

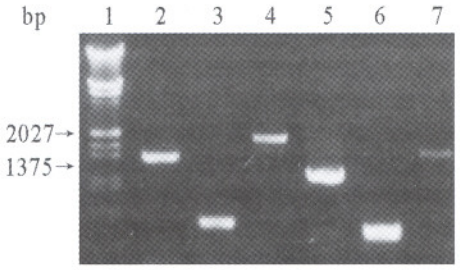

Figure 1. DNA fragments with point mutation amplified by OL-PCR
Lane 1: λDNA/*Eco*RI + *Hind* Ⅲ marker; Lane 2: pm1; Lane 3: pm2; Lane 4: pm3; Lane 5: pm4; Lane 6: pm5; Lane 7: pm6

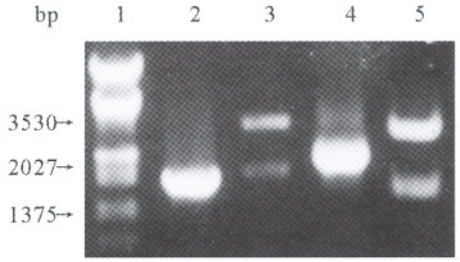

Figure 2. Identification of recombinant plasmids T-TB62 and T-TB203
Lane 1: λDNA/*Eco*RI + *Hind* Ⅲ marker; Lane 2: T-TB203 PCR assay; Lane 3: T-TB62 digested with *Cla* I + *Sph* I; Lane 4: T-TB62 PCR assay; Lane 5: T-TB203 digested with *Sph* I + *Nhe* I

3.2 Constitution and clone of plasmids TB62 and TB203

After pDVWS501 and T-TB62 were respectively digested with *Cla* I and *Sph* I and pDVWS501 and T-TB203 were respectively digested with *Sph* I and *Nhe* I, the same adhesive-ends of vectors and inserting-segments were got. After the inserting-segments were ligated to the vectors *in vitro*, the recombinant plasmids were transformed into DH5α and later the positive clones were screened with LB/Amp(+) plates. Recombinant plasmids were extracted from the picked positive clones and were mono-digested with *Cla* I, then a segment of 16151 bp in length were got. We've run PCR to plasmid TB62 with primers New6 and New2 and obtained another segment of 1356 bp. After TB203 was mono-digested with *Nhe* Ⅰ, a segment was got, which was 16151 bp in length. PCR were run to TB203 with New6 and New2 as primers, and a fragment of 1021 bp were acquired. All of the work above might show the success in constituting the full-length cDNA clone TB62 and TB203 of dengue 2 virus with point mutation (Figure 3).

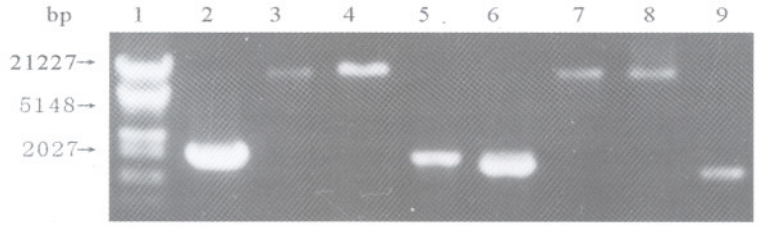

Figure 3. Identification of recombinant plasmids TB62 and TB203
Lane 1: λDNA/*Eco*RI + *Hind* Ⅲ marker; Lane 2: purified tb62; Lane 3: purified ZT62; Lane 4: TB62 digested with *Cla* I; Lane 5: TB62 PCR assay; Lane 6: purified tb203; Lane 7: purified ZT203; Lane 8: TB203 digested with *Nhe* I; Lane 9: TB203 PCR assay

3.3 Sequencing

The results of sequencing indicated that we've succeeded in constituting the full-length cDNA clones TB62 and TB203 with point mutation in sites 62 and 203 of protein E in plasmid pDVWS501.

4 Discussion

As for site-directed mutagenesis on the DNA segments larger than 1 kb, it is the most difficult problem to keep high fidelity. Among the DNA polymerase, T4 DNA polymerase, owing to its strong exonuclease activity of single and double-strand DNA 3′→5′, is the most suitable candidate for site-directed mutagengsis *in vitro*.

There are many kits for site-directed mutagengsis on plasmids. But some of them need particular vectors, which therefore depend on convenient restriction endonuclease sites in the mutated DNA segments; some of them utilize vectors designed by researchers. All of these kits are designed by similar principles that after synthesizing all sequences of the target plasmid *in vitro* by T4 DNA polymerase and ligating them together with T4 DNA ligase, the characteristic shifts of plasmid, which were easily picked out, are used as screening indicators. So the larger the plasmid is, the more difficult it is that mutagenesized-plasmid is obtained and the fidelity to those sequences except for mutation loci is guaranteed.

The aim of this research was to solve the problem of site-directed mutagenesis to plasmid pDVWS501 which is about 16 kb in length. By comparing this plasmid's zymogram, we discovered that there separately was a mono-restriction enzyme site nearby the ends of the 2 mutagenesis loci, which were 1463 bp and 1167 bp in distance respectively. But all of these restriction enzyme sites were not suitable for the point mutagenesis kits of Promega Company and the plasmid itself was beyond the applying confines of point mutagenesis kits. So, we selected 2 kinds of DNA polymerase and adopted the method of OL-PCR in this research. Pwo DNA Polymerase, whose accuracy is 10 times stronger than that of Taq DNA Polymerases, is of strong 3′→5′ exonuclease activity and more than this, its PCR product has no "A" on its 3′ ends – that are blunt ends, which avoids the mismatch and disturbance to the reaction of OL-PCR. Expand™ High Fidelity Sys is of part 3′→5′ exonuclease activity, therefore, the PCR product is the mixture with the blunt ends and 3′ ends with "A", which can be conveniently cloned into pGEM-T vectors. As is stated above, with the peculiarity of these 2 kinds of polymerase in our research, we've enhanced the fidelity to OL-PCR as possible as we could, and hence paved the way for ligating T-vectors. With expand high fidelity PCR system, if 20 effective cycles would be carried out to amplifying the segments of 1 kb, there were 92% segments identical to the templates in theory. Although the accuracy rate of these 2 kinds of DNA polymerase was lower than that of T4 DNA polymerase, owing to the amplified segments being greatly shortened *in vitro*, it still relatively lowered the error rate during replication. In this experiment, 2 clones were selected separately from T-TB62 and T-TB203 for sequencing and the expected results were got.

In the course of site-directed mutagenesizing designed by this research, there was a biggest shortcoming that was, except for the directly sequencing, no other simple ways for identifying the plasmid before and after its mutagenesizing. So, there may be false-positive results in the latter work when digesting the vectors were incompletely. In order to avoid the false-positive results, the restriction endonuclease was applied, intentionally extended the time of digestion (3 h), then another time restriction endonuclease was added at the midterm (1.5 h) which could digest the plasmid completely. After digested and purified, the plasmid was identified by PCR. The negative result proved the complete digestion of plasmid, which

would perfect the whole course of experiment and secured the comparatively high mutation rate. At last, TB62 and TB203 were transformed into DH5a and from this transformation 6 clones were picked out for identification of PCR and digestion. Among which, there were 5 and 4 positive clones respectively, and from these positive ones, 2 clones were respectively chosen to determinate their mutation sites. As a result, expected mutation sites were finally obtained.

The method of site-directed mutagenesis established by us suits for all successfully constituted plasmids. But the only limitation of this method is the 2 ends of the sites of point-mutagenesizing must have mono-digestion sites. If the amplified segments by OL-PCR were smaller than 2 kb, there were relatively high fidelity and mutation efficiency in the process of mutagenesizing.

Acknowledgments

This work was funded by Natural Science Foundation of Guangdong Province of China, No. 32833, Medical Science & Technology Foundation of Guangdong Province, No. B2003091 and Science & Technology Project of Guangzhou City, No. 2004Z2-E0214.

Correspondence to:
Hong Cao
Department of Microbiology
School of Public Health and Tropical Medicine
Southern Medical University
Guangzhou, Guangdong 510515, China
Email: gzhcao@fimmu.com

References

1. Ho SN, Hunt HD, Horton RM, *et al*. Site-directed mutagenesis by overlap extension using polymerase chain reaction. Gene 1989; 77:51－9.
2. Zhao W, Hu ZJ, Yang J, *et al*. The genomic sequence determination and virulent gene analysis of the E protein of three dengue 2 virus strains isolated in China. Chin J Zoonoses 2001; 17: 10－4.
3. Gualano RC, Pryor MJ, Cauchi MR, *et al*. Identification of a major determinant of mouse neurovirulence of dengue virus type 2 using stably cloned genomic-length cDNA. J Gen Virol 1998; 79:437－46.

Received March 10, 2006

An Overview on Bacterial Kidney Disease

Eissa AE[1], Elsayed EE[2]

1. Department of Fish Diseases and Management, Faculty of Veterinary Medicine, Cairo University, Giza, Egypt.

2. Department of Pathobiology and Diagnostic Investigation, College of Veterinary Medicine, Michigan State University, East Lansing, Michigan, 48824, USA

Abstract: Bacterial Kidney Disease (BKD) caused by a Gram-positive bacterium, *Renibacterium salmoninarum* (*R. salmoninarum*), is a systemic disease that threatens the expansion of both cultured and wild salmonids worldwide. BKD is virtually reported wherever salmonids are present, and continue to pose a threat to salmonids worldwide. Further, problems associated with BKD epizootics include high mortality rate, low growth rate, increased susceptibility to other diseases such as furunculosis and cold water disease (CWD) are another aspect of the problem. Moreover, despite the expanding risk of BKD, the pathogenesis of *R. salmoninarum* infection has only been partially elucidated, hindering the progress of competent preventive and control measures to efficiently combat this disease. For all the above mentioned reasons, scientific work and current research need to be continually updated to benefit the researchers, aquaculture sector and fisheries. The current review provides the most recent update of research work on BKD, discusses the agent and the disease it causes, with emphasis on the bacterium-host interactions in a trial for better understanding of the disease and its epizootiology. [Life Science Journal. 2006;3(3):58-76] (ISSN: 1097-8135).

Keywords: *Renibacterium salmoninarum*; bacterial kidney disease; salmon

Abbreviations: BKD: bacterial kidney disease; CWD: cold water disease; ECP: extracellular products; FAT: fluoresence antibody tests; KDM: kidney disease medium; MKDM: modified KDM; SKDM: selective KDM

1 Historical Perspectives

Bacterial Kidney Disease (BKD), caused by the Gram-positive bacterium *Renibacterium salmoninarum* (*R. salmoninarum*), is a systemic disease that afflicts salmonid fish populations worldwide. The condition was originally described as the Dee Disease because it was first observed among Atlantic salmon (*Salmo salar*) from Aberdeenshire Dee and the River Spey in Scotland in 1930 (Anonym, 1933; Smith, 1964). Other synonyms of the disease include Kidney Disease, Corynebacterial Kidney Disease and Salmonid Kidney Disease (Fryer and Sanders, 1981). Few years later, Belding and Merrill (1935) described a very similar infection that caused losses in brook trout (*Salvelinus fontinalis*), brown trout (*Salmo trutta*) and rainbow trout (*Oncorhynchus mykiss*) reared in a hatchery in Massachusetts, USA. By 1953, due to serious outbreaks, BKD had become a limiting factor in rearing brook trout, brown trout, rainbow trout, chinook salmon (*Oncorhynchus tshawytscha*), coho salmon (*Oncorhynchus kisutch*) and sockeye salmon (*Oncorhynchus nerka*) in many hatcheries in the State of Washington (Earp *et al*, 1953). In the following year, the disease was found in the feral salmon in the same state (Rucker *et al*, 1954). In 1955, BKD spread to the Great Lakes basin with the introduction of salmonines and their products from the Pacific Northwest (Allison, 1958). Reports from Canada linked the disease to mortalities in wild salmonines from Nova Scotia (Pippy, 1969; Paterson *et al*, 1979) to British Columbia (Evelyn *et al*, 1973; 1981). By 1988, the disease became widespread in Europe (England, France, Finland, Germany, Iceland, Italy, Spain, Turkey and Yugoslavia), North America (USA and Canada), and Japan (reviewed in Bullock and Herman, 1988; Fryer and Lannan, 1993). The disease continued its spread to Chile (Sanders and Barros, 1986) and there is a current consensus among fish health professionals that BKD is virtually prevalent in all parts of the world where wild or cultured salmonines exist (European Commission, 1999).

2 The Pathogen

2.1 Nomenclature and current classification of the etiological agent

Based on Gram stain properties, morphology, the causative bacterium was suggested to be a member of the genus *Corynebacterium* by Ordal and

Earp (1956) and subsequently by Smith (1964). Sanders and Fryer (1980) later refuted this classification based on the absence of mycolic acid, guanine plus cytosine (G + C) content of DNA, cell wall sugar and amino acid compositions of the peptidoglycan cell wall layer. The authors proposed that this bacterium formed a single species in a new genus *Renibacterium* and they identified the bacterium as *R. salmoninarum* (Sanders and Fryer, 1980). Sequencing of the 16S rRNA from *R. salmoninarum* (Gutenberger *et al*, 1991) and recent evaluation of G + C content (Banner *et al*, 1991) placed the organism in the Gram-positive eubacterial subdivision of actinomycetes. *Arthrobacter* and *Micrococcus* spp. are the closest relatives to *R. salmoninarum*.

2.2 Cell morphology

R. salmoninarum is a short rod (0.3 − 1.0 by 1 − 1.5 μm), Gram-positive, non-sporulated, non-capsulated, non-motile, and non acid-fast bacterium that is arranged in pairs (diplobacilli) and rarely as short chains (Sanders and Fryer, 1980). *R. salmoninarum* consists of two regions; a central region filled with lightly stained filaments (represent DNA) and a peripheral region filled with small, electron dense ribosomes (Young and Chapman, 1978).

2.3 Isolation, culture and cultural characteristics

R. salmoninarum is a slow growing organism (Sanders and Fryer, 1980). Earp *et al* (1953) cultured the bacterium on an artificial medium for the first time from infected kidney tissues on a medium that consisted of fish extract, glucose, yeast extract and meat infusion in agar. The authors achieved limited growth with first appearance of colonies after more than two weeks of incubation. When the same authors used minced chick embryo tissues embedded in 1% agar or Dorset's Egg medium, they achieved better growth. Addition of 0.05% to 0.1% L-cysteine to the Dorset's Egg medium has further enhanced the growth of *R. salmoninarum* upon primary isolation (Ordal and Earp, 1956). The authors noted that trypticase blood agar could be used for secondary cultures and bacterial maintenance. Based on years of research, Ordal and Earp (1956) formulated the Kidney Disease medium (KDM1) which consisted of: tryptose 1.0%, beef extract 0.3%, NaCl 0.5%, yeast extract 0.05%, cysteine-hydrochloride 0.1%, human blood 20 v/v and agar 1.5%. They designated this medium as "Cysteine Blood Agar Medium". While testing the *in vitro* sensitivity of *R. salmoninarum* to a large number of therapeutics, Wolf and Dunbar (1959), achieved fair growth on cysteine supplemented Mueller-Hinton medium (MH). This modified MH medium became the medium of choice for the growth of *R. salmoninarum* for several years (Bullock *et al*, 1974).

Evelyn (1977) modified Ordal and Earp's KDM1 by replacing human blood, tryptose and beef extract with 20% fetal bovine serum and peptone and designated the modified medium as KDM2. To reduce the time needed for primary isolation, Evelyn *et al* (1989) added 25 μl of heavy inoculum of *R. salmoninarum* culture (commonly known as a nurse culture) to the center of KDM2 plates. The authors reported that this modification has accelerated bacterial growth in primary cultures. Further, Evelyn *et al* (1990) were able to achieve more consistent growth of the primary culture by replacing the nurse culture with 25 μl of filter-sterilized *R. salmoninarum* spent medium. The major drawbacks of KDM2 medium, however, were the high cost and presence of serum proteins, which hampered the identification of proteins of bacterial origin.

A number of serum-free media for *R. salmoninarum* growth have also been formulated. For example, Embley *et al* (1982) described a serum-free, semi-defined growth medium that supported secondary, but not primary, growth of *R. salmoninarum*. Daly and Stevenson (1985) formulated the Charcoal Agar Medium in which they substituted activated charcoal for serum. Starliper *et al* (1998) compared the performance of 13 serum-free media and 1 serum-supplemented media for the growth of *R. salmoninarum* isolates and found that there were no significant differences among the 14 medium formulations used when mean cell counts were compared after 10, 20, 30 days incubation.

To control growth of other bacteria from fish lesions, Austin *et al* (1983) incorporated four antibiotics (Cycloheximide, D-cycloserine, Oxolinic acid and Polymyxin B) to the KDM2 medium and reduced the volume of serum from 20% to 10% (designated selective KDM or SKDM). By these modifications, the authors significantly reduced bacterial contaminants, a matter that facilitated the selected growth of *R. salmoninarum* from clinical and environmental samples. Our current lab experience (Eissa, 2005) suggested that the modification of SKDM by incorporating 1% Spent medium into the agar enhanced the growth of the *R. salmoninarum* colonies, shortened the period of incubation, and minimized the growth of contaminating bacteria.

R. salmoninarum colonies are creamy (non-

pigmented), shiny, smooth, round, raised, entire, and 1 – 2 mm in diameter on KDM2 after incubation at 15 °C for 20 days (Austin and Austin, 1999). On cysteine supplemented solid media, old colonies (i.e. 12 weeks) appeared extremely granular due to crystallization of cysteine, while in both culture media; some *R. salmoninarum* strains produced a uniform turbidity whereas others flocculated out of suspension (Austin and Austin, 1999). The organism grows slowly at 5 °C, 22 °C and optimally at 15 °C but there was no growth at 37 °C (Smith, 1964).

2.4 Preservation of cultures

Several methods have been used to preserve different species of actinomycetes including *Streptomyces*, *Actinomyces* and *Renibacterium* species. For long term preservation, methods such as lyophilization (Hopwood and Ferguson, 1969), storage under liquid nitrogen (Pridham and Hesseltine, 1975) were successfully used. Bacterial cells can also be preserved in diluted glycerol (10% – 20% v/v) and frozen at – 20 °C, but thawing, and freezing cycles can affect cell stability and viability (Wellington and Williams, 1979). To overcome this disadvantage, Feltham *et al* (1978) stored bacteria on glass beads in 10% (v/v) glycerol at – 76 ℃. The glass beads allowed removal of small samples without thawing the entire culture, which was advantageous for long-term preservation (Wellington and Williams, 1979). Preservation of small inocula of *R. salmoninarum* in KDM2 (Evelyn *et al*, 1977) or peptone saline (Starliper *et al*, 1997) and storage at – 80 °C were successfully used.

2.5 Biochemical characteristics

The organism is cytochrome oxidase negative, catalase positive, proteolytic and cysteine HCl is required for its growth (Ordal and Earp, 1956; Smith, 1964; Sanders and Fryer, 1980). Interestingly, *R. salmoninarum* isolates from different sources are identical in their biochemical characteristics (Austin *et al*, 1983; Goodfellow *et al*, 1985; Bruno and Munro, 1986a), but the result for a given test can vary depending upon the testing system used. Thus, the organism is positive for the gelatinase and DNase reactions by standard methods (Bruno and Munro, 1986a), but it was negative for these characters by the API-ZYM system (Goodfellow *et al*, 1985). The organism is β-hemolytic on media supplemented with blood (Bruno and Munro, 1986a). The organism can liquefy gelatin, degrade Tween (20 – 60), and hydrolyze casein. The bacterium is negative for esculin hydrolysis, DNase, urease, nitrate reduction, phosphatase, methyl red, indole test and carbohydrate utilization test (Table 1).

Table 1. Summary of the morphological and biochemical characteristics of *R. salmoninarum*

Test	Criteria	Notes
Gram stain	+	
PAS (Periodic Acid Schiff) stain	+	
Zeihl-Nielsen (Acid Fast) stain	–	Non acid fast
Arginine hydrolysis	–	
Bile solubility	–	
Agar hydrolysis	–	
Amylase	–	
Carbohydrate utilization	–	
Casein hydrolysis	+	
Catalase	+	
Cytochrome oxidase	–	
DNase	+	(–) By API – ZYM*
Esculin hydrolysis	–	
Esterase	–	
Gelatin liquefaction	+	(–) By API – ZYM*
Hemolytic activity	β hemolytic	Complete clearance zone around bacteria
Indole test	–	
Methyl Red	–	
Nitrate reduction	–	
Phosphatase	–	
Tween-20, 40 and 60 Hydrolysis	+	
Tween-80 hydrolysis	–	
Urease	–	

ABI – ZYM* is a bacterial enzymes based assay used for the specific identification of different bacteria.

2.6 Antibiotic susceptibility

R. salmoninarum isolates are sensitive to chloramphenicol, erythromycin, novobiocin, streptomycin, sulfamerazine, and tetracycline (Wolf and

Dunbar, 1959; Austin and Rodgers, 1980), carbenicillin, and cephaloridine (Goodfellow *et al*, 1985). *R. salmoninarum* is also sensitive to enrofloxacin (Hsu *et al*, 1994), tiamulin, cefazolin (Bandin *et al*, 1991) and azithromycin (Rathbone *et al*, 1999). Furthermore, the organism is resistant to D-cycloserine, oxolinic acid (4 μg/ml), polymyxin β and cycloheximide (Wolf and Dunbar, 1959; Goodfellow *et al*, 1985).

2.7 Antigenic characteristics and virulence factors

R. salmoninarum is an obligate intracellular pathogen that is able to invade all types of fish cells particularly phagocytic cells (Gutenberger *et al*, 1997; Ellis, 1999). The ability of *R. salmoninarum* to invade phagocytes or other cells depends upon certain virulence determinants (Gutenberger *et al*, 1997; Ellis 1999; Piganelli *et al*, 1999). It was demonstrated that *R. salmoninarum* secretes a number of extracellular products (ECP) that possess proteolytic, hemolytic and DNA degradation activities *in vitro* (Austin and Rodgers, 1980; Bruno and Munro, 1986a). When crude or precipitated culture supernatants were injected into Atlantic salmon fingerlings, 80% – 100% mortalities were reported (Shieh, 1988), but Bandin *et al* (1991) were unable to reproduce this finding using untreated culture supernatants. A 65-kDa *R. salmoninarum* zinc metalloprotease-like protein has been extracted from *R. salmoninarum* ECP that possesses hemolytic activities against a number of fish and mammalian erythrocytes. The encoding gene of the *R. salmoninarum* ECP with hemolytic activity was designated as hly (Grayson *et al*, 1995). *R. salmoninarum* secretes a water-soluble, heat stable, hydrophobic cell surface 57 kDa protein (p57) that is believed to be the major virulence determinant of this bacterium (Getchell *et al*, 1985). *In vitro*, purified p57 exhibited both hemolytic (Daly and Stevenson, 1990) and leucoagglutinating (Wiens and Kaattari, 1991) properties. Hamel (2001) reported that *R. salmoninarum* isolates differed in their pathogenicity to salmonids, a finding that correlated positively with the amount of surface associated p57.

Challenge of susceptible fish with non-auto-agglutinating strains of *R. salmoninarum* caused significantly lower mortality than auto-agglutinating strains (Daly and Stevenson, 1990). Soluble *R. salmoninarum* surface proteins possess immunosuppressive action against the salmonid specific antibody response (Turaga *et al*, 1987), which was attributed not only to the p57 protein, but also to a 22-kDa surface protein (Fredriksen *et al*, 1997). Starliper *et al* (1997) compared a number of strains of *R. salmoninarum* isolated from chinook and coho salmon from different regions in North America for virulence. The authors found that virulence differed among the used isolates and concluded that isolates retrieved from Michigan weirs in the late 1980s were the most virulent.

2.8 Molecular and genetic diversity

Although the biochemical uniformity (Bruno and Munro, 1986a) and phylogenetic homology of *R. salmoninarum* strains (Gutenberger *et al*, 1991), a minimal molecular diversity was detected among strains isolated from different parts in the world (Alexander *et al*, 2001). Alexander *et al* (2001) succeeded in differentiation between isolates of *R. salmoninarum* based on PCR amplification and length polymorphism in the tRNA intergenic spacer regions (tRNA -ILPs). Moreover, a genetic diversity was detected among 40 North American isolates by using the multilocus enzyme electrophoresis (MEE) assay with the highest genetic diversity detected in strains isolated from chinook and coho salmon spawners returning to the Little Manistee river weir in Michigan (Starliper, 1996). In particular, Michigan isolates showed a higher variation in succinate dehydrogenase and esterase loci.

3 The Disease

3.1 Disease course

Despite the fact that BKD develops slowly, progress of the disease depends on environmental factors such as water temperature (Sanders *et al*, 1978; Fryer and Sanders, 1981; Bullock and Herman, 1988), host factors (Evenden *et al*, 1993), and *R. salmoninarum* strain virulence (Starliper *et al*, 1997).

3.1.1 External signs

Affected fishes manifest a wide range of external lesions as well as behavioral changes that might vary according to the species, age of the fish affected and the virulence of the *R. salmoninarum* strain (Fryer and Sanders, 1981; Bullock and Herman, 1988; Evenden *et al*, 1993). Erratic swimming behavior, exophthalmia, superficial blebs of the skin, cavitations in muscles and deep abscesses all over the body surface have been reported in affected fish (Belding and Merrill, 1935; Smith, 1964; Fryer and Sanders, 1981; Bullock and Herman, 1988). The blebs and cavitations might contain a white to yellowish or hemorrhagic fluid (Bullock and Herman, 1988). Ascitis and peticheal hemorrhages in muscles and fins were also reported (Belding and Merrill, 1935; Earp *et al*, 1953; Evelyn, 1993). In very rare cases, the external

signs of the disease in chinook and coho salmon might only be manifested by exophthalmia with the accumulation of infective fluid containing large amount of the bacteria, pus and necrotic tissue in the enlarged eyes (Bullock and Herman, 1988).

3.1.2 Internal lesions

Kidneys of affected fishes are usually swollen and exhibit white foci that contain leucocytes, bacteria, and host cell debris (Figure 1) (Fryer and Sanders, 1981). In advanced cases the kidneys appear mostly grayish in color, the spleen may increase in size and the liver appears very pale in color (Woods and Yasutake, 1956; Fryer and Sanders, 1981). The most typical clinical lesions associated with BKD are the presence of scattered nodules of various sizes over the surface of the kidneys, spleen and liver (Belding and Merrill, 1935; Snieszko and Griffin, 1955; Klontz, 1983). In some cases, peticheal hemorrhages were noticed in the muscles lining the peritoneum with ascitic fluid accumulation (Ferguson, 1989). An opaque membrane (pseudomembrane) that covers internal organs was reported, especially in fish maintained at a temperature below 9 °C (Snieszko and Griffin, 1955; Bell, 1961; Fryer and Sanders, 1981). The pseudomembrane consists of fibrin and leucocytes (Smith, 1964). Similar membranes occur in trout at higher temperatures (12 – 13 °C) (Bullock and Herman, 1988). Hemorrhages with white or yellow viscous fluid in the hindgut and peticheal hemorrhages were often found in the peritoneum of infected Atlantic salmon (Smith, 1964).

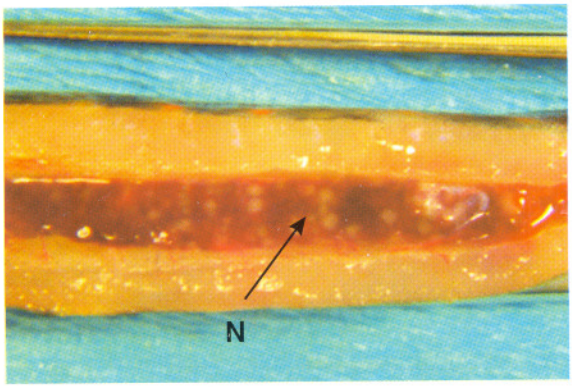

Figure 1. An Iron River brook trout fingerling with BKD. The kidney is swollen with multiple creamy-whitish nodules (N). The above case is from an outbreak of BKD that killed thousands of hatchery raised Iron River brook trout fingerlings in May 2003.

3.1.3 Histopathology

The initial histopathological description by Belding and Merrill (1935) indicated that the kidney as the major organ affected by the *R. salmoninarum* infection. All infected brook trout and brown trout exhibited microscopic lesions in the kidney, and to a lesser extent in the liver and spleen. Lesions were chronic in nature with multiple granulomas that resemble those noticed in mammalian tuberculosis (Figure 2) (Snieszko and Griffin, 1955; Wood and Yasutake, 1956). Fibrotic lesions were also noticed in kidneys, spleen, liver and intestines of the infected fish with proliferating fibroblasts forming distinct nodules that coalesced to form large masses of affected tissues (Woods and Yasutake, 1956). The granulomatous lesions apparently arose in the connective tissue stroma between the parenchymal cells of various organs (Woods and Yasutake, 1956; Jansson, 2002). It is believed that the granulomas are formed as a result of macrophages activation (Secombes, 1985) followed by its adherence to each other forming epithelioid appearance and then the fusion of a few number of these activated macrophages to form giant cells (Secombes, 1985). Both, giant cells and activated macrophages release large amounts of lytic enzymes into the surrounding tissues leading to necrosis at the central part of the granuloma (Bruno, 1986; Jansson, 2002). Interestingly, bacteria can occur intracellularly or extracellularly in the granulomas or necrotic foci (Bruno, 1986; Bullock and Herman, 1988). The hematopoietic tissue of the anterior kidney appeared to be affected firstly, followed by extensive damage to the excretory part of the kidneys (Woods and Yasutake, 1956; Jansson, 2002). Kidney pathology may contain eosinophilic granules in proximal tubules (Young and Chapman, 1978). Massive myocarditis (Wood and Yasutake, 1956), meningitis, and encephalitis (Speare, 1997) were recorded in some salmonids. In the liver, histopathological changes take the form of granulomatous nodules in the connective tissue stroma between the cords of the hepatic cells (Woods and Yasutake, 1956).

3.2 Susceptibility

There are a number of observations indicating that salmonid species and even different strain of the same species can differ in their susceptibility to BKD. For example, coho salmon of three different transferrin genotypes (AA, AC and CC) differed in resistance to experimental infection with *R. salmoninarum* (Suzumoto *et al*, 1977). Also, three populations of chinook salmon from different rivers, showed various mortality rates to experimental infection with *R. salmoninarum*. Winter *et al* (1980) reported similar results in coho salmon and steelhead trout (*Oncorhynchus mykiss*). Further, Belding and Merrill (1935) reported that brook trout was more susceptible to *R. salmoninarum* infection than the rainbow trout when ex-

perimentally infected. Mitchum and Sherman (1981) reported that brook trout were more susceptible to natural BKD infection than rainbow trout and brown trout. Eissa (2005) confirmed that the brook trout is the most susceptible species among all studied salmonids during a period of 4 years study. Moreover, he indicated that the Iron River strain of the brook trout species is more susceptible than the Assinica strain of the same species.

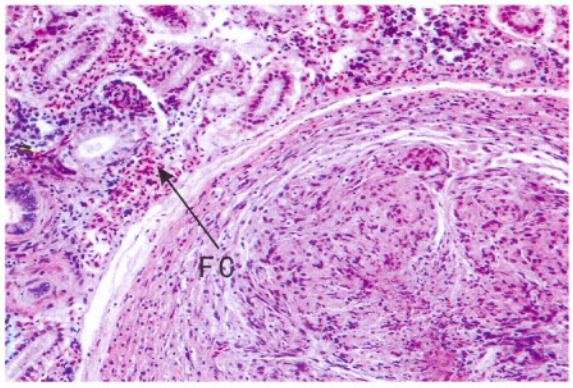

Figure 2. Hematoxylin and Eosin stained slide of kidney showing a severe granulomatous reaction that is replacing kidney tissues of a 3 years old Assinica brook trout. Notice the fibrous capsule (FC) surrounding the entire granuloma (× 100). The case is from an outbreak of BKD that killed captive 3 years old Assinica brook trout in mid September 2003.

3.3 Pathogenesis and immunity

3.3.1 Infection and pathogenesis

R. salmoninarum can induce uptake by non-phagocytic cells and can survive ingestion, which provides a means of entry into the host via the gills and the gastrointestinal tract (Evelyn, 1996; Flano *et al*, 1996; Balfry *et al*, 1996), however a study demonstrated that *R. salmoninarum* can not be internalized by healthy rainbow trout gills *in vitro* (McIntosh *et al*, 2000). *R. salmoninarum* uptake by eggs is another possibility that result in vertical transmission of the organism from parent to offspring (Evelyn *et al*, 1984; Evelyn *et al*, 1986a, 1986b; Bruno and Munro, 1986b).

R. salmoninarum is believed to spread through blood and also through intracellular habitation and replication in macrophages (Gutenberger *et al*, 1997; Ellis, 1999). Although *R. salmoninarum* is a slow growing organism, it can reach levels of 10^9 cells/g in spleen and kidney tissues before initiation of fish mortality (Evelyn, 1996).

Opsonization of the pathogen by antibody and /or complement increases the success of *R. salmoninarum* to survive and replicate within phagocytes more willingly than limit its activity as with most of other pathogens (Bandin *et al*, 1995). To survive and replicate, *R. salmoninarum* must acquire nutrients from the host. In the absence of iron, *R. salmoninarum* may produce iron reductase, which makes bound iron more available for bacterial uptake (Grayson *et al*, 1995).

R. salmoninarum produces large amounts of the p57 antigen (Wiens and Kaattari, 1989), both in serum and intracellularly. The quantity can neutralize the vast majority of antibodies that may be evoked in response to infection. These antibody-p57 complexes may remain in tissue and contribute to tissue destructive hypersensitivity resulting in granulomas (Bruno, 1986).

The p57 has immunosuppressive and tissue destructive properties. The p57 agglutinates salmon leukocytes (Wiens *et al*, 1991) and suppresses antibody production against unrelated antigens *in vitro* (Turaga *et al*, 1987). The p57 is a potent inhibitor of the phagocyte respiratory burst response (Campos-Perez *et al*, 1997) and could decrease the bactericidal activity of juvenile chinook macrophages against *Aeromonas salmonicida* (Siegel and Congleton, 1997).

Senson and Stevenson (1999) suggested that p57 and its breakdown products might form a protective layer around *R. salmoninarum* cells. Bacterial cells stripped of p57 induced stronger immune response than those not stripped of p57 (Wood and Kaattari, 1996). Cell surface associated p57 and its breakdown products may effectively block highly immunogenic areas of the bacterial cell surface from detection by host defenses (Wiens and Kaattari, 1999).

3.3.2 Effect of BKD on host immune response

Grayson *et al* (2002) studied the immunosuppressive effect of *R. salmoninarum in vitro* and *in vivo*. Within an *in vitro* assay, macrophages showed a rapid inflammatory response in which the expression of interleukin-1β, major histocompatibility complex class Ⅱ, inducible cyclooxygenase, and inducible nitric oxide synthase (iNOS) were enhanced, while tumor necrosis factor-α (TNF-α) expression was greatly reduced initially and then increased. *In vivo* study, intraperitoneal (*i. p.*) injection of *R. salmoninarum* DNA vaccine constructs (msa) reduced the expression of IL-1β, Cox-2, and MHC Ⅱ but stimulated TNF-α. In this study, the authors concluded that p57 suppresses the host immune response and hypothesized that the chronic granulomatous reaction is due to prolonged stimulation of TNF-α. The p57 possessed immunosuppressive action against salmonid specific antibody response (Turaga *et al*, 1987), tissue destructive properties (Bruno, 1986) and capable of

agglutinating salmon leukocytes (Wiens and Kaattari, 1999).

Aside from its opsonizing action, antibodies interact directly with free antigen (p57), creating immune complexes that aggregate within the tissue and cause hypersensitivity reactions, resulting in granulomas and tissue damage (Bruno, 1986). Macrophage activating factor (MAF)-activated macrophages can effectively kill *R. salmoninarum* cells (Hardie *et al*, 1996), but production of MAF in immature helper T-cells may be suppressed at low temperature (Siegel and Congleton, 1997). The proliferation and action of T cells in activating macrophages may be the primary successful immune response against *R. salmoninarum* (Secombes, 1985; Hardie *et al*, 1996).

3.3.3 Environmental factors

Effect of diet

Studies suggested that the prevalence and severity of BKD might be partly related to certain dietary and environmental factors. Diets formulated of gluten as opposed to cottonseed meal have resulted in higher BKD prevalence in several hatcheries in Washington (Wood, 1974). Wedemeyer and Ross (1973) demonstrated that BKD prevalence was similar in fish fed rations containing equivalent amounts of either gluten or cottonseed, but the non-specific stress of infection perhaps due to the increased ascorbate depletion was more severe in the corn gluten group. Sakai *et al* (1986) concluded that vitamins had no effect on BKD prevalence. Woodall and LaRoche (1964) suggested that iodine insufficiency was responsible for increased BKD incidence in juvenile chinook salmon. Paterson *et al* (1981) indicated that Vitamin A, zinc, and iron levels are significantly reduced in BKD-infected fish and subsequent feeding trials provided a lower incidence of BKD in fish fed diets high in trace elements (Fe, Cu, Mn, Co, I and F) or low in calcium (0.2%).

Effects of temperature

Several authors reported that BKD could occur over a wide range of water temperatures (Belding and Merrill, 1935; Earp *et al*, 1953; Fryer and Sanders, 1981; Bullock and Herman, 1988). For example, at 15 – 20 °C, experimentally infected juvenile salmon and trout died 21 – 34 days after inoculation, as opposed to 60 – 71 days post inoculation at 6.7 °C (Sanders *et al*, 1978). Also, Wood (1972, cited in Fryer and Sanders, 1981) reported that mortalities from BKD occurred after 30 – 35 days post exposure at temperatures above 11 °C and took 60 – 90 days at 7.2 – 10 °C. Sanders and Fryer (1981) indicated that most of epizootics occurred during the autumn and winter, under conditions of declining water temperatures; however the greatest mortality was associated with periods of highest water temperatures. Also, it was noted that during periods of low water temperatures the disease produced a slow steady death rate.

Water salinity

Despite the fact that BKD occurs mainly in freshwater, significant infections also occur in saltwater (Banner *et al*, 1983). Reports demonstrated that deaths continued in chinook, coho and pink salmon stocks after movement to salt water-rearing ponds (Earp *et al*, 1953; Bell, 1961). Frantsi *et al* (1975) reported that *R. salmoninarum* impaired the ability of Atlantic salmon smolts to acclimate to saltwater and caused a subsequent reduction in ocean survival. Ellis *et al* (1978) isolated the organism from juvenile chinook salmon that had spent two winters in the ocean. Fryer and Sanders (1981) indicated that BKD was thought to be the main cause of death among coho salmon smolts released from Siletz hatchery in Oregon. The authors reported that the majority of deaths occurred between two and four months after the fish entered saltwater. They also concluded that fish infected with BKD while in freshwater will continue to die from this disease, but at an accelerated rate, after migration to saltwater. BKD infection can impair acclimatization to seawater and cause death (Mesa *et al*, 1999). Further, Price and Schreck (2003) experimentally assessed the effect of BKD on saltwater preference of juvenile spring chinook salmon and concluded that there is a significant negative relationship between mean infection level and saltwater preference.

4 Epizootiology

4.1 Geographical distribution

BKD has been reported wherever susceptible salmonid populations are present (Fryer and Sanders, 1981; Klontz, 1983). The disease is commonly reported in cultured salmonid species from North America, Europe, Japan and South America (Fryer and Sanders, 1981; Bullock and Herman, 1988). BKD has also been observed in a wide range of wild (Pippy, 1969; Evelyn *et al*, 1973; Ellis *et al*, 1978; Paterson *et al*, 1979; Mitchum and Sherman, 1981) and feral salmonid populations from North America (Elliot and Pascho, 1991; Sanders *et al*, 1992; Holey *et al*, 1998; Jonas *et al*, 2002). The geographic range of BKD includes Canada, England, France, Finland, Germany, Iceland, Italy, Japan, Scotland, Spain, Turkey, United States, former Yugoslavia and Chile (Bullock and Herman, 1988). BKD was pre-

sumptively diagnosed and reported in Australian Victoria in the early 1970s in farmed chinook salmon however further work identified the syndrome to be nocardiosis (Humphrey *et al*, 1987). No evidence supported the presence of the disease in New Zealand, Russia. BKD was recently reported in Denmark (Lorenzen *et al*, 1997) and Norway (Jansson *et al*, 2002).

4.2 Host range

BKD has been reported in salmonids of the genera *Oncorhynchus*, *Salmo* and *Salvelinus* (Fryer and Sanders, 1981). *R. salmoninarum* has also been detected in chinook salmon (Holey *et al*, 1998), coho salmon (MacLean and Yoder, 1970), brown trout, brook trout, rainbow trout (Belding and Merrill, 1935; Mitchum *et al*, 1979), Pacific salmon, Atlantic salmon, lake trout (Bullock and Herman, 1988), pink salmon (Bell, 1961), Kokanee salmon (Awakura, 1978), Grayling (*Thymallus thymallus*) (Kettler *et al*, 1986), Lake Michigan whitefish (*Coregonus clupeformis*) and bloater (*Coregonus hoyi*) (Jonas *et al*, 2002) and whitefish (*Coregonus lavretus*) in Finland (Rimaila-Parnanen, 2002). The organism has also been detected in absence of disease in few non-salmonid species such as greenling (*Hexagrammos otaki*), flathead (*Platycephalus indicus*) and Pacific herring (*Glupea pallasi pallasi*) (Traxler and Bell, 1988). *R. salmoninarum* antigen has also been detected in Japanese sculpin (*Cottus Japonicus*) and Japanese scallops (*Patinopecten yessoensis*) (Sakai and Kobayashi, 1992). Recently, the organism has been isolated for the first time from clinically affected adult parasitic stage of Lake Ontario Sea Lamprey (*Petromyzon marinus*) (Eissa *et al*, 2006, In press).

4.3 Disease transmission

4.3.1 Source of infection

R. salmoninarum is excreted in the feces of clinically diseased trout and can survive for up to one week and two weeks in the feces and sterile seawater respectively (Balfry *et al*, 1996). The organism can also survive in non-sterile freshwater and pond sediments for up to 21 days (Austin and Rayment, 1985). Thus, the oro-fecal route of horizontal transmission may contribute significantly to the increasing prevalence of BKD in salmonids.

4.3.2 Horizontal transmission

R. salmoninarum possesses a powerful capability of inducing uptake by tissue cells including the epithelial lining of the gastro-intestinal tract (Bruno, 1986; Evelyn, 1996; Flaño *et al*, 1996). Infection is thereby likely to occur where sufficient numbers of bacteria are present within the immediate vicinity of aquatic environment. Oral-fecal route of infection can also, occur in net pens by ingestion of contaminated feces (with up to 10^7 bacteria/g of feces) during feeding (Balfry *et al*, 1996). Waterborne infection may occur through gills, eyes, lesions, wounds and ingestion (Evenden *et al*, 1993). The organism was also transmitted by feeding fish on infected or inefficiently pasteurized fish offales or fish flesh (Wood, 1974; Fryer and Sanders, 1981). Thus, uptake of *R. salmoninarum* through the intestinal wall is a likely pathway of infection (Jansson, 2002). Horizontal transmission can also occur between wild and stocked hatchery trout in natural systems (Mitchum and Sherman, 1981). Long-term exposure (180 days) of healthy fish to highly infected or dying salmon resulted in the infection and death of all exposed fish at an average water temperature of 10 ℃ (Murray *et al*, 1992).

4.3.3 Vertical transmission

Numerous studies have been conducted in the last two decades in order to study the possibility of vertical transmission of *R. salmoninarum* from mother to offspring via eggs. Allison (1958) was the first to report the development of BKD in offspring hatched from eggs transferred from a hatchery where the disease had been endemic for many years to another hatchery where it had never been detected. Bullock *et al* (1978) demonstrated transmission of *R. salmoninarum* from the broodstocks to their progeny via the eggs. Interestingly, the organism has been transmitted even after the surface disinfection of eggs which likely due to the fact that the pathogen was located within the perivitteline membrane of the egg away from the reach of the disinfectant (Evelyn, 1993). The intra-ovum route of transmission has now been firmly established (Evelyn *et al*, 1986a, 1986b) where the pathogen is located in the yolk and is protected from surface disinfectants (Evelyn *et al*, 1986a, 1986b; Bruno and Munro, 1986c). Infected coelomic fluid has been shown to be an important source of infection for the egg (Evelyn, 1993) where the organism found its way to the yolk via the micropyle due to high bacterial counts in coelomic fluid. There are some instances that intra-ovum infections can also occur prior to ovulation and directly from the ovarian tissue (Evelyn, 1993). The pathogen has been also detected in the semen (milt) of infected Brook trout brood stocks collected during spawning cycles in Michigan State hatcheries which suggests that male can play a possible role in transmission and spread of *R. salmoninarum* (Eissa, 2005).

4.3.4 Fish as possible vectors and carriers

Although there are enough satisfactory data indicating that *R. salmoninarum* is an obligate in-

tracellular pathogen of salmonid fishes and that the reservoir and carrier of infection are other infected salmonid (Woods and Yasutake, 1956; Fryer and Sanders, 1981; Klontz, 1983; Bullock and Herman, 1988), yet there are few existing data about the possibility that non-salmonids can act as a reservoir or vector for the organism. Few non-salmonid species were able to contract the infection naturally or experimentally and in turn they might become accidental carriers and play an important role in transmission of the disease to salmonid species by cohabitation. For example, Pacific herring (*Clupea harengus pallasi*) living in net pens with *R. salmoninarum* infected coho salmon have been reported as infected (Paclibare *et al*, 1988). Also, Pacific herring (Traxler and Bell, 1988), sablefish (*Anoplopoma fumbria*) (Bell *et al*, 1990), Common shiner (*Notropis cornutus*) (Hicks *et al*, 1986), and the fathead minnow (*Pimephales promelas*) (Hicks *et al*, 1986) were able to contract infection by *i. p.* injection of *R. salmoninarum*. The organism was also detected in moribund Pacific hakes (*Merluccius productus*) (Kent *et al*, 1998). In addition, Greenlings (*Hexagrammos otakii*) and flathead (*Platycephalus indicus*) were also reported as possible vectors for the disease (Sakai and Kobayashi, 1992).

4.3.5 Possible vectors other than fish

A limited number of studies have been conducted in the last two decades that have lead to the assumption that animals other than fish can act as possible vectors for the transmission of *R. salmoninarum* to salmonids. For example, the Japanese scallop (*Patinopecten yessoensis*) has been reported as a possible vector for *R. salmoninarum* transmission to coho salmon pen-raised in the neighboring seawater (Sakai and Kobayashi, 1992).

Some blood-sucking ectoparasites, like salmon lice (*Lepeophteirus salmonis*), can act as vectors for the pathogen. Although, salmon lice can occasionally harbor the pathogen, no record of active transmission of *R. salmoninarum* between sea lice infected and non-infected fish exists (Richards *et al*, 1985; Frerichs and Roberts, 1989).

4.3.6 Reservoirs

Clinically infected, subclinically infected or latent carrier salmonids are the main reservoir of infection (Klontz, 1983; Richards *et al*, 1985, Bullock and Herman, 1988). Bacterial laden-feces and *R. salmoninarum* rich pond sediment can also act as a reservoir of infection (Balfry *et al*, 1996; Austin and Rayment, 1985). In addition, inefficiently pasteurized infected salmon viscera are a confirmed reservoir of infection (Wood, 1974).

5 Diagnosis of BKD

5.1 Isolation and bacteriological identification of the agent

A number of culture media have been successfully used for the primary isolation of *R. salmoninarum* from clinically infected fish. Among these media cysteine blood agar (Ordal and Earp, 1956), KDM2 (Evelyn *et al*, 1977), SKDM (Austin *et al*, 1983) and charcoal agar medium (Daly and Stevenson, 1985) were used with varying degrees of success. The most common drawback of bacterial culture is the slow growing nature of *R. salmoninarum*, which requires up to 12 weeks to achieve bacterial growth. Most recently, Eissa (2005) has suggested a modified KDM medium (MKDM) which enhanced *R. salmoninarum* growth, minimized other bacterial contaminants and ultimately shortened the incubation time to 5–10 days.

The optimal incubation temperature for the isolation of *R. salmoninarum* on culture media is 15 °C (Sanders and Fryer, 1980). The organism is differentiated from other Gram-positive bacteria using the morpho-chemotaxonomic features described by Sanders and Fryer (1980).

5.2 Antigen-antibody reactions

5.2.1 Agglutination test

Although easy and rapid to perform, the test requires that bacteria are first cultured which conveys no advantage if compared with that of other diagnostic methods. Kimura and Yoshimizu (1981) used *Staphylococci* specifically sensitized with antibody against *R. salmoninarum* to develop a coagglutination test to detect *R. salmoninarum* in kidney tissues with limited success.

5.2.2 Immunofluorescence

Direct and indirect fluorescent antibody tests (FAT) have commonly been used to detect *R. salmoninarum* in infected tissues including fixed and paraffin embedded tissues. Bullock and Stuckey (1975) were first to describe the indirect fluorescent antibody technique (IFAT) to visualize the *R. salmoninarum* cells in tissues of infected fish. They concluded that IFAT is more sensitive than Gram stain and can detect the bacteria in subclinical infections. Several methods to quantify *R. salmoninarum* utilizing FAT have been used, including a subjective scoring of fluorescence intensity (1+ to 4+) in tissue smears (Bullock *et al*, 1980). In a later procedure, bacteria are immobilized on filter-paper grids and titers expressed as cells per unit of tissue or ovarian fluid (Elliot and Barila, 1987).

Elliot and McKibben (1997) compared two

fluorescent antibody techniques (FATs) (membrane filtration FAT or MF-FAT and Smear-FAT or S-FAT) for detection of *R. salmoninarum* in ovarian fluid from naturally infected chinook salmon. They reported greater sensitivity of MF-FAT compared to the S-FAT and concluded that MF-FAT was preferable for detection of low numbers of bacteria. Cross reactivity of other bacterial species with antisera prepared against *R. salmoninarum* have been reported (Bullock *et al*, 1980; Austin *et al*, 1985; Brown *et al*, 1995), thus the inclusion of any FAT of control material from *R. salmoninarum*-positive fish is necessary for comparison of cell morphology and staining properties of bacteria in test and control samples (Elliot and McKibben, 1997). Inter-laboratory comparisons revealed that FAT reproducibility is poor when used in detection of very low levels of infection (Armstrong *et al*, 1989).

5.2.3 Enzyme linked immunosorbent assay (ELISA)

Hsu *et al* (1991) developed an improved monoclonal antibody based ELISA for detection of the p57 protein of *R. salmoninarum*. The assay was both specific and sensitive for detection of soluble *R. salmoninarum* antigen at concentrations as low as 50 – 100 ng/ml. A double antibody sandwich ELISA, also known as quantitative ELISA (Q-ELISA), provides accurate indication about the real prevalence of BKD in the tested fish population because it determines both prevalence and intensity of the infection (Pascho *et al*, 1998). The procedures are fairly standardized by the studies of Pascho and Mulcahy (1987) and Pascho *et al* (1991). A positive threshold has been computed and proposed for Q-ELISA results interpretation (Meyers *et al*, 1993; Pascho *et al*, 1998). The positive-negative cutoff absorbance for the kidney homogenate was determined as 0.10. Pascho *et al* (1998) assigned the following antigen level categories for tested positive kidney samples: low (0.10 to 0.19), medium (0.20 – 0.99) and high (1.00 or more).

5.2.4 Immunohistochemistry (IHC)

Hoffmann *et al* (1989) compared various staining techniques (Gram, PAS, IFAT and indirect peroxidase procedures) for their ability to detect *R. salmoninarum* in the tissues of rainbow trout fixed by various methods (Fresh frozen tissue, frozen formalin-fixed tissue, formalin or Bouin's fixed paraffin-embedded tissue) and concluded that only the indirect peroxidase technique gave satisfactory results regardless of the fixation method used. IHC has the advantage of visualizing *R. salmoninarum* and the tissue alteration they cause simultaneously (Jansson *et al*, 1991; Evensen *et al*, 1994). IHC has been used to detect BKD natural and experimental infections. For example, using *in situ* IHC, Lorenzen *et al* (1997) reported the first demonstration of BKD in rainbow trout in Denmark. Evensen *et al* (1994) detected the organism *in situ* by using IHC in paraffin embedded tissue specimens from Atlantic salmon and they reported the use of monoclonal antibodies specific for the *R. salmoninarum* p57 protein. However, it has been reported that prolonged preservation of tissue samples in formalin has very deleterious effect on the antigen detection and retrieval in immunohistochemical assays (Evensen *et al*, 1994). A typical picture of how bacteria and tissue look like after IHC adopted on an infected kidney tissue is indicated in Figure 3 and Figure 4 (Eissa, 2005).

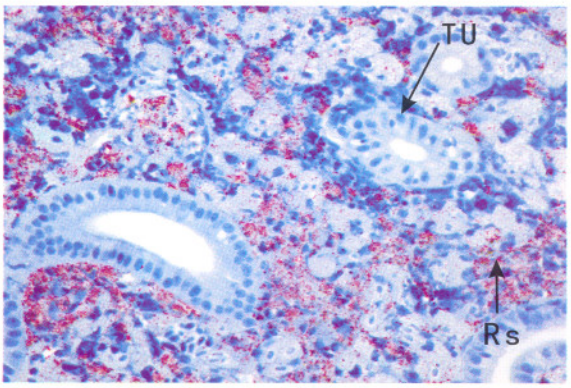

Figure 3. Kidney tissue of Iron River brook trout fingerling exhibiting heavy *R. salmoninarum* infection. Kidney section was stained using an anti-*R. salmoninarum* antibody based streptavidin-immunoperoxidase immmunolbeling (×400). Sections were counterstained with Mayer's hematoxylin (Blue background)
Rs: *R. salmoninarum* soluble antigens with the red staining affinity. Tu: Non-affected kidney tubules with blue counterstaining affinity.

5.3 Polymerase chain reaction (PCR)

PCR has been successfully used to detect *R. salmoninarum* DNA within individual chinook salmon eggs with a detection sensitivity of 2 bacterial cells/egg (Brown *et al*, 1994). A nested PCR (nPCR) has been developed by Chase and Pascho (1998) to amplify a 320 bp fragment of the gene encoding the p57 protein and they recorded no specific fragments amplification when other fish bacterial pathogens were used as templates for nPCR. The sensitivity of the method increased one hundred fold compared to a conventional PCR method (Pascho *et al*, 1998). The authors compared the sensitivities of nPCR, ELISA and FAT assays to detection *R. salmoninarum* in kidneys of infected chinook salmon and concluded that nPCR showed the highest sensitivity (61%), followed by ELISA

(47%) then FAT (43%). Pascho *et al* (1998) reported that nPCR detected *R. salmoninarum* in 100% of the tested ovarian fluid samples and thereby concluded that nPCR was the most accurate and sensitive method for detection of *R. salmoninarum*. Hong *et al* (2002) designed a pair of specific primer for nested amplification of 501 bp and 314 bp DNA fragments of the sequence coding p57 of *R. salmoninarum* respectively and they also recorded no specific fragments amplification when other principal fish bacterial pathogens were used as templates in PCR and nPCR tests. However, Miriam *et al* (1997) have cautioned that PCR positive samples may contain some proportion of dead *R. salmoninarum* with detectable level of DNA. This means that kidney tissues containing non-culturable *R. salmoninarum* can be falsely positive when tested with nPCR. In a recent study, Eissa (2005) used three diagnostic technique namely culture, Q-ELISA and nPCR to detect *R. salmoninarum* in kidney tissues of returning spawners salmon and concluded that nPCR is much more sensitive than the other two methods in discovering the very early infection.

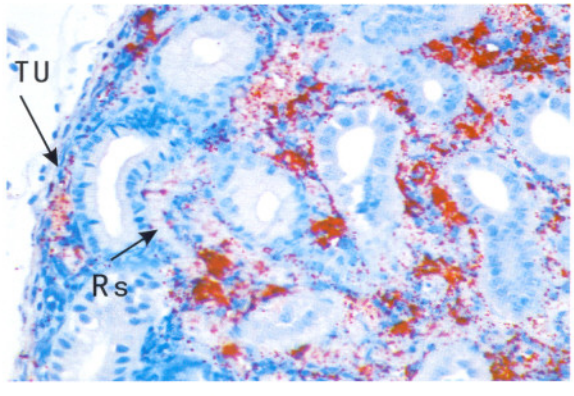

Figure 4. Kidney tissue of Iron River brook trout fingerling exhibiting heavy *R. salmoninarum* infection after enhanced antigen retrieval procedures using alkaline phosphatase red and goat anti-*R. salmoninarum* antibody. Sections were counterstained with Mayer's Hematoxylin (Blue background) (×400). This case is from an outbreak of BKD that killed thousands of hatchery raised Iron River brook trout fingerlings in May 2003.
Rs: *R. salmoninarum* soluble antigens with the red staining affinity. Tu: Non-affected kidney tubules with blue counterstaining affinity.

6 Differential Diagnosis

External manifestations of BKD are non-pathognomonic, but the course of the disease and the granulomatous nature of the kidney lesions may provide presumptive indications. The disease can be differentiated from other kidney diseases of chronic progression including pseudo-kidney disease (*Carnobacterium piscicola*) (Ross and Toth, 1974), nephrocalcinosis (calcium deposits) (Peddie, 2004) and proliferative kidney disease (lymphoid hyperplasia) in response to myxozoan parasite *Tetracapsula bryosalmonae*) (Clifton-Hadley *et al*, 1984). Differentiation is mainly based on observation and detection of the organism or its antigens using immunofluorescence, IHC, ELISA, PCR. In case of nephrocalcinosis, differentiation is mainly based on bacteriological assessment to rule out the presence of the bacterium, however on-farm examination of lesion consistency can help to discriminate between these conditions as BKD lesions are soft whilst those caused by nephrocalcinosis have a gritty texture (Peddie, 2004).

R. salmoninarum can be differentiated from coryneform group of bacteria, which includes the genera of *Listeria*, *Erysipelothrix*, *Corynebacterium*, *Actinomyces*, *Celullomonas*, *Curtobacterium*, *Arthrobacter* and *Brevibacterium* by cell wall composition and G+C contents of DNA (Stuart and Welshimer, 1974; Sanders and Fryer, 1980).

Although *R. salmoninarum* share certain characteristics with *Actinomyces pyogenes* (formerly *Corynebacterium pyogenes*), they differ in a number of other characteristics. *A. pyogenes* is facultatively anaerobic, catalase negative and produce acid from carbohydrates. The genus *Renibacterium* can be separated from pathogenic *Corynebacteria* and genus *Caseobacter* by the presence of lysine in the cell wall and the absence of mycolic acids. The genus *Caseobacter* is further differentiated by a mol % G + C of 60 – 67 (Crombach, 1978). Genus *Celullomonas* contains the diamino acid ornithine in its cell wall peptidoglycan and has a mol % G + C ranging from 65 – 72.

Interestingly some of the coryneform groups of bacteria have an overlapping characteristics and phylogenetic homology. Among this group of bacteria a cell wall peptidoglycan containing lysine occurs primarily in *Arthrobacter* and *Brevibacterium*. DNA homology studies showed close relationship between several species in these two genera. However, these bacteria have usually been isolated from the environment, are chemoorganotrophic, show a progression of morphological changes during the growth cycle and have a mol % G + C above 60. Interestingly, all these characteristics are distinctly different from that of *Renibacterium*.

7 Control

7.1 Chemotherapy

Since the early 1950s a relatively large number of chemotherapeutics have been intensively tested *in vivo* and *in vitro* for efficacy in treating BKD. Rucker *et al* (1951) was first to use antimicrobial agents against clinical BKD and their results showed a definite decrease in mortalities when sulfadiazine was incorporated into fish diets. Although treatment did not completely cure clinically sick fish, sulfamerazine reduced BKD mortalities alone and combined with sulfaguanidine and sulfadiazine (Allison, 1958). Wolf and Dunbar (1959) tested 34 therapeutic agents including erythromycin thiocyanate and sulfamerazine on 16 strains of *R. salmoninarum* using the disk method for drug sensitivity screening followed by *in vivo* feeding trials with experimentally infected fish. They concluded that erythromycin fed at the rate of 100 mg/kg of fish for 5 consecutive days gave the best results. Generally, due to the occurrence of the bacterium intracellularly as well as extracellularly, these treatments only suppressed the systemic spread of the organism and induced partial relief (Amos 1977). Intramuscular (*i.m.*) and *i.p.* administration of sulfonamide drugs significantly reduced prespawning mortality among chinook salmon broodstocks being hold prior to spawning (Amend and Fryer, 1968). However, sulfonamides administered by *i.m.* or *i.p.* routes often produced sterile abscesses at the injection site in adults and induced mortalities and teratogenicity with their progeny (Amos, 1977).

In an attempt to reduce or prevent vertical transmission of BKD, salmon eggs were water hardened for 1 hour in 2 ppm erythromycin (Amos, 1977). However, erythromycin was rapidly eliminated and dropped below detectable level within 24 hours after water hardening (Evelyn *et al*, 1986a). Monthly subcutaneous (*S.C.*) injection of adult female Pacific salmon with 11 mg/kg erythromycin reduced pre-spawning mortality due to BKD (Klontz, 1983). Interestingly, erythromycin remains in the eggs of injected females for up to 60 days before spawning (Evelyn *et al*, 1986; Moffitt, 1991). It is believed that erythromycin residues in the eggs assist in preventing vertical transmission of *R. salmoninarum* from parents to their offspring (Lee and Evelyn, 1994). Detectable amounts of erythromycin often remain in the perfused tissues of both juvenile and adult salmon long after they are no longer detected in the plasma and muscle (Moffitt, 1991; Haukenes and Moffitt, 1999) and this possibly contributes to the efficacy of erythromycin against the slow growing *R. salmoninarum*. Feeding erythromycin can efficiently reduce mortalities of infected hatchery raised salmonids (Wolf and Dunbar, 1959; Austin, 1985; Moffitt and Bjornn, 1989). A dose of 200 mg/kg body weight for 21 days was most effective (Moffitt, 1992). Erythromycin is only available as an Investigational New Animal Drug (INAD) through the Food and Drug Administration (FDA) (Moffitt, 1992).

Austin (1985) tested more than 70 antimicrobial compounds both *in vivo* and *in vitro* and found that clindamycin, erythromycin, kitasamycin, penicillin G and spiramycin were useful for combating early clinical BKD cases while cephradine, lincomycin and rifampicin were effective prophylactically but had limited use therapeutically. Hsu *et al* (1994) tested the efficacy of enrofloxacin in treating BKD *in vitro* and *in vivo* and they concluded that low minimal inhibition concentrations (MICs), high bioavailability and large volume distribution of the antibiotic make it good candidate for use as effective therapeutic against BKD.

7.2 Adult segregation

Broodstock segregation is a more practical method for reducing the prevalence and levels of *R. salmoninarum* in hatchery-reared salmon (Pascho *et al*, 1991) and for increasing survival during their downriver migration and entry into seawater (Pascho *et al*, 1993; Elliot *et al*, 1995). This procedure aims to interrupt vertical transmission of *R. salmoninarum* by isolating or destroying eggs from brood fish that exhibit clinical signs of BKD or test positive, with a high titer, against *R. salmoninarum* antigens. The method is used successfully in a number of U.S states and Canadian provinces such as Washington, Idaho, Michigan, Wisconsin, and Ontario.

7.3 Eradication

Due to the complicated nature of BKD and its obvious threats to fisheries, Hoskins *et al* (1976) recommended complete destruction of the infected stocks and disinfection of the holding facilities to achieve complete eradication of the disease. However, this procedure is considered by fisheries managers as impractical due to the widespread occurrence of *R. salmoninarum* (Sanders and Fryer, 1980).

Eradication can be of value in single fish farms or hatcheries that receive their water supply from specific pathogen free source (European Commission, 1999). Eradication procedures should be followed by standard, cleaning and disinfection procedures. Although some trials have been made to eradicate BKD from fish farmed in open waters (e.g. sea and lake cages) or from farms and hatcheries with water supply from rivers, results were very

discouraging.

After eradication procedures have been applied in the fish farm and hatcheries, restocking should only utilize certified BKD-free stocks. Restocking should be followed by two inspections and laboratory examinations per year for a total period of two years before the facility can be designated as "BKD-free" (European Commission, 1999).

7.4 Prophylaxis

7.4.1 Reducing the risk of BKD introduction

Special attention should be paid to prevent the introduction of infected fish or their gametes (Evelyn *et al*, 1984; Yoshimizu, 1996). This can only be achieved through prior examination and quarantine. Special requirements of water supply, wild birds and amphibians' control. In addition, restriction of movement of vehicle, visitors as well as utensils from infected into free areas is equally important. Repopulation must be accompanied with certificate issued by the competent authority certifying that the fish or eggs are specific pathogen free.

7.4.2 Vaccination

In the last two decades, vaccination against BKD has achieved different levels of success. Paterson *et al* (1981) reported that an inactivated suspension of *R. salmoninarum* mixed 1:1 with Freunds adjuvant (FCA) administered by *i. p.* injection, reduced the level of infection of *R. salmoninarum* in yearling salmon but, did not completely eliminate the infection. Sakai *et al* (1993; 1995) found that although vaccination evoked specific antibodies, these antibodies did not endow with a protection. Piganelli *et al* (1999) demonstrated that oral administration of *R. salmoninarum* expressing low levels of cell associated p57, resulted in an extension of the mean time to death after challenge and they concluded that the protection was not due to humoral antibody. This conclusion supported earlier histopathological indications of an involvement of the cell mediated immune response in recovery, due to intracellular survival and the composition of inflammatory cells in connection with signs of regression (Munro and Bruno, 1988). Rhodes *et al* (2004) presented DNA adjuvants and whole bacterial cell vaccines against *R. salmoninarum* that were tested in chinook salmon fingerlings. These authors concluded that whole cell vaccines of either a nonpathogenic *Arthrobacter* spp. or an attenuated *R. salmoninarum* strain produced limited protection against acute *i. p.* challenge with virulent *R. salmoninarum*. They also concluded that the addition of either synthetic oligodeoxynucleotides or purified *R. salmoninarum* genomic DNA as adjuvants did not increase protection, however a combination of both whole cell vaccines significantly increased survival among fish naturally infected with *R. salmoninarum*. Also, the surviving fish treated with the combination vaccine exhibited reduced levels of bacterial antigens in the kidney.

References

1. Alexander SM, Grayson TH, Chambers EM, Coopers LF, Barker GA, Gilpin ML. Variation in the spacer regions separating tRNA genes in *R. salmoninarum* distinguishes recent clinical isolates from the same location. Journal of Clinical Microbiology 2001; 39: 119-28.
2. Allison LN. Multiple sulfa therapy of kidney disease among brook trout. Progressive Fish Culturists 1958; 20: 66-8.
3. Amend DF, Fryer JL. The administration of sulfonamide drugs to adult salmon. Progressive Fish Culturists 1968; 30:168-72.
4. Amos KH. The control of Bacterial Kidney Disease in spring chinook salmon. M. S. thesis, University of Idaho, Moscow 1977:20.
5. Anonym. Second intrim report of the Furunculosis committee. Edinburgh: H. M. S. O., 1933; 81.
6. Armstrong RD, Evelyn TPT, Martin SW, Dorwand W, Ferguson HW. Erythromycin levels in eggs and alevins derived from spawning broodstock Chinook salmon (*Oncorhynchus tshawytscha*) injected with the drug. Diseases of Aquatic Organisms 1989; 6: 33-6.
7. Austin B. Evaluation of antimicrobial compounds for the control of bacterial kidney disease in rainbow trout, *Salmo gairdneri Richardson*. Journal of Fish Diseases 1985; 8: 209-20.
8. Austin B, Austin DA. Bacterial Fish Pathogens, Diseases in Farmed and Wild Fish. Third Edition. Springer-Praxis, Chichester, UK. 1999.
9. Austin B, Bucke D, Feist S, Rayment JN. A false positive reaction in the fluorescent antibody test for *R. salmoninarum* with a coryneform organism. Bulletin of the European Association of Fish Pathologists 1985; 5:8-9.
10. Austin B, Embley TM, Goodfellow M. Selective isolation of *Renibacterium salmoninarum*. FEMS Microbiology Letters 1983; 17: 111-4.
11. Austin B, Rayment JN. Epizootiology of *Renibacterium salmoninarum*, the causal agent of Bacterial Kidney Disease in salmonid fish. Journal of Fish Diseases 1985; 8: 505-9.
12. Austin B, Rodgers CJ. Diversity among strains causing bacterial kidney disease in salmonid fish. Current Microbiology 1980; 3:231-5.
13. Awakura T. Bacterial Kidney Disease in mature salmonid. Fish Pathology 1978; 13:53-4.
14. Balfry SK, Albright LJ, Evelyn TPT. Horizontal transfer of *Renibacterium salmoninarum* among farmed salmonids via the fecal-oral route. Diseases of Aquatic Organisms 1996; 25:63-9.
15. Bandin I, Rivas C, Santos Y, Secombes CJ, Barja JL, Ellis AE. Effects of serum factors on the survival of *Renibacterium salmoninarum* within rainbow trout macrophages. Diseases of Aquatic Organisms 1995; 23:

221 – 7.

16. Bandin I, Santos Y, Bruno DW, Raynard RS, Toranzo AE, Barja JL. Lack of biological activities in the extracellular products of *Renibacterium salmoninarum*. Canandian Journal of Fisheries and Aquatic Science 1991; 48:421 – 5.
17. Banner CR, Rohovec JS, Fryer JL. *Renibacterium salmoninarum* as a cause of mortality among Chinook salmon in salt water. Journal of the World Mariculture Society 1983; 14:236 – 9.
18. Banner CR, Rohovec JS, Fryer JL. A new value for mol percent guanine + cytosine of DNA for the salmonid fish pathogen *Renibacterium salmoninarum*. FEMS Microbiology Letters 1991; 79:57 – 9.
19. Belding DL, Merrill B. A preliminary report upon a hatchery disease of the salmonidae. Transactions of the American Fisheries Society 1935; 65:76 – 84.
20. Bell GR. Two epidemics of apparent kidney disease in cultured pink salmon (*Oncorhynchus gorbuscha*). Journal of the Fisheries Research Board of Canada 1961; 18: 559 – 62.
21. Bell GR, Hoffman RW, Brown LL. Pathology of experimental infections of the sablefish, *Anoplopoma fimbria* (Pallas), with *Renibacterium salmoninarum*, the agent of Bacterial Kidney Disease in salmonids. Journal of Fish Diseases 1990; 13:355 – 67.
22. Brown LL, Evelyn TPT, Iwama GK, Nelson WS, Levine RP. Bacterial species other than *Renibacterium salmoninarum* cross react with antisera against *R. salmoninarum*, but are negative for the p57 gene of *R. salmoninarum* as detected by the polymerase chain reaction (PCR). Diseases of Aquatic Organisms 1995; 21: 227 – 31.
23. Brown LL, Iwama GK, Evelyn TPT, Nelson WS, Levine RP. Use of PCR to detect DNA from *Renibacterium salmoninarum* within individual salmonid eggs. Diseases of Aquatic Organisms 1994; 18:165 – 71.
24. Bruno DW. Histopathology of Bacterial Kidney Disease in laboratory infected rainbow trout, *Salmo gairdneri Richardson*, and Atlantic salmon, *Salmo salar* L., with reference to naturally infected fish. Journal of Fish Diseases 1986; 9:523 – 37.
25. Bruno DW. The relationship between auto-agglutination, cell surface hydrophobicity and virulence of fish pathogen *Renibacterium salmoninarum*. FEMS Microbiology Letters 1988; 51:135 – 40.
26. Bruno DW, Munro ALS. Uniformity in the biochemical properties of *Renibacterium salmoninarum* isolates obtained from several sources. FEMS Microbiology Letters 1986a; 33:247 – 50.
27. Bruno DW, Munro ALS. Observation on *Renibacterium salmoninarum* and the salmonid egg. Diseases of Aquatic Organisms 1986b; 1: 83 – 7.
28. Bruno DW, Munro ALS. Haematological assessment of rainbow trout, *Salmo gairdneri Richardson*, and Atlantic Salmon, *Salmo salar* L., infected with *Renibacterium salmoninarum*. Journal of Fish Diseases 1986c; 9: 195 – 204.
29. Bullock GL, Griffin BR, Stuckey HM. Detection of *Corynebacterium salmoninus* by direct fluorescent antibody tests. Canadian Journal of Fisheries and Aquatic Science 1980; 37: 719 – 21.
30. Bullock GL, Herman RL. Bacterial Kidney Disease of salmonid fishes caused by *Renibacterium salmoninarum*. Fish Disease Leaflet 78, US Fish and Wildlife Service, Washington, DC, 1988.
31. Bullock GL, Stuckey HM. Fluorescent antibody identification and detection of the *Corynebacterium* causing the Kidney Disease of salmonids. Journal of the Fisheries Research Board of Canada 1975; 32: 2224 – 7.
32. Bullock GL, Stuckey HM, Chen PK. Corynebacterial Kidney Disease of salmonids: Growth and serological studies on the causative bacterium. Applied Microbiology 1974; 28: 811 – 4.
33. Bullock GL, Stuckey HM, Mulchay D. Corynebcaterial Kidney Disease: Egg transmission following iodophore disinfection. Fish Health News 1978; 7:51 – 2.
34. Campos-Perez JJ, Ellis AE, Secombes CJ. Investigation of factors influencing the ability of *Renibacterium salmoninarum* to stimulate rainbow trout macrophage respiratory burst activity. Fish and Shellfish Immunology 1997; 7: 555 – 66.
35. Chase DM, Pascho RJ. Development of a nested polymerase chain reaction for amplification of a sequence of the p57 gene of *Renibacterium salmoninarum* that provides a highly sensitive method for detection of the bacterium in salmonid kidney. Diseases of Aquatic Organisms 1998; 34: 223 – 9.
36. Clifton-Hadley RS, Bucke D, Richards RH. Proliferative Kidney Disease of salmonid fish; a review. Journal of Fish Diseases 1984; 7: 363 – 77.
37. Crombach WHJ. Caseobacter polymorphus gen. nov., sp. nov., a coryneform bacterium from cheese. International Journal of Systematic Bacteriology 1978; 28:354 – 66.
38. Daly JG, Stevenson RM. Charcoal agar, a new growth medium for the fish disease bacterium *Renibacterium salmoninarum*. Applied and Environmental Microbiology 1985; 50:868 – 71.
39. Daly JG, Stevenson RM. Characterization of the *Renibacterium salmoninarum* haemagglutinin. Journal of General Microbiology 1990; 136: 949 – 53.
40. Earp BJ, Ellis CH, Ordal EJ. Kidney Disease in young salmon. Special Report Ser. No. 1, Department of Fisheries, Washington State, 1953;73.
41. Eissa A, Elsayed EE, McDonald R, Faisal M. First record of *Renibacterium salmoninarum* in the sea lamprey (*Petromyzon marinus*). Journal of Wildlife Diseases 2006; (in press).
42. Eissa A. Bacterial kidney disease (BKD) in Michigan salmonids. Ph. D. Dissertation, Michigan State University, East Lansing, Michigan 2005; 210.
43. Elliot DG, Barila TY. Membrane filtration-fluorescent antibody staining procedures for detecting and quantifying *Renibacterium salmoninarum* in coelomic fluid of Chinook salmon (*Oncorhynchus tshawytscha*). Canadian Journal of Fisheries and Aquatic Science 1987; 44: 206 – 10.
44. Eliott DG, McKibben CL. Comparison of two fluorescent antibody techniques (FATs) for detection and quantification of *Renibacterium salmoninarum* in coelomic fluid of spawning Chinook salmon *Oncorhynchus tshawytscha*. Diseases of Aquatic Organisms 1997; 30: 37 – 43.
45. Elliott DG, Pascho RJ. Juvenile fish transportation: im-

pact of Bacterial Kidney Disease on survival of spring/summer chinook salmon stocks. Annual Report, 1989. Prepared by the U.S. Fish and Wildlife Service, Seattle, Wash., for the U.S. Army Corps of Engineers 1991.
46. Elliott DG, Pascho RJ. Juvenile Fish Transportation: Impact of Bacterial Kidney Disease on survival of spring/summer chinook salmon stocks. Annual Report, 1993. U.S. Army Corps of Engineers 1995.
47. Elliott DG, Pascho RJ, Palmisano AN. Broodstock segregation for the control of Bacterial Kidney Disease can affect mortality of progeny Chinook salmon (*Oncorhynchus tshawytscha*) in seawater. Aquaculture 1995; 132: 133－44.
48. Ellis AE. Immunity to bacteria in fish. Fish and Shellfish Immunology 1999; 9: 291－308.
49. Ellis RW, Novotny AJ, Harrell LW. Case Report of Kidney Disease in wild Chinook salmon (*Oncorhynchus tshawytscha*) in the sea. Journal of Wildlife Diseases 1978; 14:121－3.
50. Embley TM, Goodfellow M, Austin B. A semi-defined growth medium for *Renibacterium salmoninarum*. FEMS Microbiology Letters 1982; 14:299－301.
51. European Commission. Bacterial Kidney Disease. Report of the Scientific Committee on Animal Health and Animal Welfare. European Commission, Health and Consumer Protection, Brussels, 1999; 1－44 (also available at: www. europa. eu. int/comm/food/fs/sc/scah/out36-en. pdf)
52. Evelyn TPT. An improved growth medium for the kidney disease bacterium and some notes on using the medium. Bulletin de L' Office International des Epizooties 1977; 87: 511－3.
53. Evelyn TPT. Bacterial Kidney Disease－BKD. In: Inglis V, Roberts RJ, Bromage NR. (Eds). Bacterial Diseases of Fish. Blackwell Scientific Publications, Oxford, UK, 1993; 177－95.
54. Evelyn TPT. Infection and disease. In: Iwama G & Nakanishi T (Eds), The fish immune system. Academic Press, San Diego, United States 1996; 339－66.
55. Evelyn TPT, Bell GR, Prosperi-Porta L, Ketcheson JE. A simple technique for accelerating the growth of the Kidney Disease bacterium *Renibacterium salmoninarum* on a commonly used culture medium (KDM2). Diseases of Aquatic Organisms 1989; 7: 231－4.
56. Evelyn TPT, Hoskins GE, Bell GR. First Record of Bacterial Kidney Disease in an apparently wild salmonid in British Columbia. Journal of the Fisheries Research Board of Canada 1973; 30: 1578－80.
57. Evelyn TPT, Ketcheson JE, Prosperi-Porta L. The clinical significance of immunofluorescence-based diagnoses of bacterial kidney disease carrier. Fish Pathology 1981; 15: 293－300.
58. Evelyn TPT, Ketcheson JE, Prosperi-Porta L. Further evidence for the presence of *Renibacterium salmoninarum* in salmonid eggs and for the failure of providoniodine to reduce the intra-ovum infection rate in the water. Journal of Fish Disease 1984; 7:173－82.
59. Evelyn TPT, Ketcheson JE, Prosperi-Porta L. Experimental intraovum infection of salmonid eggs with *Renibacterium salmoninarum* and vertical transmission of the pathogen with such eggs despite their treatment with erythromycin. Diseases of Aquatic Organims 1986a; 1: 197－202.
60. Evelyn TPT, Ketcheson JE, Prosperi-Porta L. Use of erythromycin as a means of preventing vertical transmission of *Renibacterium salmoninarum*. Diseases of Aquatic Organisms 1986b; 2:7－11.
61. Evelyn TPT, Prosperi-Porta L, Ketcheson JE. Two new techniques for obtaining consistent results when growing *Renibacterium salmoninarum* on KDM2 culture medium. Diseases of Aquatic Organisms 1990; 9: 209－12.
62. Evenden AJ, Grayson TH, Gilpin ML, Munn CB. *Renibacterium salmoninarum* and bacterial kidney disease－the unfinished jigsaw. Annual Review of Fish Diseases 1993; 3:87－104.
63. Evensen O, Dale OB, Nilsen A. Immunohistochemical identification of *Renibacterium salmoninarum* by monoclonal antibodies in paraffin-embedded tissues of Atlantic salmon (*Salmo salar* L.), using paired immunoenzyme and paired immunofluorescence techniques. Journal of Veterinary Diagnostic Investigation 1994; 6:48－55.
64. Feltham RKA, Power AK, Pell PA, Sneath PHA. A simple method for storage of bacteria at －76 degree C. Journal of Applied Bacteriology 1978; 44:313－6.
65. Ferguson HW. Systemic pathology of fish. Iowa State University Press. Ames, United States 1989; 263.
66. Flaño E, Kaattari SL, Razquin B, Villena AJ. Histopathology of the thyumus of coho salmon *Onchorhynchus kisutch* experimentally infected with *Renibacterium salmoninarum*. Diseases of Aquatic Organisms 1996; 26: 11－8.
67. Frantsi CJ, Flewelling TC, Tidswell KG. Investigations on corynebacterial kidney disease and diplostomulum sp. (eye-fluke) at Margaree Hatchery, 1972－1973, Technical Seport Serial No. Mar/T－75－9. Research Development Branch, Fish and Marine Services, Department of Environment. Halifax, Nova Scotia, Canada 1975; 30.
68. Fredriksen A, Endresen C, Wergeland HI. Immunosuppressive effect of a low molecular weight surface protein from *Renibacterium salmoninarum* on lymphocytes from Atlantic salmon (*Salmo salar* L.). Fish and Shellfish Immunology 1997; 7: 273－82.
69. Frerichs G, Roberts R. Fish Patology (Roberts R, Second Edition) Bailliere Tindal, London 1989.
70. Fryer JL, Sanders JE. Bacterial Kidney Disease of Salmonid Fish. Annual Review of Microbiology 1981; 35: 273－98.
71. Fryer JL, Lannan CN. The history and current status of *Renibacterium salmoninarum*, the causative agents of Bacterial Kidney Disease in Pacific salmon. Fisheries Research 1993; 17:15－33.
72. Getchell RG, Rohovec JS, Fryer JL. Comparison of *Renibacterium salmoninarum* isolates by antigenic analysis. Fish Pathology 1985; 20:149－59.
73. Goodfellow M, Embley TM, Austin B. Numerical taxonomy and emended description of *Renibacterium salmoninarum*. Journal of General Microbiology 1985; 131:2739－52.
74. Grayson TH, Bruno DW, Evenden AJ, Gilpin ML, Munn CB. Iron acquisition by *Renibacterium salmoninarum*; contribution by iron reductase. Diseases of Aquatic Organisms 1995; 22:157－62.
75. Grayson TH, Coopers LF, Wrathmell AB, Roper J, Evenden AJ, Gilpin ML. Host responses to *Renibacteri-*

um salmoninarum and specific components of the pathogen reveal the mechanisms of immune suppression and activation. Journal of Immunology 2002; 106: 273 – 83.

76. Gutenberger SK, Giovannoni SJ, Field KG, Fryer JL, Rohovec JS. A phylogenetic comparison of the 16S rRNA sequence of the fish pathogen, *Renibacterium salmoninarum*, to Gram-positive bacteria. FEMS Microbiology Letters 1991; 77: 151 – 6.
77. Gutenberger SK, Duimstra JR, Rohovec JS, Fryer JL. Intracellular survival of *Renibacterium salmoninarum* in trout mononuclear phagocytes. Diseases of Aquatic Organisms 1997; 28:93 – 106.
78. Hamel O. The Dynamic and effects of Bacterial Kidney Disease in Snake River spring chinook salmon (*Oncorhynchus tshawytscha*). Ph. D. Dissertation. University of Washington. Washington DC, USA. 2001.
79. Hardie LJ, Ellis AE, Secombes CJ. *In vitro* activation of rainbow trout macrophages stimulates inhibition of *Renibacterium salmoninarum* growth concomitant with augmented generation of respiratory burst products. Diseases of Aquatic Organisms 1996; 27:175 – 83.
80. Haukenes AH, Moffitt CM. Concentrations of erythromycin in maturing salmon following intraperitoneal injection of two drug formulations. Journal of Aquatic Animal Health 1999; 11: 61 – 7.
81. Hicks BD, Daly JG, Ostland VE. Experimental infection of minnows with Bacterial Kidney Disease bacterium *Renibacterium salmoninarum*. Abstract, Third Annual Meeting, Aquaculture Association of Canada, July 1986, Guelph, Ontario, 1986.
82. Hoffmann RW, Bell GR, Pfeil-Futzien C, Ogawa M. Detection of *Renibacterium salmoninarium* in tissue sections by different methods – a comparative study with special regard to the indirect Immunohistochemical peroxidase technique. Fish Pathology 1989; 24:101 – 4.
83. Holey ME, Elliot RE, Marcqueneski SV, Hnath JG, Smith KD. Chinook salmon epizootics in Lake Michigan: Possible contributing factors and management implications. Journal of Aquatic Animal Health 1998; 10: 202 – 10.
84. Hong I, Longying G, Xiujie S, Yulin J. Detection of *Renibacterium salmoninarum* by nested-PCR. Journal of Fisheries of China / Shuichan Xuebao 2002; 26:453 – 8.
85. Hopwood DA, Ferguson HM. A rapid method for lyophilizing Streptomyces culture. Journal of Applied Bacteriology 1969; 32: 434 – 6.
86. Hoskins GE, Bell GR, Evelyn TPT. The occurrence, distribution and significance of infectious disease and neoplasms observed in fish in the Pacific Region up to the end of 1974. Technical Report – Fisheries and Marine Service Research Development 1976; 609: 37.
87. Hsu H, Bowser PR, Schachte JH. Development and evaluation of a monoclonal-antibody-based enzyme-linked immunosorbent assay for the diagnosis of *Renibacterium salmoninarum* infection. Journal of Aquatic Animal Health 1991; 3:168 – 75.
88. Hsu H, Wooster GA, Bowser PR. Efficacy of enrofloxacin for the treatment of salmonids with bacterial kidney disease, caused by *Renibacterium salmoninarum*. Journal of Aquatic Animal Health 1994; 6:220 – 3.
89. Humphrey JD, Lancaster CE, Gudkovs N, Copland JW. The disease status in Australia of Australian salmonids: bacteria and bacterial diseases. Journal of Fish Disease 1987; 10:403 – 10.
90. Jansson E. Bacterial Kidney Disease in salmonid fish: Development of methods to assess immune functions in salmonid fish during infection by *Renibacterium salmoninarum*. Doctoral Thesis, University of Upsala, Sweden, 2002.
91. Jansson E, Hongslo T, Lindberg R, Ljungberg O, Svensson BM. Detection of *Renibacterium salmoninarum* and Yersinia ruckeri by the peroxidase-antiperoxidase immunohistochemical technique in melanin-containing cells of fish tissues. Journal of Fish Disease 1991; 14: 689 – 92.
92. Johnson DC, Hnath JG. Lake Michigan Chinook salmon mortality-1988. Michigan Department of Natural Resources. Fisheries Division Technical Report No. 91 – 4, 1991.
93. Jonas JL, Schneeberger PJ, Clapp DF, Wolgamood M, Wright G, Lasee B. Presence of the BKD-causing bacterium *Renibacterium salmoninarum* in lake whitefish and bloaters in the Laurentian Great Lakes. Archive of Hydrobiology. Special Issue Advances Limnology 2002; 57:447 – 52.
94. Kent ML, Traxler GS, Kieser D, Richard J, Dawe SC, Shaw RW, Prosperi PL, Ketcheson J, Evelyn TPT. Survey of salmonid pathogens in ocean-caught fishes in British Columbia, Canada. Journal of Aquatic Animal Health 1998; 10: 211 – 9.
95. Kettler S, Pfeilputzien C, Hoffman R. Infection of grayling (Thymallus) with the agent of bacterial kidney disease (BKD). Bulletin of the European Association of Fish Pathologists 1986; 6: 69 – 71.
96. Kimura T, Yoshimizu M. Rapid Methods for Detection of bacterial kidney disease of salmonid (BKD) by coagglutination of antibody sensitized protein A-containing *Staphylococci*. Bulletin of the Japanese Society of Scientific Fisheries 1981; 47: 1173 – 83. In Japanese with English summary. SFA 27 (1). (Lab. Microbiol., Fac. Fish, Hokkaido Univ, Minato-3, Hakkodate 041, Japan).
97. Klontz GW. Bacterial Kidney Disease in Salmonids: An Overview. In: Anderson DP, Dorson M, Dubourget PH (Eds). Antigens of Fish Pathogens: Development and Production for Vaccines and Serodiagnostics. Collection Fondation Marcel Merieux, Lyons, France, 1983; 177 – 200.
98. Lee E, Evelyn TPT. Prevention of vertical transmission of the bacterial kidney disease agent *Renibacterium salmoninarum* by broodstock injection with erythromycin. Diseases of Aquatic Organisms 1994; 18:1 – 4.
99. Lorenzen E, Olesen NJ, Korsholm H, Heuer OE, Evensen OE. First demonstration of *Renibacterium salmoninarum* /BKD in Denmark. Bulletin of the European Association of Fish Pathologists 1997; 17:140 – 4.
100. MacLean DG, Yoder WG. Kidney Disease among Michigan salmon in 1967. Progressive Fish Culturists 1970; 32:26 – 30.
101. McIntosh D, Austin B, Flaño E, Villena JA, Tarazona Martinez-Pereda JV. Lack of uptake of *Renibacterium*

salmoninarum by gill epithelia of rainbow trout. Journal of Fish Biology 2000; 56:1053 – 61.

102. Mesa MG, Maule AG, Poe TP, Schreck CB. Influence of Bacterial Kidney Disease on smoltification in salmonids: is it a case of double jeopardy? Aquaculture 1999; 174:25 – 41.
103. Meyers TR, Short S, Farrington C, Lipson K, Geiger HJ, Gates R. Establishment of negative-positive threshold optical density value for the enzyme-linked immunosorbent assay (ELISA) to detect soluble antigen of *Renibacterium salmoninarum* in Alaskan Pacific salmon. Diseases of Aquatic Organisms 1993; 16: 191 – 7.
104. Miriam A, Griffiths SG, Lovely JE, Lynch WH. PCR and Probe-PCR assays to monitor broodstock Atlantic salmon (*Salmo salar* L.) ovarian fluid and kidney tissues for the presence of DNA of the fish pathogen *Renibacterium salmoninarum*. Journal of Clinical Microbiology 1997; 35:1322 – 6.
105. Mitchum DL, Sherman LE, Baxter GT. Bacterial kidney disease in Feral Populations of Brook Trout (*Salvelinus fontinalis*), Brown Trout (*Salmo trutta*), and Rainbow Trout (*Salmo gairdneri*). Journal of Fisheries Research Board of Canada 1979; 36:1370 – 6.
106. Mitchum DL, Sherman LE. Transmission of bacterial kidney disease from wild to stocked hatchery trout. Canadian Journal of Fisheries and Aquatic Science 1981; 36:547 – 51.
107. Moffitt CM. Oral and injectable applications of erythromycin in salmonid fish culture. Veterinary and Human Toxicology 1991;3: 49 – 53.
108. Moffitt CM. Survival of juvenile chinook salmon challenged with *Renibacterium salmoninarum* and administered oral doses of erythromycin thiocyanate for different durations. Journal of Aquatic Animal Health 1992; 4: 119 – 25.
109. Moffitt CM, Bjornn TC. Protection of chinook salmon smolts with oral doses of erythromycin against acute challenges of *Renibacterium salmoninarum*. Journal of Aquatic Animal Health 1989; 1: 227 – 32.
110. Murray CB, Evelyn TPT, Beacham TD, Ketcheson LW, Prosperi-Porta L. Experimental induction of bacterial kidney disease in chinook salmon by immersion and cohabitation challenges. Diseases of Aquatic Organisms 1992; 12: 91 – 9.
111. Munro ALS, Bruno DW. Vaccination against Bacterial Kidney Disease. In: Ellis, AE (Ed.) Fish Vaccination, Academic Press, London, England, 1988, 125 – 34.
112. Ordal EJ, Earp BJ. Cultivation and transmission of the etiological agent of Bacterial Kidney Disease. Proceedings of the Society for Experimental Biology and Medicine 1956; 92: 85 – 8.
113. Paclibare JO, Albright LJ, Evelyn TPT. Investigations on the occurrence of the Kidney Disease Bacterium *Renibacterium salmoninarum* in non-salmonids on selected farms in British Columbia. Bulletin of the Aquaculture Association Canada 1988; 88:113 – 5.
114. Pascho RJ, Chase D, McKibben CL. Comparison of the membrane-filtration fluorescent antibody test, the enzyme-linked immunosorbent assay and the polymerase chain reaction to detect *Renibacterium salmoninarum* in salmonid ovarian fluid. Journal of Veterinary Diagnostic Investigation 1998; 10:60 – 6.
115. Pascho RJ, Elliot DG, Streufert JM. Broodstock segregation of spring chinook salmon *Oncorhynchus tshawytscha* by use of enzyme-linked immunosorbent assay (ELISA) and the fluorescent antibody technique (FAT) affects the prevalence and levels of *Renibacterium salmoninarum* infection in progeny. Diseases of Aquatic Organisms 1991; 12: 25 – 40.
116. Pascho RJ, Elliott DG, Achord S. Monitoring of the in-river migration of smolts from two groups of spring chinook salmon, *Oncorhynchus tshawytscha* (Walbaum), with different profiles of *Renibacterium salmoninarum* infection. Aquaculture and Fisheries Management 1993; 24:163 – 9.
117. Pascho RJ, Mulcahy D. Enzyme-linked immunosorbent assay for a soluble antigen of *Renibacterium salmoninarum*, the causative agent of salmonid bacterial kidney disease. Canadian Journal of Fisheries and Aquatic Science 1987; 44:183 – 91.
118. Paterson WD, Gallant C, Desautels D, Marshall L. Detection of Bacterial Kidney Disease in wild salmonids in the Margaree River system and adjacent waters using an indirect fluorescent antibody technique. Journal of Fisheries Research Board of Canada 1979; 36:1464 – 8.
119. Paterson WD, Lall SP, Desantels D. Studies on bacterial kidney disease in Atlantic salmon (*Salmo salar*) in Canada. Fish Pathology 1981; 15: 283 – 92.
120. Peddie S. Nephrocalcinosis. Fish farmers 2004; 27: 37.
121. Piganelli JD, Wiens GD, Xhang JA, Christensen JM, Kaattari SL. Evaluation of a whole cell p57-vaccine against *Renibacterium salmoninarum*. Diseases of Aquatic Organisms 1999; 36:37 – 44.
122. Pippy JHC. Kidney disease in Juvenile Atlantic salmon (*Salmo salar*) in the Margaree River. Journal of Fisheries Research Board of Canada 1969; 26:2535 – 7.
123. Price CS, Schreck CB. Stress and saltwater-entry behavior of juvenile chinook salmon (*Oncorhynchus tshawytscha*): conflicts in physiological motivation. Canadian Journal of Fisheries and Aquatic Sciences 2003; 60: 910 – 8.
124. Pridham TG, Hesseltine CW. Culture collections and patent depositions. Advances in Applied Microbiology 1975; 19:1 – 23.
125. Rathbone CK, Harrell LW, Peterson ME, Poysky FT, Strom MS. Preliminary Observations on the Efficacy of Azithromycin for Chemotherapy of Bacterial Kidney Disease. Western Fish Disease Workshop, Fish Health Section/American Fisheries Society Annual Meeting, Twin Falls, Idaho, 1999, June 9 – 11.
126. Rhodes LD, Rathbone CK, Corbett SC, Harrell LW, Strom MS. Efficacy of cellular vaccines and genetic adjuvants against Bacterial Kidney Disease in chinook salmon (*Oncorhynchus tshawytscha*). Fish and Shellfish Immunology 2004; 16:461 – 74.
127. Richards RH, Roberts RJ, Schlotfeldt HJ. Bakterielle Erkrankungen der Knochenfische. In: Roberts RJ and Schlotfeldt HJ (Eds.), Grundlagen der Fischpathologie, Verlag Paul Parey, Hamburg, Germany, 1985; 174 – 207.
128. Rimaila-Parnanen. First case of Bacterial Kidney Disease (BKD) in whitefish (*Coregonus lavaretus*) in Fin-

land. Bulletin of the European Association of Fish Pathologists 2002; 22:403－4.
129. Ross AJ, Toth RJ. Lactobacillus－a new fish pathogen? Progressive Fish Culturist 1974; 36: 191.
130. Rucker RR, Bermer AF, Whipple WJ, Burrows RE. Sulfadiazine for Kidney Disease. Progressive Fish Culturists 1951; 13:135－7.
131. Rucker RR, Earp BJ, Ordal EJ. Infectious diseases of pacific salmon. Transaction of the American Fisheries Society 1954; 83: 297－312.
132. Sakai M, Atsuta S, Kobayashi M. The immune response of Rainbow trout (*Oncorhynchus mykiss*) injected with five *Renibacterium salmoninarum* bacterins. Aquaculture 1993; 113: 11－8.
133. Sakai MS, Kobayashi M. Detection of *Renibacterium salmoninarum* the causative agent of Bacterial Kidney Disease in salmonid fish, from pen-cultured coho salmon. Applied and Environmental Microbiology 1992; 58:1061－3.
134. Sakai DK, Nagata M, Iwami T, Koide N, Tamiya Y, Ito Y, Atoda M. Attempt to control BKD by dietary modification and erythromycin chemotherapy in hatchery-reared Masu salmon *Oncorhynchus masou* Brevoort. Bulletin of the Japanese Society of Scientific Fisheries 1986; 52: 1141－7.
135. Sakai M, Terutoyo Y, Masanori K. Influence of the immuno-stimulant, EF203, on the immune responses of rainbow trout (*Oncorhynchus mykiss*) to *Renibacterium salmoninarum*. Aquaculture 1995; 138: 61－7.
136. Sanders JE, Barros JR. Evidence by the fluorescent antibody test for the occurrence of *Renibacterium salmoninarum* among salmonid fish in Chile. Journal of Wildlife Diseases 1986; 22: 255－7.
137. Sanders JE, Fryer JL. *Renibacterium salmoninarum* gen. nov., sp. nov., thecausative agent of bacterial kidney disease in salmonid fishes. Irrternational Journal of Systematic Bacteriology 1980; 30:496－502.
138. Sanders JE, Long JJ, Arakawa CK, Bartholomew JL, Rohovec JS. Prevalence of *Renibacterium salmoninarum* among downstream-migrating salmonids in the Columbia River. Journal of Aquatic Animal Health 1992; 4:72－5.
139. Sanders JE, Pilcher KS, Fryer JL. Rlation of water temperature to Bacterial Kidney Disease in coho salmon (*Onchorhynchus kisutch*), sockeye salmon (*O. nerka*), and steelhead trout (*Salmo gairdneri*). Journal of Fisheries Board Canada 1978; 35:8－11.
140. Secombes CJ. The *in vitro* formation of teleost multinucleate giant cells. Journal of Fish Disease 1985; 8:461－4.
141. Senson PR, Stevenson RM. Production of the 57 kDa major surface antigen by a non-agglutinating strain of the fish pathogen *Renibacterium salmoninarum*. Diseases of Aquatic Organisms 1999; 38: 23－31.
142. Shieh HS. An extracellular toxin produced by fish Kidney Disease bacterium, *Renibacterium salmoninarum*. Microbiological Letters 1988; 38: 27－30.
143. Siegel DC, Congleton JL. Bactericidal activity of juvenile chinook salmon macrophages against *Aeromonas salmonicida* after exposure to live or heat-killed *Renibacterium salmoninarum* or to soluble proteins produced by *R. salmoninarum*. Journal of Aquatic Animal Health 1997; 9:180－9.
144. Smith IW. The occurrence and pathology of Dee Disease. Freshwater Salmon Fisheries Research 1964; 34:1－13.
145. Snieszko SF, Griffin PJ. Kidney Disease in brook trout and its treatment. Progressive Fish Culturists 1955; 17: 3－13.
146. Speare DJ. Differences in patterns of meningoencephalitis due to Bacterial Kidney Disease in farmed Atlantic and chinook salmon. Research in Veterinary Science 1997; 62: 79－80.
147. Starliper CE. Genetic diversity of North American isolates of *Renibacterium salmoninarum*. Diseases of Aquatic Organisms 1996; 27:207－13.
148. Starliper CE, Smith DR, Shatzer T. Virulence of *Renibacterium salmoninarum* to salmonids. Journal of Aquatic Animal Health 1997;9:1－7.
149. Starliper CE, William BS, Jay M. Performance of serum-free broth media for growth of *Renibacterium salmoninarum*. Diseases of Aquatic Organisms 1998; 34:21－6.
150. Stuart SE, Welshimer HJ. Taxonomic reexamination of *Listeria pirie* and transfer of *Listeria grayi* and *Listeria murrayi* to a new genus *Murraya*. International Journal of Systematic Bacteriology 1974; 24: 177－85.
151. Suzumoto BK, Schreck CB, McIntyre JD. Relative resistances of three transferring genotypes of coho salmon (*Oncorhynchus kisutch*) and their hematological responses to Bacterial Kidney Disease. Journal of Fisheries Research Board of Canada 1977; 34: 1－8.
152. Traxler G, Bell G. Pathogens associated with impounded Pacific herring *Clupea harengus pallasi*, with emphasis on viral erythrocytic necrosis (VEN) and atypical *Aeromonas salmonicida*. Diseases of Aquatic Organisms 1988; 5: 93－100.
153. Turaga PS, Weins GD, Kaattari SL. Analysis of *Renibacterium salmoninarum* antigen production *in situ*. Fish Pathology 1987; 22:209－14.
154. Wedemeyer GA, Ross AJ. Nutritional factors in the biochemical pathology of Corynebacterial Kidney Disease in the coho salmon (*Oncorhynchus kisutch*). Journal of Fisheries Research Board of Canada 1973; 30:296－8.
155. Wellington EMH, Williams ST. Preservation of actinomycete inoculum in frozen glycerol. Microbios Letters 1979; 6:151－7.
156. Wiens GD, Kaattari SL. Monoclonal antibody analysis of common surface protein(s) of *Renibacterium salmoninarum*. Fish Pathology 1989; 24:1－7.
157. Wiens GD, Kaattari SL. Monoclonal antibody characterization of a leukoagglutinin produced by *Renibacterium salmoninarum*. Infection and Immunity 1991; 59: 631－7.
158. Wiens GD, Kaattari SL. Bacterial Kidney Disease (*Renibacterium salmoninarum*). In: Woo PTK and Bruno DW (eds.), Fish Diseases and Disorders, CABI Publishing, New York, USA 1999; 269－302.
159. Wiens GD, Chein MS, Winton JR, Kaattari SL. Antigenic and functional characterization of p57 produced by *Renibacterium salmoninarum*. Diseases of Aquatic Organisms 1999; 37: 43－52.
160. Winter GW, Schreck CB, McIntyre JD. Resistance of different stocks and transferrin genotypes of coho salmon,

Oncorhynchus kisutch, and steelhead trout, *Salmo gairdneri*, to Bacterial Kidney Disease and vibriosis. United States National Marine Fisheries Service Fishery Bulletin 1980; 77:795 – 802.

161. Wolf K, Dunbar CE. Tests of 34 therapeutic agents for control of Kidney Disease in trout. Transactions of the American Fisheries Society 1959; 88:117 – 24.
162. Wood JW. Diseases of Pacific Salmon, Their Prevention and Treatment. Olympia, Washington: Department of Fisheries, Hatchery Division, 2nd Edition. 1974, 82.
163. Wood EM, Yasutake WT. Histopathology of Kidney Disease in fish. American Journal of Pathology 1956; 32: 845 – 57.
164. Wood PA, Kaattari SL. Enhanced immunogenicity of *Renibacterium salmoninarum* in chinook salmon after removal of the bacterial cell surface-associated 57 kDa protein. Diseases of Aquatic Organisms 1996; 25: 719.
165. Woodall AN, LaRoche G. Nutrition of salmonid fishes. 11. Iodide requirements of chinook salmon. Journal of Nutrition 1964; 82: 475 – 82.
166. Young CL, Chapman GB. Ultrastructural aspects of the causative agent and renal histopathology of Bacterial Kidney Disease in brook trout (*Salvelinus fontinalis*). Journal of Fisheries Research Board Canada 1978; 35:1234 – 48.
167. Yoshimizu M. Disease problems of salmonid fish in Japan caused by international trade. Bulletin de l' Office International des Epizooties 1996; 15: 533 – 49.

Received June 5, 2006

Effects of Breed and Weight on the Reproductive Status of Zebu Cows Slaughtered in Imo State Nigeria

Maxwell Nwachukwu Opara[1], Emelia Chioma Nwachukwu[1], Oluwatoyin Ajala[2], Ifeanyi Charles Okoli[1]

1. *Tropical Animal Health and Production Research Group, Department of Animal Science and Technology, Federal University of Technology, P.M.B. 1526, Owerri, Nigeria*

2. *Department of Veterinary Surgery and Reproduction, University of Ibadan, Ibadan Oyo State, Nigeria*

Abstract: Gross morphological studies of 200 zebu cows (*Bos indicus*) slaughtered in Owerri abattoir, southeastern Nigeria was carried between the months of September and November, 2005 to determine the effects of breed and weight on the reproductive activities of such animals. Seventy seven (38.5%) of these cows were White Fulani, 75 (37.5%) and 48(24.0%) Sokoto Gudali and Cross-breeds. Among these cows examined, 77 (38.5%) of them weighed between 351 – 400 kg, 76 (38.0%) weighed 301 – 350 kg while the cows that were within the 451 – 500 kg and 601 – 650 kg weight groups each recorded 1 (0.5%) against them. Macroscopic examination of the ovaries for corpus luteum in the different breeds revealed that 130 (65.0%) of the cows were undergoing active estrous cycle, with 53 (40.8%), 48 (36.9%) and 29 (22.3%) falling within the Sokoto Gudali, white Fulani and Cross-breed cows respectively. Presence of corpus albicans on their ovaries showed that 178 (89.0%) had calved before, again with Sokoto Gudali breed recording 70 (39.3%), while the White Fulani and Cross-breeds recorded 65 (36.5%) and 43 (24.2%) number of corpus albicans. Mean ovarian measurements (pole to pole, border to border) showed no gross difference among the breeds. However, the cross-breed had more follicles than the pure breeds. Weight of the cows positively affected the ovarian measurements. A number of atrophied ovaries were recorded which equally reduced the mean ovarian measurements and weight for cows in the 451 – 500 kg body weight range. It was concluded that breed and weight could be veritable tools to ascertain the reproductive status of cows brought for slaughter in order to stop the indiscriminate slaughtering of reproductively active animals thereby depleting the Nigerian livestock population. [Life Science Journal. 2006;3(3):77 – 81] (ISSN: 1097 – 8135).

Keywords: breed weight; reproductive status; cows; Imo state; Nigeria

Abbreviations: CA: corpus albicans; CH: corpus haemorrhagicum; CL: corpus luteum

1 Introduction

More than 80% of livestock population in Nigeria is in the hands of the illiterate Fulani nomads[1]. These livestock include cattle, sheep and goats. Typical of their traditional, the Fulanis perceive ownership of livestock more as symbol of status than as meat animals[2,3]. Proper economic management of food animals demands that those sold for slaughter should be males and females that are reproductively inactive. Thus, information on the reproductive status, breed and weight of animals sent for slaughter should be continually evaluated to avoid wastage through the slaughtering of reproductively active females. It is recommended that cattle be sold based on their weights, breeds and sometimes age, as consumers prefer very big cattle to smaller ones because of their meat proportion[3] and palatability[4]. The total reliance on these indices however may be misleading as some breeds reproduce more than others[5].

Research studies on data from abattoirs have revealed high occurrence of fetal wastage among cows slaughtered in Nigeria[6-9]. These studies may not reveal the exact magnitude of the problem since they depict mainly the prevalence of indiscriminate slaughtering of pregnant cows in the country. Ovaries collected from slaughter houses have been noted to contain evidence of the present and past reproductive status of such animals in the form of follicles in varying degrees of development, corpus haemorrhagicum (CH) and corpus albicans (CA) among others[2,10].

Studies on ovarian morphology could yield valuable information on the present reproductive conditions and history of cows of different breeds and weights slaughtered within a locality.

This study was thus designed to investigate the influence of breed and weight on the reproductive activities of cows brought in for slaughter at the Owerri municipal abattoir of Imo state, southeastern Nigeria.

2 Materials and Methods

Gross morphological studies of ovaries of 200 *Bos indicus* cows slaughtered at Owerri municipal abattoir Imo state were carried out between the months of September and November, 2005 to determine the effects of breed and weight on the reproductive activities of such slaughtered cows. The abattoir was visited twice in a week and during each visit, the cows were identified before slaughter, their breeds and weights equally noted.

After the slaughter, pairs of ovaries from each of the cows were harvested and put into properly labeled clean glass dishes and taken to the laboratory where morphological examinations were carried within 3 hours. In addition, the uterus of each cow was excised and inspected for fetal materials. The weights of the ovaries were determined in grams, using an electronic balance, while their dimensions (lengths of pole to pole and border to border) were measured in millimeter using a venier calipers. The number of corpus luteum (CL), CA, and CH and other gross observations such as adhesions and atrophy were equally recorded for each pair of ovaries. The data generated were analyzed, using simple averages, percentages and statistics.

3 Results

Breeds and weights of cows slaughtered in the abattoir at Owerri are reported in Table 1. Out of 200 slaughter cows examined, 77 (38.5%) were White Fulani breed, while 75 (37.5%) and 48 (24.0%) were Sokoto Gudali and Cross-breeds respectively. Across these breeds too, 77 (38.5%) of them weighed between 351 – 400 kg. Also, 41 (54.7%) of the cows belonged to the Sokoto Gudali breed while 27 (35.1%) and 9 (18.8%) were of the White Fulani breed and Cross-breed respectively. Seventy-six (38.0%) of the cows examined belonged to the 301 – 350 kg weight range, where 33 (42.9%) of them were of White Fulani breed 25 (33.3%) and 18 (37.5%) were Sokoto Gudali and Cross-breed.

Table 1. Weight and breeds of cows slaughtered at the abattoir in Owerri, Imo state

Weight(kg)	No.(%)WF	No.(%)SG	No.(%)CB	Total (%)
200 – 250	6(7.8)	–	–	6(3.0)
251 – 300	8(10.4)	7(9.3)	21(43.8)	36(18.0)
301 – 350	33(42.9)	25(33.3)	18(37.5)	76(38.0)
351 – 400	27(35.1)	41(54.7)	9(18.8)	77(38.5)
401 – 450	2(2.6)	1(1.3)	–	3(1.5)
451 – 500	1(1.3)	–	–	1(0.5)
501 – 550	–	–	–	–
551 – 600	–	–	–	–
601 – 650	–	1(1.3)	–	1(0.5)
Total	77(38.5)	75(37.5)	48(24.0)	200(100)

WF = White Fulani, SG = Sokoto Gudali, CB = Cross-Breed.

The result of the effect of breed on the number of CL from cows slaughtered at the abattoir in Owerri is reported in Table 2. Of the 200 cows examined, 130 (65.0%) had CL, while 70 (35.0%) of them had no CL. Among the cows whose ovaries had CL, 53 (40.8%) were Sokoto Gudali followed by 48 (36.9%) and 29 (22.3%) of the White Fulani and Cross-breeds respectively. Nineteen (27.1%) of the Cross-breed had no CL, while 29 (41.4%) of White Fulani and 22(31.4%) of Sokoto Gudali breeds had no CL.

The effect of breed on the number of CA from cows slaughtered at the abattoir in Owerri is shown in Table 3. Out of the total number of cows examined, 178 (89.0%) of them had CA on their ovaries whereas 22 (11.0%) had none. Of the cows with CA, 70 (39.3%) of them were Sokoto Gudali, while 65 (36.5%) and 43 (24.2%) were White Fulani and Cross-breed respectively. Majority, 12 (54.5%) of the cows without CA were of White Fulani breed, whereas Sokoto Gudali and Cross-breed each was 5 (22.7%).

Table 4 shows the mean ovarian measurements in cows of different breeds slaughtered at the abattoir in Owerri. Out of the 70 cows examined here, 28 of them were Sokoto Gudali with mean ovarian

weight of 6.649 ± 0.34, while 26 White Fulani and 16 Cross-breed cows had mean ovarian weights of 6.04 ± 0.31 and 5.543 ± 0.40 respectively. The mean pole to pole length of the ovaries harvested from 28 Sokoto Gudali was 3.21 ± 0.70, followed by 2.34 ± 0.09 and 2.30 ± 0.09 from ovaries collected from 16 Cross-breed and 26 White Fulani cows respectively. The mean border to border measurements of ovaries from 16 Cross-breed was 2.01 ± 0.15, followed by 1.80 ± 0.08 and 1.80 ± 0.06 from 26 White Fulani and 28 Sokoto Gudali cows. The mean number of follicles measured was highest for the 16 Cross-breed cows which recorded 7.25 ± 0.97 followed by 6.535 ± 0.96 and 5.577 ± 0.78 mean number of follicles on ovaries belonging to 28 Sokoto Gudali and 26 White Fulani breeds of cows.

Table 2. Effect of Breed on number of CL from cows slaughtered at the abattoir in Owerri, Imo state

Breed of cows	Cows with CL (%)	Cows without CL (%)	Total examined (%)
F	48(36.9)	29(41.4)	77(38.5)
SG	53(40.8)	22(31.4)	75(37.5)
CB	29(22.3)	19(27.1)	48(24.0)
Total	130(65.0)	70(35.0)	200

Table 3. Effect of breed on number of CA from cows slaughtered at the abattoir in Owerri, Imo state

Breed of cows	Cows with CA(%)	Cows without CA(%)	Total (%)
WF	65(36.5)	12(54.5)	77
SG	70(39.3)	5(22.7)	75
CB	43(24.2)	5(22.7)	48
Total	178(89.0)	22(11.0)	200

The effect of weight on ovarian measurements of cows slaughtered at the abattoir in Owerri is reported in Table 5. The longest pole to pole length was obtained from ovaries of cows weighing 601 – 650 kg body weight, followed by 3.05 ± 0.51 and 2.73 ± 0.23 measurements from ovaries of cows that weighed 351 – 400 kg and 401 – 450 kg body weights respectively. The least pole to pole dimension was from ovaries of cows in 200 – 250 kg body weight range. The mean border to border dimensions of ovaries were highest for those harvested from cows weighing between 401 – 450 kg. Again the least border to border measurement was obtained from ovaries belonging to cows that weighed 200 – 250 kg body weight, which was 1.6 ± 0.13. The mean ovarian weight was highest (8.25 ± 0.0) for cows that weighed between 601 – 650 kg, followed by 7.94 ± 0.0 got for cows weighing 401 – 450 kg. The least ovarian weights of 2.571 ± 4.49 and 5.70 ± 0.0 were recorded against cows which weighed between 200 – 250 kg and 451 – 500 kg respectively.

4 Discussion

Very useful information on the reproductive states of cows could be obtained from the ovaries of such animals sent for slaughter. This study shows that over 75% of the cows slaughtered in Owerri abattoir were of Sokoto Gudali and White Fulani breeds and also that about this population of cows weighed between 301 – 400 kg. This finding agrees with earlier reports[3,6,9], that people prefer these breeds of cattle as meat because of their big sizes. That about 65% of the cows slaughtered possessed corpora lutea, shows that they were still reproductively active. Over 75% of these animals were Sokoto Gudali and White Fulani breeds of cattle. This again confirms our earlier reports[2] and others[6-9] that most animals slaughtered in our abattoirs are usually those still having high reproductive ability.

Breed seemed not to have obvious effect on the number of CA on the ovaries of Sokoto Gudali and White Fulani cows examined. Although the percentages of cows with CA show a gross difference between the Sokoto Gudali, White Fulani and Cross-breed, there is lack of literature to support this trend. This is the first report of the effect of breed on the reproductive status of cows slaughtered for meat at the abattoirs in Owerri, Nigeria. CA count from pairs of ovaries from slaughtered animals showed that this may be a good tool to highlight the problem of reproductive wastage among cows slaughtered in Nigeria. It has been document-

ed[10,11] that previous reproductive history in the form of fibrosed remains of CL of pregnancy (CA) persist for life in majority of cows and this preserves a record of the number of pregnancies undergone by each animal. Our reports showed that 89% of the cows had calved while 11% had not, again depicting the insufficiency of fetal wastage measurements as a major tool in evaluating reproductive wastage among slaughtered animals.

Table 4. Mean ovarian measurement in cows of different breeds slaughtered at the abattoir in Owerri, Imo state

Parameter	Breeds of cows ($n=70$)		
	WF No./mean	SG No./mean	CB No./mean
Wt. of ovary(g)	26(6.04±0.31)	28(6.649±0.34)	16(5.543±0.40)
Pole to pole(cm)	26(2.30±0.09)	28(3.21±0.70)	16(2.34±0.09)
Border to border(cm)	26(1.80±0.08)	28(1.80±0.06)	16(2.01±0.15)
No. of follicles	26(5.577±0.78)	28(6.535±0.96)	16(7.25±0.97)

Table 5. Effect of weight on ovarian measurement of cows slaughtered at the abattoir in Owerri, Imo state

Weight(kg)	Pole to pole (cm)	Border to border (cm)	Weight of ovaries (g)
200 – 250	1.86±0.14	1.60±0.13	2.57±4.49
251 – 300	2.26±0.05	1.73±0.04	6.68±0.52
301 – 350	2.44±0.04	1.87±0.04	6.01±0.36
351 – 400	3.05±0.51	1.88±0.05	6.05±0.29
401 – 450	2.73±0.23	2.20±0.32	7.94±0.0
451 – 500	2.50±0.0	1.70±0.0	5.70±0.0
501 – 550	–	–	–
551 – 600	–	–	–
601 – 650	3.10±0.0	1.80±0.0	8.25±0.0

Breed of cows slaughtered in Owerri abattoir seems to influence the ovarian measurements. The ovaries harvested from White Fulani and Sokoto Gudali were heavier than those of the Cross-breed cows. Also, Sokoto Gudali cows had longer pole to pole measurement of their ovaries than the other breeds. The Cross-breed cows had wider border to border measurements of their ovaries than the pure breeds. The Cross-breed equally had higher number of follicles than the pure breeds. These findings are in agreement with a similar work carried out among small ruminants in Ogun state, southwestern Nigeria[5]. The difference that existed between the Cross-breed and pure breeds might be revealing an improvement in the reproductive traits of the Cross-breed cows as a result of combined genetic make ups.

The ovarian measurements seem to increase as the cows attained bigger body weights. In the pole to pole measurements, exceptions to this trend were among the ovaries collected from cows within the weight of 401 – 500 kg. The cows seemed to have ovaries which were wider than they were long. But the ovaries belonging to cows that weighed 451 – 500 kg had shorter border to border measurements. The difference in these orders may be attributed to the presence of some atrophied ovaries in the group encountered during this study. Weight also seemed to increase the weight of the ovaries. Exceptions here were ovaries of cows that weighed 451 – 500 kg, this again is explained by the presence of atrophied ovaries as supported by Arthur[10].

5 Conclusion

Our studies revealed that about 65% of different breeds of cows slaughtered at Owerri abattoir for meat, irrespective of their weights were still in their active reproductive states but are being sent for slaughter for reasons other than reproductive inactivity. Breeds seemed to positively influence the reproductive performance of our indigenous cows, however cross breeding also slightly improved this trait. Ovarian measurements increased with the body weight of the cows. Age[2] and body weight

of animals sent for slaughter could be a future reliable index to ascertain the reproductive status of such animals before they are finally passed for slaughter.

Correspondence to:
Opara MN
Tropical Animal Health and Production Research Group
Department of Animal Science and Technology
Federal University of Technology
P.M.B. 1526, Owerri, Nigeria.
Email: oparamax@yahoo.com

References

1. Ogunyemi G. Meat hygiene in Nigeria. The Vet. Surgeon 1982; 7: 23-9.
2. Opara MN, Nwachukwu EC, Okoli IC. Ovarian activities in cows of different ages slaughtered in Imo state, Nigeria. Asian Journal of Information Technology 2005; 4(7): 640-3.
3. Aladi NO. Current trends in the production, handling and sales of meat in Nigeria. B. Agric. Tech. Project Report, Federal University of Technology Owerri, Nigeria 1999.
4. Okeudo NJ. Emperical studies of the living conditions of domestic animals in Nigeria. In: Studies in sustainable agriculture and Animal Science in sub-Saharan Africa. Malu UC, Gottwald F (Eds.), Frankfurt, Peter Lang 2004.
5. Abiola SS, Onwuka CFI. Reproductive performance of West African dwarf sheep and goats at village levels in Ogun state, Nigeria. Nig J Anim Prod 1998; 28:79-82.
6. Matthew T, Adeola CO, Matthew A. The recovery of fetuses from slaughtered cattle in the abattoirs in Nigeria and its economic implication to the nation: five year study (1975-1980). Nig Vet Med Assoc, 19th Ann. Conf. Book of abstracts, 1982, 45.
7. Oyekunle MA, Olubanjo Fasina OF. Fetal wastage in abattoirs and its implication; solution report for Ogun state, Nigeria. Nig J Anim Prod 1992; 19:57-63.
8. Wekhe SN, Berepubo NA, Ekpenyong CE. Prevalence and implication of inadvertent slaughtering of pregnant ruminants in Port-Harcourt, Nigeria. Delta Agric 1992; 1: 43-5.
9. Okoli IC, Nwokeocha JR, Herbert U, Anyanwu GA. Analysis of meat inspection records for Imo state, Nigeria (11): Assessment of the magnitude of fetal wastage in state abattoirs. Trop Anim Prod Invest 2001; 4:29-35.
10. Arthur GH, Moakes DE, Pearson H. Veterinary Reproduction and Obstetrics. 5th edn, Bailliere Tindall, London 1982.
11. Dawson FLM. Observations on the corpora albicantes in the ovaries of normal and infertile dairy cows. J Agric Sci 1958; 50: 322-30.

Received March 16, 2006

Gaseous Formaldehyde-induced DNA-protein Crosslinks in Liver, Kidney and Testicle of Kunming Mice

Guangyin Peng, Xu Yang, Wei Zhao, Junjun Sun, Yi Cao, Qian Xu, Junlin Yuan, Shumao Ding

College of Life Science, Central China Normal University, Wuhan 430079, China

Abstract: To explore the effect of distant-site toxicity, this study detected the amount of DNA-protein crosslinks (DPC) with KCl-SDS assay in liver, testicle and kidney of the purebred Kunming mice treated with gaseous formaldehyde (FA). The results showed that gaseous FA couldn't cause DPC or could cause few DPC at the lower concentration (0.5 mg/m^3), while could cause significant DPC at higher concentrations (1.0 mg/m^3 and 3.0 mg/m^3) ($P<0.01$). The results suggested that FA could induce DPC in the distant organs (liver, testicle and kidney) of mice at relatively high concentrations, which indicated that FA might induce distant-site toxicity. [Life Science Journal. 2006;3(3):82-87] (ISSN: 1097-8135).

Keywords: formaldehyde; distant-site toxicity; DNA-protein crosslinks; KCl-SDS assay

Abbreviations: DPC: DNA-protein crosslinks; FA: formaldehyde; DSB: DNA strand breaks; IARC: International Agency for Research; NO: nitric oxide; SDS: sodium dodecyl sulfate

1 Introduction

Formaldehyde (FA) is a colorless, highly flammable gas at ambient temperature, which is present in the environment from both natural processes and manmade sources. As a major industrial chemical, it can be found in construction materials, resins, textiles, leather goods, paper, and consumer products. At the same time, as a naturally occurring biological compound, it is present in tissues, cells, and body fluids. In addition, some reviews have reported that FA is a genotoxic and mutagenic compound and has been classified as a human carcinogen (class AI) by IARC (International Agency for Research) recently[1]. Due to its extensive sources, high level, long-term and high toxicity, it is important to study FA toxic effect and mechanism.

Studies have shown that FA has extensive genotoxicity, including DNA-protein crosslinks (DPC) and DNA strand breaks (DSB)[2,3,4]. DPC is the primary genotoxic effect of FA, which is formed through covalent bond where deoxyribonucleic acid is linked to an endogenous protein. Regions of DNA that are covalently linked with protein are typically considered to be non-functional and can block normal functions of the nuclear matrix, such as replication and transcription, and can form the foci for double strand breaks, which can lead to chromosomal aberrations and sister-chromatid exchanges. Furthermore high amounts of DPC can cause the expression of critical regulatory genes change. For the significance of DPC, the content of it may be of value in the assessment of FA-induced genotoxicity. Casanova *et al* have proved that acute FA inhalation could induce DPC in nasal mucosa of rats and monkeys by experiments *in vivo*[5,6,7]. Kuykendall exposed rat nasal epithelial cells to FA and found DPC content increased remarkably above the concentration of 100 μmol/L[4]. In addition, in our laboratory, Liu *et al* exposed human peripheral blood lymphocytes to FA and found that there was no significant difference in the DPC coefficient between the groups treated with 5 μM, 25 μM FA and the control group, while there was a significant difference between the groups treated with 125 μM, 625 μM FA and the control group ($P<0.01$). The results showed that FA could not induce DPC at low concentrations but could induce DPC significantly at high concentrations[8].

These studies above either chose organs located at exposure site, or were conducted *in vitro* to estimate FA toxicity. Few of them proved whether FA could induce distant-site toxicity. At present, there are still controversies on whether inhaled FA can induce distant-site toxicity, mainly because of the rapid metabolism and removal of FA *in vivo*[9,10]. Recently, Franks developed a mathematical model for estimating the absorption and metabolism of FA by humans. This model was used to analyze the increase of FA concentration in the blood after exposure to FA, and results showed that the increase was insignificant, indicating FA

could be removed rapidly in the blood[11]. This is consistent with previous reports declaring that inhaled FA could be removed rapidly[9,10]. However, some work also support FA has the distant-site toxicity. For example, Shaham *et al* examined DPC in peripheral blood lymphocytes of workers exposed to FA, and they found a significantly positive correlation between FA and DPC concentrations. In their early work, they also found a linear relationship between years of FA exposure and the amount of DPC[12,13]. Epidemiological studies on workers also suggested that the possible relations between FA exposures and leukemia[14,15]. These authors proposed that although inhaled FA was metabolized rapidly at contact sites, FA might be transported by unknown mechanism and cause cancers like leukemia subsequently.

To investigate FA-induced genotoxicity in the distant organs such as liver, kidney and testicle of mice, in this study, the content of FA-induced DPC in the organs of mice was detected by KCl-SDS assay. At the same time, the results will give more information to understand whether FA has distant-site toxicity. Additionally, this study may be helpful to understand the genotoxicity and the carcinogenicity of FA comprehensively and systematically, providing a scientific basis for constituting secure professional concentration standard of FA.

2 Materials and Methods

2.1 Reagents and apparatus

10% formalin, calf thymus DNA and fluorescence dye Hoechst 33258 were purchased from Sigma(USA). Sodium dodccyl sulfate (SDS) and proteinase K were purchased from Merck(Germany). PBS (without Ca^{2+} and Mg^{2+}), trypan blue solution of 0.4% and other chemicals were of analytical grades.

A WH-2 type environmental chamber (WH-2, Yu-Xin Inc, China) as FA generator, a 4160 type digital electrochemical FA analyzer (Interscan Inc, USA), glass low inhalation chamber, temperature centrifuge (Eppendof-5415R), fluorescence spectrophotometer (RF-4500, HITACHI, Japan) were used in the experiments.

2.2 Animal

24 male Kunming mice were supplied by the Experimental Animal Center of Hubei Province, China. Animals' weight were 19 ± 1 g.

2.3 Mice exposure to gaseous FA

24 male Kunming mice were divided randomly into 4 testing groups ($n = 6$ each) and were exposed to different concentrations of FA: 0, 0.5, 1.0 and 3.0 mg/m^3. The inhaled groups were exposed to gaseous FA for 72 hours continuously. During the exposure the mice were allowed to drink and eat twice at fixed time each day. FA inhaled groups were placed into glass inhalation chambers. The chamber temperature was 23 ℃ ± 0.5 ℃, and the humidity was 45% ± 0.5%, and the gas flux was 1 ± 0.01 L/min. A 4160 type digital electrochemical analyzer was used to measure the concentrations of gaseous FA.

2.4 Preparation of cells

Mice were executed immediately after exposure and livers, kidneys and testicle were obtained. The tissues were minced with scissors and homogenized with seven to eight strokes in PBS (pH 7.5). The homogenate was filtered through four layers of cheesecloth and then the cells were collected by centrifugation at 1500 rpm for 5 min. After re-suspending, the cell density was regulated with PBS and cell viability was analyzed with the method of trypan blue exclusion. Cell viability was above 95% and density was $10^5 - 10^6$ cells per ml.

2.5 KCl-SDS assay

In this study the KCl-SDS assay was based on Zhitkovich and Chakrabarti methods with some modification to detect FA-induced DPC[16,17]. Cells were harvested by centrifugation at 1500 rpm for 5 min. The cells were resuspended in 0.5 ml of PBS, pH 7.5, followed by lysis with 0.5 ml of 2% SDS solution with gentle vortexing. The lysate solution was heated at 65 °C for 10 min and then 0.1 ml of pH 7.4 and 10 mM Tris-HCl containing 2.5 M KCl was added, followed by passing the resultant mixture six times through a 1 ml polypropylene pipette tip to favor shearing of DNA for a uniform length. Since SDS binds tightly to protein but not to DNA, the free protein and protein-DNA complexes are precipitated with added SDS while free DNA is remained in the supernatant. The SDS-KCl precipitate (containing the protein and DNA-protein crosslinks complexes) was formed by placing the samples in ice for 5 min and was then collected by centrifugation at 10,000 rpm for 5 min. The supernatants containing the unbound fraction of DNA were collected in different labeled tubes. The pellets (containing DPC) were washed three times by resuspending in 1 ml washing buffer (0.1 M KCl, 0.1 mM EDTA, and 20 mM Tris-HCl, pH 7.4) followed by heating at 65 °C for 10 min, chilling in ice for 5 min, and centrifugating as described above. The latter supernatants from each wash were added into the previous one with unbound fractions of DNA. The final pellet was resuspended in 1 ml proteinase K solution (0.2 mg/ml soluble in a wash buffer) and digested for 3 h at

50 °C. The resultant mixture was centrifuged at 12,000 rpm for 10 min and the supernatant was collected (the supernatant contained the DNA previously involved in DNA-protein crosslinks). 1 ml of either the supernatant containing the unbound fraction of DNA or the supernatant containing the DNA previously involved in DNA-protein crosslinks was then mixed with 1 ml freshly prepared fluorescent dye Hoechst 33258 (400 ng/ml soluble in 20 mM Tris-HCl), and then the tubes were allowed to stand for 30 min in the dark[18]. The sample fluorescence was measured using a RF-4500 fluorescence spectrofluorimeter with excitation wavelength 350 nm and emission wavelength 450 nm. The DNA contents of the samples were determined quantitatively through a corresponding DNA standard curve (as Figure 1 shows and regression equation is $y = 2.4423 + 0.0028x$, $r^2 = 0.9974$) generated from a set of calf thymus DNA. The DPC coefficient was measured as a ratio of the percentage of the DNA involved in DPC over the percentage of the DNA involved in DPC plus unbound fraction of DNA.

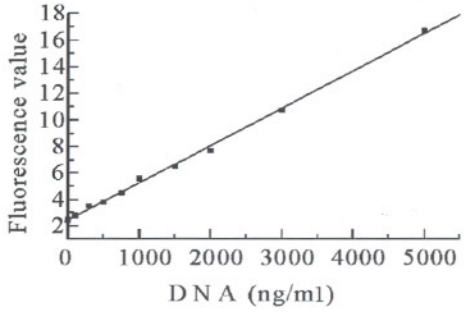

Figure 1. The standard curve of DNA concentration

2.6 Statistical analysis

Results were analyzed by software Origin 6.0. Student's t-test was applied to evaluate the significance of the differences in the results between treated and control groups. A level of $P<0.05$ was defined to be statistically significant.

3 Results

3.1 Effect of FA-induced DPC in the livers of mice

Figure 2 showed the effect of gaseous FA exposure on DPC levels in livers of mice. There was no significant difference in DPC coefficient between 0.5 mg/m^3 FA inhaled group and 0 mg/m^3 control group. However, the DPC levels at 1.0 mg/m^3 and 3.0 mg/m^3 groups were significantly ($P<0.01$) higher than that in the control group, demonstrating that as the inhaled gaseous FA concentrations increased, the DPC levels ascended.

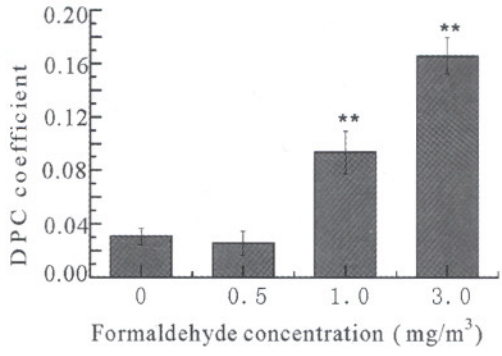

Figure 2. DPC formation in mice liver cells at different FA concentrations

* * : $P<0.01$, compared with control group

3.2 Effect of FA-induced DPC in the kidneys of mice

Figure 3 showed the effect of gaseous FA on DPC levels in kidneys of mice. There was significant difference in the DPC levels between control group and FA inhaled groups($P<0.01$). The results indicated that the DPC levels ascended with the increasing of inhaled gaseous FA concentrations.

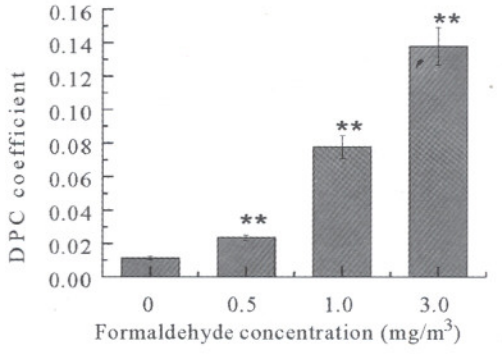

Figure 3. DPC formation in mice kidney cells at different FA concentrations

* * : $P<0.01$, compared with control group

3.3 Effect of FA-induced DPC in the testicles of mice

Figure 4 showed that the DPC coefficient of 0.5 mg/m^3 FA-treated group was significantly higher than that of control group ($P<0.05$), and there were significant difference in DPC coefficient between 1.0 mg/m^3, 3.0 mg/m^3 FA-treated groups and the control group ($P<0.01$). It indicated that there was a clearly dose-dependent rela-

tionship between the DPC coefficient and the concentrations of FA.

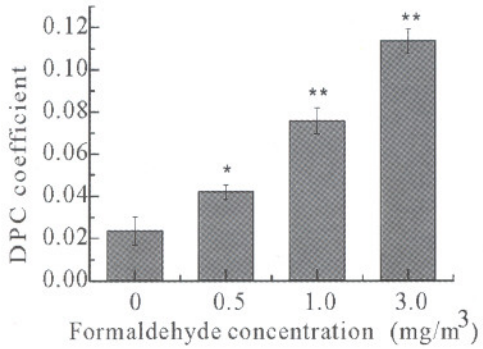

Figure 4. DPC formation in mice testicle cells at different FA concentrations
*: $P<0.05$; **: $P<0.01$, compared with control group

4 Discussion

4.1 Parameters of chamber and the concentrations of gaseous FA

The concentrations of gaseous FA generated by small environmental chamber were measured 3 times per day for 3 days. The measurement results (0.03 ± 0.03 mg/m^3, 0.49 ± 0.03 mg/m^3, 1.03 ± 0.04 mg/m^3 and 3.03 ± 0.08 mg/m^3) were very close to the anticipative concentrations (0 mg/m^3, 0.5 mg/m^3, 1.0 mg/m^3 and 3.0 mg/m^3). It indicated that the gaseous FA from chamber emission was quite stable and reliable.

In the previous studies, gaseous FA was generated from paraformaldehyde. Then high level of FA was diluted with clean, filtered air to achieve the desired gas concentrations[19]. In this way, it was very difficult to control the temperature (T), the humidity (RH) and the gas flux (F) of gaseous FA. It is well-known that the alterations of temperature and humidity could affect the experimental results remarkably. The gas flux of FA is also important to the inhalational quality of mice. In the present study, different concentrations of gaseous FA were generated by small environmental chamber with formalin. In this method, the temperature, the humidity and the gas flux could be set by the chamber before exposure. The parameters of the chamber will be very stable after 3 hours of operation. The results were showed in Figure 5. Thus, this experimental method has great improvement for better reliability and higher reproducibility.

4.2 Comparison of the effect of FA-induced DPC in the three different organs of mice

According to the effect of FA-induced DPC in the three different organs of mice, we could conclude that FA could induce DPC with a dose-dependent relationship between the DPC coefficient and the concentrations of FA. We also found that the DPC level of 3.0 mg/m^3 FA inhaled groups of liver was the highest and that of testicle was the lowest, which indicated that gaseous-FA-induced genotoxicity in the liver of mice was the most severe, then was kidney and the least was testicle.

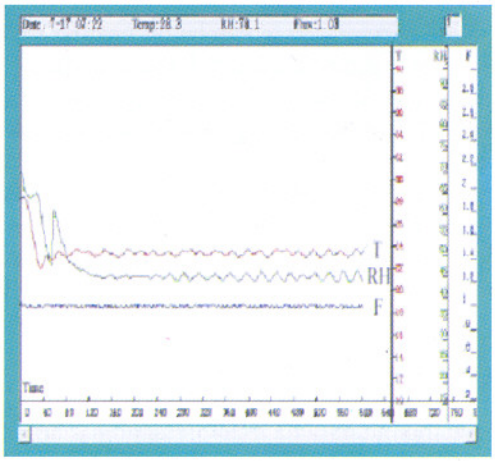

Figure 5. The parameters of the small environmental chamber

4.3 The mechanism of the FA-induced DPC

DPC is relatively permanent in the cells. Due to the poor repair capacity, DNA-protein complexes may be present during DNA replication and possibly cause a loss and inactivity of the important genes such as tumor suppressor genes, and may be responsible for tumor formation. For the electrophilicity of carbonyl and smaller steric hindrance, FA is apt to form DPC. Initially, a hydroxymethyl intermediate is formed by the addition of FA to a primary amine of either DNA or protein. The hydroxymethyl group then condenses with a second primary amine to produce a methylene bridge between DNA and protein. The form of DPC can be expressed as histone-NH-CH_2-NH-DNA. Additionally, as a inhibitor to antioxidases, FA could induce the formation of DPC indirectly, for example, by increasing the content of DPC resulted from the depletion of GSH and the inhibition of glutathioneperoxidase and superoxide dismutase which can clear hydroxy radical and oxygen-derived free radicals[6,13,20,21].

4.4 FA and distant-site toxicity

Whether the FA does have the distant-site toxicity and what is the mechanism still is unknown. Thrasher proposed that rapid removal of FA was insufficient to support that FA could not induce distant-site toxicity, because FA might form adducts with amino acid or other biological molecule in blood, and the adducts could be sent to remote

sites by blood circular system and generate FA again, so these adducts were responsible for tumors caused by FA[22]. In fact, as biochemical active as nitric oxide (NO), it is also able to induce physiological and toxicological effects at distant sites, probably by forming adducts[23,24]. NO is active to sulfhydryl and amino groups, and interestingly, recent work showed that it was also the cause for FA[25]. Therefore, it would be interesting to investigate which kind of adduct formed in blood after exposure to FA, since it had been proposed that the amount of free FA in blood was not altered after exposure.

In the present study, significant DPC could be detected in the three organs of liver, kidney and testicle when the mice were exposed to gaseous FA of higher concentrations, which evidently indicated that FA might induce distant-site toxicity.

5 Conclusions

In this study, KCl-SDS assay was applied to detect the amount of DPC in liver, kidney and testicle of mice. According to the results, we could conclude that FA could induce DPC significantly at the higher concentrations, the results also indicated that FA might induce distant-site toxicity.

Acknowledgments

This work is supported by China National Science Foundation (project coded 30570799).

Correspondence to:
Xu Yang
College of Life Sciences
Huazhong Normal University
No. 152, Luo-Yu Road, Wuhan 430079, China
Email: yangxu@mail.ccnu.edu.cn

References

1. International Agency for Research on Cancer. 2004. IARC classifies formaldehyde as carcinogenic to humans. 2004-06-15, http://www.iarc.fr/ENG/Press-Releases/archives/pr153a,html.
2. Bunde RL, Jarvi EJ, Rosentreter JJ. A piezoelectric method for monitoring formaldehyde induced crosslink formation between poly-lysine and poly-deoxyguanosine. Talanta 2000; 51: 159-71.
3. Conaway CC, Whysner J, Verna LK. Formaldehyde mechanistic data and risk assessment: endogenous protection from DNA adduct formation. Pharmacol Ther 1996; 71: 29-55.
4. Kuykendall JR, Trela BA, Bogdanffy MS. DNA-protein crosslink formation in rat nasal epithelial cells by hexamethylphosphoramide and its correlation with formaldehyde production. Mutat Res 1995; 343: 209-18.
5. Casanova M, Deyo DF, Heck HD. Covalent binding of inhaled formaldehyde to DNA in the nasal mucosa of Fischer 344 rats: analysis of formaldehyde and DNA by high-performance liquid chromatography and provisional pharmacokinetic interpretation. Fundam Appl Toxicol 1989; 12: 397-417.
6. Casanova M, Morgan KT, Gross EA. DNA-protein cross-links and cell replication at specific sites in the nose of F344 rats exposed subchronically to formaldehyde. Fundam Appl Toxicol 1994; 23: 525-36.
7. Casanova M, Morgan KT, Steinhagen WH, *et al*. Covalent binding of inhaled formaldehyde to DNA in the respiratory tract of Rhesus monkeys: pharmacokinetics, rat-to-monkey interspecies scaling, and extrapolation to man. Fundam Appl Toxicol 1991;17: 403-28.
8. Liu YS, Lu ZS, Yang JW, *et al*. Quantification study on the DNA-protein in crosslinks of human blood lymphocytes induced by formaldehyde. Hubei journal of preventive medicine 2004; 15: 4-7.
9. Heck HD, Casanova M. The implausibility of leukemia induction by formaldehyde: a critical review of the biological evidence on distant-site toxicity. Regul Toxicol Pharmacol 2004; 40: 92-106.
10. Collins JJ, Ness R, Tyl RW. A review of adverse pregnancy outcomes and formaldehyde exposure in human and animal studies. Regul Toxicol Pharmacol 2001; 34: 17-34.
11. Franks SJ. A mathematical model for the absorption and metabolism of formaldehyde vapour by humans. Toxicology and Applied Pharmacology 2005;206: 309-20.
12. Shaham J, Bomstein Y, Gurvich R. DNA-protein crosslinks and p53 protein expression in relation to occupational exposure to formaldehyde. Occup Environ Med 2003; 60: 403-9.
13. Shaham J, Bomstein Y, MeltzerA, *et al*. DNA-protein crosslinks, a biomarker of exposure to formaldehyde-*in vitro* and i*n vivo* studies. Carcinogenesis 1996; 17: 121-5.
14. Coggon D, Harris EC, Poole J. Extended follow-up of a cohort of British chemical workers exposed to formaldehyde. J Natl Cancer Inst 2003; 95: 1608-15.
15. Hauptmann M, Lubin JH, Stewart PA. Mortality from lymphohematopoietic malignancies among workers in formaldehyde industries. J Natl Cancer Inst 2003; 95: 1615-23.
16. Zhitkovich A, Costa M. A simple, sensitive assay to detect DNA-protein crosslinks in intact cells and *in vivo*. Carcinogenesis 1992; 13:1485-9.
17. Chakrabarti SK, Bai CJ, Subramanian KS. DNA-protein crosslinks induced by nickel compounds inisolated rat renal cortical cells and its antagonism by specific amino acids and magnesium ion. Toxicol Appl Phamacol 1999; 154: 245-55.
18. Cesarone CF, Bolognesi C, Santi L. Improved microfluorometric DNA determination in biological materical using 33258 Hoechst. Anal Biochem 1979; 100: 188-97.
19. Fujimaki H, Kurokawa Y, Kunugita N, *et al*. Differential immunogenic and neurogenic inflammatory responses in an allergic mouse model exposed to low levels of formaldehyde. Toxicology 2004; 197: 1-13.
20. Speit G, Schutz P, Merk O. Induction and repair of formaldehyde-induced DNA-protein crosslinks in repair-deficient human cell lines. Mutagenesis 2000; 15: 85-

90.
21. Takashima H, Boerkoel CF, John J. Mutation of TDP1, encoding a topoisomerase I-dependent DNA damage repair enzyme, in spinocerebellar ataxia with axonal neuropathy. Nature Genet 2002; 32: 267 – 72.
22. Thrasher JD, Kilburn KH. Embryo toxicity and teratogenicity of formaldehyde. Arch Environ Health 2001; 56: 300 – 11.
23. Hogg N. The biochemistry and physiology of S-nitrosothiols. Annu Rev Pharmacol Toxicol 2002; 42: 585 – 600.
24. Weinberger B, Laskin DL, Heck DE, *et al*. The toxicology of inhaled nitric oxide. Toxicol Sci 2001; 59: 5 – 16.
25. Metz B, Kersten GF, Hoogerhout P, *et al*. Identification of formaldehyde-induced modifications in proteins. Biol Chem 2004; 279: 6235 – 43.

Received June 5, 2006

Microarchitecture Fabrication Process of the Artificial Bone

Zhongzhong Chen[1], Cheng Li[1], Zhiqiang Jiang[2], Zhiying Luo[3]

1. College of Mechanical Engineering, Zhengzhou University, Zhengzhou, Henan 450001, China
2. Department of Mechanical Engineering, Zhengzhou Institute of Aeronautics, Zhengzhou, Henan 450015, China
3. The Second Internal Hospital of Zhengzhou University, Zhengzhou University, Zhengzhou, Henan 450002, China

Abstract: By using bionic modeling and rapid prototyping technology, a novel system based on air-pressure jet solidification (AJS) technique is developed to fabricate porous microarchitecture of the artificial bone. Acting as transitional carrier of the bone implant, the porous scaffolds formed could provide proper porosity and interconnections for the growth of bone tissue and nutrient transport. This approach is better than traditional fabrication processes, because the latter methods cannot fabricate a microarchitecture with spatial bending micropores so as to satisfy biological requirements. [Life Science Journal. 2006;3(3):88-93] (ISSN: 1097-8135).

Keywords: rapid prototyping; scaffolds; air-pressure jet solidification

Abbreviations: AJS: air-pressure jet solidification; DS: denatured sucrose; FDM: fused deposition modeling; RP: rapid prototyping

1 Introduction

In the view of tissue engineering, the osteo-replacement tissue must have proper aperture and porosity for bone repair so as to accelerate bone regeneration. Moreover, it must serve as three-dimensional (3-D) template for initial cell attachment and subsequent tissue regeneration[1-3]. Conventional wisdom states that scaffolds should be designed to match healthy tissue morphological characteristics and have an interconnected pore network for cell migration and nutrient transport. Furthermore, the simulation design of the inter-connective architecture has a decisive effect on the activation of bone substitute. The traditional methods to fabricate scaffolds include polymer foaming technique, particulate-leaching, solid-liquid phase separation, textile technique and extrusion process, etc[4-10]. But with these methods, the bionic architecture similar in morphological characteristics to the inter-microstructure of the natural bone could not be ensured, which is essential to vascularization and tissue regeneration.

Based on the building principle of fused deposition modeling (FDM) in rapid prototyping (RP) technology, a new forming technique - AJS system is developed, which can build up the bone scaffolds with a novel fabrication material. The formed scaffold possesses an exterior mould exactly coincident with the replaced bone and interior porous architecture simulating the microstructure of the natural bone tissue. By filling self-setting calcium phosphate cement (CPC, a kind of biomaterial for bone substitute) and rhBMP (recombinant human bone morphogentic protein, a kind of growth factor) into the scaffolds, the fabricated scaffolds are dissolved with the solidification of CPC, and then the simulated interior microstructure is formed.

2 Materials and Methods

2.1 Fabrication material

A kind of fabrication material - denatured sucrose(DS) is developed to form the 3-D scaffolds. As a forming material, DS has proper plasticity, ductility and viscosity, so that the 3-D scaffolds can be built up and will not distort after solidification. Equally important, as an implantable biomaterial, DS has some proper histological performance and can be served as a biomaterial stabilizer of protein to maintain the activation of rhBMP.

2.2 AJS system

AJS system is designed to fabricate the artificial bone based on the layer-by-layer manufacturing principle of RP[11]. In the process, refined DS is fed into two controllable jets and melted into a semi-molten state by a heating system. Each jet has a

small nozzle on the tip, the diameter of the nozzle is 0.2 mm. Both jets are connected to an air compressor. Fine DS filament can be expressed through the nozzle by applying compressed air. Under the control of a computer, the on-off operation of the pressure air can be controlled by electromagnetic valves, then a 3-D working platform moves according to the processed data generated from the bionic modelling. So the filament is deposited layer-by-layer, and finally, a 3-D part is built in the areas defined by CAD model (Figure 1).

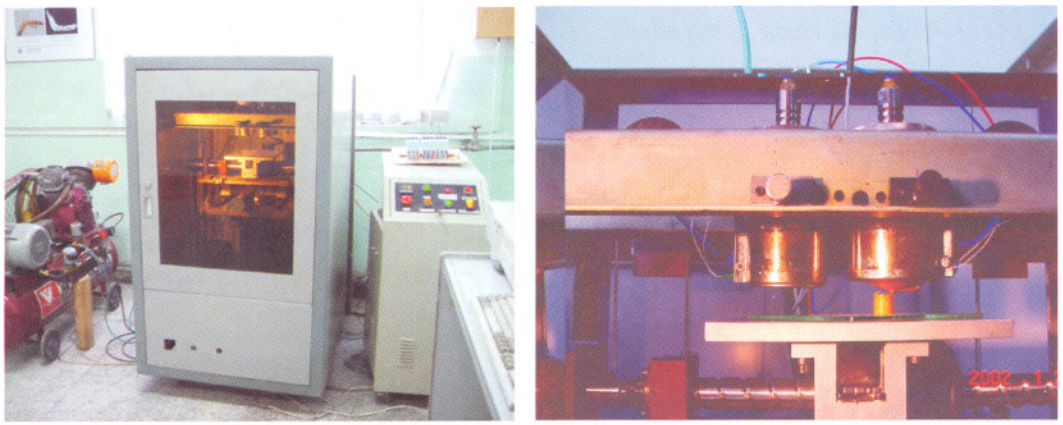

Figure 1. AJS system and its key part—two pressure jets

2.3 Diameter of filament

AJS system has many technical parameters, such as temperature of jet, squeezing and scanning velocity etc, all of these are the important process variables which determine the quality of the part. Due to the scaffolds fabricated, the key index is the diameter of filament in the fabrication process, which determine the configuration of the microarchitecture in the interior of artificial bone.

A calculation modeling is built up according to the matching relation of squeezing and scanning velocity of the jet. DS is a kind of thermoplastic material with a certain viscoelasticity. According to the viscoelastic and rheologic theory, it will keep in a semi-molten state in the whole fabrication process. Through double actions of air pressure and the traction force of the solidified layer, the shearing stress in DS would be occurred. Therefore, the tensile process is belong to non-Newtonia fluid and stretching flow. According to the theory analysis and expriments result, after the filament expressed from jet, the cross-section of filament can be concluded as Figure 2(a) in the tensile region, which is a rectangular CFGH (Ⅲ) in the center and two conics at both ends.

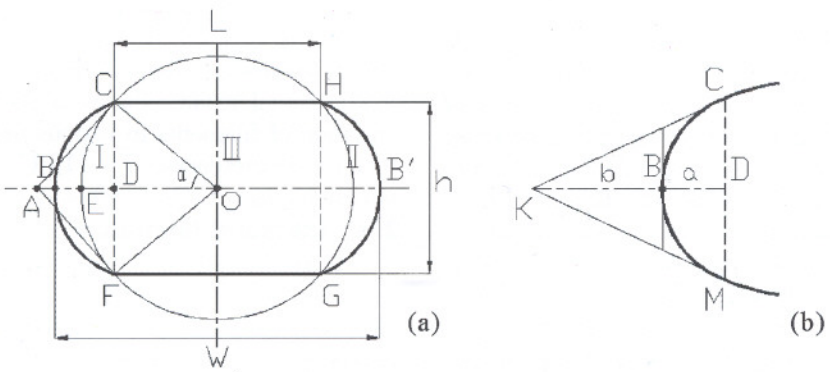

Figure 2. Illustration of solidification filament model in cross-section

According to the conic in Figure 2(b), line KC, KM are tangent to arc MBC, given MC = h,

KB = b and BD = a, ρ is defined as $a/(a+b)$, from spline geometrics, it can be educed that the contour of conic, namely the type of arc MBC can be determined by ρ, and a serial of conclusions could be derived as

1) $0.05<\rho<0.5$, the conic is ellipse;

2) $\rho=0.5$, the conic is parabola;

3) $0.5<\rho<0.95$, the conic is hyperbola.

For easy to analysis and calculation, Figure 2 is simplified as follows:

a) While the squeezing velocity V_p is slow, namely while $\rho<0.3$, the cross-section contour of filament can be simplified as rectangle Ⅲ in Figure 2(a). Due to the filament flow in unit time is equal to the forming volume required, an expression should be derived as

$$V_p \cdot \pi d^2/4 = V_s \cdot L \cdot h \tag{1}$$

$$W = L = \frac{\pi d^2 V_p}{4hV_s} \tag{2}$$

Where h is defined as the height between the nozzle and fabricated layer, d is the diameter of nozzle, V_p is the squeezing velocity, Vs is the scanning velocity of jet, L is the width of rectangle Ⅲ, W is the diameter of filament.

b) The area of conic must be taken into account while Vp is increased to a certainty. If the contour of conic is difficult to describe, arc FEC can be used for approximate the conic (Figure 2 (a)). It belongs to the circle which include the four border point of rectangle Ⅲ, where O is defined as center of circle, segment AC, AF are tangent to arc CEP. Given FD = DC = $h/2$, OD = $L/2$, then the equation of ρ should be deduced as

$$\rho = \frac{ED}{BD} = \frac{\frac{\sqrt{L^2+h^2}-L}{2}}{\frac{h}{L}\cdot\frac{h}{2}}$$

$$= [1+\sqrt{1+(\frac{h}{L})^2}]^{-1} \quad (0<\frac{h}{L}<1) \tag{3}$$

While h/L is taken values in the interval of (0, 1), according to expression (3), it can be concluded that variation range of ρ is in the interval of (0.414, 0.5). Due to in the fabrication process, h/L is taken values in the interval of (0, 0.5). Generally speaking, ρ is be in the interval of (0.472, 0.5), namely ρ is set in the middle of value 0.05 and 0.95, therefore, the curvature range is between ellipse and hyperbola, which is approach parabola. Therefore, arc FEC is served as substitutional curve to calculate area I and Ⅱ approximately.

Therefore, while Vp is increased to a certainty, ρ is equal or greater than 0.3, the cross-section area of filament can be expressed as:

$$A_{\mathrm{I}} = A_{\mathrm{sector(OFEC)}} - A_{\mathrm{triangle(OPC)}}$$

$$= \frac{1}{2}\left(\sqrt{\frac{L^2+h^2}{2}}\right)^2 \cdot 2\alpha - \frac{L\cdot h}{4}$$

$$\approx \frac{1}{2}\left(\sqrt{\frac{L^2+h^2}{2}}\right)^2 \cdot 2\frac{h}{\sqrt{L^2+h^2}} - \frac{L\cdot h}{4}$$

($since$ $\sin\alpha \approx \alpha$, $|\alpha| \ll 1$)

$$= \frac{h}{4}(\sqrt{L^2+h^2}-L) \tag{4}$$

$$A_{\text{section of filament}} = A_{\text{rectangle Ⅲ}} + 2A_{\mathrm{I}}$$

$$= L\cdot h + 2\cdot\frac{h}{4}(\sqrt{L^2+h^2}-L)^2$$

$$= \frac{h}{2}(\sqrt{L^2+h^2}+L) \tag{5}$$

From the principle of equal volume, it can be deduced that

$$\frac{\pi}{4}d^2\cdot V_p = A_{\text{section of filament}}\cdot V_s$$

$$= \frac{h}{2}(\sqrt{L^2+h^2}+L)\cdot V_s \tag{6}$$

If $\zeta = \frac{\pi d^2 V_p}{2hV_s}$, it follows that

$$L = \frac{\zeta^2 - h^2}{2\zeta} \tag{7}$$

In Figure 2(a), by using the length of segment AD as the distance of conic vertex to rectangular border CF, the value L can be deduced according to the expression (7), consequently, the expression of filament diameter can be derived

$$W = L + 2\cdot AD = L + 2\cdot\frac{h^2}{2L} = \frac{L^2+h^2}{L} \tag{8}$$

c) Illustration and analysis

In the fabrication process of filaments, given $d = 0.3$ mm, $h = 0.2$ mm, $Vp = 15$ mm/s, $Vs = 20$ mm/s, value W can be calculated from expression (2) and (8), which is 0.265 mm and 0.403 mm respectively. Comparing with the actual measurement result, which is 0.4 mm, it can be concluded that the calculation modeling of expression (8) is feasible, so that the calculation value is close to the actual result. Figure 3 shows the diameter variation of filaments in various processing parameter, for concreteness, $T = 115$ ℃, $P = 0.95$ Mpa, parameter h_k, Vs is variable.

2.4 Integrated fabrication

According to the bionic CAD modelling[12], some anatomical characteristic can be conclude that Haversian canals are connected by Volkmann's canals with a constant angle, the average diameter of Haversian canal is approximately 300 μm, the average diameter of Volkmann's canal is approximately 200 μm. In view of these considerations and the fabrication characteristic of AJS system, a

forming process can be designed to form conduction of osteons in one cross section by expressing the filament from point to point. Furthermore, in order to ensure the interconnection of osteons between upper and lower cross-sections, the jet should pause temporarily at the point of Haversian canals so that the filament can be expressed downwards further. In this way, the integrated fabrication of Haversian and Volkman's canals can be realized (Figure 4).

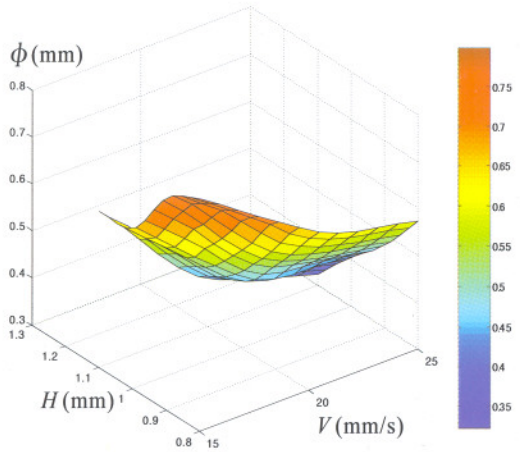

Figure 3. Diameter variation of filaments in various processing parameter

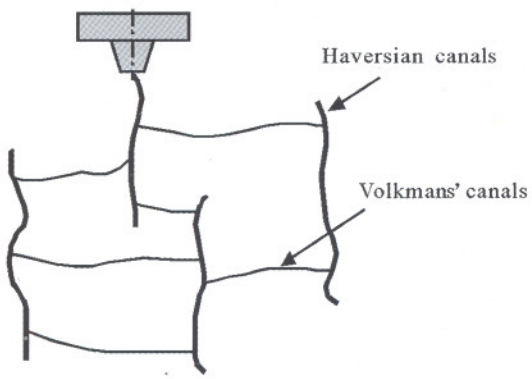

Figure 4. Schematic illustration of the microarchitecture forming process in vertical direction

From the mathematical model of the interior microstructure, the integrated fabrication of Haversian and Volkman's canals can be realized in the fabrication direction. After feeding DS into two jets, jet I and jet Ⅱ are heated to 90 ℃ and 120 ℃ respectively and kept unchanged during the whole forming process. Jet I expresses fine filament with the platform moving in X-Y directions according to the processed data of exterior contour. After one layer of exterior contour is fabricated, the platform moves 0.2 mm downwards, and continues to fabricate the next layer, so the exterior mould can be built up layer-by-layer. Until the required height reaches to build the interior scaffolds, jet I is cut off, and the platform moves horizonally to the position under jet Ⅱ, then jet Ⅱ begins to express fine filament. Therefore, in the whole process, with the platform moving according to the processed data, the fabrication of exterior mould and interior scaffolds can be built up by controlling the two jets cooperatively, so the 3-D scaffolds can be fabricated (Figure 5).

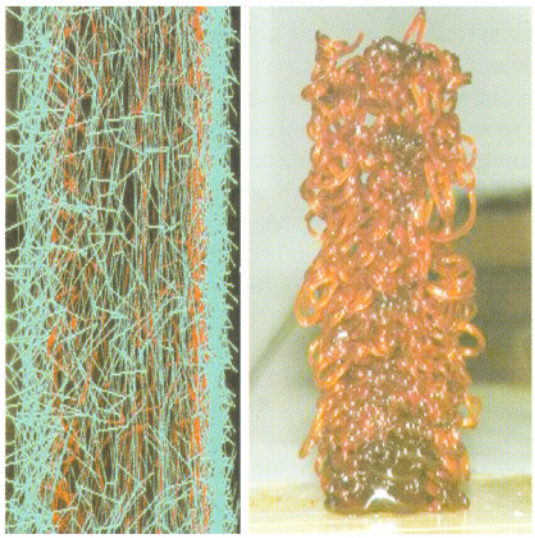

Figure 5. Simulated building of the interior 3-D scaffolds and corresponding scaffolds fabricated on AJS system

3 Results

3.1 Porous microstructure, porosity and pore dimension

After filling CPC into the cavities of bone scaffolds and solidifying process, the artificial bone can be produced. It can be concluded that the compressive strength of the bone substitute, the degradation rate and osteogenesis as well as osteogenetic quality are all associated closely with porosity. Equally important, the pore dimension is also a key index in osteoconduction, which plays an important role in infiltration of tissue fluid and osteogenesis. In view of medichine, the porosity of 60% or more and the pores dimension ranging from 200 to 500 μm in bone substitue are suitable for the bone regeneration[13]. The CPC porosity is 40%, and the average micropore dimension is about 5 μm. So the porous architecture of the bone scaffolds must include fabricated micropores and the inherent micropores of CPC. Therefore, the average diameters of Haversian canals and Volkman's canals should be controlled within 200 μm and 350 μm respectively.

The porosity can be adjusted by changing the height (H). Experiments determine that if fabricating two layer filament scaffolds within 1 mm, the interference or destruction between two adjacent filament scaffolds will occur, furthermore, the thermal field of the nozzle would melt the previous filament scaffolds. On the other hand, if fabricating two layer filament scaffolds to 4 mm or more, the interior architecture will distort and could not satisfy the necessary porosity. According to the experimental analysis, the suitable porosity can be well ensured if H is 2 mm, which can ensure the simulation accuracy and give enough space for heat dissipation.

The porous morphologies of the bone scaffolds are examined by gross observation, microscope and scanning electron microscopy (SEM). The bone scaffolds is cut off with a scalpel in both horizontal and vertical directions. Macroscopically, clear channels and micropores can be seen in both vertical and horizontal directions (Figure 6).

Under microscope (Keyence Company VH-8000, Japan), the porous morphologies encompassing Haversian canals and Volkman's canals are visible. There is no remarkable difference in shape or size between the filament scaffolds and the porous architecture formed in the bone scaffolds. The porosity of the bone scaffolds is 63.2% measured by toluene infiltration displacement method, which can satisfy the histological criterion of carrier scaffolds in bone tissue engineering.

The porous morphologies of the scaffold are examined by SEM at 20 KV (JEOL Company DJM-840, Japan) (Figure 7). From the energy spectrum analysis of line scanning between two micropores centers in a cross-section, it can be seen that there is no any chemical element in the center of micropore, the carbon content (the main element of DS) is the highest in the border of micropores, and decreases gradually outwards; at the same time, the content of calcium and phosphorus (the main elements of CPC) increase gradually. These findings suggest that micropores can be formed with the 3-D scaffolds of DS dissolving gradually during the solidification of CPC. So the validity of using filament scaffolds to fabricate the interior microstructure of bone scaffolds is confirmed.

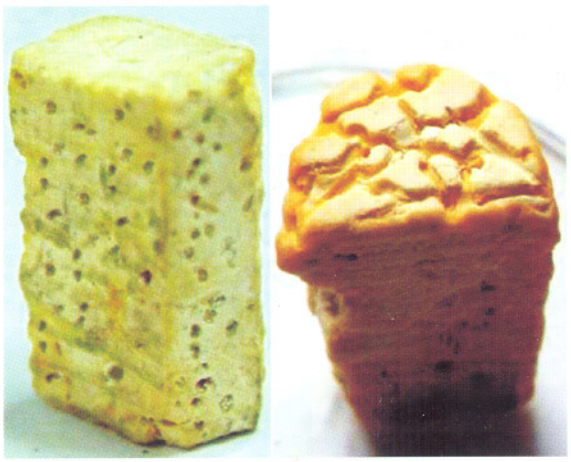

Figure 6. The fabricated bone scaffold

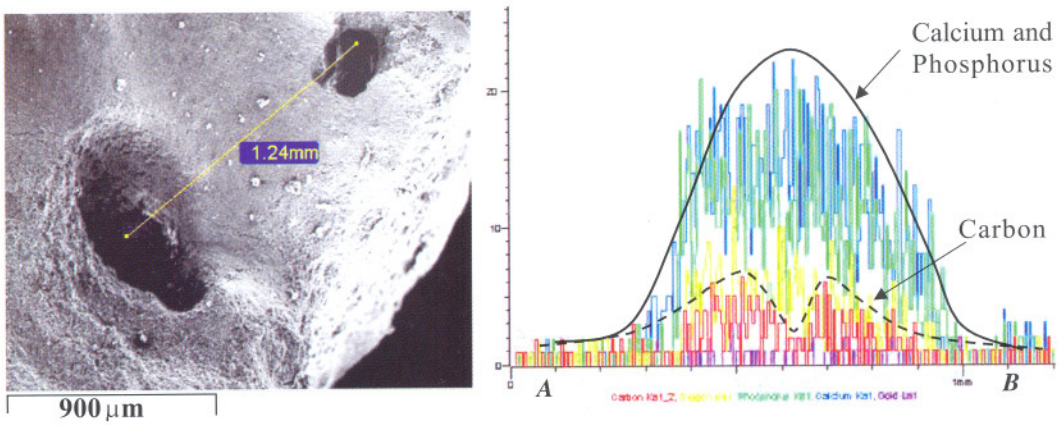

Figure 7. SEM image of the macropores in scaffolds

4 Conclusions

According to previous bionic CAD modelling for artificial bone, bone scaffolds can be produced through the fabrication system built and integrated fabrication method, which has the exact external contour of replaced bone and tissue-like 3-D scaffolds simulating the interior of natural bone. In this study, matching relation of processing parameters is determined through theory analysis and experiment, moreover, results show that some necessary

indexes of biology, such as porous microstructure, porosity and pore dimension can be obtained accurately, which can provide an inherent network of channels for tissue fluid circulation and realize bone transformation.

Correspondence to:
Zhongzhong Chen, Ph.D.
College of Mechanical Engineering
Zhengzhou University
Zhengzhou, Henan 450001, China
Telephone: 86-371-6778-1235
Email: zzchen@zzu.edu.cn

References

1. Sherwood JK, Riley SL, Palazzolo R, *et al*. A three-dimensional osteochondral composite scaffold for articular cartilage repair. Biomaterials 2002; 23(24): 4739－51.
2. Goldstein AS, Juarez TM, Helmke CD, *et al*. Effect of convection on osteoblastic cell growth and function in biodegradable polymer foam scaffolds. Biomaterials 2001; 22 (11): 1279－88.
3. Deng Y, Lin XS, Zheng Z, *et al*. Poly (hydroxybutyrate-co-hydroxyhexanoate) promoted production of extracellular matrix of articular cartilage chondrocytes *in vitro*. Biomaterials 2003; 24(23): 4273－81.
4. Vaz CM, van Tuijl S, Bouten CVC, *et al*. Design of scaffolds for blood vessel tissue engineering using a multilayering electrospinning technique. Acta Biomaterialia 2005; 1(5): 575－82.
5. Shum AWT, Li J, Mak AFT. Fabrication and structural characterization of porous biodegradable poly(dl-lactic-co-glycolic acid) scaffolds with controlled range of pore sizes. Polymer Degradation and Stability 2005; 87(3): 487－93.
6. Ang TH, Sultana FSA, Hutmacher DW, *et al*. Fabrication of 3D chitosan-hydroxyapatite scaffolds using a robotic dispensing system. Materials Science and Engineering: C 2002; 20(1－2): 35－42.
7. Ma JB, Wang HJ, He BL, *et al*. A preliminary *in vitro* study on the fabrication and tissue engineering applications of a novel chitosan bilayer material as a scaffold of human neofetal dermal fibroblasts. Biomaterials 2001; 22 (4): 331－6.
8. Thomson RC, Mikos AG, Beahm E, *et al*. Guided tissue fabrication from periosteum using preformed biodegradable polymer scaffolds. Biomaterials 1999; 20 (21): 2007－18.
9. Lin ASP, Barrows TH, Cartmell SH, *et al*. Microarchitectural and mechanical characteri-zation of oriented porous polymer scaffolds. Biomaterials 2003; 24(3): 481－9.
10. Gomes ME, Godinho JS, Tchalamov D, *et al*. Alternative tissue engineering scaffolds based on starch: processing methodologies, morphology, degradation and mechanical properties. Materials Science and Engineering: C 2002; 20(1－2):19－26.
11. Hutmacher DW, Sittinger M, Risbud MV. Scaffold-based tissue engineering: rationale for computer-aided design and solid free-form fabrication systems. Trends in Biotechnology 2004; 22(7):354－62.
12. Petzold R, Zeilhofer HF, Kalender WA. Rapid prototyping technology in medicine-basics and applications. Computerized Medical Imaging and Graphics 1999; 23(5): 277－84.
13. Nakagawa T, Sugiyama T, Kamei T, *et al*. An immuno-light- and electron-microscopic study of the expression of bone morphogenetic protein-2 during the process of ectopic bone formation in the rat. Archives of Oral Biology 2001; 46(5): 403－11.

Received June 13, 2006

Author Index

Subject Index

Instructions to Authors

1. General Information

(1) **Goals:** As an international journal published both in print and on internet, *Life Science Journal* is dedicated to the dissemination of fundamental knowledge in all areas of life science. The main purpose of *Life Science Journal* is to enhance our knowledge spreading in the world under the free publication principle. It publishes full-length papers (original contributions), reviews, rapid communications, and any debates and opinions in all the fields of life science.

(2) **Categories of publication:** Research articles, reviews, objective descriptions, research reports, opinions/debates, news, letters to editor, meeting report.

(3) **Cover feature:** The covers of *Life Science Journal* feature illustrations the Editor-in-Chief selects from the articles scheduled for publication in that issue. Authors whose articles are chosen for a cover feature will be asked to provide a high-quality version of the selected illustration as well as a brief legend (four to five sentences) describing the significance of the image. In light of the rapid production schedule for journal covers, authors are expected to provide the requested material within 3 days.

(4) **Publication costs:** US $ 30 per printed page of an article to defray costs of the publication will be paid by the authors when it is accepted. Extra expense for color reproduction of figures will be paid by authors (estimate of cost will be provided by the publisher for the author's approval). For the starting, publication fee will be waived for the current issues and they will be supported by Zhengzhou University.

(5) **Journal copies to authors:** Two hard copies of the journal will be provided free of charge for each author.

(6) **Additional copies bought by authors:** Additional hard copies could be purchased with the price of US $ 4/issue (mailing and handling cost included).

(7) **Distributions:** Web version of the journal is freely opened to the world without payment or registration. The journal will be distributed to the selected libraries and institutions for free. US $ 5/issue hard copy is charged for the subscription of other readers.

(8) **Advertisements:** The price will be calculated as US $ 400/page, i. e. US $ 200/a half page, US $ 100/a quarter page, etc. Any size of the advertisement is welcome.

2. Manuscripts Submission

(1) **Submission methods:** Electronic submission through email is encouraged and hard copies plus an IBM formatted computer diskette would also be accepted.

(2) **Software:** The Microsoft Word file will be preferred.

(3) **Font:** Normal, Times New Roman, 10 pt, single space.

(4) **Indent:** Type 4 spaces in the beginning of each new paragraph.

(5) **Manuscript:** Do not use "Footnote" or "Header and Footer".

(6) **Title:** Use Title Case in the title and subtitles, e. g. "**Debt and Agency Costs**".

(7) **Figures and tables:** Use full word of figure and table, e. g. "**Figure** 1. Annul income of different groups", **Table** 1. Annual increase of investment".

(8) **References:** Number the references in the order of their first mention in the text. References should include all the authors' last names and initials, title, journal, year, volume, issue, and pages etc.

Reference examples:

Journal article: Hacker J, Hentschel U, Dobrindt U. Prokaryotic chromosomes and disease. Science 2003;301(34):790 – 3.

Book: Berkowitz BA, Katzung BG. Basic and clinical evaluation of new drugs. In: Katzung BG, ed. Basic and Clinical Pharmacology. Appleton & Lance Publisher. Norwalk, Connecticut, USA. 1995:60 – 9.

(9) **Submission address:** America: lifesciencej@gmail.com, Marsland Press, P. O. Box 21126, Lansing, Michigan 48909, USA.

China: lifesciencej@zzu. edu. cn, Zhengzhou University, 100 Science Road, Zhengzhou, Henan 450001, China.

(10) **Reviewers:** Authors are encouraged to recommand 2 – 8 competent reviewers with their names and email addresses.

3. Manuscript Preparation

Each manuscript is suggested to include the following components but authors can do their own ways:

(1) Title. Including each author's full name; institution (s) with which each author is affiliated, with city, state/province, zip code, and country.

(2) Abstract. Including Background, Materials and Methods, Results, and Discussion.

(3) Keywords.

(4) Abbreviations. All abbreviations needed are listed here, so that they could be used directly in the article.

(5) Introduction.

(6) Materials and Methods.

(7) Results.

(8) Discussion.

(9) Acknowledgments.

(10) Correspondence. Correspondence author's full name, institution, city, state/province, zip code, country, telephone number, facsimile number (if available), and email address are listed here.

(11) References.

4. Copyright and Permissions

Life Science Journal

Acta Zhengzhou University Overseas Edition
Volume 3 Number 3, September 2006

Published by:
Zhengzhou University
Marsland Press

Sponsor:
North American Branch of Zhengzhou University Alumni

Zhengzhou University
100 Science Road
Zhengzhou, Henan 450001, China
Telephone: 86-371-6778-1272
Email:lifesciencej@zzu.edu.cn
Website:http://life.zzu.edu.cn

Marsland Press
P. O. Box 21126
Lansing, Michigan 48909, USA
Telephone: 517-980-4106
Email: lifesciencej@gmail.com
Website: http://www.sciencepub.org

ISSN 1097-8135
9 771097 813064

Life Science Journal
Volume 3 Number 3 September 2006